

SOL-898

DOE/ET/20567-1/2(Bk.1)

**SOLAR CENTRAL RECEIVER HYBRID POWER SYSTEMS SODIUM-COOLED
RECEIVER CONCEPT. FINAL REPORT**

Volume 2, Book 1. Conceptual Design, Sections 1 through 4

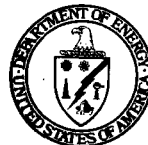
January 1980

Work Performed Under Contract No. AC03-78ET20567

**Rockwell International
Energy Systems Group
Canoga Park, California**



U.S. Department of Energy



Solar Energy

9

DISCLAIMER

"This book was prepared as an account of work sponsored by an agency of the United States Government. Neither the United States Government nor any agency thereof, nor any of their employees, makes any warranty, express or implied, or assumes any legal liability or responsibility for the accuracy, completeness, or usefulness of any information, apparatus, product, or process disclosed, or represents that its use would not infringe privately owned rights. Reference herein to any specific commercial product, process, or service by trade name, trademark, manufacturer, or otherwise, does not necessarily constitute or imply its endorsement, recommendation, or favoring by the United States Government or any agency thereof. The views and opinions of authors expressed herein do not necessarily state or reflect those of the United States Government or any agency thereof."

This report has been reproduced directly from the best available copy.

Available from the National Technical Information Service, U. S. Department of Commerce, Springfield, Virginia 22161.

Price: Paper Copy \$16.00
Microfiche \$3.50

**SOLAR CENTRAL RECEIVER HYBRID POWER SYSTEMS
SODIUM-COOLED RECEIVER CONCEPT
FINAL REPORT**

**VOLUME II, BOOK 1
CONCEPTUAL DESIGN
SECTIONS 1 THROUGH 4**

JANUARY 1980

**PREPARED FOR THE
U.S. DEPARTMENT OF ENERGY
AS PART OF**

CONTRACT NO. DE-AC03-78ET20567 (ET-78-C-03-2233)



Rockwell International
Energy Systems Group



MCDONNELL DOUGLAS



CORPORATION

Salt River Project
WATER ♦ POWER



Babcock & Wilcox



CONTENTS

	Page
1.0 Introduction	11
1.1 Objectives	11
1.2 Technical Approach	13
1.3 Technical Team	17
2.0 Market Analysis	19
2.1 Introduction	28
2.2 Solar/Fossil/Nuclear Plant, Economic and Performance Assumptions	28
2.3 Comparison with Fossil/Nuclear Plants	34
2.4 Comparison with Solar-Only Plants	38
2.5 Market Assessment	39
3.0 Parametric Analysis	67
3.1 Introduction	68
3.2 Collector Subsystem	68
3.3 Receiver Subsystem	118
3.4 Storage Subsystem	197
3.5 Non-Solar Subsystem	206
3.6 Electrical Power Generation Subsystem	218
3.7 Master Control	227
3.8 Dynamic Analyses	231
4.0 Selection of Preferred System	237
4.1 Selection Process	237
4.2 Selection Criteria	238
4.3 System Analyses	239
Abbreviations and Acronyms	275

(Sections 5 and 6 are in Vol II, Book 2.)

(References are in Vol II, Book 2.)

TABLES

		Page
1-1.	Summary of Hybrid Plants	15
2-1.	Financial Assumption for Market Assessment of Hybrid Fossil Solar Units.	29
2-2.	Economic and Performance Assumptions for Market Assessment of Hybrid Fossil Solar Units and Competing Power Plants	31
2-3.	Comparison of Hybrid/Fossil/Nuclear Levelized Busbar Electricity Cost Estimates	37
2-4.	Stand-Alone Solar Plant Capital Costs.	39
2-5.	Comparison of Hybrid/Stand-Alone Solar Plant Levelized Busbar Electricity Cost Estimates.	40
2-6.	Sample Calculation Base Load Markets	44
2-7.	Utilities Examined for Capacity Requirement, 1977.	47
2-8.	Projected Additional Base Load Capacity Requirements and Potential Markets for Generating Equipment, Western United States 1987-1989 and 1990-2001, GW.	53
2-9.	Projected Additional Intermediate Level Capacity Requirements and Potential Markets, Western United States 1987-1989 and 1990-2001, GW.	54
2-10.	Summary of Markets for New Generating Capacity, Western United States, GW.	56
2-11.	Comparison of Normal and Expanded Markets Due to Retirement of All Oil and Gas Before 1986 for Base Load Generating Equipment, Western United States 1987-1989 and 1990-2001, GW.	58
2-12.	Comparison of Normal and Expanded Markets Due to Retirement of Remaining Oil and Gas After 1990 for Base Load Generating Equipment, Western United States 1987-1989 and 1990-2001, GW	59
2-13.	Comparison of Normal and Expanded Markets Due to Retirement of All Oil and Gas Before 1986 for Intermediate Load Generating Equipment, Western United States 1987-1989 and 1990-2001, GW	60
2-14.	Comparison of Normal and Expanded Markets Due to Retirement of Remaining Oil and Gas After 1990 for Intermediate Load Generating Equipment, Western United States 1987-1989 and 1990-2001, GW	61
2-15.	Effect of Time of Changeover From Oil and Gas to Coal/Solar Systems on Market Size	62
2-16.	Summary of Demand for New Electric Generating Capacity, Western United States 1990-2001, Based on Specific Utilities Only (GW) . . .	64
2-17.	Summary of Demand for New Electric Generating Capacity for Entire Western United States 1990-2001 (GW).	64

TABLES

	Page
2-18. Summary of Demand for New Electric Generating Capacity for the United States	65
2-19. Utility Systems with Limited Capacity to Accept Hybrid Fossil Solar Units of Specified Sizes.	66
3-1. Factors Influencing Field Optimization.	70
3-2. Component Dependent Cost Models	71
3-3. Fixed Cost Changes.	74
3-4. Other Changes to Cost Model	76
3-5. Sample Performance Summary.	83
3-6. Performance Summary 120m Focal Height	86
3-7. 1962 Albuquerque (BOES) Visual Range vs Sky Cover	90
3-8. Number of Panels vs Temperature Gradient.	134
3-9. Engineering Basis for Material Selection.	141
3-10. Receiver Quadrant Flow and Heat Input	146
3-11. Assumptions for Thermal Loss Study.	150
3-12. Derived Temperature Values in Solar Panel	160
3-13. Drips Predicted Stress (psi).	163
3-14. Computed Thermal Gradient Stresses.	164
3-15. Summary of B31.1 Stress Evaluation.	165
3-16. Relaxation-Fatigue Evaluation	167
3-17. Tower Displacements and Accelerations	172
3-18. Tower Displacements and Accelerations	175
3-19. Conventional Free-Surface Pump Characteristics.	178
3-20. Summary of "Compact Tube" Steam Generator Experience.	186
3-21. Comparison of Evaporator Surface Area with CRBRP.	194
3-22. Comparison of Candidate Thermal Storage Concepts, 0.8-SM.	196
3-23. Heat Transfer Surfaces.	207
3-24. Ash System Comparison	216
3-25. EPGS Performance Characteristics	221
3-26. EPGS Performance Characteristics	222

TABLES

		Page
4-1.	Estimated Additional Capital Cost Required for Series Configuration	245
4-2.	University of Houston Isolation Model Monthly Clear Day Percentages	248
4-3.	Relative Output of Fields Operating with Various FRPR Cutoffs . . .	250
4-4.	Derives System Costs for System Constrained to Operate at 208 MWt Peak but Sized at Higher FRPR	250
4-5.	Economic Assumptions.	256
4-6.	Fuel Selection Non-economic Considerations.	261
4-7.	Requirements and Selection Criteria	265
4-8.	Optimum Plant Selection Study Economic Climate and Conditions . . .	266
4-9.	Optimum Plant Selection Study Parameter Ranges.	267

FIGURES

1-1.	Solar Central Receiver Hybrid Power System Energy Flow Diagram	10
1-2.	Solar Central Receiver Hybrid Power System Without Storage	12
1-3.	Solar Central Receiver Hybrid Power System With Storage	14
2-1.	U.S. Solar Insolation Regions (Direct Normal Insolation in kWh/m ² -Day)	36
3-1.	Optimization Envelope - 240 m Tower	78
3-2.	Optimization Envelopes for Different Focal Heights	79
3-3.	Optimization Envelopes for 150 m Tower	80
3-4.	Optimization Envelope for 120 m Tower	82
3-5.	Trim Control Vector	84
3-6.	Envelopes of Optimization Envelopes for Different Tower Heights	88
3-7.	Figure of Merit vs Power	92
3-8.	Figure of Merit vs Power Optimums	93

FIGURES

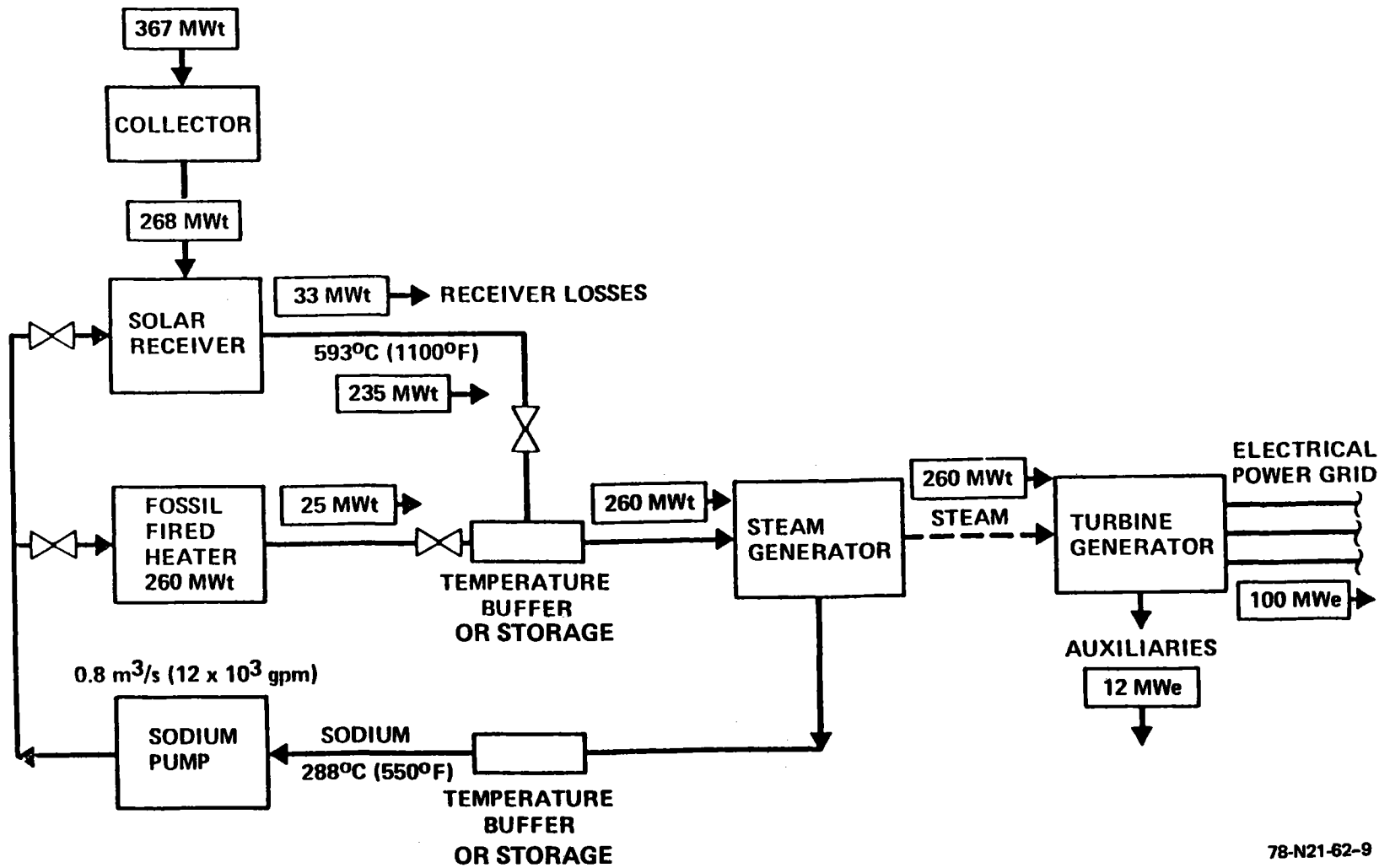
	Page
3-9. Figure of Merit vs Power Expanded Scale	94
3-10. Figure of Merit vs Power Expanded Scale	95
3-11. Figure of Merit vs Annual Energy (GWT)	96
3-11A. Cost of Optimum Solar Systems	97
3-11B. Effects of Aerosol Extinction on Transmittance from Heliostat to Receiver	98
3-11C. Atmospheric Attenuation for Low and High Visibility – Comparison of Mirvel and University of Houston Models	99
3-11D. Effects on Visual Range on Solar Optimization	101
3-11E. Visual Range Effects on Preferred Commercial Optimization	102
3-11F. Visual Range Effects on Preferred Commercial Optimization	103
3-12. Figure of Merit vs Equinox Noon Power	104
3-13. Figure of Merit vs Equinox Noon Power	105
3-14. Normalized Incident Flux on Receiver	106
3-15. Effect of Heliostat Size on Normalized Cost	110
3-16. External Receiver Concept	122
3-17. Baseline Receiver Design Layout for 0.9 SM Hybrid Plant	123
3-18. Panel Concept	124
3-19. 0.8 SM Receiver – Buffer Tanks in Tower	126
3-20. Buffer Tanks in Tower – Alternate 1	129
3-21. Diurnal Variation in Circumferential Flux Distribution	132
3-22. Transient Incident Panel Powers	133
3-23. Solar Multiple – 0.8 Receiver Size Selection	136
3-24. Solar Multiple – 1.4 Receiver Size Selection	138
3-25. Receiver Sizing Preferred Commercial System	140

FIGURES

	Page
3-26. Receiver Heat Flux Distribution	142
3-27. Normalized Receiver Heat Flux Profiles: Based on Equinox Noon	144
3-28. ΔT Through Tube Wall and Na Film	148
3-29. Axial Temperature Distribution on Solar Panel Tubes	149
3-30. Combined Heat Transfer Coefficient	152
3-31. Heat Transfer in Combined Free and Forced Flows	155
3-32. Advanced Receiver Tube Temperature Profile Equinox Noon — North Side	156
3-33. Derived Temperature Relationships	158
3-34. DRIPS Computer Model of Solar Receiver	161
3-35. DRIPS Predicted Thermal Displacements (Exaggerated)	162
3-36. Receiver Tower (100 MWe, 1.4 SM)	170
3-37. Receiver Tower (100 MWe, 0.8 SM)	174
3-38. Coal Fired Hybrid Riser Costs Versus Pipe ID	176
3-39. Coal Fired Hybrid Downcomer Costs	176
3-40. Key Differences Between the Fermi and Hallam Free Surface Pumps . .	180
3-41. Decarburization of 0.095-in. Thick 2-1/4 Cr — 1 Mo Steel by Sodium (One Side)	182
3-42. Highlights of LMEC/SCTI Test of MSG	187
3-43. Heat Transfer Results from LMEC/SCTI Test of MSG (100% Power in Combined Evaporator-Superheater Mode)	188
3-44. Stress Range vs Allowable Stress Cycles	190
3-45. Pinch Point Diagram — % Basis	192
3-46. Pinch Point Diagram — Length Basis	192
3-47. Effect of Sodium ΔT on Plant Costs	195
3-48. Ground Level, Atmospheric Tank Storage Concept	198
3-49. Ground Level, High Pressure Storage Concept	199
3-50. Buffer Tanks, T_1 and T_2 , Located at the Receiver Elevation	200
3-51. Corrosion of Type 316 Stainless Steel by Flowing Sodium	204
3-52. Coal-Ash Corrosion	208
3-53. Decarburization of 2-1/4 Cr — 1 Mo Alloy Furnace Tube in Sodium	210
3-54. Direct Firing System for Pulverized Coal	211

FIGURES

	Page
3-55. Negative Pressure Pneumatic Conveyor	214
3-56. Negative and Positive Pressure Pneumatic Conveyor	215
3-57. Solar Central Receiver Hybrid Power System	217
3-58. Turbine Cycle Configuration	220
3-59. Sulzer Cycle Startup/Shutdown System	223
3-60. Annual Improvement in Logic Gate Density	228
3-61. Cost per Megabit of Data Storage — 1978 and 1980	228
3-62. Annual Improvement for Power Consumption	228
3-63. Data Acquisition Costs — Conventional Hardwired vs Data Hiway . .	228
3-64. Loss of Pump Transient	232
3-65. Buffered System Response to Loss of Pump Transient	234
3-66. 1.4 SM Receiver Pump Head vs Flow Curve	236
4-1. Simplified Diagram — Solar Hybrid Plant Series Configuration Solar Receiver Followed by Fossil Heater	240
4-2. Simplified Diagram — Solar Hybrid Plant Series Configuration Fossil Heater Followed by Solar Receiver	242
4-3. Simplified Diagram — Solar Hybrid Plant Parallel Configuration . .	243
4-4. Figure of Merit and Annual Output vs Peak Power	246
4-5. Commercial System Collection Characteristics	249
4-6. Tower Cost vs Peak Power	251
4-7. Effect of Field/Receiver Power Ratio on FOM	252
4-8. Busbar Energy Cost vs Field/Receiver Power Ratio	254
4-9. Coal Solar Multiple Trade Study	257
4-10. Oil and Coal Hybrid Busbar Energy Costs	262
4-11. EPGS Size vs Storage Capacity	268
4-12. Nth Coal Hybrid Busbar Costs; 364 MWt Receiver	269
4-13. Nth Coal Hybrid Busbar Costs, 1000 MWt Receiver	270
4-14. Busbar Cost vs Receiver and Plant Size and Storage	271
4-15. Intermediate Load Candidate Comparisons	274



78-N21-62-9

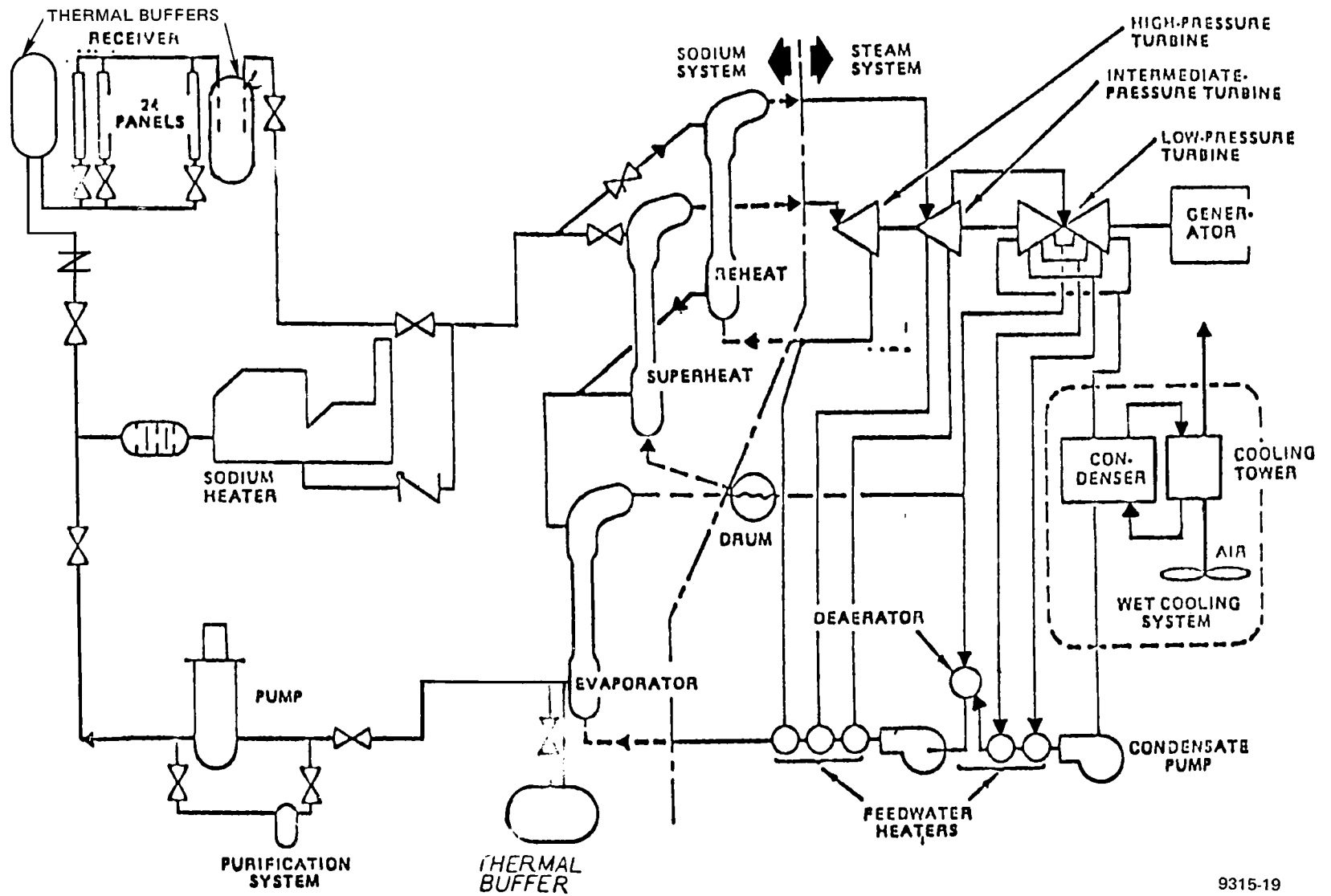
Figure 1-1. Solar Central Receiver Hybrid Power System Energy Flow Diagram

I.0 INTRODUCTION

1.1 OBJECTIVES

The overall, long-term objective of the Solar Central Receiver Hybrid Power System program is to identify, characterize, and ultimately demonstrate the viability and cost effectiveness of solar/fossil, steam Rankine cycle, hybrid power systems that: (1) consist of a combined solar central receiver energy source and a nonsolar energy source at a single, common site, (2) may operate in the base, intermediate, and peaking capacity modes, (3) produce the rated output independent of variations in solar insolation, (4) provide a significant savings (50% or more) in fuel consumption, and (5) produce power at the minimum possible cost in mills/kWh. It is essential that these hybrid concepts be technically feasible and economically competitive with other systems in the near to mid-term time period (1985-1990) on a commercial scale.

The program objective for Phase I is to identify and conceptually characterize solar/fossil steam Rankine cycle, commercial-scale, power plant systems that are economically viable and technically feasible. The basic process constituting the hybrid solar concept as developed to date is shown in Figure 1-1. The principal advantages of this system, when compared with a solar stand-alone plant, for example, is that the solar hybrid plant can operate day and night and during poor insolation conditions. Consequently, full capacity credit can be taken for the plant, and there is no requirement to start up and shut down the steam plant daily. The amount of energy storage that may be required in a hybrid plant can vary from that which will provide only a few minutes of operation (provides a smooth transition from solar to fossil and back) to that which will allow operation for several hours. The amount of storage depends heavily upon the assumptions made for the future cost of coal and oil and the power schedule of the utility grid. Large amounts of storage can readily be accomplished if it is economically viable to do so. In addition, such a plant would exhibit additional operational flexibility. Consequently, our second objective was to develop a conceptual design of a sodium-cooled Hybrid Central Solar Receiver plant which can supply 3 to 4 full power hours of electrical energy from a thermal storage system



9315-19

Figure 1-2. Solar Central Receiver Hybrid Power System Without Storage

The third objective was to select a scaled-up version of a hybrid plant with at least 3 full power hours of thermal storage. The plant size to be set by minimizing the busbar energy costs, consistent with technical and economic acceptability.

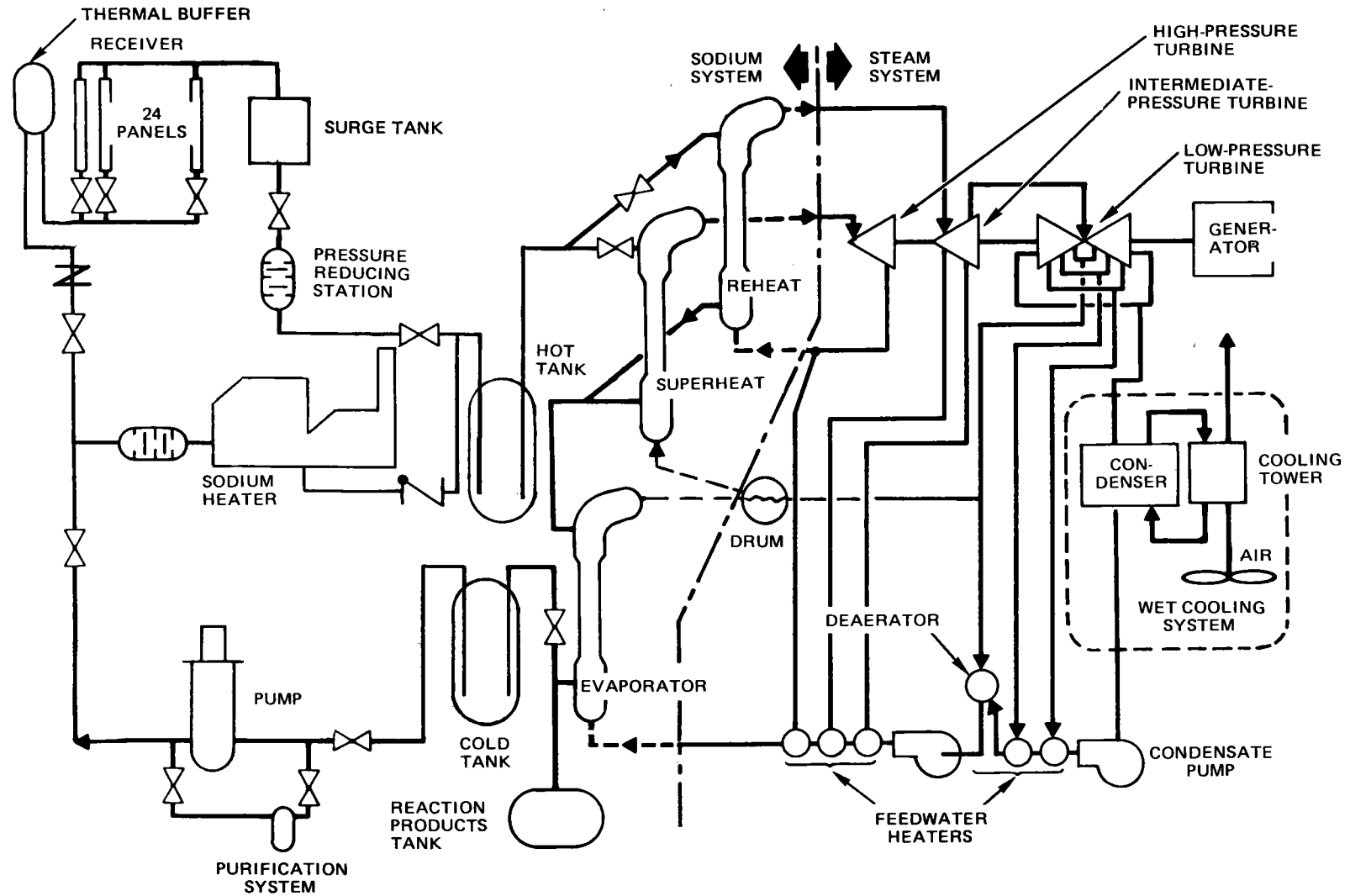
A typical flow diagram for a hybrid system without storage is shown in Figure 1-2. A hybrid system incorporating storage is shown in Figure 1-3. The two concepts are essentially the same except for the larger sodium tanks, the addition of a pressure-reducing station, and a second pump. Referring to Figure 1-2, 500⁰F sodium is pumped to the top of the tower, where it enters the receiver, and absorbs the solar energy collected on the surface of a series of panels. The sodium exits the receiver at a temperature of 1100⁰F, descends the tower, flows into a hot thermal buffer tank, and then enters a sodium-to-steam steam generator. The steam produced by the steam generator is fed to a conventional turbine that drives a generator, producing electrical power. From the steam generator, the sodium flows into a cold (550⁰F) thermal buffer tank, and then is pumped back to the top of the tower.

In parallel with the receiver is a fossil-fuel-fired heater that can heat the sodium from 550 to 1100⁰F. When solar energy is not adequate to supply the required power, the fossil-fuel-fired heater is turned up. Thus, the electrical output of the plant may be made constant at all times, and the system has an availability typical of a conventional, fossil-fuel-fired utility power plant.

A summary of the characteristics of the hybrid plants studied is given in Table 1-1.

1.2 TECHNICAL APPROACH

The technical approach that was used on this program was to review and transfer all of the pertinent technical data available from the Advanced Central Receiver Program to the Hybrid Central Receiver Program, add the fossil-fired heater, and establish a reference baseline configuration. System, subsystem, and component level trade studies and parametric analysis were then conducted to



42400-1096E

Figure 1-3. Solar Central Receiver Hybrid Power System With Storage

TABLE 1-1
SUMMARY OF HYBRID PLANTS
(Sheet 1 of 2)

	<u>UNITS</u>	<u>PLANTS</u>			
		<u>BASELINE</u>	<u>BUFFERED</u>	<u>STORAGE</u>	<u>STORAGE</u>
<u>EPGS*</u>					
NET POWER MWE		<u>100</u>	100	100	<u>430</u>
TURBINE PRESSURE	MN/M ² (PSIA)	12.5 (1,815)	12.5 (1,815)	12.5 (1,815)	16.6 (2,415)
CAPACITY FACTOR	PERCENT	80	80	80	40
FSPA*	PERCENT	<u>25</u>	25	<u>50</u>	<u>85</u>
<u>HEATER</u>					
THERMAL POWER		<u>260 (10)</u>	260 (20)	260 (0)	<u>1,115 (5)</u>
RATED MWT (MIN %)					
<u>FUEL</u>		<u>OIL</u>	COAL	COAL	<u>OIL/COAL</u>

*ELECTRIC POWER GENERATION SYSTEM – GROSS CYCLE EFFICIENCY PERCENT 43.5 (BL 43.1) (COMMERCIAL 43.7)

**FRACTION SOLAR POWER ANNUAL

SUPERHEATER/REHEATER °C (°F) 538/538 (1000/1000)

79-S7-48-50

TABLE 1-1
SUMMARY OF HYBRID PLANTS
(Sheet 2 of 2)

	<u>UNITS</u>	<u>PLANTS</u>			
		<u>BASELINE</u>	<u>BUFFERED</u>	<u>STORAGE</u>	<u>STORAGE</u>
<u>RECEIVER</u>					
SOLAR MULTIPLE	—	0.9	0.8	1.4	1.44
FRPR***	PERCENT	1.0	1.1	1.0	1.0
THERMAL POWER	MWT	234	208	364	1,600
MIDPOINT ELEVATION	M (FT)	<u>135 (443)</u>	124 (407)	154 (505)	<u>334 (1,096)</u>
HEIGHT	M (FT)	<u>12.3 (40.4)</u>	13.5 (44.3)	15.3 (50)	<u>28.5 (94)</u>
DIAMETER	M (FT)	<u>12.3 (40.4)</u>	10.4 (34.1)	13 (43)	25 (82)
<u>STORAGE ENERGY</u>	MWE-H	0	4.2	300	1,720
<u>COLLECTOR</u>					
MIRROR AREA	KM ² (FT ² x 10 ⁶)	<u>0.41 (4.5)</u>	0.417 (4.6)	0.66 (7.1)	<u>3 (32)</u>
NUMBER HELIOSTATS 10 ³		<u>8.5</u>	8.5	13.5	<u>61</u>
AVERAGE FIELD					
DIAMETER 10 ³	M (FT)		1.6 (5)	2.0 (6.5)	<u>4 (13)</u>

*** FIELD RECEIVER POWER RATIO – SODIUM TEMPERATURE °C (°F) 288/593 (550/1100)

modify the baseline into an optimized cost-effective system. Systems and components were then sized in sufficient detail to permit an accurate cost estimate to be made. The optimized configuration was then scaled up to define and cost the commercial plant.

1.3 TECHNICAL TEAM

The following organizations and their areas of responsibility are given here.

HYBRID PROGRAM

Principal Technical Contributors

Rockwell International

Bill Willcox
Anarg Frangos
Jan Ives
Joe Miller
Ed Mouradian
John Page

Dale Cipra
John Auleta
John Pfouts
Tom Springer
Lyle Glasgow

University of Houston

Mike Walzel
Lorin Vant Hull

SRI International

Ed Kinderman
Paul Meagher
Gwen Crooks

Babcock & Wilcox

John Slavens
Bill Clancy
Earl Coulter

Salt River Project

Steve Chalmers
Dick Durning
Don Squire

McDonnell-Douglas

Dave Carey

Stearns-Roger

Allen McKenzie
William Lang

PARTICIPATING ORGANIZATIONS AND
PRINCIPAL TECHNICAL CONTRIBUTORS

Rockwell International (Energy Systems Group)

- . Overall System Integration
- . Sodium Subsystems
- . Receiver
- . Steam Generator
- . Storage Subsystem
- . Stack Gas Cleanup System

Babcock & Willcox

- . Fossil-Fueled Sodium Heater and Auxiliary

McDonnell-Douglas Corporation (Astronautics Company)

- . Collector Subsystem
 - . Master Control Subsystem
- University of Houston

Stearns Roger, Alan McKensie - William Lang

- . Electric Power Generation Subsystem
- . Plant Layout
- . Tower and Stack (chimney)
- . Fuel Handling (in part)
- . Ash Handling
- . Balance of Plant

Salt River Project - Dick Durning - Steve Chalmers - Don Squire

- . Utility Consultants - for Operations, Design, and Cost
- . Utility Viewpoint Guidance - Investment, Utility Planning,
Grid Integration, and Utility
Acceptance

Stanford Research International (Nuclear and Utility Systems)

- . Independent Economic Parameter Assessment
- . Market Penetration Analysis

2.0 MARKET ANALYSIS

SUMMARY

This section includes an analysis of potential markets for electric generating units in the western United States and estimates of similar requirements in the eastern portion to the year 2001. It also contains estimates of the cost of electric power from solar-hybrid units and compares these costs with their potential competitors - solar only, fossil only, and nuclear-fueled units under a variety of conditions. Finally, market shares and market penetration to the year 2010 for solar hybrid units are presented. Plant sizes referred to in this section are in megawatts electric.

The commercialization of new systems is expedited if the market requirements for these systems are understood early in their design and development. In the case of hybrid fossil-solar central power units, the insolation conditions under which they might prove competitive with other electric power producers were established. This information guided the designer and enabled him to select unit designs with greater commercial potential. Furthermore, the total market potential was estimated for all competitive systems and the likely share of that total that the hybrid could obtain in order to estimate realistically the manufacturing requirements and costs. Finally, the rate of market penetration (sales) was estimated. This latter parameter will dictate the speed at which the systems will be sold.

The market analysis reported here consists of estimates of overall market size derived from projections of electric power growth, examination of utility plans, and projections of potential governmental (regulatory) action. Market shares for the solar hybrids are projected by comparisons of the levelized costs of busbar power produced by these units with costs of other electric power producers such as coal only, nuclear and solar only units. In these comparisons, standard economic and performance assumptions were applied to all plants.

Projections of market penetration are dependent upon evaluation of utility attitudes toward new technologies and of potential environmental and other constraints to acceptance of hybrid fossil-solar systems.

No severe impediments to adoption were identified and normal penetration parameters were used in calculations to estimate rates of sales for solar hybrid systems.

Under favorable conditions (high insolation, relatively high coal price and inflation rate) as many as 53 430-MW solar-oil hybrid units could be installed in intermediate service by year 2010 in the western United States. Eight to 57 615-MW solar-coal hybrids could be installed in base load service in the same time interval. The lower number assumes that the larger coal-only plants compete with hybrids, the high assumes that competition is limited to smaller coal-only units.

Markets for hybrid fossil-solar electric generating units are defined by three primary considerations. First, they are limited by the expected growth in demand for new electric generating units of all kinds. The definition of this expected market was an important part of the market assessment. The second important factor in the assessment of hybrid solar markets is the economic competitiveness of this system with all systems that could be used to produce electric power in the market period. This comparison is used to compute an ultimate or equilibrium share of the total demand for capacity that should be captured by the hybrid fossil-solar units. Finally, markets (sales) in the near-term are limited by the rate at which customers (electric utilities) accept a new technology (product).

Estimated overall markets are determined by examining projected demand (sales) of electricity and computing the electric generating capacity needed to meet this demand. The calculations required:

- 1) Regional projections of electric power demand
- 2) Allocation of this demand to the individual states
- 3) Allocation of state demand among the major utilities (primary power producers)
- 4) Calculation of capacity requirements to meet demand for these utilities (representing ~75% of total area capacity)
- 5) Estimates of markets represented by all utilities in the region
- 6) Estimation of the ultimate market share.

The regional demand projections were based on previous SRI projections of regional markets for electricity. These projections were derived from a detailed

and regionalized computer analysis of energy supply and demand in the United States and the price competition that determines the choice between fuels (or between fuels and electricity).

The nationwide electricity growth was projected at 5.3% for the period 1975-1985, and 3.8% for the period 1985 to 2000. This latter period is of greatest interest, although the lower growth rates, generally between 2.0 and 2.5%, predicted by SRI for electricity growth over the period 2000 to 2022 will also have an impact on the long-term solar hybrid markets. The forecast demand (sales) in the West North Central, West South Central, Mountain and Pacific regions was allocated to the individual states.

The sales demand was translated to capacity. Average capacity factors were estimated for each state. These factors include the reserve margins actually maintained by the utility.

The overall generation allocation for each state was divided into requirements for base, intermediate, and peak load service, and this distribution was extended to the major utilities in each state examined.

Actual and planned capacity was projected by state and for each major utility. Existing capacity by state and utility was obtained from DOE, EEI, and individual utility data. This was corrected for each category -- base, intermediate, peak for:

- 1) Announced addition (+)
- 2) Expected retirements (after 30 years) (-)
- 3) Expected transfers from base (-, +) to intermediate
(units <400 MW and >15 years old)
- 4) Entitlements (+)

The difference between capacity need and capacity available at selected times defined the total expected market for electric generating equipment. These are summarized in Tables S-1 through S-3.

Table S-1 presents data summed by state and by power pool for the major utilities in the western United States. These currently have 75% of the installed electric generating capacity in that area, and are estimated to represent 90% of the potential market. Requirements in the period 1990 to 2001 when solar units will first be introduced are summarized in Table S-2 that presents data based on specific utilities and Table S-3 that represents the total market.

TABLE S-1
SUMMARY OF MARKETS FOR NEW GENERATING CAPACITY
WESTERN UNITED STATES, GW
(Normal Retirement)

Western States Coordinating Council	1987-1989		1990-2001	
	Base	Intermediate	Base	Intermediate
By state	0.5	5.7	14.7	26.0
By pool	0	7.8	5.0	26.6
Electric Reliability Council of Texas				
	1.7	3.9	26.0	17.6
Mid-Atlantic Area Council				
By state	0.1*	0.7*	1.3	4.0
By pool	0*	0.8*	0	4.0
Southwest Power Pool				
By state	0	3.1	11.0	13.2
By pool	0	3.1	10.8	13.2
Total by states	2.3	13.4	53.0	60.8
Total by pool	1.7	15.6	41.8	61.4

*Differences because of rounding.

TABLE S-2

SUMMARY OF DEMAND FOR NEW ELECTRIC
GENERATING CAPACITY, WESTERN UNITED STATES
[1990-2001, BASED ON SPECIFIC UTILITIES ONLY (GW)]*

	Base Load	Intermediate Load
Normal retirement only	42-53	61-61
Normal retirement, with 1987-89 needs added	44-55	74-77
Forced retirement with 1990-2001 needs only	61-73	75

TABLE S-3

SUMMARY OF DEMAND FOR NEW ELECTRIC GENERATING
CAPACITY FOR ENTIRE WESTERN UNITED STATES*
[1990-2001 (GW)]

	Base Load	Intermediate Load	Total
Normal retirement	46-58	67-69	113-127
Normal retirement with 1986-89 needs added	48-61	82-85	130-146
Forced retirement with 1990-2001 needs only	67-80	82-83	149-163

* Data rounded to nearest GW.

The 30-year levelized costs of electricity for various systems are shown in Table S-4. The solar hybrid costs are presented as a function of assumed direct normal solar insolation characteristic of western U.S. regions.

The equilibrium market share for these assumed conditions are shown in Table S-5. Under favorable conditions, the equilibrium market share could be quite large.

The initial units sold will have first plant rather than Nth plant costs. Penetration calculations must consider this factor as well as the fact that markets traditionally resist, or slowly adopt, new equipment. A brief examination of factors that could unduly delay acceptance was performed.

Environmental and materials considerations, especially sodium availability, were addressed.

The several potential impacts of the use of fossil-solar hybrid central station power units discussed here are not severe. Land is definitely available. Water requirements are no greater than those for other power producing units needed (or installed) in the same area. Disturbance of semi-arid ecosystems may cause small effects. Many of the effects will be smaller than those for a coal-only unit. Thus, the environmental impacts, including land and water requirements, are not likely to prove impediments to selection of fossil-solar hybrid units by electric utilities. Sodium availability and price are not factors in limiting fossil-solar hybrid unit use.

The hybrid market penetration analysis considered five time periods (1990, 1995, 2000, 2005, and 2010) and twelve regions that were developed by roughly grouping utilities according to solar insolation level.

The hybrid unit sizes and costs used in the analysis were selected by Rockwell. The company also suggested some of the combinations of presumably competitive systems used in the final comparisons. The interpretation of results is that of SRI.

Three separate cases have been considered in the final market penetration analyses. The first deals with the marketability of the 430 MW solar-oil hybrid with storage in intermediate load service. It has been assumed that the major competition this hybrid will face consists of coal and oil-fired steam-cycle power plants of ~400 MW capacity, and smaller oil-fired combined cycle facilities in the size range of 200 to 250 MW. The second and third cases analyzed the

TABLE S-4

COMPARISON OF HYBRID/FOSSIL/NUCLEAR LEVELIZED
BUSBAR ELECTRICITY COST ESTIMATES

Intermediate Load (40% Capacity Factor)	Plant Capacity (MWe)	Levelized Busbar Electricity Costs (mills/kWh, 1979 dollar basis)							
		8%/Yr coal price escalation*				10%/Yr coal price escalation			
		Solar Insolation (kWh/m ² day)				Solar Insolation (kWh/m ² day)			
		4.5	5.5	6.5	7.5	4.5	5.5	6.5	7.5
Solar-Oil Hybrid, 1st plant cost	430	182	164	149*	149*	182	164	149*	149*
Solar-Oil Hybrid, Nth plant cost	430	150	132	117*	117*	150	132	117*	117*
Coal (small plant) ^f	100	_____		131	_____		152		_____
Coal	400	_____		113	_____		135		_____
Oil	400	_____		147	_____		147		_____
Oil combined-cycle	250	_____		126	_____		126		_____
Base Load (70% Capacity Factor)									
Solar-Coal Hybrid, 1st plant cost	615	103	100	98	95	118	114	110	106
Solar-Coal Hybrid, Nth plant cost	615	88	85	82	79	103	99	95	91
Coal (small plant) ^f	100	_____		94	_____		115		_____
Coal	400	_____		84	_____		107		_____
Coal	1,000	_____		72	_____		94		_____
Coal combined-cycle	1,000	_____		77	_____		97		_____
Nuclear (LWR)	1,000	_____		64	_____		64		_____
Cases: 1990 start-up for all plants; oil (residue) price is \$2.92/MMBtu and coal price is \$1.40 in 1979; fuel price escalation rates are 9.5% for nuclear and 10% for oil.									

* At this solar insolation level, the plant fuel cost is calculated as zero, indicating that some of the collected solar energy is not being used. This is an unrealistic situation, since a plant with a lower solar multiple would be less expensive and more suitable under these conditions.

^f Economic and operational data developed by Rockwell International.

• Initial coal cost at \$1.40/MMBtu

TABLE S-5

PROJECTED EQUILIBRIUM MARKET SHARES FOR FOSSIL-SOLAR HYBRIDS
(No "Behavioral Lag" Is Considered; 1990 Start-Up)

Intermediate Load (40% Capacity Factor)	Plant Capacity (MWe)	Equilibrium Market Share (% Captured in 1990)							
		8%/Yr coal price escalation				10%/Yr coal price escalation			
		Solar Insolation (kWh/m ² day)							
		4.5	5.5	6.5	7.5	4.5	5.5	6.5	7.5
Solar-Oil Hybrid, 1st plant cost	430	0.0	0.0	0.3	0.3	0.0	0.4	2.6	2.6
Solar-Oil Hybrid, Nth plant cost	430	0.3	3.7	29.9	29.9	2.3	23.0	76.9	76.9
Base Load (70% Capacity Factor)*									
Solar-Coal Hybrid, 1st plant cost	615	0.1	0.1	0.2	0.3	0.6	1.3	2.6	5.3
Solar-Coal Hybrid, Nth plant cost	615	1.4	2.7	5.4	10.6	9.0	17.9	33.2	54.1

*Nuclear power plants are not considered among the competing plant types.

marketability of ~615 MW coal-solar hybrids in base load service with two major competitors - large (1000 MW) and small (400 MW) coal-only facilities.

At a 10% coal price escalation, 9 units would be placed in intermediate load service by year 2000 and 53 units could be in use by year 2010. Only one unit would be in service in base load markets by 2000 and 8 by 2010, if large coal-only plants form the competition. On the other hand, 13 units could be in service in year 2000 and 57 in year 2010 if small coal-only plants formed the competition. This is summarized in Table S-6.

The solar units will first be used in the southwest, particularly to serve the Arizona-Southern California markets. Northern California markets and those in Texas can also be important by year 2010.

Subsidies can accelerate market acceptance.

TABLE S-6
SUMMARY OF SOLAR HYBRID UNIT MARKETS
(Coal at \$1.40/MMBtu, 10% escalation)

	2000	2010
Oil Solar	9	53
Coal Solar (Large plant competition)	1	8
Coal Solar (Small plant competition)	9	53

2.1 INTRODUCTION

Market requirements for the hybrid fossil-solar central power units, provided in this study, guided the designer and enabled him to select unit designs with the greatest commercial potential. Cost estimates for competitive systems led to realistic estimates of equilibrium market shares. The rate of market penetration as a function of time was estimated. This latter parameter dictates the speed at which the systems will be sold and new manufacturing facilities will be needed. This estimate of sales prospects will also be useful in establishing cash flow expectations and financial viability of new ventures.

Predictions of the potential use of solar electric generating systems and of the fossil fuel savings they make possible are useful to planners who are attempting to forecast the need for fossil fuels and the productive structure needed to supply them.

The market analysis reported here consists of estimates of overall market size derived from projections of electric power growth, examination of utility plans, and projections of potential governmental (regulatory) action (see Section 2.5). Market share is projected by comparisons of the levelized costs of busbar power [Busbar Energy Costs (BBEC)] produced by hybrid fossil-solar units with costs of other electric power producers such as coal only, nuclear and solar only units (see Sections 2.3 and 2.4). In these comparisons, standard economic and performance assumptions were applied to all plants (see Section 2.2).

Projections of market penetration are dependent upon evaluation of utility attitudes toward new technologies and of potential environmental and other constraints to acceptance of hybrid fossil-solar systems. These evaluations will be reported as part of Section 6.

2.2 SOLAR/FOSSIL/NUCLEAR PLANT ECONOMIC AND PERFORMANCE ASSUMPTIONS

Comparisons between units with differing ratios of capital to operating and fuel costs are frequently highly sensitive to the economic, financial, and performance assumptions made. Comparisons between fuel types have similar sensitivity. The influence of these assumptions is particularly strong in this instance, since the comparison is based on plants intended to go into operation in 1990 and to operate 30 years thereafter. The high rates of inflation that the prudent planner now uses intensifies the differences. Therefore, the financial parameters set forth in Table 2-1 were chosen only after careful consideration and discussion among the project team members. They are viewed as conservative estimates.

Table 2-1

FINANCIAL ASSUMPTION FOR MARKET ASSESSMENT OF
HYBRID FOSSIL-SOLAR UNITS

Debt fraction	0.5
Return on debt	0.10
Stock fraction	0.5
Return on stock	0.15
Cost of capital after tax [*]	0.10
Income tax rate, fraction	0.5
Annual insurance and other taxes, fraction	0.0225
Depreciation method	SOYD
Depreciation life, years	22
Fixed charge rate, fraction [*]	0.179

* Computed from other stated values.

The values set forth in Table 2-2 were derived by SRI from a variety of sources. Primary reliance was placed on data found in the Technical Assessment Guide* prepared by the Electric Power Research Institute.

Capital costs assumed for the plants against which the hybrid fossil-solar units were tested fall within the DOE range[†] with one exception. The cost assumed for the intermediate load residual-fired steam generating plant falls ~10% above the DOE range. This plant is far from competitive, so the difference is not significant. Construction times of five years were assumed for all hybrid units.

The heat rates used are also generally in agreement with DOE assumptions. Intermediate load residual-fired steam turbine units are assumed to have heat rates ~9% above the upper figure selected by DOE. The differences do not significantly affect the competitive status of the hybrid units.

Delivered, long-term contract coal costs listed for 1979 were \$1.00 and \$1.40 per million Btu. The lower cost is representative of regions characterized by competitive markets, mine-mouth western coal, and/or captive mines. The higher cost is representative of coals shipped long distances or without competitive market. Actual coal prices can vary widely. SRI has estimated delivered 1979 coal prices (long-term contract) ranging from \$1 to \$2 per million Btu. While both coal costs were used in earlier analyses, the value of \$1.40 was used in the final analysis of market share and penetration. Both 8 and 10% coal cost inflation rates were used in conjunction with these analyses reported in Section 6.

O&M costs are similar to those suggested by DOE. The differences have no bearing on further conclusions as O&M costs range from only 2 to 18% of the total levelized costs (depending on plant type), and the differences between units in similar service are generally on the order to 2 mills per kWh or less.

A number of different methods of cost calculation are available for use in this type of analysis. First year costs, average cost of service, and levelized costs, which are discounted costs averaged over time, are frequently used. The choice made here can also influence the competitive status of the alternate

*Report EPRI PS-866-SR (June 1978).

†RDD

TABLE 2-2
 ECONOMIC AND PERFORMANCE ASSUMPTIONS FOR MARKET ASSESSMENT
 OF HYBRID FOSSIL-SOLAR UNITS
 AND COMPETING POWER PLANTS
 (Sheet 1 of 2)

Item	Value	
	Used	Prior DOE Assumption (if different)
Base Year for Costs	1979	
Year of Commercial Operation	1990	
Plant Life (years)	30	
Capital Cost (\$/kWe)		
Solar-Oil Hybrid, SM = 1.44 (430) ^{*†} 1st plant cost	1,822	
Solar-Oil Hybrid, SM = 1.44 (430) [†] Nth plant cost	1,431	
Solar-Coal Hybrid, SM = 1.0 (615) [§] 1st plant cost	1,515	
Solar-Coal Hybrid, SM = 1.0 (615) [§] Nth plant cost	1,190	
Coal, intermediate load (400) [†]	890	550-1,065
Coal, base load (1,000) [§]	720	550-1,065
Coal, cc ^{**} , base load (1,000) [§]	790	550-1,065
Coal, Rockwell, base or intermediate load (100)	1,067	
Nuclear, base load (1,000) [§]	870	825-1,100
Oil, resid-steam, intermediate load (400) [†]	485	330-440
Oil, resid, cc ^{**} intermediate load (250) [†]	330	330-440
Heat Rate (Btu/kWh)		
Solar-Oil Hybrid (430)	9,500	
Solar-Coal Hybrid (615)	10,200	
Coal, intermediate load (400)	11,000	
Coal, base load (1,000)	10,500	9,000-10,500
Coal, cc, base load (1,000)	9,500	9,000-10,500
Coal, Rockwell, base or intermediate load (100)	10,200	9,00-10,500

*Unit size, MW

§Capacity factor, 70%

†Capacity factor, 40%

**Combined cycle

TABLE 2-2
 ECONOMIC AND PERFORMANCE ASSUMPTIONS FOR MARKET ASSESSMENT
 OF HYBRID FOSSIL-SOLAR UNITS
 AND COMPETING POWER PLANTS
 (Sheet 2 of 2)

Item	Value	
	Used	Prior DOE Assumption (if different)
Nuclear, base load (1,000)	10,500	10,400-10,800
Oil, resid-steam, intermediate load (400)	9,500	8,700-8,900
Oil, resid, cc, intermediate load (250)	8,500	8,700-8,900
Fuel Costs (\$/MMBtu)		
Coal	\$1.40	
Oil, resid	\$2.92	\$2.20-2.75
Nuclear	\$0.57	\$0.27
Fuel Escalation (%/year)*		
Coal	8, 10%	
Oil, resid	10%	
Nuclear	9.5%	
O&M Cost (first year)		
Solar-Oil Hybrid (430)	1% capital + 10% 1st year fuel	
Solar-Coal Hybrid (615)	1% capital + 30% 1st year fuel	
Coal, intermediate load (400)	3.5 mills/kWh	
Coal, base load (1,000)	2.3 mills/kWh	
Coal, cc, base load (1,000)	4.6 mills/kWh	
Coal, Rockwell, base or intermediate load (100)	0.75% capital + 30% 1st year fuel	
Nuclear, base load (1,000)	2.6 mills/kWh	
Oil, resid-steam, intermediate load (400)	1.0 mills/kWh	
Oil, resid, cc, intermediate load (250)	2.0 mills/kWh	

Sources: DOE, SRI International, EPRI.

*These values are consistent with the SRI long-range for cost (To the year 2000).

systems under evaluation. Levelized costs computed in a manner similar to that set forth by Doane* were used in the calculations and comparisons of Sections 2.3 and 2.4.

All plants are assumed to start up in 1990 or beyond and all results are expressed in 1979 dollars.

*J. W. Doane, The Cost of Energy from Utility-Owned Solar-Electric Systems, Jet Propulsion Laboratory (June 1976).

2.3 COMPARISON WITH FOSSIL/NUCLEAR PLANTS

Many characteristics of fossil-solar hybrid power systems, such as high capital cost, and ability to operate at high capacity factors, indicate that these plants can be considered as being most suited to base and intermediate load service. Vying for a share of these markets could prove difficult, however, because of the competition that any emerging alternative technology faces. This competition comes not only in the form of conventional nuclear and fossil-fired system such as low-Btu gas, combined-cycle facilities. Within the intermediate load power market, the stiffest competition is likely to be from steam-cycle coal plants ranging up to 400 MW in capacity, and somewhat smaller (about 250 MW) in capacity, combined-cycle, oil fired plants. In order to be consistent within this analysis, these plants are assumed to operate at a "typical" intermediate load capacity of 40%.

In the base load market, nuclear, steam-cycle coal, and combined-cycle coal plants, all in the 800 to 1,000 MW size range, are likely competitors. A 70% capacity factor has been chosen as representative of base load facilities. As discussed later, nuclear units were not considered in the final market share computations.

The important economic, financial, and performance assumptions used to characterize the competing power plants were presented in Section 2.2. As can be seen in Table 2-2, a number of varying assumptions are made about the design and costs of the hybrid systems. Two plant designs are considered with solar multiples of 1.44 and 1.0. The first is oil-fired and has heat storage capability; the second employs coal as a backup energy source and incorporates no storage. In addition, for both of these plant types, two capital cost estimates are used; these represent the 1st and the Nth commercial plants. Assumptions about the costs and performance of the competing plant types are also listed in Table 2-2.

Using these assumptions within the framework of the costing methodology that was noted in Section 2.2, levelized busbar electricity cost estimates were computed for the various plant types considered.

Since the cost of power from a solar-thermal electric facility is highly dependent upon the availability of direct normal solar insolation, regional variations in this parameter were considered in performing the busbar cost

calculations. Characteristic insolation levels were developed for the various regions used in this study. As shown in Figure 2-1, these direct normal insolation levels ranged from a high of 7.5 kWh per m² day (annual average) in limited portions of the southwestern U.S. to a low of 4.5 kWh per m² day or less in northwestern, mid-western, and southern portions of the country.

The results of the cost analysis that include variations in insolation are presented in Table 2-3. These are levelized busbar costs, expressed in 1979 dollars, for plants that start up in 1990. Results for coal price escalation rates of 8 and 10% per year are presented in Table 2-3.

The cost projections for intermediate load power can be seen to vary widely depending upon plant type, insolation level, and the rate at which coal prices increase with time. At the assumed 8% per year coal price escalation rate, the 400-MWe coal-fired plant provides the least expensive power in every insolation region. At the highest insolation levels, the 430-MWe solar-oil hybrid BBEC cost approaches the BBEC cost of the 400-MWe coal plant if Nth plant capital costs are used for the hybrid.

At the higher coal price escalation rate of 10% per year, the economic attractiveness of the solar-oil hybrid is increased substantially in relation to the conventional coal-fired plants. At Nth plant costs, the hybrid is computed to have an advantage over all other plant types in the 6.5 and 7.5 kWh/m² day insolation regions.

In the base load market, the availability of nuclear power and larger (1,000 MW) coal-fired plants substantially reduces the ability of the 615-MW solar-coal hybrid plant to obtain an economic advantage. Light water reactor facilities are estimated to be able to generate base load electricity at lower cost than the hybrid under all options considered. At a 10% per year coal price escalation rate, and assuming Nth plant hybrid capital costs, however, the 615-MW solar-coal hybrid appears likely to be competitive with the large coal-fired power plants in regions with favorable insolation levels.

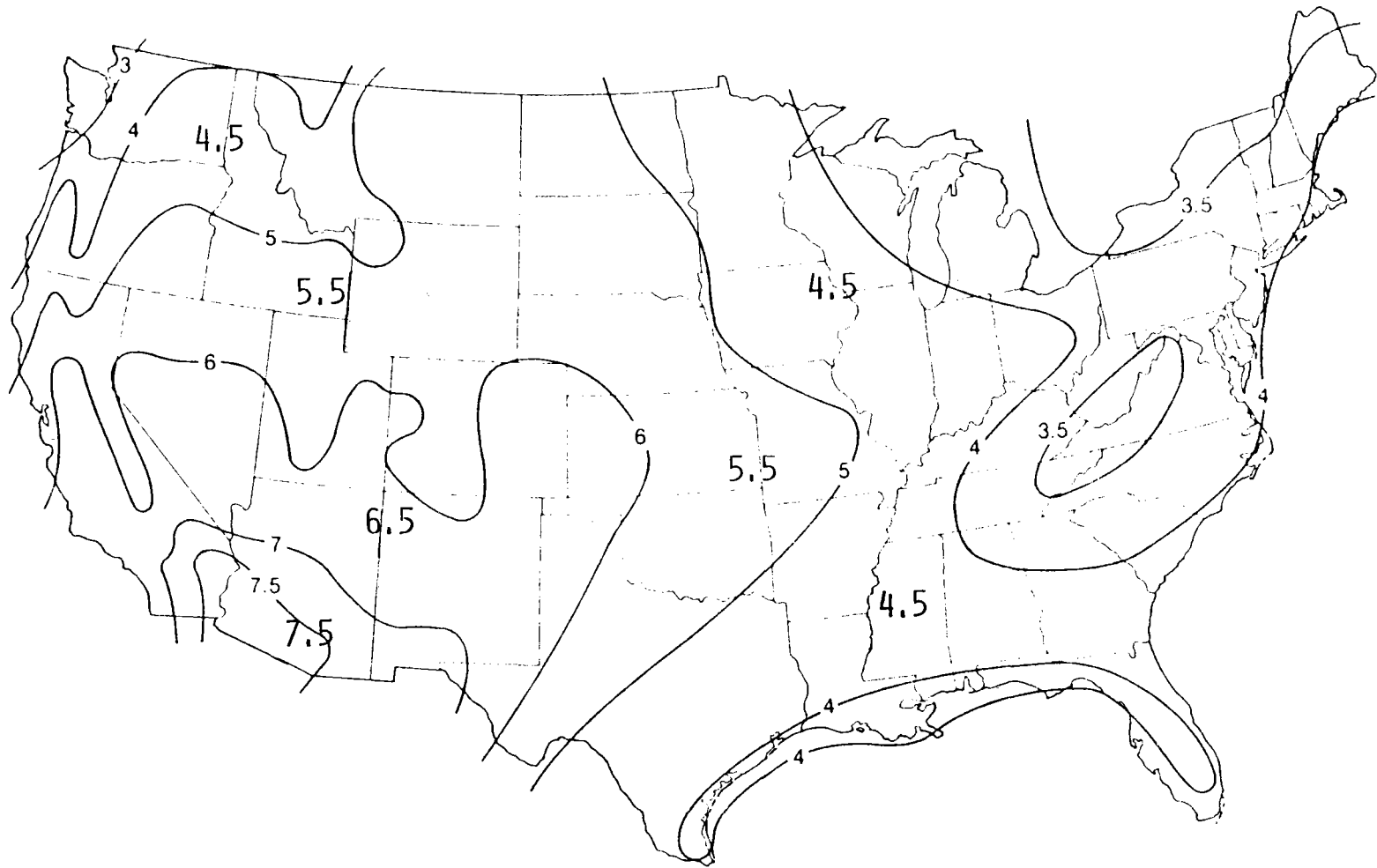


Figure 2-1. U.S. Solar Insolation Regions (Direct Normal Insolation in kWh/m²-Day)

TABLE 2-3

COMPARISON OF HYBRID/FOSSIL/NUCLEAR LEVELIZED
BUSBAR ELECTRICITY COST ESTIMATES

Intermediate Load (40% Capacity Factor)	Plant Capacity (MWe)	Levelized Busbar Electricity Costs (mills/kWh, 1979 dollar basis)							
		8%/Yr coal price escalation				10%/Yr coal price escalation			
		Solar Insolation (kWh/m ² day)				Solar Insolation (kWh/m ² day)			
		4.5	5.5	6.5	7.5	4.5	5.5	6.5	7.5
Solar-Oil Hybrid, 1st plant cost	430	182	164	149*	149*	182	164	149*	149*
Solar-Oil Hybrid, Nth plant cost	430	150	132	117*	117*	150	132	117*	117*
Coal (small plant)†	100			131			152		
Coal	400			113			135		
Oil	400			147			147		
Oil combined-cycle	250			126			126		
<u>Base Load (70% Capacity Factor)</u>									
Solar-Coal Hybrid, 1st plant cost	615	103	100	98	95	118	114	110	106
Solar-Coal Hybrid, Nth plant cost	615	88	85	82	79	103	99	95	91
Coal (small plant)†	100			94			115		
Coal	400			84			107		
Coal	1,000			72			94		
Coal combined-cycle	1,000			77			97		
Nuclear (LWR)	1,000			64			64		

Bases: 1990 start-up for all plants; oil (reside) price is \$2.92/MMBtu and coal price is \$1.40 in 1979; fuel price escalation rates are 9.5% for nuclear and 10% for oil.

* At this solar insolation level, the plant fuel cost is calculated as zero, indicating that some of the collected solar energy is not being used. This is an unrealistic situation, since a plant with a lower solar multiple would be less expensive and more suitable under these conditions.

† Economic and operational data developed by Rockwell International.

2.4 COMPARISON WITH SOLAR-ONLY PLANTS

Although the major competition that fossil-solar hybrids will face in the 1990s will be from fossil fueled plants, other alternative energy systems that are based upon renewable resources can be expected to vie for a share of the power market. One of the most important of these alternative concepts is likely to be the stand-alone solar plant. The competition from this type of plant has the potential to significantly affect the market penetration of hybrid power systems (especially in areas of high solar insolation). As a result, it is important to consider the expected economic viability of stand-alone solar plants in comparison with fossil-solar hybrids. A preliminary analysis was performed; the design bases used for the stand-alone solar plants were those available in March 1979, consisting of the results of the ACR Program. [Ⓜ]

The stand-alone solar thermal electric power plant considered in this analysis is based upon a conceptual design developed by Rockwell International. Similar to the solar portion of the hybrid design, it incorporates a sodium coolant loop, with a secondary loop of water that acts as the plant's working fluid. The amount of thermal energy storage capacity that the plant contains can range from 0 to 13.2 h, and for storage capacity of >1 h, the plant's annual capacity factor varies nearly linearly with the storage capacity.

The number of hours of storage and the plant capital investments required to achieve the representative 40 and 70% intermediate and base load plant capacity factors are shown in Table 2-4. (These data are based upon a direct normal insolation of 6.3 kWh per m² day that is characteristic of Barstow, California.) As with the fossil-solar hybrid, capital costs for 1st and Nth commercial facilities are considered. First year operation and maintenance costs are assumed to be 1% of the plant capital investment.

The results of the preliminary hybrid/stand-alone solar cost comparison are presented in Table 2-5. The levelized busbar costs are expressed in 1979 dollars, but are for plants that begin operation in 1990.

For intermediate and peaking applications, high insolation and fuel costs, the stand-alone solar plant appears likely to be an economically viable alternative to the hybrid coal-solar system. For example, in comparing Nth plant

[Ⓜ] Advanced Central Receiver Final Report.

TABLE 2-4
 STAND-ALONE SOLAR PLANT CAPITAL COSTS
 (Based Upon Barstow Solar Insolation Data)

<u>Load Category</u>	<u>Capacity Factor Percent</u>	<u>Storage Capability Hours</u>	<u>Plant Capital Cost (1979 dollars/kWe)</u>	
			<u>1st Plant</u>	<u>Nth Plant</u>
Intermediate	40	3	\$1,822	\$1,431
Base	70	11	3,190	2,380

capital costs of intermediate load facilities, the stand-alone plant is estimated to produce electricity less expensively in the two highest insolation regions. If the more realistic (for the 1990 time frame) 1st plant costs are assumed the intermediate load stand-alone plant has an advantage only at the highest insolation level of 7.5 kWh/m² day.

In the base load market at the assumed fuel escalation rate, the all sodium stand-alone solar-coal economics does not fare well against the solar-coal hybrid. (See Table 2-5.) The basic reason is that the additional high temperature thermal storage capability required to reach higher capacity factors in the stand-alone solar facility adds a substantial capital cost penalty. This penalty is enough to negate any economic advantage from fuel saving by the stand-alone plant, even under the conditions of high direct normal insolation and high coal escalation rate.

2.5 MARKET ASSESSMENT

2.5.1 Methods of Analysis

Markets for hybrid fossil-solar electric generating units are defined by three primary considerations. First, they are limited by the expected growth in demand for new electric generating units of all kinds. The definition of this expected market was an important part of the market assessment. The second important factor in the assessment of hybrid solar markets is the economic competitiveness of this system with all systems that could be used to produce electric power in the market period. This comparison, discussed in Sections 2.3 and 2.4, is used to compute an ultimate or equilibrium share of the total demand for capacity that should be captured by the hybrid fossil-solar units. Finally,

TABLE 2-5

COMPARISON OF HYBRID/STAND-ALONE SOLAR PLANT
LEVELIZED BUSBAR ELECTRICITY COST ESTIMATES †

(Preliminary Data)

Levelized Busbar Electricity Costs
(mills/kWh, 1979 dollar basis)

Intermediate Load (40% Capacity Factor)	Plant Capacity (MWe)	8%/Yr coal price escalation				10%/Yr coal price escalation			
		Solar Insolation (kWh/m ² -day)				Solar Insolation (kWh/m ² -day)			
		4.5	5.5	6.5	7.5	4.5	5.5	6.5	7.5
Solar-Oil Hybrid, 1st plant cost 430		182	164	149	149	182	164	149	149
Solar-Oil Hybrid, Nth plant cost 430		150	132	117	117	150	132	117	117
Stand-alone solar, 1st plant cost 100		230	188	159	138	230	188	159	138
Stand-alone solar, Nth plant cost 100		167	136	115	100	167	136	115	100
<u>Base Load (70% Capacity Factor)</u>									
Solar-Coal Hybrid, 1st plant cost 615		103	100	98	95	118	114	110	106
Solar-Coal Hybrid, Nth plant cost 615		88	85	82	79	103	99	95	91
Stand-alone solar, 1st plant cost 100		266	218	184	160	266	218	184	160
Stand-alone solar, Nth plant cost 100		199	163	138	119	199	163	138	119

Basis: 1990 start-up for all plants; oil (resid) price is \$2.92/MMBtu and coal price is \$1.40 in 1979; fuel price escalation rate for oil is 10% per year.

†Economic and operational data developed by Rockwell International.

markets (sales) in the near term are limited by the rate at which customers (electric utilities) accept a new technology (product). The approach to the equilibrium can be rapid, as in the case of jet aircraft, or slow as in the case of new steel production facilities.

In the following paragraphs, the definition of overall market and market share under varying competitive situations will be described.

Estimated overall markets are determined by examining projected demand (sales) of electricity identifying the requirements by base, intermediate and peak loads, noting additions, entitlements, retirements and transfers and computing the new electric generating capacity needed to meet this adjusted demand.

The calculations required:

- A. Regional projections of electric power demand
 - B. Allocation of this demand to the individual states
 - C. Allocation of state demand among the major utilities (primary power producers)
 - D. Calculation of capacity requirements to meet demand for these utilities (representing ~80% of total area capacity)
 - E. Estimates of markets represented by all utilities in the region
 - F. Estimation of the ultimate market share.
- A. The regional demand projections were based on previous SRI projections of regional markets for electricity.* These projections were derived from a detailed and regionalized computer analysis of energy supply and demand in the United States and the price competition that determines the choice between fuels (or between fuels and electricity).

The analysis emphasized those fuels used in electricity production and those other fuels in competition with electricity for heating. The nationwide electricity growth was projected at 5.3% for the period 1975-1985, and 3.8% for the period 1985-2000. This latter period is of greatest interest, although the lower growth rates, generally between 2.0 and 2.5%, predicted by SRI for electricity growth over the period 2000-2022 will also have an impact on the long-term solar hybrid markets. The effect of differences in growth rates is important to the market projections. If instead of 5.3 and 3.8% annual growth

*Electric Power Research Institute, Fuel and Energy Price Forecasts, EPRI-433, Palo Alto, CA (1977).

rates for the periods 1975-85 and 1986-2000 the rates were 4.8 and 3.3%, the gross market would drop by 17%. If the rates were to drop to 4.3 and 2.8%, the markets would be reduced by 30%. Increased electricity sales would show equivalent increases in capacity demand and markets for new units. Thus, while the projected markets are based on what we believe to be reasonable estimates of growth in electric power demand, the actual markets could vary substantially from those projected on the basis of 5.3 and 4.8% annual growth.

B. The forecast demand (sales) in the West North Central, West South Central, Mountain, and Pacific regions was allocated to the individual states. Reported sales for 1976 were used as a base. Trends were deducted by examination of the years 1970 and 1973.* Line losses (7%) were added to the state sales to obtain generation load requirements. Average capacity factors were estimated for each state. These factors include the reserve margins actually maintained by the utility. These factors as for the state-by-state distribution of regional sales were based on 1976 data and projected forward using recent trends as guidance.† It was assumed in the projection that capacity factors would be improved with the installation of modern equipment selected with the idea of obtaining improved on-line availability and performance as this is now a major utility industry concern.

C. The overall generation allocation for each state was divided into requirements for base, intermediate, and peak load service. By dividing the hours of use for each load type into the proportion of generating capacity, the total capacity required to satisfy the load was derived. The average allocation of capacity was: base, 50%; intermediate, 31%; and peak, 19%. These allocations are hypothetical and can only be used as rough guides. A utility will operate its units as base, intermediate, or peak load depending on need, the unit capability, and the direct cost of power. The lowest cost generation unit (or mix of units) will be preferred by the dispatcher.

*Edison Electric Institute Statistical Yearbooks of the Electric Utility Industry, Edison Electric Institute, New York, N.Y. (1970, 1973, 1976).

†Data obtained from Moody's Public Utilities Manual, Congressional hearings and individual utility reports.

The study was extended to the major utilities in each state examined. Again, 1976 was used as base year, and trends from 1970 were considered in the projection of the allocations of the state totals.* Adjustments to sales were necessary for those utilities with sales in more than one state. Also, the individual utility sales were adjusted for interchange. The adjusted sales figures used were for sales within the service areas. Entitlements, i.e., sales by governmental organizations to preferred customers, were included in available peak capacity.† Correction for average line loss experienced by each utility was applied to sales to calculate capacity requirements.

D. Capacity requirements for the individual utilities were projected using the projected sales corrected for system line loss, observed trends in system capacity, and the allocation of capacity as before (i.e., 50% base, 31% intermediate, and 19% peak).

E. Existing capacity by state and utility was obtained from DOE,§ EEI,** and individual utility data.†† This was corrected for each category — base, intermediate, peak for:

- 1) Announced additions (+)
- 2) Expected retirements (after 30 years) (-)
- 3) Expected transfers from base (-,+) to intermediate (units <400 MW and >15 years old)
- 4) Entitlements (+).

Announced additions include those through January 1979. They were obtained from DOE, trade journals,§§ and various other utility reports. Jointly owned capacity was allocated to the individual owners and to the state of ownership to be matched against electric power demand in that state.

*Ibid., EEI.

†Ibid., EEI.

§Department of Energy, Office of Utility Project Operations, Inventory of Power Plants in the United States, DOE/RA-0061 (December 1977).

**Edison Electric Institute, Statistical Yearbook of the Electricity Utility Industry.

††Uniform Statistical Reports of the Individual Utilities, Utility Annual Reports.

§§"New Generating Plants," Power Engineering. Technical Publishing Co., Energy Daily, Wall Street Journal, etc. (1978).

TABLE 2-6

SAMPLE CALCULATION
BASE LOAD MARKETS

<u>Actual Capacity, 1977</u>	<u>Actions, 1978-1986</u>			<u>Projected Capacity 1986</u>	<u>Need[*] 1986</u>	<u>Buy Available Units (if deferred)[†]</u>	<u>Hybrid Market</u>
	<u>Announced Additions</u>	<u>Normal Retirement</u>	<u>Transfer to Intermediate</u>				
16.7	6.3	1 ^{**}	2 ^{**}	20.0	26.1	6.1	0 to 6.1
<u>Expected Capacity, 1986</u>	<u>Actions, 1987-1989</u>			<u>Projected Capacity 1986</u>	<u>Need[*] 1986</u>	<u>Buy Available Units (if deferred)[†]</u>	<u>Hybrid Market</u>
	<u>Announced Additions</u>	<u>Normal Retirement</u>	<u>Transfer to Intermediate</u>				
26.1	3.7	0.7	0	29.1	29.5	0.4 (6.5) [†]	0 to 6.5
<u>Expected Capacity, 1989</u>	<u>Actions, 1990-2001</u>			<u>Projected Capacity 1986</u>	<u>Need[*] 1986</u>	<u>Buy Available Units (if deferred)[†]</u>	<u>Hybrid Market</u>
	<u>Announced Additions</u>	<u>Normal Retirement</u>	<u>Transfer to Intermediate</u>				
29.5	2.6	1.2	0	30.9	44.2	13.3 (19.8) [†]	13.3 to 19.8

* Annual growth rate of overall demand to 1985 at 5.3 percent, from 1986-2001 at 3.8 percent.

† Quantity to buy if previous requirements were not filled.

** Example quantities.

As indicated, SRI assumes that base load units would be transferred to intermediate service after 15 years. However, units with capacities above 400 MW are expected to remain in base load service. All plants are expected to be retired after 30 years of service. While these assumptions are in general accord with electric utility practice, it must be recognized that retirements and shifts in service function can occur earlier or later than predicted by these arbitrarily selected criteria. If individual utility operations indicated a surplus of base load and a deficit of intermediate load capacity, a frequent occurrence, the few suitable base load fossil units would be switched to intermediate power service. Such factors as siting or other regulatory delays or difficulty in attracting capital funds at acceptable rates of interest could cause the utility to retain plants in service beyond 15 or 30 years. Borrowing or pooling of electricity or even reduction of reserve margin may be used to defer ordering of new or replacement equipment.

The general thrust of such practice is a delay in ordering of new plants. With a given growth over time, the need for new generating equipment between 1980 and 2000 will remain constant. By delaying orders until 1990, for example, the utility concentrates the market in the period 1990-2000. This delay is advantageous to systems such as the hybrid fossil-solar generating system that will not be demonstrated until the mid to late 1980s. That effect is indicated in Table 2-6.

F. For each utility and group of utilities (state and power pool), the forecast of capacity need (Column 6 of Table 2-6) was compared with capacity calculated to be available in the years 1986, 1989, and 2001 (Column 5). If calculated available capacity exceeded forecast capacity requirement, no additional generating units were required and there was no market. If projected capacity was not sufficient to meet the forecast capacity demand, then new capacity was assumed to be ordered before the end of the period, i.e., before 1986, 1989, and 2001 (Column 7). As a final approximation, capacity ordered in 1986 and 1989 was added to the capacity calculated to be available in the succeeding period to arrive at a total potential capacity market (Column 8). Also shown in Table 2-6 are the adjustments made for announced additions, retirements, and transfers.

The requirements stated are for installed capacity; orders would be placed four to five years earlier. Thus, the markets indicated for the period 1987-1989 are not likely to be available to a hybrid solar system. The information was included to indicate the incentive (potential increase in sales of solar units) that could result from an accelerated hybrid development program.

It was not feasible within the constraints of this project to analyze the hundreds of utilities in the western states separately. Major utilities for each state considered were analyzed. In the analysis, major utility totals were accumulated by state and power pool or coordinating council. (Pooling of electric generation within states and within power pools is a normal mode of utility operation.)

2.5.2 Estimated Markets for New Generating Capacity

The utilities examined in detail are set forth in Table 2-7. The utilities listed own from 72 to 91% of the total capacity in the states considered. As shown in the table, the utilities were categorized by utility coordinating council for later analysis.

The analysis concentrated on base and intermediate power plant requirements. These are the most likely markets for hybrid systems that have baseload capacity. (The peak load capacity requirements are generally about 40% of baseload or 60% of intermediate load.) The projected demand for electric generating capacity in these markets is set out in Tables 2-8 and 2-9. In these tables, the capacity needed has been calculated on two bases:

- 1) Generated power is shared by all utilities within a state (state needs summed)
- 2) Generated power is shared by all utilities within a power pool or reliability council (pool needs summed).

The latter of these is indicated by the word pooled.

If perfect pooling is assumed, the total demand for new installations of base load generating units is estimated at 1.7 GW of base and 14.6 of intermediate load units in the 1987-89 period. In this period, a marked surplus of base load units can be found in three of the four power pools considered. However, it is unlikely that the intermediate power demand will be filled by derating additional units.

TABLE 2-7
 UTILITIES EXAMINED FOR CAPACITY REQUIREMENT, 1977
 (1977 Capacity in Thousands of Megawatts)
 (Sheet 1 of 5)

<u>Western States Coordinating Council</u>		<u>Total State Capacity (estimated)</u>	<u>Total Capacity Reported by Utilities Listed</u>	<u>Percentage[†] of State Capacity in Utilities Examined</u>
Washington	Seattle Dept. Lighting Washington Water Power Washington Public Power Supply System BPA* to Washington public power agencies Total	18.4	10.6	
Oregon	Pacific Power and Light (excludes Wyoming) Portland General Electric Puget Sound Power and Light BPA* to Oregon public power agencies Total	7.9	10.5	
California	Los Angeles Dept. Water & Power Pacific Gas and Electric Co. San Diego Gas and Electric Co. Southern California Edison Co. Sacramento Municipal District Total	35.7	32.0	
Nevada	Nevada Power Co. ** Sierra Pacific Power Co. ** Total	3.6 ¹	2.0	

* Includes municipals, public power districts, rural electric cooperatives, and wholesale deliveries to large industrial companies.
[†] Utility capacity is frequently located among several states.
 ** Service territory extends to other states.

TABLE 2-7
(Sheet 2 of 5)

<u>Western States Coordinating Council</u>		<u>Total State Capacity (estimated)</u>	<u>Total Capacity Reported by Utilities Listed</u>	<u>Percentage[†] of State Capacity in Utilities Examined</u>
Utah	Utah Power and Light Co. **	1.6	2.3 ²	
Arizona	Arizona Public Service Co. ** Tucson Gas and Electric Co. Salt River Project			
	Total	8.7	6.8	
Colorado	Public Service Co. of Colorado **	4.7 ³	2.6	
New Mexico	Public Service Co. of New Mexico	4.5 ⁴	0.9	
Montana	Montana Power Co.	3.1 ⁵	1.1	
Idaho	Idaho Power Co. **	1.8	1.8 ⁶	
Wyoming	Pacific Power and Light Co., Wyoming portion only	3.3 ⁵	1.8	
	Total of above states and utilities	93.3	72.4	77.6%
<u>Electric Reliability Council of Texas</u>				
Texas	Central Power & Light Co. (Central & Southwest Corp.) Community Public Service Co. Dallas Power and Light Co. (Texas Utilities) El Paso Electric Co. **			

† Ibid.
** Ibid.

TABLE 2-7
(Sheet 3 of 5)

<u>Electric Reliability Council of Texas (contd)</u>		<u>Total State Capacity (estimated)</u>	<u>Total Capacity Reported by Utilities Listed</u>	<u>Percentage^f of State Capacity in Utilities Examined</u>
	Gulf States Utilities ^{**}			
	Houston Lighting & Power Co.			
	San Antonio Public Service Board ^{**}			
	Southwestern Public Service Co.			
	Texas Electric Service Co. (Texas Utilities)			
	Texas Power and Light Co. (Texas Utilities)			
	West Texas Utilities (Central and Southwest)			
	Total for above states and utilities	46.0	42.0	91.3%
<u>Mid-Atlantic Area Council</u>				
Dakota	Montana-Dakota Utility Co. ^{**}			
	Otter Tail Power Co. ^{**}			
	Total	2.1 ⁵	0.9	
Dakota	Black Hills Power & Light Co. ^{**}			
	Northwestern Public Service Co.			
	Total	2.2 ⁵	0.4	
Minnesota	Minnesota Power & Light Co. ^{**}			
	Northern States Power Co. ^{**}			
	Total	8.2	7.1	

^f Ibid.

^{**} Ibid.

TABLE 2-7
(Sheet 4 of 5)

Mid-Atlantic Area Council (concluded)		Total State Capacity (estimated)	Total Capacity Reported by Utilities Listed	Percentage [†] of State Capacity in Utilities Examined
Nebraska	Nebraska Public Power District Omaha Public Power District			
	Total	3.9	2.9	
Iowa	Interstate Power Co. ** Iowa Electric Light & Power Iowa-Illinois Gas & Electric Iowa Power & Light Co. Iowa Public Service Co. Iowa Southern Utilities			
	Total	<u>6.2</u>	<u>5.0</u>	
	Total of above state and utilities	22.6	16.3	72.1%
<hr/> Southwest Power Pool <hr/>				
Kansas	Kansas Gas & Electric Co. Kansas Power & Light Co.			
	Total	6.8 ⁷	3.5	
Oklahoma	Oklahoma Gas & Electric Co. Public Service Co. of Oklahoma (Central and Southwest Corp.)			
	Total	9.2	6.9	

† Ibid.

** Ibid.

TABLE 2-7
(Sheet 5 of 5)

<u>Southwest Power Pool (concluded)</u>		<u>Total State Capacity (estimated)</u>	<u>Total Capacity Reported by Utilities Listed</u>	<u>Percentage[†] of State Capacity in Utilities Examined</u>
Missouri	Empire District Electric Co. ** Kansas City Power & Light Co. ** Missouri Public Service Co. Union Electric Co.			
	Total	13.4	11.7	
Arkansas	Arkansas Power & Light Co. (Middle South Utilities)	4.8	3.3	
Louisiana	Central Louisiana Electric Co., Inc. (Middle South Utilities) Louisiana Power & Light Co. (Middle South Utilities) New Orleans Public Service Co. (Middle South Utilities) ** Southwestern Electric Power Co. ** (Central and Southwest Corp.)			
	Total	<u>12.9</u>	<u>9.6</u>	
	Total of above states and utilities	47.1	35.0	74.3%

† Ibid.

** Ibid.

NOTES TO TABLE 2-7

- 1 Large amounts of power are owned by the federal government and out-of-state utilities.
- 2 Utility also supplies Wyoming and Idaho.
- 3 Capacity includes a large number of federal, municipal, and cooperative installations.
- 4 The majority of capacity is owned by utilities that have been listed within the WSCC.
- 5 State capacity includes equipment owned by utilities in adjacent states. Those utilities have been included in this study.
- 6 Utility also supplies Nevada and Oregon.
- 7 The state capacity includes various small municipal and cooperative installations.

TABLE 2-8

PROJECTED ADDITIONAL BASE LOAD CAPACITY REQUIREMENTS AND
POTENTIAL MARKETS FOR GENERATING EQUIPMENT, WESTERN UNITED STATES
1987-1989 and 1990-2001, GW

	Additional Needed Capacity			Markets	
	1986	1989	2001	1987-1989	1990-2001
<u>Western States Coordinating Council</u>					
Arizona	S	S	S	0	0
California	6.1	6.5	19.8	0.4	13.3
Colorado	S	S	0.6	0	0.6
Idaho	S	S	S	0	0
Montana	0	0.1	0.9	0.1	0.8
Nevada	S	S	S	0	0
New Mexico	S	S	S	0	0
Oregon	S	S	S	0	0
Utah	S	S	S	0	0
Washington	S	S	S	0	0
Wyoming	S	S	S	0	0
Pooled	S	S	5.0	0	5.0
Sum of States	6.1	6.6	21.3	0.5	14.7
<u>Electric Reliability Council of Texas</u>					
Texas	S	1.7	27.7	1.7	26.0
Pooled	S	1.7	27.7	1.7	26.0
<u>Mid-Atlantic Area Council</u>					
Iowa	0.1	S	0.5	0	0.5
Minnesota	S	S	S	0	0
Nebraska	S	S	S	0	0
North Dakota	0.3	0.3	0.9	0	0.6
South Dakota	0.1	0.2	0.4	0.1	0.2
Pooled	S	S	S	0	0
Sum of States	0.5	0.5	1.8	0.1*	1.3
<u>Southwest Power Pool</u>					
Arkansas	S	S	2.7	0	2.7
Kansas	S	S	S	0	0
Louisiana	S	S	6.8	0	6.8
Missouri	S	S	0.2	0	0.2
Oklahoma	S	S	1.3	0	1.3
Pooled	S	S	10.8	0	10.8
Sum of States	S	S	21.8	0	11.0
Total Western United States (Pooled)				1.7	41.8
Total Western United States (Individual States)				2.3	53.0

S = Surplus, no additional units needed.

* Difference caused by change from deficit to surplus in Iowa between 1986-1989.

TABLE 2-9

PROJECTED ADDITIONAL INTERMEDIATE LEVEL CAPACITY REQUIREMENTS
AND POTENTIAL MARKETS, WESTERN UNITED STATES
1987-1989 and 1990-2001, GW

	Additional Needed Capacity			Markets	
	1986	1989	2001	1987-1989	1990-2001
<u>Western States Coordinating Council</u>					
Arizona	S	0	2.5	0	2.5
California	3.2	6.6	21.9	3.4	15.3
Colorado	S	S	1.1	0	1.1
Idaho	S	S	S	0	0
Montana	S	S	S	0	0
Nevada	S	S	0.7	0	0.7
New Mexico	0.3	0.4	0.5	0.1	0.1
Oregon	3.3	4.8	7.6	1.5	2.8
Utah	0.2	0.4	1.3	0.2	0.9
Washington	5.0	5.5	8.1	0.5	2.6
Wyoming	S	S	S	0	0
Pooled	9.7	16.5	43.1	7.8	26.6
Sum of States	12.0	17.7	43.7	5.7	26.0
<u>Electric Reliability Council of Texas</u>					
Texas	12.7	16.6	34.2	3.9	17.6
Pooled	12.7	16.6	34.2	3.9	17.6
<u>Mid-Atlantic Area Council</u>					
Iowa	1.6	1.6	2.6	> 0.1*	1.0*
Minnesota	1.8	2.2	3.5	0.5*	1.2*
Nebraska	0.6	0.7	1.9	0.1	1.1*
North Dakota	0.2	0.3	0.8	0.1	0.4*
South Dakota	0.2	0.2	0.4	> 0.1*	0.2
Pooled	4.3*	5.1*	9.1*	0.8*	4.0
Sum of States	4.4*	5.0*	9.2*	0.7*	4.0
<u>Southwest Power Pool</u>					
Arkansas	1.5	2.0	3.9	0.5	1.9
Kansas	0.3	0.3	1.0	0	0.7
Louisiana	2.2	3.5	8.5	1.3	5.0
Missouri	3.0	3.4	5.5	0.4	2.1
Oklahoma	1.7	2.6	6.1	0.9	3.5
Pooled	8.8*	11.8	25.0	3.1	13.2
Sum of States	8.7*	11.8	25.0	3.1	13.2
Total Western United States (Pooled)				14.6	61.4
Total Western United States (Individual States)				12.9	60.8

* Differences due to rounding.

S = Surplus, no additional units needed.

The single exception is in the Western Systems Coordinating Council (WSCC). This power pool will have surplus base load unit capacity in 1986 and 1989 (21.5 and 23.7 GW, respectively). The Bonneville Power Administration (BPA) manages power produced by several government agencies. If BPA could change its supply contracts, some of the 13.2 GW of BPA managed hydroelectric capacity could be shifted to cover intermediate power demands. This would relieve at least some of the estimated deficits of 9.7 and 16.5 GW capacity in 1986 and 1989, respectively. This would have the effect of deferring purchase of units until sometime after 1990 and of increasing the intermediate power unit market in the WSCC region from 26.6 to perhaps as much as 35 GW for the period 1990-2001.

Perfect pooling is unlikely. An approximation of the effect of imperfect pooling was obtained by considering state pooling rather than regional pooling. The effect is marked but not overwhelming. The potential market increase is 11.8 GW for base and 2.8 GW for intermediate load capacity. Like deferred retirement of generating units or purchase of power from others, pooling has the effect of deferring purchases by the individual utilities. The more the pooling, the later the demand for new capacity arises. There are substantial planned surpluses in several regions at present, especially for baseload units, because large baseload units must be planned or ordered well before need (up to 15 years for a large nuclear unit), and utilities until 1973-74 were operating on historical growth rates of 6 to 8%. As noted earlier, SRI demand forecasts assume 5.3% annual growth to 1985 and 3.8% until year 2000.

The difference in 1990 capacity requirements under an 8% growth assumption and the SRI lower growths is ~50%.

Given the assumptions above and with no deferral of equipment purchase, the projected need for installed additional electric generating capacity in 1986=89 and 1990-2001 is shown in Table 2-10.*

*Some of the near-term, recorded capacity surpluses are diminishing as utilities defer construction because of cash flow and capital market pressures. Any deferred effects on the market are likely to be felt before 1990.

TABLE 2-10

SUMMARY OF MARKETS FOR NEW GENERATING CAPACITY
WESTERN UNITED STATES, GW
(Normal Retirement)

<u>Western States Coordinating Council</u>	<u>1987-1989</u>		<u>1990-2001</u>	
	<u>Base</u>	<u>Intermediate</u>	<u>Base</u>	<u>Intermediate</u>
By state	0.5	5.7	14.7	26.0
By pool	0	7.8	5.0	26.6
<u>Electric Reliability Council of Texas</u>				
	1.7	3.9	26.0	17.6
<u>Mid-Atlantic Area Council</u>				
By state	0.1*	0.7*	1.3	4.0
By pool	0*	0.8*	0	4.0
<u>Southwest Power Pool</u>				
By state	0	3.1	11.0	13.2
By pool	0	3.1	10.8	13.2
Total by states	2.3	13.4	53.0	60.8
Total by pool	1.7	15.6	41.8	61.4

* Differences because of rounding.

Additional generating capacity would be needed if all oil and gas (except) peaking units were retired. Such a retirement could call for repowering with hybrid fossil-solar heating units replacing the oil and gas firing equipment and steam boilers but using the existing turbogenerators. In other, perhaps most, cases, complete new generating units would be required. The effect of such early retirement is shown in Tables 2-11 through 2-15. Tables 2-11 through 2-14 consider base and intermediate load requirements separately and for two time periods for retirement, before 1986 and after 1990. The overall effect is summarized in Table 2-15. Early retirement of existing plants will require replacement units be placed on-line before hybrid fossil-solar units are available. These plants will be relatively new and will not be retired in the time period (1987-2001) of first interest to this assessment. On the other hand, later retirement will create a market for new generating equipment in the time frame of concern. Retirements of existing oil- and gas-fired units (excepting those used for peaking service) after 1990 will create additional markets of ~20 GW for base load and 14 GW for intermediate load applications. Thus, the expected base load market will increase by 38 to 48%, and the intermediate load market will increase by 48 to 58% if all non-peaking oil and gas units were removed from service after 1990.

The markets analyzed in detail represent only about 40% of U.S. installed capacity but a much larger proportion of the market is likely to be available to hybrid fossil-solar units. As indicated in Figure 2-1, unfavorable insolation regions are more prevalent in the eastern United States, and the higher hybrid unit power costs (shown in Sections 2.3 and 2.4) will result in smaller market shares.

As indicated, SRI has not examined every utility in detail. In general, the ones not examined were small and publicly owned. These utilities are more likely to purchase electricity, and their demand has been covered partly in the reported sales of major utilities. Also, they will have preferential access to federal and state produced electricity. Finally, they are usually too small to require units as large as 100 MW or to venture into new technology. For these reasons, we project that, although the excluded utilities represent about 25% of the total capacity in the western United States, the additional market they represent is no more than 10% of the western U.S. markets. The markets without and with these small utilities are shown in Tables 2-16 and 2-17, respectively.

TABLE 2-11

COMPARISON OF NORMAL AND EXPANDED MARKETS DUE TO RETIREMENT OF
ALL OIL AND GAS BEFORE 1986 FOR BASE LOAD GENERATING EQUIPMENT, WESTERN UNITED STATES
1987-1989 AND 1990-2001, GW

Western States Coordinating Council	Markets					
	Normal		Expanded		Difference	
	1987-1989	1990-2001	1987-1989	1990-2001	1987-1989	1990-2001
Pooled	0	5.0	0	10.9	0	5.9
Sum of states	0.5	14.7	0.1	13.8	0.4	-0.9
<u>Electric Reliability Council of Texas</u>						
Pooled	1.7	26.0	2.3	19.4	0.6	-6.6
<u>Mid-Atlantic Area Council</u>						
Pooled	0	0	0	0	0	0
Sum of states	0.1	1.3	0.2	1.5	0.1	0.2
<u>Southwest Power Pool</u>						
Pooled	0	10.8	0.7	14.9	0.7	4.1
Sum of states	0	11.0	1.8	10.8	1.8	-0.2
Total western U.S. (pooled)	1.7	41.8	3.0	45.2	1.3	3.4
Total western U.S. (individual states)	2.3	53.0	4.4	45.5	2.1	-7.5

TABLE 2-12

COMPARISON OF NORMAL AND EXPANDED MARKETS DUE TO RETIREMENT OF
REMAINING OIL AND GAS AFTER 1990 FOR BASE LOAD GENERATING EQUIPMENT, WESTERN UNITED STATES
1987-1989 AND 1990-2001, GW

Western States Coordinating Council	Markets					
	Normal		Expanded		Difference	
	1987-1989	1990-2001	1987-1989	1990-2001	1987-1989	1990-2001
Pooled	0	5.0	0	10.9	0	5.9
Sum of states	0.5	14.7	0.5	20.9	0	6.2
<u>Electric Reliability Council of Texas</u>						
Pooled	1.7	26.0	1.7	34.8	0	8.8
<u>Mid-Atlantic Area Council</u>						
Pooled	0	0	0	0	0	0
Sum of states	0.1	1.3	0.2	1.5	0.1	0.2
<u>Southwest Power Pool</u>						
Pooled	0	10.8	0	15.7	0	4.9
Sum of states	0	11.0	0	15.9	0	4.9
Total western U.S. (pooled)	1.7	41.8	1.7	61.4	0	19.6
Total western U.S. (individual states)	2.3	53.0	2.4	73.1	0.1	20.1

TABLE 2-13

COMPARISON OF NORMAL AND EXPANDED MARKETS DUE TO RETIREMENT OF
ALL OIL AND GAS BEFORE 1986 FOR INTERMEDIATE LOAD GENERATING EQUIPMENT, WESTERN UNITED STATES
1987-1989 AND 1990-2001, GW

Western States Coordinating Council	Markets					
	Normal		Expanded		Difference	
	1987-1989	1990-2001	1987-1989	1990-2001	1987-1989	1990-2001
Pooled	7.8	26.6	5.0	19.5	-2.8	-7.1
Sum of states	5.7	26.0	4.5	20.3	-1.2	-5.7
<u>Electric Reliability Council of Texas</u>						
Pooled	3.9	17.6	3.7	12.0	-0.2	-5.6
<u>Mid-Atlantic Area Council</u>						
Pooled	0.8	4.0	0.8	3.8	0	-0.2
Sum of states	0.7	4.0	0.8	3.8	0.1	-0.2
<u>Southwest Power Pool</u>						
Pooled	3.1	13.2	2.3	9.8	-0.8	-3.4
Sum of states	3.1	13.2	2.3	9.8	-0.8	-3.4
Total western U.S. (pooled)	14.6	61.4	11.8	45.1	-2.8	-16.3
Total western U.S. (individual states)	12.9	60.8	11.3	45.9	-1.6	-14.9

TABLE 2-14

COMPARISON OF NORMAL AND EXPANDED MARKETS DUE TO RETIREMENT OF
REMAINING OIL AND GAS AFTER 1990 FOR INTERMEDIATE LOAD GENERATING EQUIPMENT, WESTERN UNITED STATES
1987-1989 AND 1990-2001, GW

	Markets					
	Normal		Expanded		Difference	
	1987-1989	1990-2001	1987-1989	1990-2001	1987-1989	1990-2001
<u>Western States Coordinating Council</u>						
Pooled	7.8	26.6	6.8	32.9	-1.0	6.3
Sum of states	5.7	26.0	5.7	32.3	0	6.3
<u>Electric Reliability Council of Texas</u>						
Pooled	3.9	17.6	3.9	23.1	0	5.5
<u>Mid-Atlantic Area Council</u>						
Pooled	0.8	4.0	0.8	4.1	0	0.1
Sum of states	0.7	4.0	0.8	4.1	0.1	0.1
<u>Southwest Power Pool</u>						
Pooled	3.1	13.2	3.2	15.1	0.1	1.9
Sum of states	3.1	13.2	3.2	15.1	0.1	1.9
Total western U.S. (pooled)	14.6	61.4	14.7	75.2	0.1	13.8
Total western U.S. (individual states)	12.9	60.8	13.6	74.6	0.7	13.8

TABLE 2-15

EFFECT OF TIME OF CHANGEOVER FROM OIL AND GAS TO
COAL/SOLAR SYSTEMS ON MARKET SIZE

	Change			
	Before 1986		After 1990	
	Base Load	Intermediate Load	Base Load	Intermediate Load
<u>Western States</u>				
Pooled States	+5.9	-7.1	5.9	6.3
	-0.9	-5.7	6.2	6.3
<u>Electric Reliability Council of Texas</u>				
Pooled States	-6.6	-5.6	8.8	5.5
	-6.6	-5.6	8.8	5.5
<u>Mid-Atlantic Area Council</u>				
Pooled States	0	-0.2	0	0.1
	+0.2	-0.2	0.2	0.1
<u>Southwest Power Pool</u>				
Pooled States	4.1	-3.4	4.9	1.9
	-0.2	-3.4	4.9	1.9
<u>Total Western U.S.</u>				
Pooled Individual states	3.4	-16.3	19.6	13.8
	-7.5	-14.9	20.1	13.8

Extension of the total market estimates from the western region to the remainder of the United States was by approximation only. As will be shown below, the market share projected for hybrid solar units in regions with insolation of 4.5 kWh/m^2 day or less is very small, and thus the accurate estimation of market size is of little consequence.

As a first approximation, the growth in demand for electricity (and for new capacity will proceed at the same rate over the eastern and western U.S. The current and near-term projected sales (capacity) for the regions is in the ratio 60/40. Using this ratio and the data of Table 2-17, we estimate total U.S. markets as shown in Table 2-18. The actual markets will be limited by economic and other factors. These are discussed briefly in Section 6. Also to be discussed are the rates of market penetration to be expected.

2.5.3 Unit Size

A potentially important factor that could influence the economics of hybrid fossil-solar units and therefore the market share of the concept is the unit size. Larger units should be more economic and gain a larger share of the total available market set out above.

An analysis was made of the 61 electric utility systems used to establish the total available market in the western U.S. to see if there were limitations on plant size. As shown in Table 2-19, only five utility systems with 3-GW capacity (8% of total number and about 1.5% of expected capacity in 1989) would not be able to use units as large as 100 MW. Twelve representing 66% of the expected capacity could use even larger units. A 300-MWe unit design would be suitable for ~80% of all utility systems. A standard design plant of 300 to 400 MW would fit well with the market requirements. Final design units were 430 and 615 MW.

TABLE 2-16

SUMMARY OF DEMAND FOR NEW ELECTRIC
GENERATING CAPACITY, WESTERN UNITED STATES
1990-2001, BASED ON SPECIFIC UTILITIES ONLY (GW) *

	<u>Base Load</u>	<u>Intermediate Load</u>
Normal retirement only	42-53	61-61
Normal retirement, with 1987-89 needs added	44-55	74-77
Forced retirement with 1990-2001 needs only	61-73	75

* Data rounded to nearest GW.

TABLE 2-17

SUMMARY OF DEMAND FOR NEW ELECTRIC GENERATING
CAPACITY FOR ENTIRE WESTERN UNITED STATES †
1990-2001 (GW)

	<u>Base Load</u>	<u>Intermediate Load</u>	<u>Total</u>
Normal retirement	46-58	67-69	113-127
Normal retirement with 1986-98 needs added	48-61	82-85	130-146
Forced retirement with 1990-2001 needs only	67-80	82-83	149-163

† Also includes Louisiana.

TABLE 2-18

SUMMARY OF DEMAND FOR NEW ELECTRIC GENERATING
CAPACITY FOR THE UNITED STATES (GW)

	<u>Western U.S.</u>		<u>Eastern U.S.</u>		<u>Total U.S.</u>	
	<u>Baseload</u>	<u>Intermediate</u>	<u>Baseload</u>	<u>Intermediate</u>	<u>Baseload</u>	<u>Intermediate</u>
Normal retirement	46-58	67-69	69-87	100-105	115-145	167-173
Normal retirement with 1986-89 needs added	48-61	82-85	72-92	123-128	120-153	205-213
Forced retirement with 1990-2001 needs only	67-80	82-83	100-120	150-180	167-200	232-273

TABLE 2-19

UTILITY SYSTEMS WITH LIMITED CAPACITY TO
ACCEPT HYBRID-FOSSIL-SOLAR UNITS OF SPECIFIED SIZES

<u>Size of Acceptable Unit (MW)</u>	<u>Number of Systems</u>	<u>Total Systems' Capacity (Rounded) (GW)</u>
100	5	3
100-199	12	18
200-299	12	25
300-399	9	29

Unit should be no more than 20 percent of total capacity or one-third of intermediate load capacity.

3.0 PARAMETRIC ANALYSIS

SUMMARY

For the Receiver Subsystem, a trade study comparing parallel vs series arrangement for receiver and fossil-fired sodium heater resulted in the selection of the parallel configuration for the conceptual design. Based on previous work for the ACR design study, an external receiver with many small diameter vertical tubes cooled by upward flowing sodium was selected as the preferred configuration. For the 0.8 SM concept, the cold and hot buffer tanks, were mounted on top of the receiver tower, to provide thermal protection for the receiver for the loss of receiver pump event and to buffer the steam generators for the cloud transient event. Tube orificing of the 0.8 SM receiver was investigated but was not considered feasible nor cost effective in the smaller receiver sizes. Several other trade studies were performed to determine the feasibility of varying the size of the receiver, insulating to reduce heat losses, and improving reliability by reducing the number of receiver control valves. These changes were not cost effective for the 100 MWe plants.

Thermal performance and structural analysis of the receiver showed that the design of a structurally adequate receiver appeared feasible. Tower analysis results are presented showing tower column and mat dimensions.

A trade study to size the riser/downcomer piping resulted in the selection of 51 cm (20 in.) pipe for both riser and downcomer for the 0.8 SM plant design. For the 1.4 SM case however, the riser pipe size selected was 61 cm (24 in.) and the downcomer pipe size was 30.5 cm (12 in.). The hockey stick configuration was selected for the steam generator based on ESG experience with these units - pumps, valves and piping were selected, based on previous operating experience with these components in sodium systems.

Three storage concepts were examined for the 0.8 SM plant. The tower level, low pressure hot and cold tank thermal buffer system was adopted for this plant. For the 1.4 SM plant, the ACR all sodium storage system concept was adopted. Details of the alternative concepts are presented and compared. Storage size, storage media, containment and steam system materials selection are some of the topics covered in this section. Thermal performance analysis for the 0.8 SM hot

and cold buffer tanks is reviewed. More details are given in Appendix A. Containment vessel structural analysis is briefly discussed. The methods for ullage maintenance analysis and fluid maintenance analysis are described. Pumps, piping and valve analysis have been previously covered in the receiver subsystem.

The EPGS concept considered for parametric analysis was limited to the steam Rankine cycle utilizing a reheat steam turbine. Seventeen steam cycles were analyzed and the most cost effective steam cycle was determined to be the 1815 psia, 1000^oF/1000^oF, single reheat cycle with heater ahead of reheat point (HARP). This cycle was selected for both 0.8 SM and 1.4 SM hybrid plants.

The following section reports on the component level studies which were done during conceptual design.

3.1 INTRODUCTION

Parametric analyses of the major subsystems, consisting of the Collector, Receiver, Storage, Non-solar; Electric Power Generation, and Master Control Subsystems were conducted over a wide range of independent parameters in order to define subsystem operation and interfaces for use in the preferred system selection studies. A reference baseline system configuration was established, based on the ACR study described in Reference 3-1, and subsystems trade studies and parametric analyses were developed in the context of this baseline system.

Following is a detailed discussion of the parametric analyses conducted for each of the major subsystems.

3.2 COLLECTOR SUBSYSTEM (SOLAR SYSTEM OPTIMIZATION)

An analysis was made to define the most cost effective collector field and receiver combinations over a wide range of peak powers to allow the selection of solar subsystem sizes and identify their associated costs and performance of any of several design points. These data were then used along with the balance of plant data to select discrete operating points for the solar hybrid power plant.

By way of introduction, Table 3-1 lists the parameters that influence field optimization.

Tower, receiver, and field size are each influenced by numerous factors. For example, restricted or expensive land favors a taller tower so blocking will be reduced and heliostats can be packed more densely. Simultaneously, it favors a smaller field (compared to a baseline system) because the peripheral heliostats use ground inefficiently. In contrast, cheap land favors a larger field, limited primarily by beam spillage and atmospheric attenuation; the heliostats can be distributed sparsely, as required by the necessity to eliminate blocking. A larger field may allow the required power level to be reached with a shorter tower.

The chart should be used with some wisdom to distinguish between factors favoring smaller systems versus those favoring a smaller tower, or receiver or field irrespective of system size.

The last item, high cost competition, for example, should really be applied to smaller systems, as competition at 100 MWE may be a diesel at 10 ¢/KW hr, compared to a coal plant at 2 ¢/KW hr for a 500 MWe system.

3.2.1 Field Design (Optimization Model) Input Data

The input data required to perform the field optimization falls into two categories: cost and performance.

The assumed cost factors or pertinent algorithms are listed in Table 3-2. The bases for these costs in 1978 dollars were the final optimization costs.

TABLE 3-1
FACTORS INFLUENCING FIELD OPTIMIZATION

FAVORS LARGER TOWERS

- o LARGE FIXED COST
- o TOWER COST SUB QUADRATIC
- o RESTRICTED OR EXPENSIVE LAND

FAVORS LARGER RECEIVERS

- o LOW RECEIVER COST/M²
- o LOW RECEIVER LOSSES/M²
- o LARGE FLAT HELIOSTAT
- o SEVERE ABERRATIONS
- o LARGE BEAM SPREAD

FAVORS LARGER FIELD

- o EXPENSIVE RECEIVER SS
- o CHEAP HELIOSTATS
- o CHEAP LAND AND WIRE
- o LOW ATMOSPHERIC ATTENUATION

FAVORS SMALLER TOWERS

- o ZERO FIXED COST
- o TOWER COST SUPER QUADRATIC
- o LARGE BEAM SPREAD

FAVORS SMALLER RECEIVERS

- o HIGH RECEIVER COST/M²
- o HIGH RECEIVER LOSSES/M²
- o HIGH PERFORMANCE HELIOSTAT
- o SMALLER HELIOSTAT

FAVORS SMALLER FIELDS

- o EXPENSIVE HELIOSTATS
- o CHEAP RECEIVER SS
- o EXPENSIVE LAND OR WIRE
- o HIGH ATMOSPHERIC ATTENUATION
- o RESTRICTED AREA
- o HIGH COST COMPETITION

TABLE 3-2

COMPONENT DEPENDENT COST MODELS

(Sheet 1 of 2)

(NOTE)

FIXED*	\$4.39 M	CONSTANT BASED ON WATER/STEAM STUDY
HELIOSTAT*	\$71.96/m ²	EXCLUDING LAND AND WIRING INCLUDING NONHELIOSTAT LOCATION DEPENDANT O&M
LAND* (HELIOSTAT FIELD)	\$1.45/m ²	\$5,871/ACRE - INCLUDING ROUGH SITE PREP.
LAND* (CENTRAL AREA)	\$28.67/H ²	H = RECEIVER CENTERLINE ELEVATION (m)
WIRING, } TRENCHING, } ELECT. DIST., }	{ .0412 R { .04237 ΔR { 4.72 Δaz	COST PER HELIOSTAT R = DISTANCE FROM TOWER TO COMPUTATIONAL CELL (m) ΔR = RADIAL SPACING IN CELL (m)
LOC: DEP* O&M	8.525 Δaz	Δaz = AZIMUTHAL SPACING IN CELL (DISTANCES IN m)
SODIUM PUMP	40.7 P (H + 66 m)	COST OF APPROXIMATELY \$1000/HP P = ABSORBED POWER (MW)

*CHANGED OR ADDED SINCE ADVANCED CENTRAL RECEIVER (ACR) STUDY

TABLE 3-2
 COMPONENT DEPENDENT COST MODELS
 (Sheet 2 of 2)

RECEIVER*

$$\$6.0 \text{ M} \left(\frac{D}{16.1} \right)^{.6} \left(\frac{L}{16.1} \right)^{.2}$$

L = RECEIVER LENGTH (m)

D = RECEIVER DIAMETER (m)

TOWER

$$\text{COST} = \$109 (\text{FL} - 22\text{m})^{2.1}$$

FL = REC EQUATOR ELEV
 ABOVE GRADE - 4m

BASED ON WATER/STEAM STUDY

PIPING NETWORK

PIPING

55 · D (IN.)

\$/FT (STAINLESS STEEL)

30 · D (IN.)

\$/FT (CARBON STEEL)

VALVES

\$2,000 · D (IN.)

6" - 17" VALVES

\$3,000 · D (IN.)

17" - 24" VALVES

EXPANSION
 AND BENDS

X (1.5)

ADJUSTMENT TO PIPE LENGTH

VERTICAL FACTOR

5% INCREASE PER 60 FEET

M = 10⁶

ESG-79-30, Vol I, Book 1
72

*CHANGED OR ADDED SINCE ADVANCED CENTRAL RECEIVER (ACR) STUDY

used in the Advanced Central Receiver (ACR) Study Phase I. The costs were reviewed in light of recent work on other studies, and those costs marked with an asterisk were changed, or added, such as the cost of location-dependent heliostat operations and maintenance (O&M). Recent analyses showed that the previous value used for heliostat cost in the ACR study ($\$65.67/\text{m}^2$) could be reduced to $\$60.12/\text{m}^2$. This value excludes the cost of wiring, trenching, and electrical distribution which is accounted for elsewhere. The previous cost also did not include heliostat O&M present values, amounting to $\$11.84/\text{m}^2$. The derivation of the O&M costs is given in Section 3.2.3. This value does not include heliostat location-dependent O&M costs accounted for elsewhere. This cost is primarily associated with the labor involved in cleaning the heliostat, a cost that is directly related to the time to wash the heliostats and to move from heliostat to heliostat. The total distance travelled is related to the distance between heliostats, which is represented by the following:

Total distance = Σ azimuthal spacing + the distance from the tower to the farthest heliostat.

The first term is much larger than the second and, therefore, the cost per heliostat was defined as

Location-Dependent (Loc. Dep.) O&M Cost/Heliostat = $8.525 \Delta\text{Az}$,

where ΔAz is the azimuthal spacing between heliostats. The constant was derived by dividing the Loc. Dep. O&M cost/heliostat ($\$131$) by the average azimuthal spacing. The average spacing was determined by averaging the azimuthal spacing in the 100 MWe ACR field. This value was found to be 15.37 meters.

Table 3-3 shows a comparison of the elements of the fixed costs (independent of system size) used in the hybrid study with those used during the ACR study along with summary comments pertaining to the source of the change, which are discussed in more detail below.

Calibration equipment was originally (during ACR Study) an educated guess, later updated using a bottoms-up estimate of a newly defined Beam Characterization Subsystem.

TABLE 3-3
FIXED COST CHANGES

	<u>COST 10⁶ \$</u>		<u>NOTE</u>
	<u>ACR</u>	<u>HYB</u>	
CALIBRATION EQUIPMENT	.10	.17	BCS RE-EVALUATED
DESIGN AND SUPPORT ENGINEERING	1.74	1.84	INFLATION FACTOR (BASED ON PDR)*
MASTER CONTROL	1.78	.75	DOES NOT INCLUDE INTERFACE CONTROLLERS FOR VALUES AND MOTORS TO BE SUBCONTRACTOR DEFINED AND COSTED
INDIRECT A&E	1.35	1.43	INFLATION FACTOR (BASED ON PDR)
CONTINGENCY		.20	TO COVER UNCERTAINTY IN DIFFERENCES TO PDR
TOTAL		4.39	

*PDR - "Preliminary Design Report" SAN-1108-76-8
MDC - G6776, Oct. 77

Design and Support Engineering costs were originally based on the allocation of engineering costs from the PDR* and were inflated six percent to bring them up to date.

Master Control costs decreased considerably from the PDR (commercial) due to the fact that interface controllers for valves, motors, etc., are to be costed by the subsystem and not included in master control costs. Software costs were estimated by sizing against the PDR. Some learning was assumed.

Indirect A&E Services were originally estimated at 10 percent over the PDR Pilot Plant and inflated six percent to bring them up to date.

Other changes to the cost model are defined in Table 3-4. Land costs are estimated by realtors in the area at \$500 to 5,000/acre for desert land. The low side is for land that is inaccessible and without power lines, sewer drainage, etc. The higher priced land is improved, more easily accessible (roads already in), has utilities in close proximity, and is usually located fairly close to a populous area (i.e., Barstow).

The receiver cost algorithms were derived for this study using scaling factors for the receiver defined during the ACR study.

Performance models were based on optical losses associated with the heliostat including cosine, reflectivity, shadowing and blocking, atmospheric attenuation, and interception, and thermal loss models for the various receiver sizes and configurations. The thermal loss model assumed for the external receivers included consideration of surface absorption, radiation, and convection losses combined to equal 22.1 Mwt for a 16.15 m receiver (identical diameter and height). It was assumed that the loss is constant over all periods of energy collection and scales with surface area for smaller receivers.

3.2.2 Field Analysis (Optimization)

Initial Optimizations

Optimizations were done over a wide range of receiver focal heights, where focal height equals receiver centerline elevation -4 m (the height of the

*See footnote on Table 3-3.

TABLE 3-4
OTHER CHANGES TO COST MODEL

LAND COSTS:

RAW LAND, \$5000/ACRE = 1.24/M² LAND

RANGES FROM \$500 ± \$5000/ACRE DEPENDING ON PROXIMITY TO
URBAN DEVELOPMENT AND PRESENCE OF ROADS, RAIL, UTILITIES

YARDWORK: CENTRAL AREA = \$46,600/ACRE = \$11.52/M² LAND

HELIOSTAT FIELD = \$871/ACRE = \$0.21/M² LAND

HELIOSTAT LAND = \$1.24 + \$.21 = \$1.45/M² LAND

CENTRAL LAND = $\frac{(46,600 + 5,000) \text{ 8 ACRES}^*}{120 \text{ M X } 120 \text{ M}} = 28.67/H^2$ H = TOWER HEIGHT

RECEIVER COST: = $\$6 \times 10^6 \left(\frac{D}{16.1}\right)^{.6} \left(\frac{L}{16.1}\right)^{.2}$ BASED ON SCALING ACR RECEIVER

*BASED ON 8 ACRES FOR 120M TOWER AND $\frac{\text{RADIUS OF EXCLUSION CIRCLE}}{\text{TOWER HEIGHT}} = \text{CONSTANT}$

center of a heliostat above ground). This was done to obtain data over a corresponding range of peak power loads. For each focal height (hereafter referred to as "tower height"), a range of external cylindrical receiver sizes were investigated. Figure 3-1 shows the results of this analysis for a 240-m tower height. Each "parabolic" curve represents the output figure of merit versus design point power for a range of field size (i.e., trim lines) for a specific input figure of merit (FOM - system cost/annual thermal output in MWh, \$/annual MWht). A completely optimized system would have an input figure of merit equal to the output figure of merit achieved at the low power on the curve, e.g., on Figure 3-1 at 80.1 and 1040, the input figure of merit was 80.2, very close to convergence. By investigating a range of input conditions (receiver dimensions and input figure of merit), an envelope of achievable output figure of merits versus equinox noon power is obtained for each focal height (vertical distance from receiver centerline to the plane of the heliostat center points).

In Figure 3-1, we see that a 240 m focal height with a 16 acre central exclusion area leads to an equinox noon power output of 1000 MWt and a minimum figure of merit of 80.1 \$/annual MWht for a receiver about 25 m tall and 20 to 21 m in diameter.

In Figure 3-2, if the performance envelopes are plotted for each focal height considered, an envelope of envelopes is defined which is indicative of the performance which could be achieved if the optimum focal height were chosen for a desired equinox noon power and then the correct receiver size were selected. Note that at lower powers (< 500 MWt) this baseline design curve begins to rise and at 200 MWt it is very steep. Reasons for this rise will be discussed later. Because of this rising design curve, the smaller systems cannot be optimized in the usual way; the minimum of the "parabolic" design envelope does not represent the contact with the baseline design curve. Rather, this contact occurs on the low power side of the envelope where it defines the baseline design envelope.

The consequence of this rising baseline design curve is that the critical portion of the envelope for the smaller systems is not the bottom of the "parabola," but the left side, i.e., the area of contact. Consequently, the

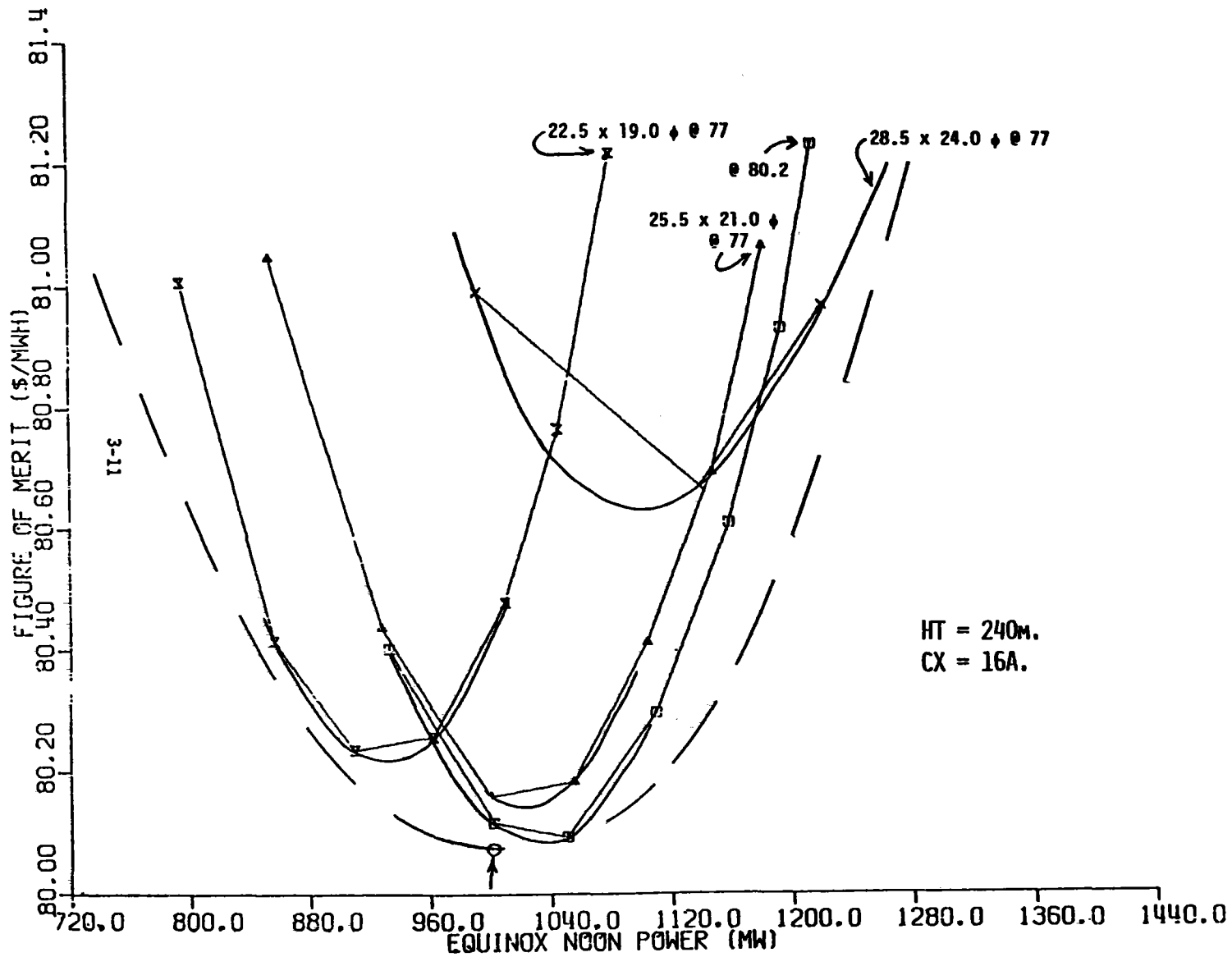


Figure 3-1. Optimization Envelope - 240 m Tower

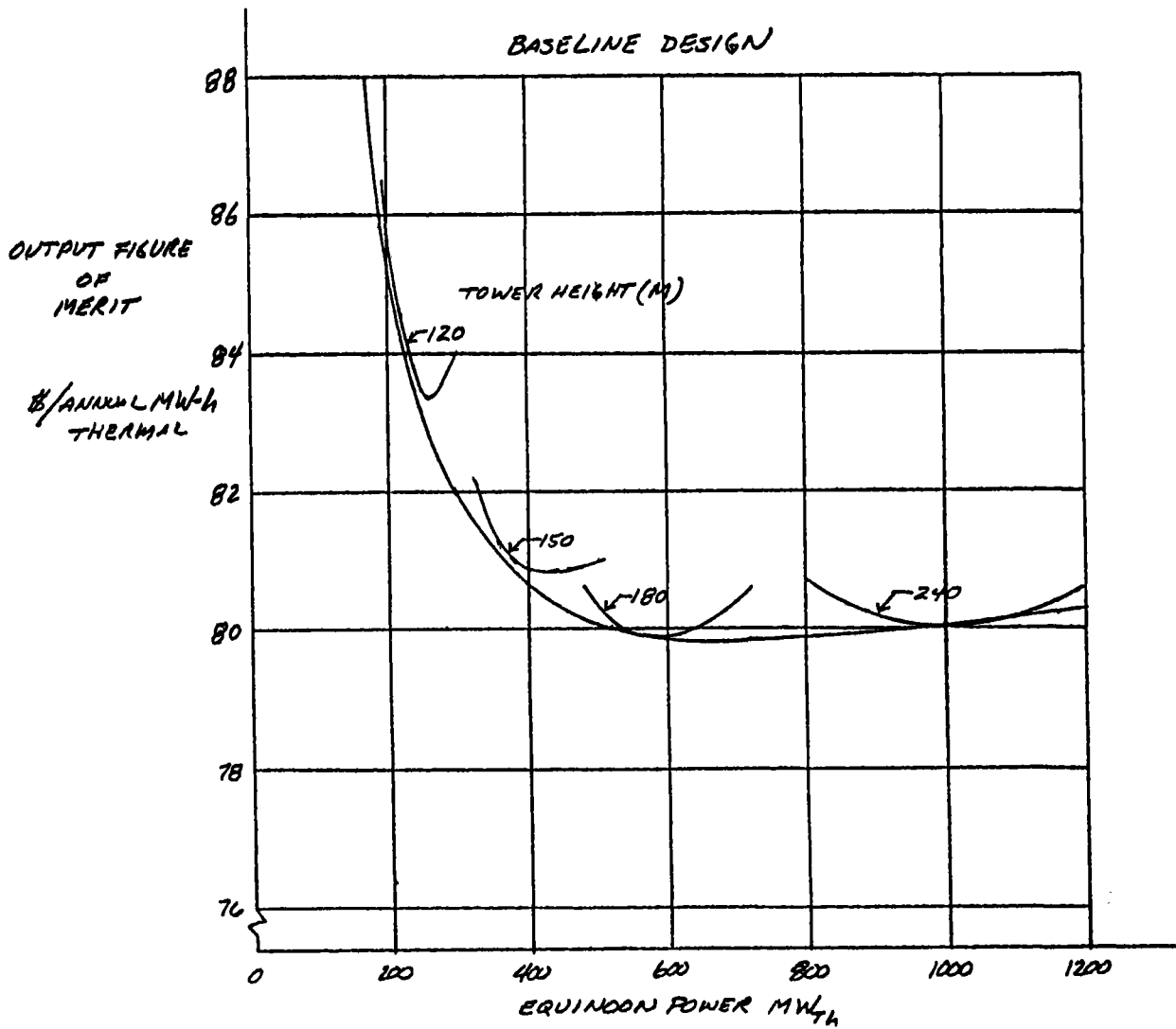


Figure 3-2. Optimization Envelopes for Different Focal Heights

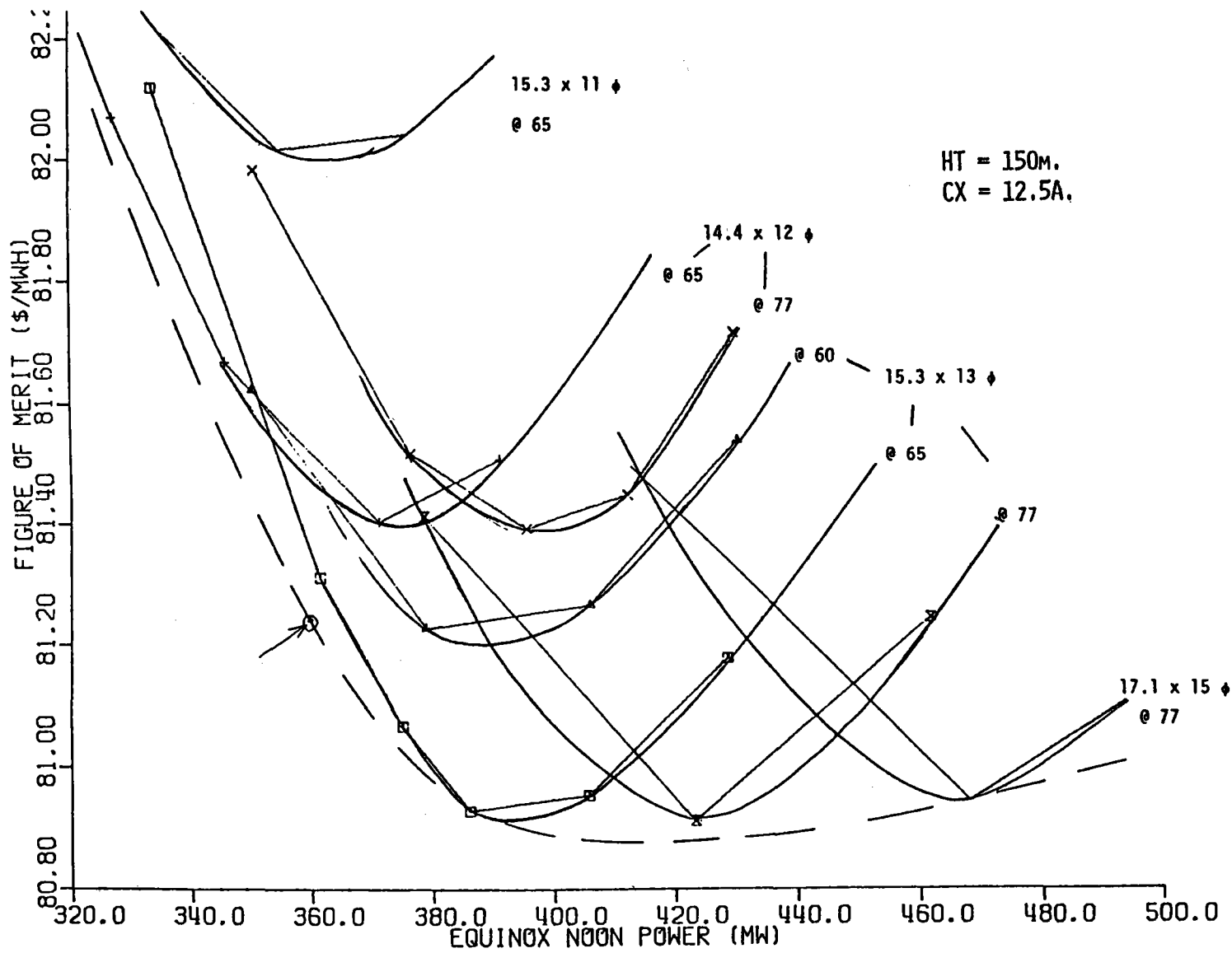


Figure 3-3. Optimization Envelopes for 150 m Tower

design data for the smaller systems concentrates on defining the left side of the "parabolas." This is accomplished most effectively by using an input figure of merit substantially less than the output, or converged, value. Thus, for the 150-m focal height case, shown in Figure 3-3, the definitive curves have an input figure of merit of 65 rather than 80. At 150 m, the exclusion area in the center of the field has been scaled to 12.5 acres and the optimum receiver would be about 15 m tall by 12.5 m in diameter. The contact point with the baseline design curve occurs at a figure of merit of 81.2 and an equinox noon power of 360 Mwt. In contrast, the lowest figure of merit for this focal height is 80.9 at 420 Mwt.

For a 120-m focal height, shown in Figure 3-4, the baseline design curve is rising so fast that the ordinate has been compressed 10 fold relative to the previous curves. With an 8-acre exclusion area, this system provides the required 208 Mwt (solar multiple = 0.8) essentially at the point of contact with the baseline design curve. An input figure of merit of 65 has been used to reduce the system size below the 260 Mwt achieved for an optimized system at this focal height.

Table 3-5 is an example of a performance summary page from the optimization runs representing the best constrained system providing the desired 208 Mwt at the equinox noon design point with an insolation of 950 W/m^2 . On the upper right is given the number of heliostats required, the total glass area and the total land area (the ratio gives an average glass density of 21.7%). The three matrices show the east half-field of the cellwise design. Each cell has an area of $5 H^2/4 = 18,000 \text{ m}^2$. The tower is centered in the cell marked with a zero in the middle of the leftmost column.

The "trim control" matrix (of 4's) shows the cell occupation number in quarters, three corresponding to a cell which lies 75 percent inside of the useful heliostat field. In the "limits" matrix, the 3's indicate cells in which mechanical limits have been active in defining the heliostat spacing (three refers to the diagonal neighbor).

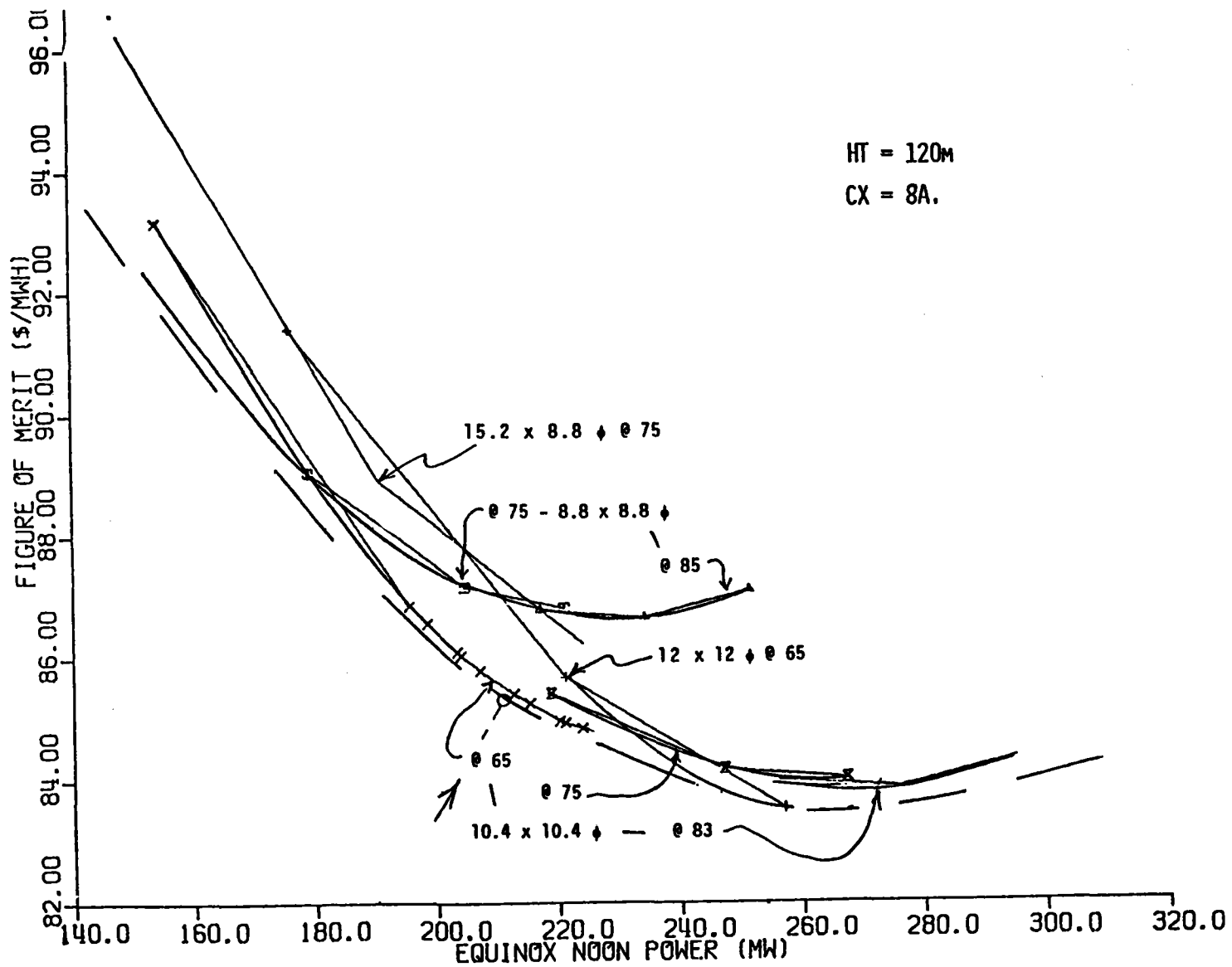


Figure 3-4. Optimization Envelope for 120 m Tower

TABLE 3-5
SAMPLE PERFORMANCE SUMMARY

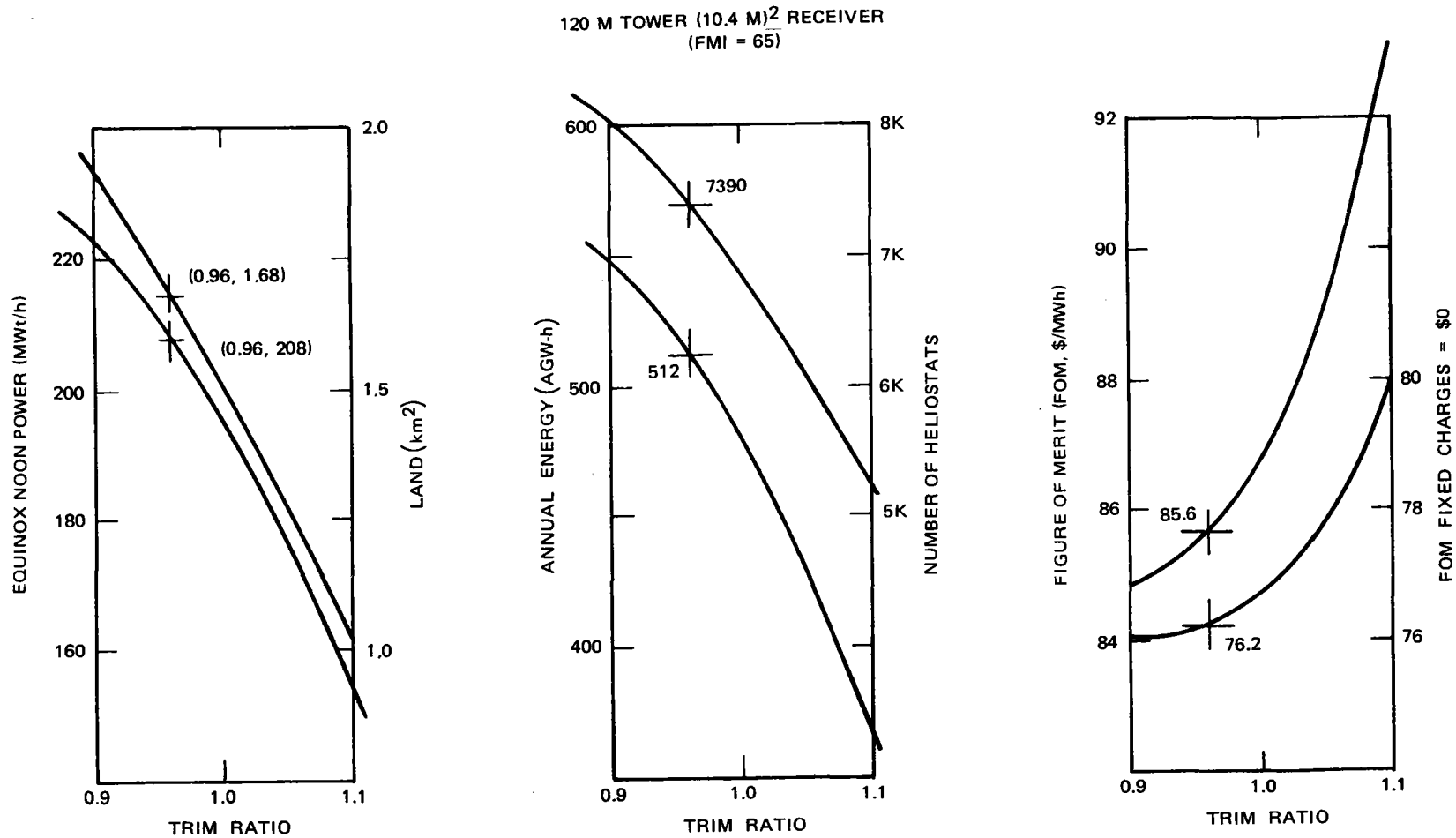
TRIM CONTROL	LIMITS				
00000000	00000000				
00000000	00000000				
44410000	00000000	MAX. NUMBER OF HELIOS./CELL=	367.0	:	HGLASS/DMIR**2 = 0.8963
44442000	00000000				
44444200	00000000				
44444400	00000000				
44444400	00000000				
34444400	33000000				
03444400	03000000				
44444300	33000000				: TOTAL GLASS = 0.35967E 06
44443000	00000000				: TOTAL LAND = 0.16560E 07
44420000	00000000				
11100000	00000000				
00000000	00000000				

***** NUMBER OF HELIOSTATS PER CELL***** ; HT = 120.0 METERS

0.	0.	0.	0.	0.	0.	0.	0.
0.	0.	0.	0.	0.	0.	0.	0.
46.6	91.9	86.9	19.9	0.	0.	0.	0.
57.6	112.4	105.8	95.9	42.2	0.	0.	0.
71.6	139.7	128.4	114.4	98.4	41.4	0.	0.
92.6	177.6	157.7	134.4	113.3	93.4	0.	0.
128.6	236.5	194.1	155.3	125.7	102.2	0.	0.
117.4	310.7	233.5	173.9	135.1	107.5	0.	0.
0.	233.6	252.4	180.4	138.0	108.5	0.	0.
156.8	321.9	229.1	170.6	132.1	78.1	0.	0.
125.3	226.6	183.1	146.3	88.3	0.	0.	0.
83.4	161.3	142.8	60.2	0.	0.	0.	0.
14.6	29.2	26.9	0.	0.	0.	0.	0.
0.	0.	0.	0.	0.	0.	0.	0.

PERFORMANCE SUMMARY AND COST BREAKDOWN FOR OPTIMIZED COLLECTOR FIELD - TRIM LINE AT 0.960

EQNOON POWER	=	218.903	207.068	IN MW - (SCALED TO 950 W/M2)
ANNUAL ENERGY	=	506.465	IN GWH	
FIXED COSTS	=	4.8030	IN \$M	
TOWER COST	=	9.1788	2.4388	4.2298 0.9428 1.5674 IN \$M FOR 950. EQUINOON F
LAND COST	=	2.4012	IN \$M	
WIRING COST	=	1.1786	IN \$M	
HELIOSTAT COST	=	20.7064	25.8821	31.0578 IN \$M
TOTAL COST	=	38.2680	43.4437	48.6194 IN \$M
FIGURE OF MERIT	=	75.559	85.778	95.998 IN \$/MWH , FOR AN INPUT OF 65.000 USING HELIOS



9315-20

Figure 3-5. Trim Control Vector

The "number of heliostats per cell" matrix represents a sum over the right and left half-fields, thus, although only the right half-field is depicted, the heliostat number is 7,332. Variations in heliostat packing across the field are obvious, although the heliostats in those cells with trim control numbers <4 (i.e., at the perimeter of the field) are packed into a fraction of a cell.

The performance summary shows first the equinox noon power delivered to sodium using the University of Houston's insolation model (about 1002 W/m^2) and then the Sandia dictated 950 W/m^2 . The annual energy is all collected when the sun is above 10° elevation. Monthly, the long term average values appropriate to the southwestern desert of cloud cover, turbidity and precipitable water are used in developing this estimate. The fixed costs include the cost of preparing the central exclusion area for construction. The tower cost gives first the total, then the costs of the tower, the receiver, the vertical plumbing and the riser pump. The land cost includes only the heliostat field. The wiring cost includes the present value of the O&M components associated with azimuthal spacing (Category 3). The heliostat cost is given for a baseline case and $\pm 20\%$. Thus, we are interested in the center column, where the "heliostat cost" is based on an area cost of $71.96 \text{ \$/m}^2$. This includes a capital cost of $60.12 \text{ \$/m}^2$ and O&M of $11.84 \text{ \$/m}^2$. The Figure of Merit is the output value, computed as the ratio of the Total Cost divided by the Annual Energy. The input figure of merit is listed to the right.

The extent of the heliostat field is defined by the trim control matrix which is set by the trim control to include those cells with a trim ratio greater than that defined by the "trim line," given as 0.960 in this case. The trim line should be close to unity at the design power for an optimal constrained system.

By taking outputs at several trim lines, a range of system sizes is defined, allowing interpolation to an exact desired point. In Figure 3-5, we see a set of such interpolation curves for our design case. The

TABLE 3-6

PERFORMANCE SUMMARY 120m FOCAL HEIGHT

NOON = 4.0 MAX. NUMBER OF HELIOS./CELL = 367.0 ; AHELI/DMIR**2 = 0.8963 ; TOTAL GLASS = 0.5205
 TRIM CONT L LIMITS 10612. HELIOS AHELI 54.7263 ASEG= 54.7263 ; TOTAL LANS = 0.2556

10000000	00000000
44430000	00000000
44444100	00000000
44444400	00000000
44444430	00000000
44444440	00000000
44444441	00000000
34444442	33000000
03444441	00000000
44444440	03000000
44444430	00000000
44444400	00000000
44443000	00000000
44310000	00000000

***** NUMBER OF HELIOSTATS PER CELL ***** HT = 120.0 METERS

8.7	0.	0.	0.	0.	0.	0.	0.
42.3	83.6	80.1	56.0	0.	0.	0.	0.
51.0	100.7	96.4	89.0	80.9	17.8	0.	0.
62.0	122.1	115.2	105.6	94.0	82.4	0.	0.
77.4	150.2	139.3	124.3	108.6	93.4	59.4	0.
99.5	191.9	169.8	146.1	123.5	103.6	87.2	0.
139.6	256.2	210.3	168.8	138.0	113.0	93.6	19.1
117.3	311.4	256.8	190.2	149.0	120.1	97.8	39.6
0.	236.8	283.1	200.7	153.7	122.4	98.9	19.9
157.9	321.3	264.1	192.9	149.6	119.7	95.9	0.
151.4	275.2	218.6	170.4	136.6	110.7	67.3	0.
106.3	202.0	173.9	144.9	119.7	98.1	0.	0.
77.9	152.0	137.8	118.8	75.4	0.	0.	0.
57.8	113.8	79.4	23.4	0.	0.	0.	0.

PERFORMANCE SUMMARY AND COST BREAKDOWN FOR OPTIMIZED COLLECTOR FIELD - TRIM LINE AT 1.000

EQUINOON POWER	=	291.577	275.970	IN MW	- (SCALED TO 950 W/M2)			
ANNUAL ENERGY	=	685.525	IN GWH					
FIXED COSTS	=	4.3000	IN \$M					
TOWER COST	=	9.7207	2.4388	4.1045	1.0884	2.0890	IN \$M FOR 950. EQUINOON POWER	
LAND COST	=	3.7062	IN \$M	4.2113				
WIRING COST	=	1.5985	IN \$M					
HELIOSTAT COST	=	29.9669	37.4574	44.9478	IN \$M			
TOTAL COST	=	49.8924	57.3828	64.8732	IN \$M			
FIGURE OF MERIT	=	72.780	83.206	94.633	IN \$/MWH	FOR AN INPUT OF	83.000	USING HELIOSTAT

86
 ESG-79-30, Vol II, Book 1

leftmost curve shows the origin of the trim line of 0.960, as this is the number required to deliver 208 Mwt. Comparison with the previous figure shows that the three-point interpolation curves drawn here were not perfect, missing the actual design values by 1/2 to 1%.

The performance summary page for the optimal converged design at a 120 m focal height is shown in Table 3-6. The power level is 276 Mwt and the output figure of merit is 83.87 \$/annual MWh.

Figure 3-6 again shows figure of merit over a range of peak power and corresponding tower heights.

The steep rise of the baseline design curve for systems smaller than 400 Mwt is of interest. A first order study of the effect of the fixed cost is shown in the lower curve. The actual fixed cost was subtracted from the total cost and the figure of merit recomputed for appropriate cases. The resulting curve is substantially lower, and shows a minimum in the range of 300 to 600 Mwt compared to a minimum in the range of 500 to 1000 Mwt for the baseline design. The curve below 300 Mwt is not very well defined because the design studies for the 120 m case concentrated on defining the point of contact with the baseline design curve, i.e., the left side of the design envelope, rather than the bottom. Thus, these two envelopes may still come down somewhat more. However, before further optimizations were done to better establish the minimum, an additional review of the costs included in the fixed cost model was made. The subsequent analysis of these costs revealed that two of the components of the fixed cost, namely, the costs associated with Design and Support Engineering and Indirect A&E, were based on first plant costs. For the sake of consistency, these costs were updated (reduced) to reflect estimates for Nth plant (the basis for other costs used in the optimization). The following summarizes these changes:

<u>Item</u>	<u>1st Plant (10⁶ \$)</u>	<u>Nth Plant (10⁶ \$)</u>
Design and Support Engineering	1.84	1.0
Indirect A&E	1.43	.70
Total Fixed Cost	4.19	2.62

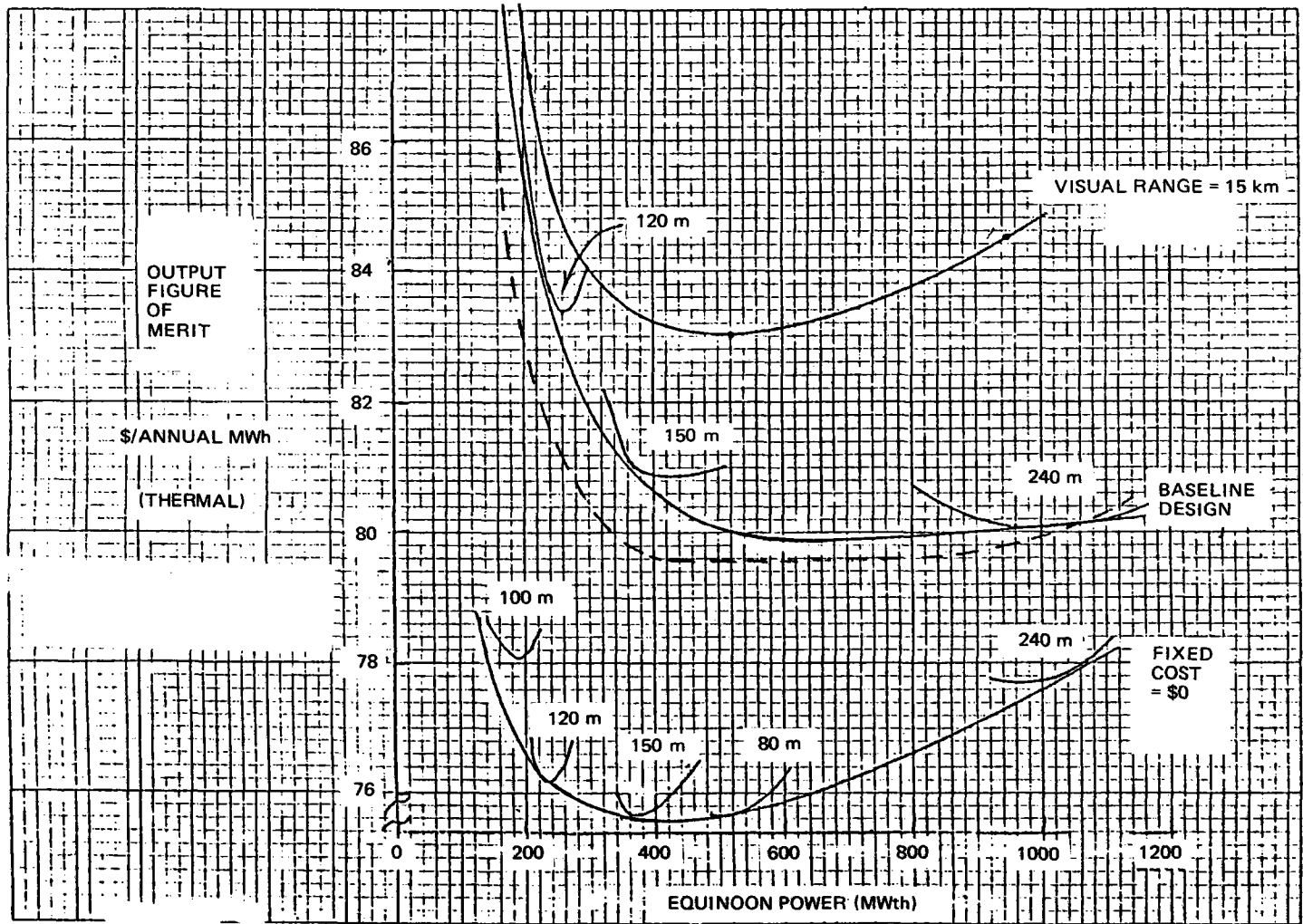


Figure 3-6. Envelopes of Optimization Envelopes for Different Tower Heights

The application of those revised fixed costs was made during further optimization runs and a revised fixed cost baseline curve is shown as the dotted line on Figure 3-6.

Also shown on this figure is the effect of reducing the assumed visual range (50 km) used in the baseline optimization to 15 km. As can be seen, this reduction on visual range and its associated drop in field performance due to increased atmospheric absorption between the heliostat and receiver has a detrimental effect on figure of merit.

To determine if a visual range of 15 km (10 miles) makes any sense in a desert environment, the 1962 Albuquerque data tapes "sanitized" by Eldon Boes were analyzed. Table 3-7 was generated giving the number of hours in which a given visual range and fraction of sky cover coexisted. The leftmost column in the table corresponds to perfectly cloudless hours, and we see that of the 2,051 such hours, 220 had visual ranges of 50 miles (80 km) and 1,723 had visual ranges of 60 miles or greater (100 km). In contrast, most of the days with short visual range were associated with high cloud cover.

Alongside and below the table we have calculated the several reasonable sums, percentages, and cumulative percentages. "Beam hours" is taken as the product of $(1 - \text{sky cover})$ and the total number of occurrences. We can see from this computation that 95% of the annual daylight hours had a visual range of 30 miles (50 km) or greater, and 96% of the hours with over 50% clear sky had a visual range of 40 miles (64 km) or greater. It is also useful to note that 94% of the "beam hours" satisfy this condition. Thus, it appears that our standard visual range of 50 km may considerably overestimate the atmospheric attenuation of reflected light, and that 75 km might be a more realistic estimate. Surely 15 km is not of program interest; we chose it only to be certain of showing an effect in the parametric study.

TABLE 3-7

1962 ALBUQUERQUE (BOES) VISUAL RANGE vs SKY COVER

VISUAL MILES	SKY COVER S											Σ	%	%	Σ	%	%
	0.	.1	.2	.3	.4	.5	.6	.7	.8	.9	1.0						
1	0	0	0	0	1	1	0	1	0	0	9	12	.3	100	2	.1	100
2	0	0	0	0	1	1	0	1	1	0	9	13	.3	99.7	2	.1	100
4	0	0	0	0	0	0	2	0	1	1	12	16	.3	99.4	0	0	99.8
10	2	1	2	6	6	2	1	1	3	4	38	66	1.4	99.1	19	.6	99.8
15	5	1	7	0	2	0	1	3	2	1	20	42	.9	97.7	15	.5	99.2
20	15	5	3	3	1	0	0	0	7	8	33	75	1.6	96.8	27	.9	98.7
25	5	0	0	0	0	0	0	1	0	0	3	9	.2	95.2	5	.2	97.8
30	20	5	3	5	2	5	7	8	8	12	75	150	3.2	95.0	40	1.3	97.6
35	5	1	1	0	0	2	0	2	2	1	3	17	.4	91.8	9	.3	96.3
40	46	15	12	12	13	5	9	17	21	35	80	265	5.6	91.4	103	3.3	96.0
45	10	3	1	5	1	1	1	0	1	1	5	29	.6	85.8	21	.7	92.7
50	220	44	41	34	27	41	32	62	69	80	203	853	17.8	85.2	407	13.0	92.0
55	0	0	0	0	0	0	0	0	0	0	0	0	0	67.4	0	0	79
60	1723	278	143	156	97	84	92	136	156	131	217	3213	67.4	67.4	2481	79	79
Σ	2051	353	213	221	151	142	145	232	271	274	707	4760	100		3131	100	
%	43	7	4	5	3	3	3	5	6	6	15	100					
% (cum)	43	50	54	59	62	65	68	73	79	85	100						

Final Optimizations

In order to better define the optimum (minimum figure of merit as a function of peak power) to point, to enable the selection of the preferred commercial system operating point, further optimization runs were made. These runs incorporate the aforementioned revisions to the cost model and were expanded over a larger range of peak powers and corresponding tower heights (1600 MWt and 330 m high). The results of these updated, expanded computations are shown in the following figures.

Figure 3-7 shows figure of merit over the entire range of peak power. Figure 3-8 identifies the tangent point for each tower height/field size variation parabola used in defining the envelope of optimum solar systems. Figures 3-9 and 3-10 show the lower portion of the curve in varying degrees of scale expansion to allow even finer definition of the optimum point. As can be seen, the optimum occurs in the neighborhood of 500 to 600 MWt. Figure 3-11 shows the relationship of annual output, in GWh, to figure of merit. This shows that the optimum system produces slightly less than 1500 GWh at a peak power (from the previous figures) of \sim 500 MWt.

The product of figure of merit and annual output yields the solar system cost. This cost includes the capital cost of all the equipment necessary to obtain the solar power (see Section 3.2.1). In order to determine the optimum operating power level, the solar system cost must be added to the balance of plant costs and levelized energy costs derived. Figure 3-11A shows the solar system costs as a function of both peak power and annual energy outputs which were used in the total hybrid power system optimization.

Visual Range (Atmospheric Attenuation) Trades

The effect of visual range (atmospheric attenuation) on the final optimization was analyzed. Figure 3-11B shows the visual range loss model used by the University of Houston computer model. The baseline performance used in this study is based on a curve fit of the 50 km visual range data shown on this figure. A comparison of this loss model with that used in the MIRVAC codes is shown in Figure 3-11C. The data in both figures have been adjusted

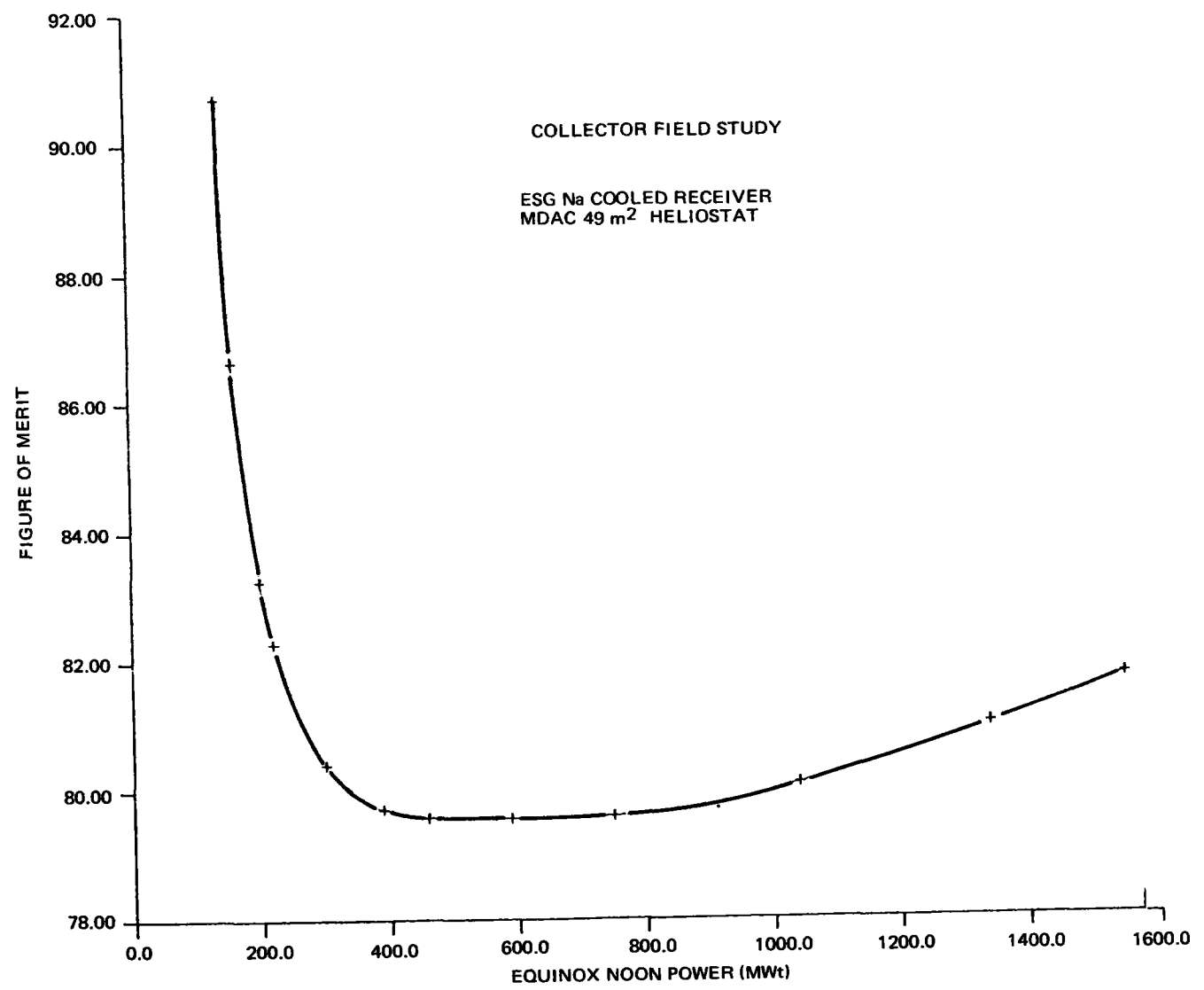


Figure 3-7. Figure of Merit vs Power

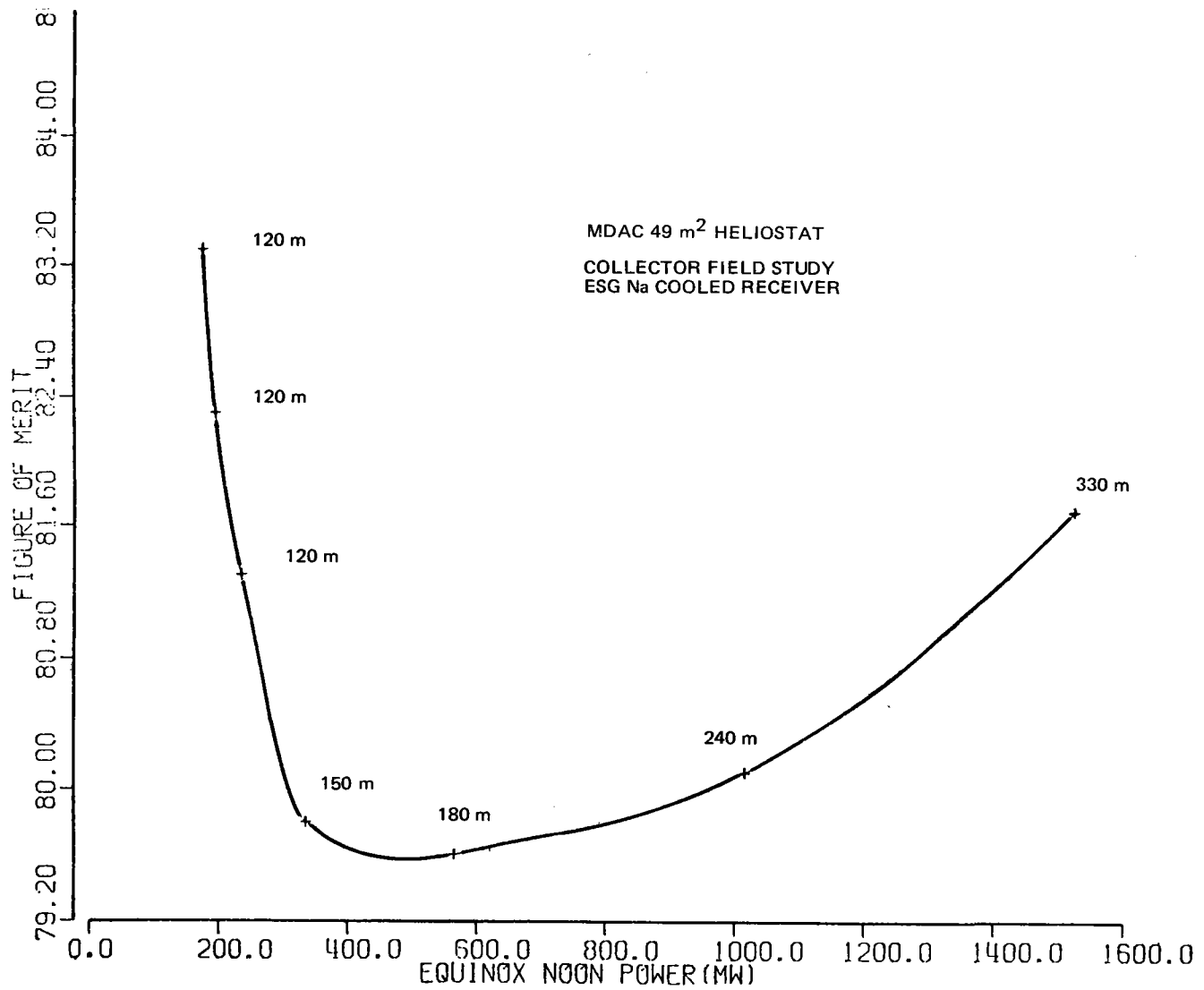


Figure 3-8. Figure of Merit vs Power Optimums

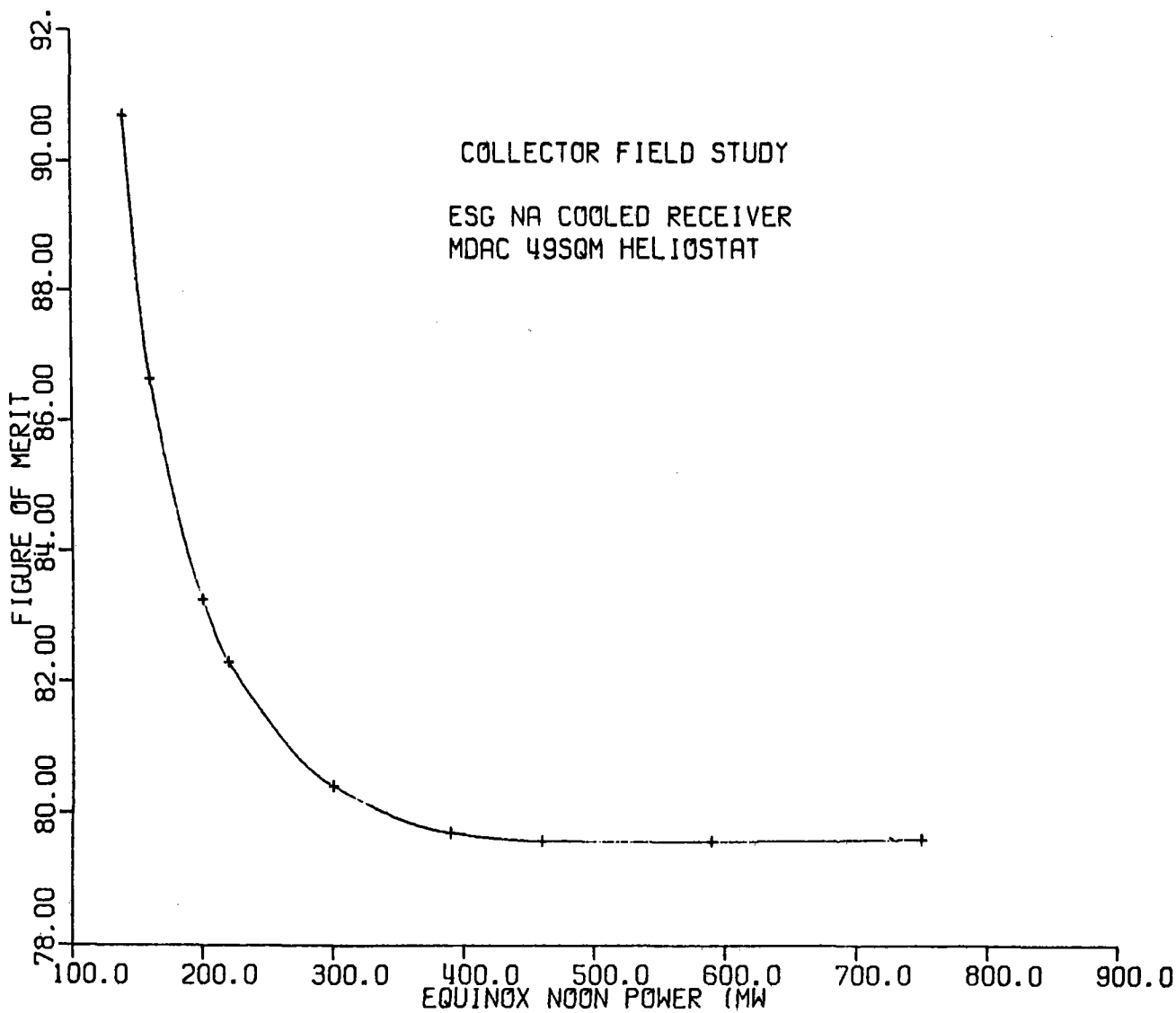


Figure 3-9. Figure of Merit vs Power Expanded Scale

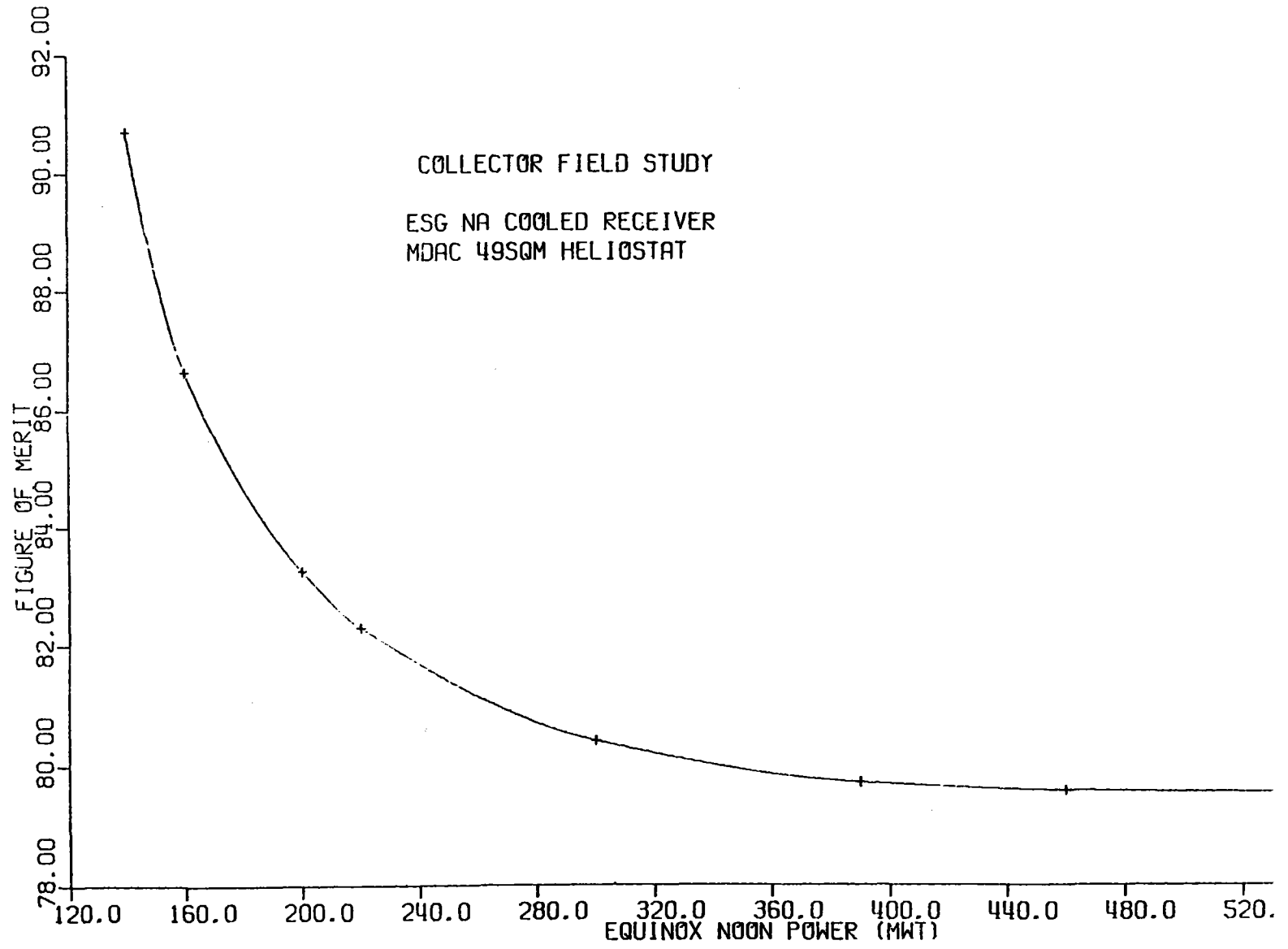


Figure 3-10. Figure of Merit vs Power Expanded Scale

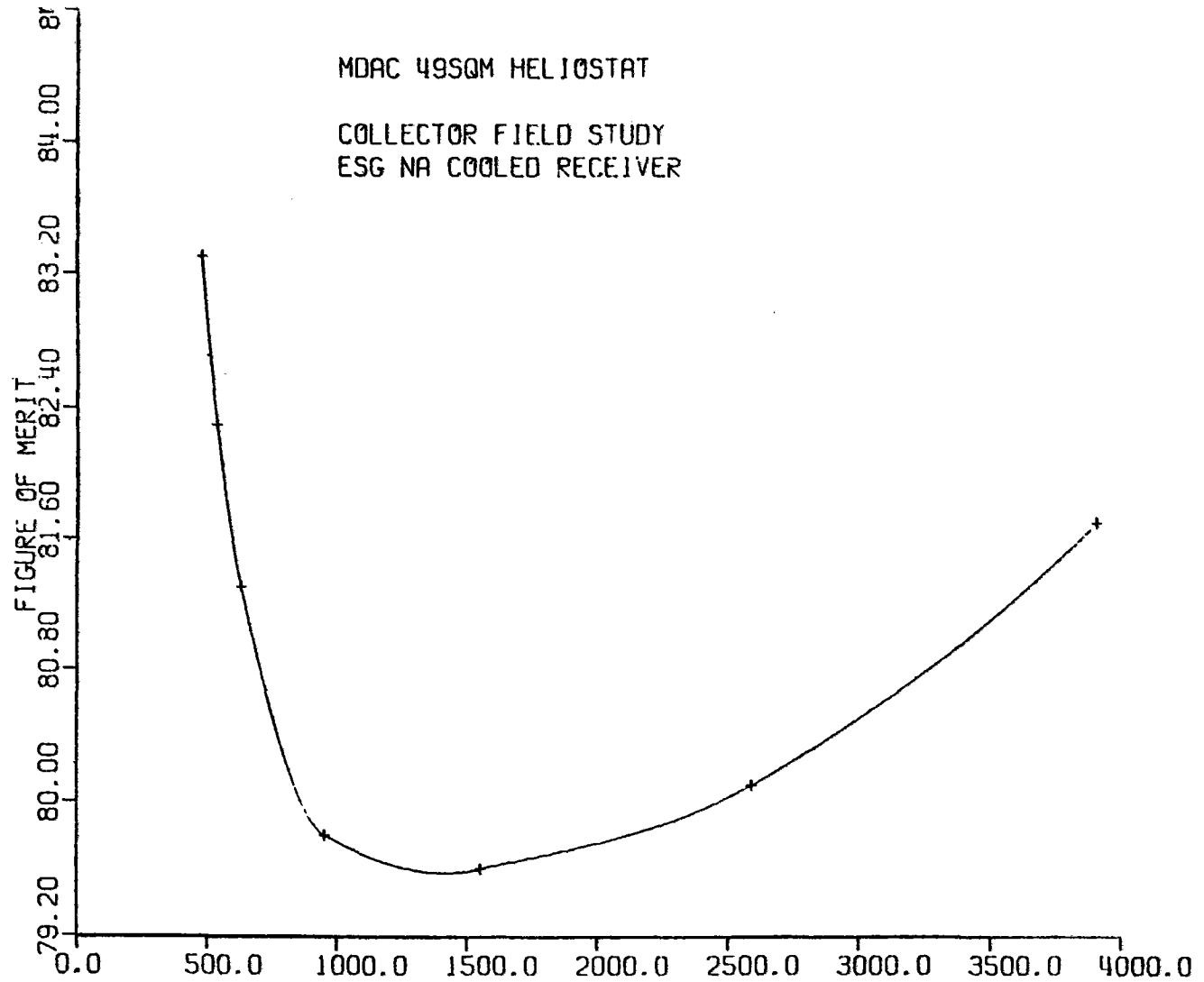


Figure 3-11. Figure of Merit vs Annual Energy (GWT)

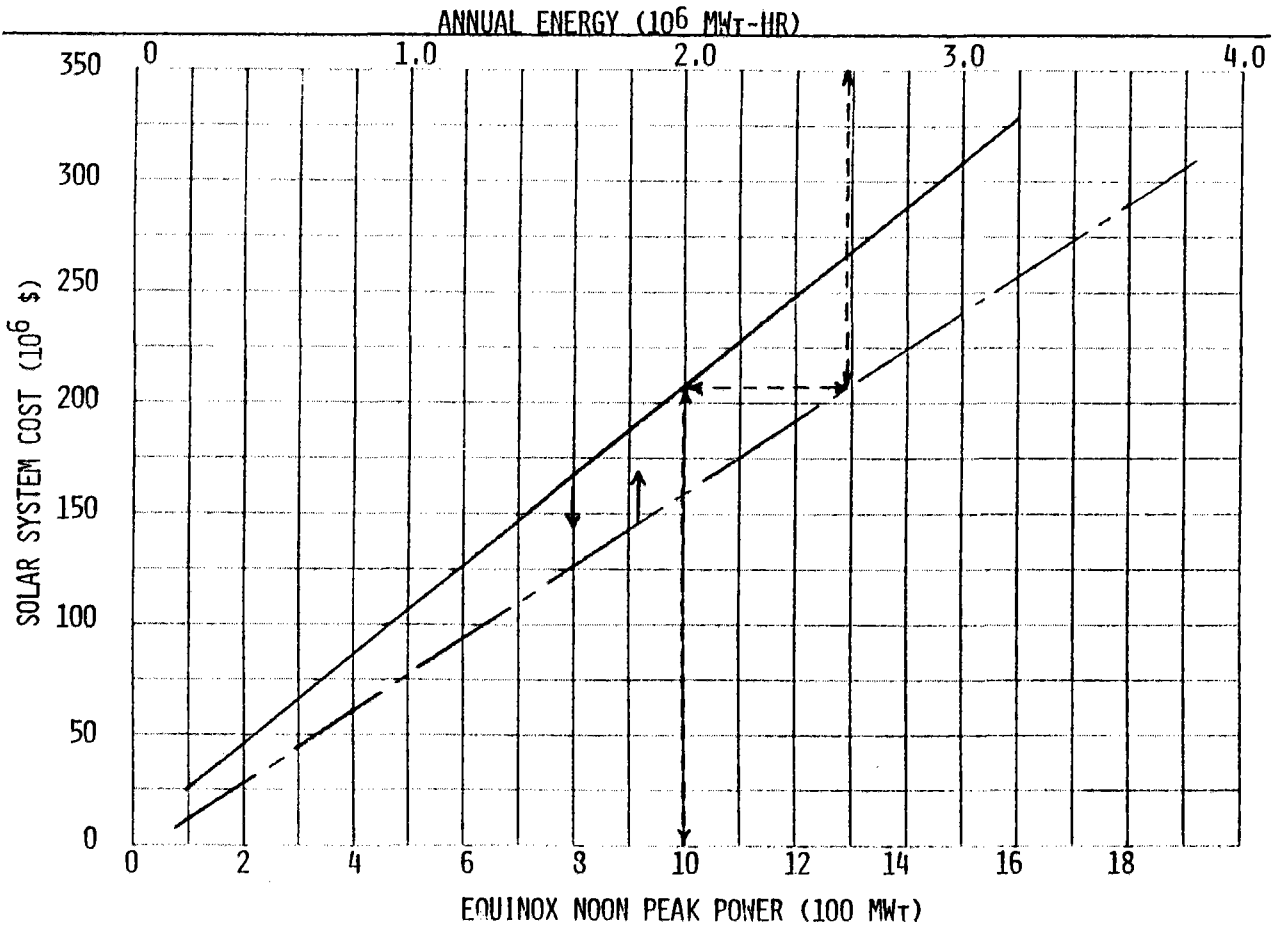
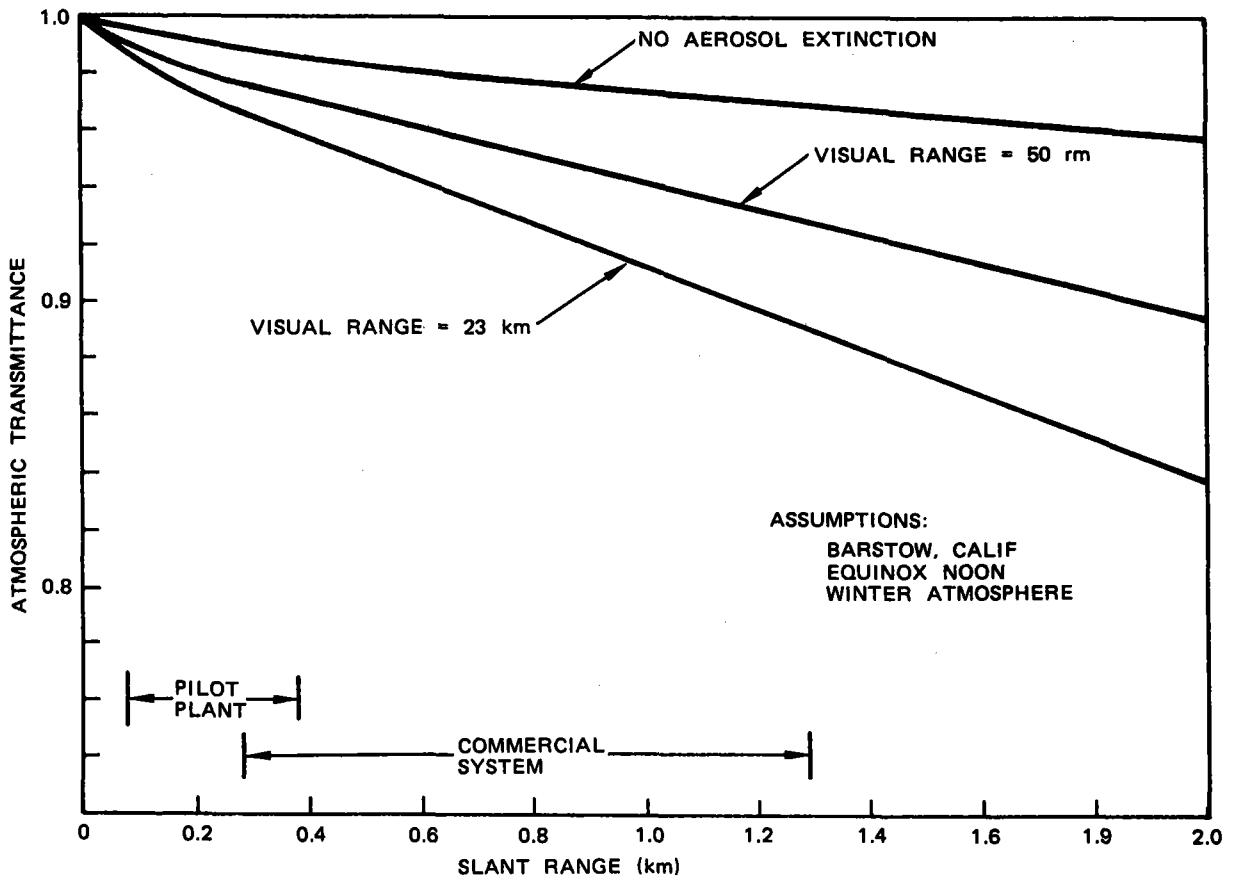


Figure 3-11A. Cost of Optimum Solar Systems



9315-21

Figure 3-11B. Effects of Aerosol Extinction on Transmittance from Heliostat to Receiver

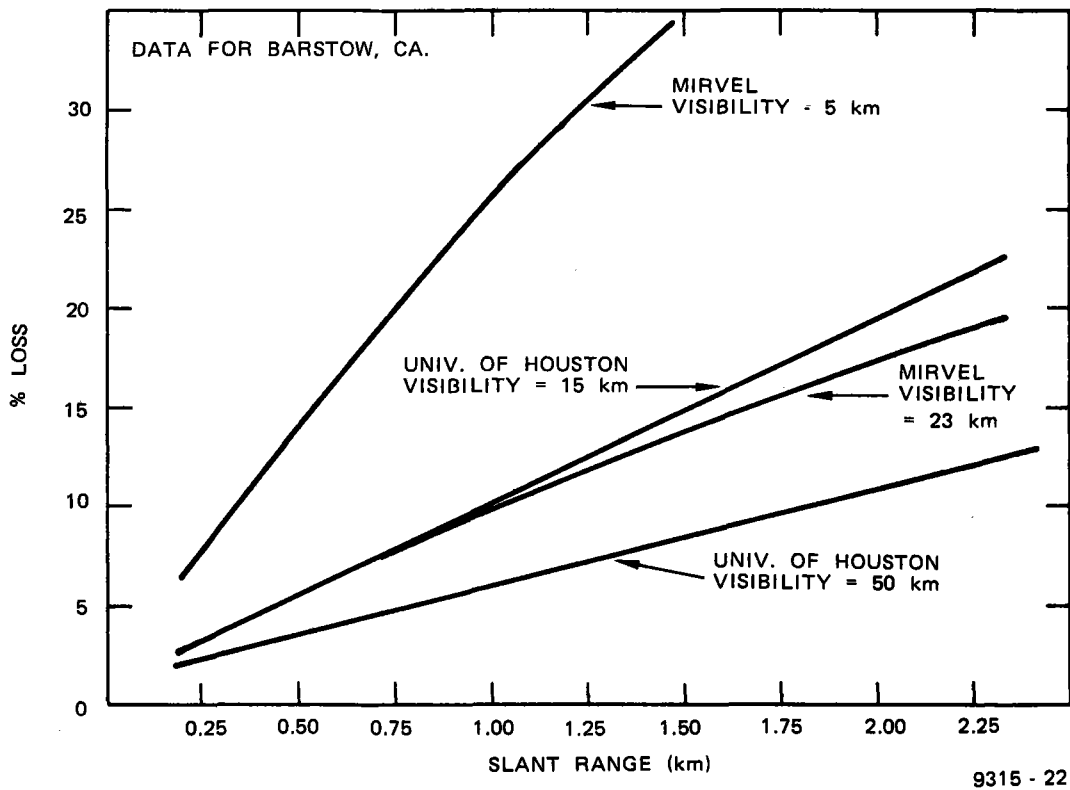


Figure 3-11C. Atmospheric Attenuation for Low and High Visibility – Comparison of Mirvel and University of Houston Models

for the altitude at Barstow, California. The effects of reducing visual range from 50 km to 15 km (this reduction is considered extremely conservative, as previously discussed in the initial optimization write-up) on the figure of merit can be seen in Figure 3-11D. The effect is more pronounced at higher power levels (larger system) amounting to an ~6% increase in figure of merit for the 330-m tower. A more detailed presentation of the effect on the preferred commercial system (330 m tower) can be seen on the much expanded scale of Figure 3-11E. To put the data in a more realistic perspective, Figure 3-11F presents the same data on a "zeroed" scale. In conclusion, the effect of visual range assumption on the system optimization is relatively small over an extreme variation in visual range and based on the previously discussed Albuquerque data the 50-km assumption was considered justified.

Aim Strategy Trade Study

Further optimizations were made for the solar system with the 120-m tower. These involved analyzing larger elongated receivers. The sizes included 12.0-m length by 10.4-m diameter, 13.5-m length by 10.4-m diameter, and 15.0-m length by 10.4-m diameter receivers. Two different aim strategies were investigated (single point equatorial aim and a high-low two-point aim). This was done to determine the effect on the peak flux incident on the receiver. Single point aim resulted in peak fluxes on the order of 1.9 MW/m^2 , which exceeded the receiver allowable flux of $\approx 1.5 \text{ MW/m}^2$, with the high-low two-point aim showing a marked reduction in peak flux to $< 1.4 \text{ MW/m}^2$. The two-point aim was only practical on the 13.5 and 15.0-m long receivers due to excess spillage on smaller receivers.

The results of the optimizations can be compared on Figures 3-12 and -13. Also shown for reference on Figure 3-12 is the previously analyzed 10.4-m x 10.4-m receiver. The input figure of merit (FMI) was increased from 65 to 72, and this variation can be compared directly for the 12.0-m long by 10.4-m diameter receiver. The FMI affects field density in an inverse fashion. Increasing the FMI tends to increase the optimum power level for a given receiver size due to a change in the allowable field density. The receiver/tower combination with the lowest figure of merit at the required solar multiple = 0.8, power level (228.9 MWt), (208 MWt required with a field/receiver power ratio of

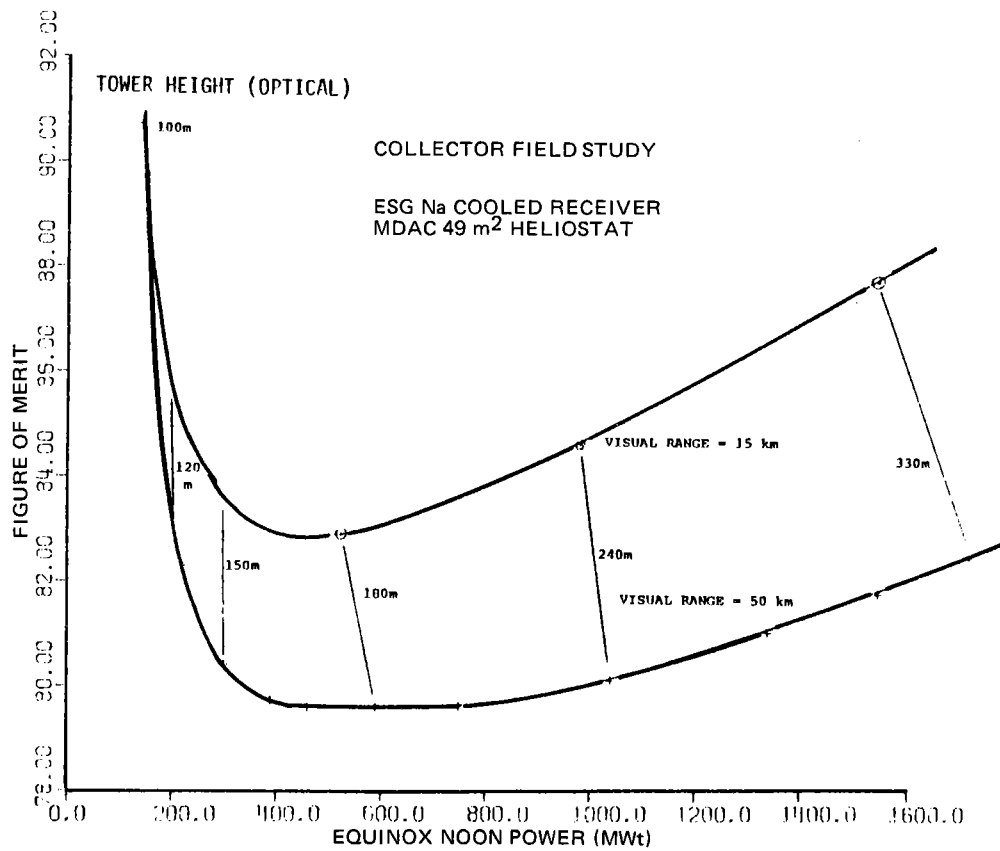


Figure 3-11D. Effects on Visual Range on Solar Optimization

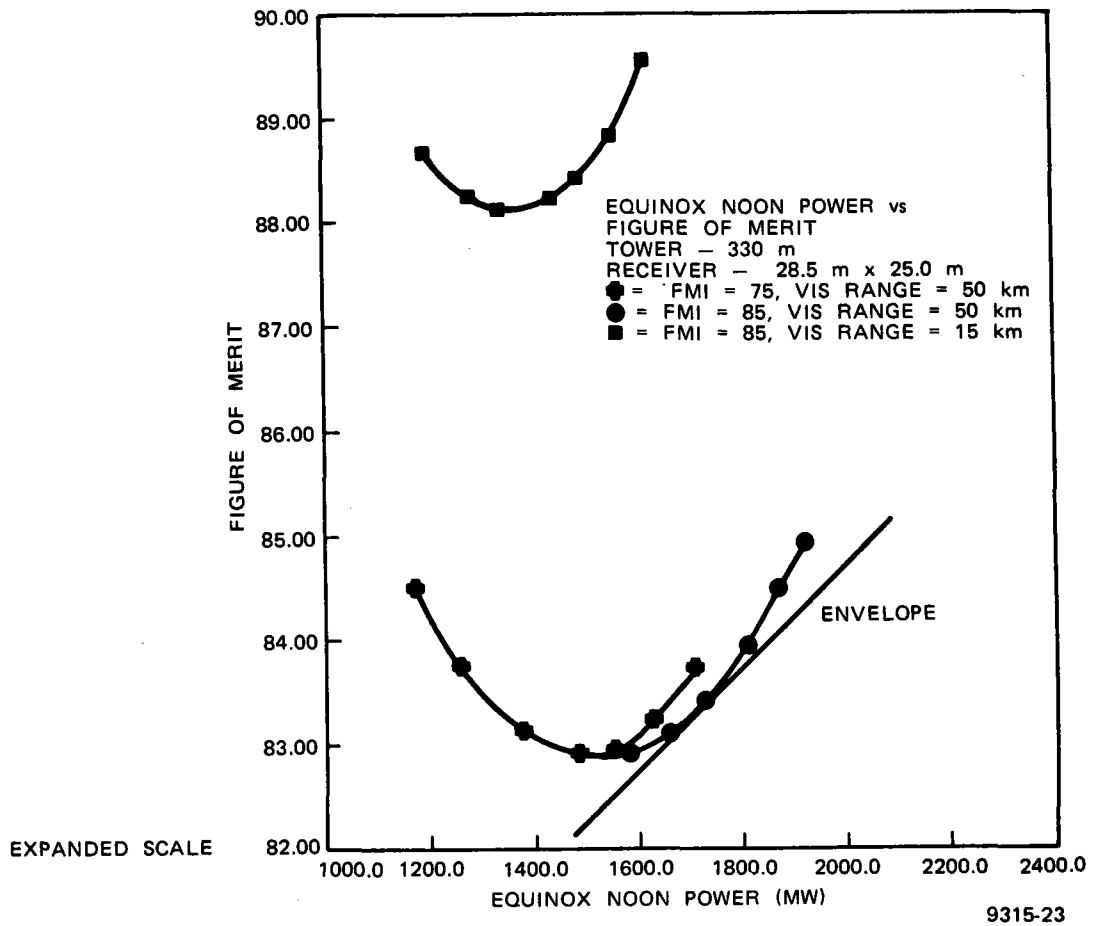


Figure 3-11E. Visual Range Effects on Preferred Commercial Optimization

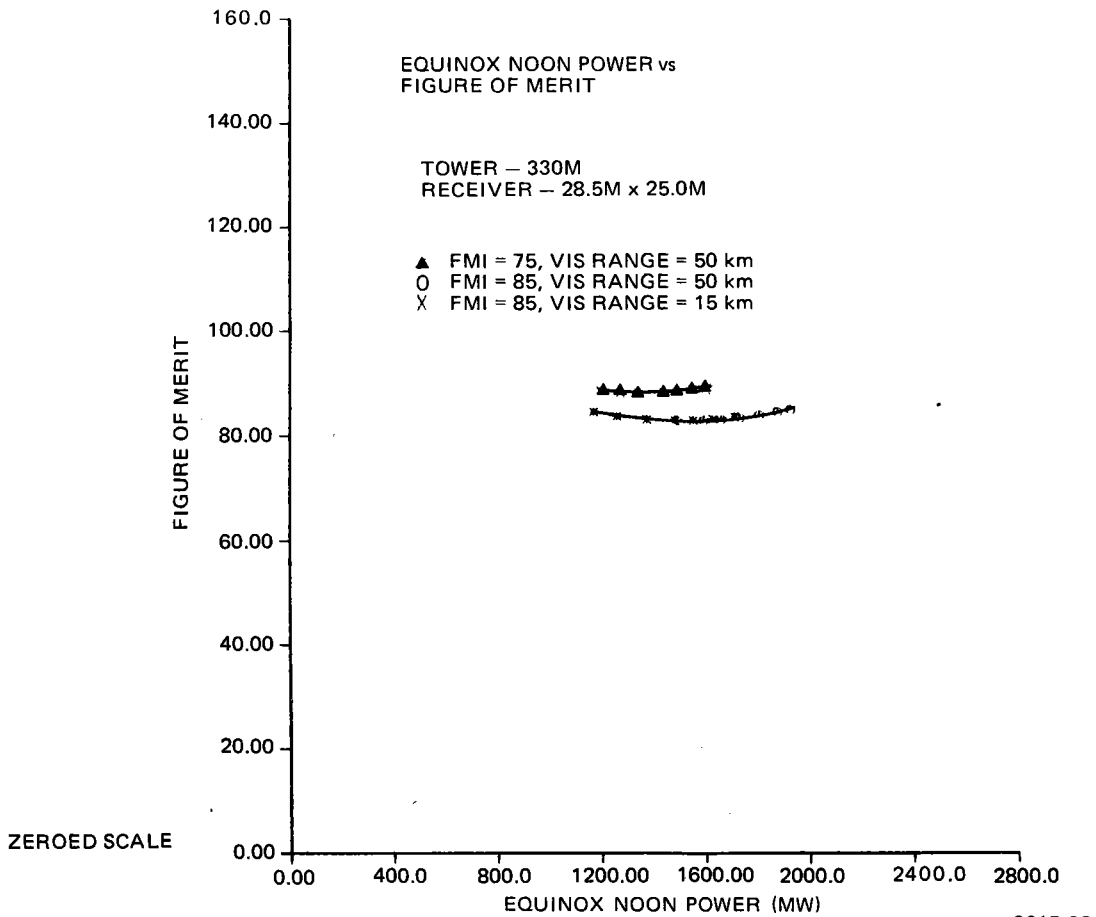
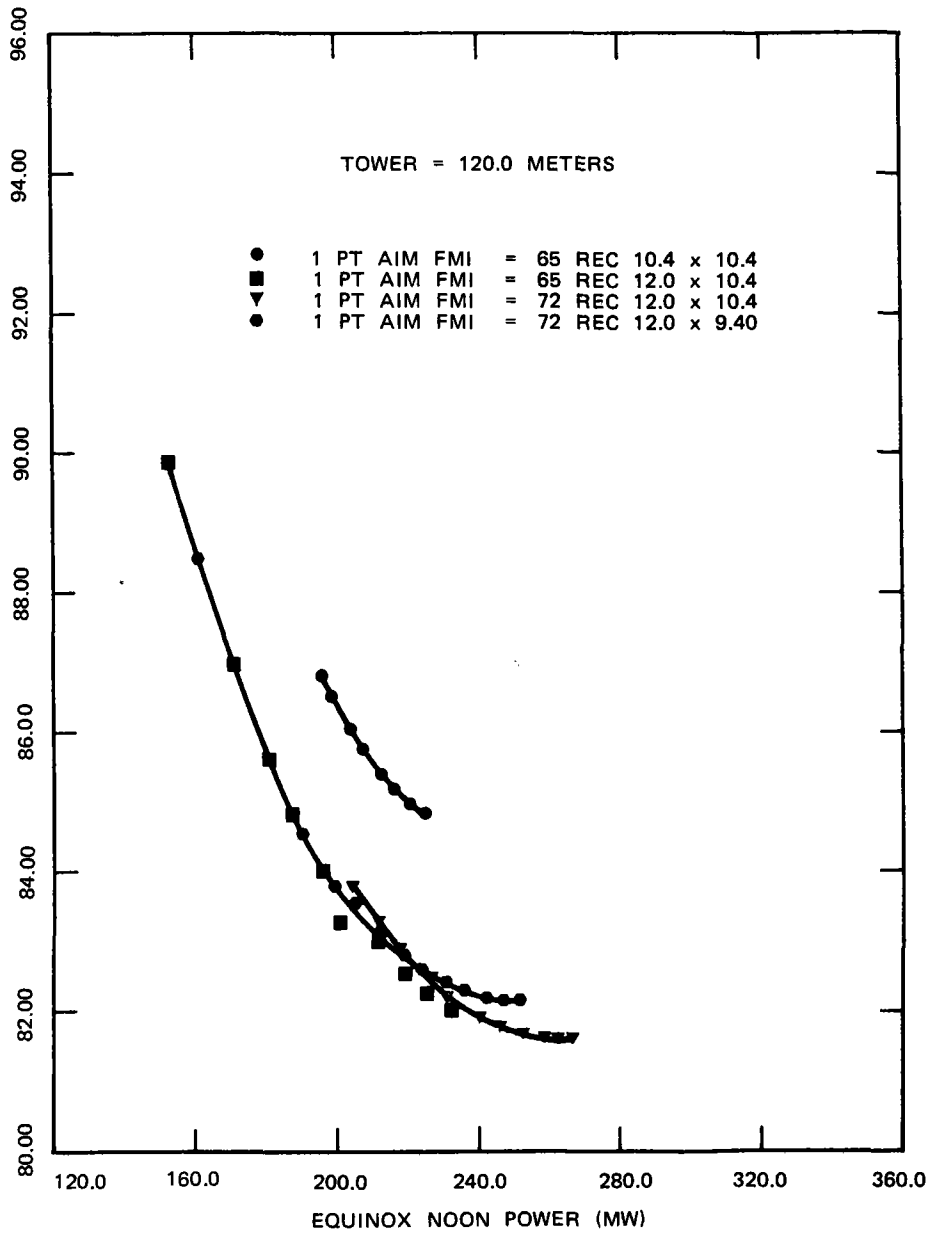


Figure 3-11F. Visual Range Effects on Preferred Commercial Optimization



9315-24

Figure 3-12. Figure of Merit vs Equinox Noon Power

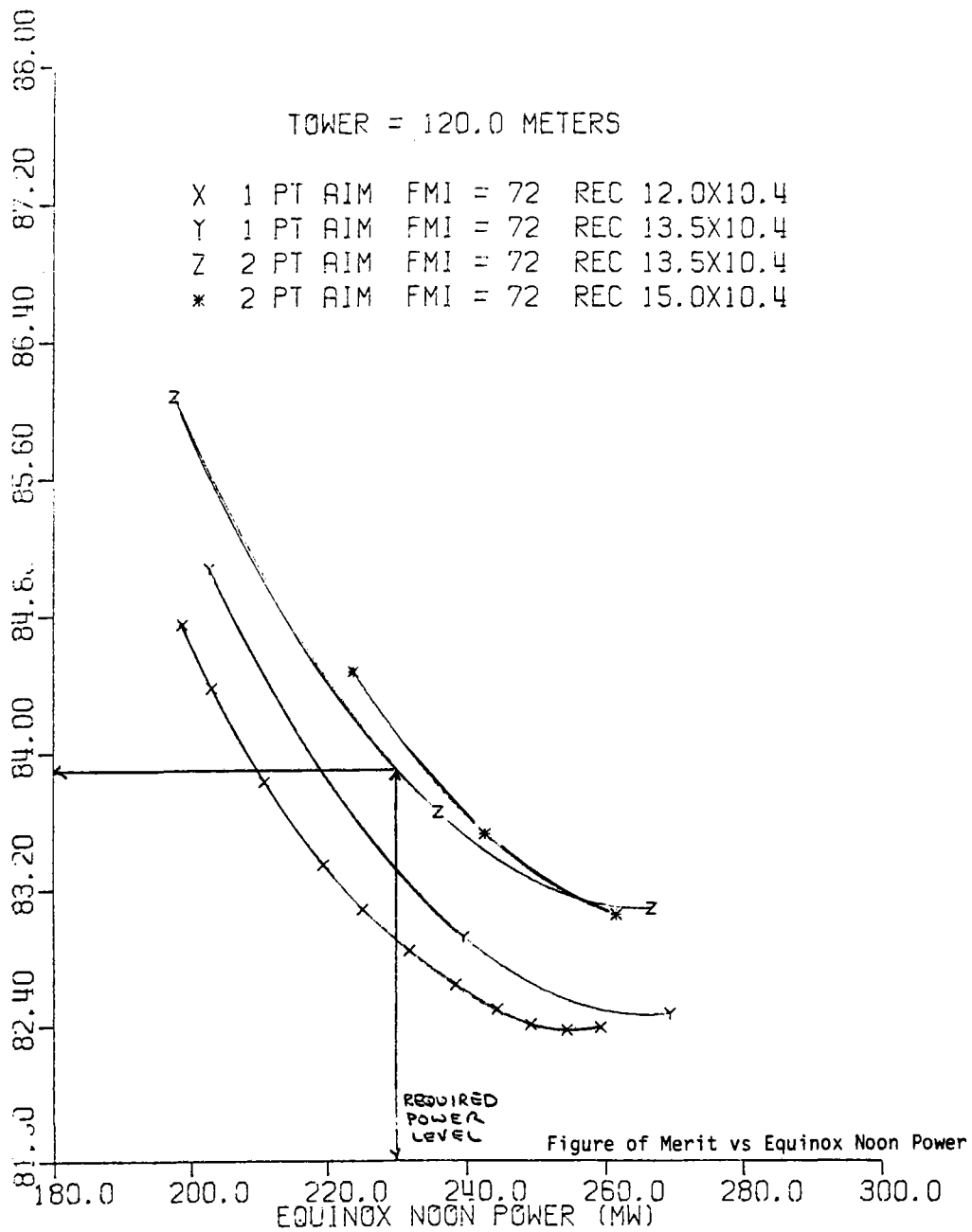
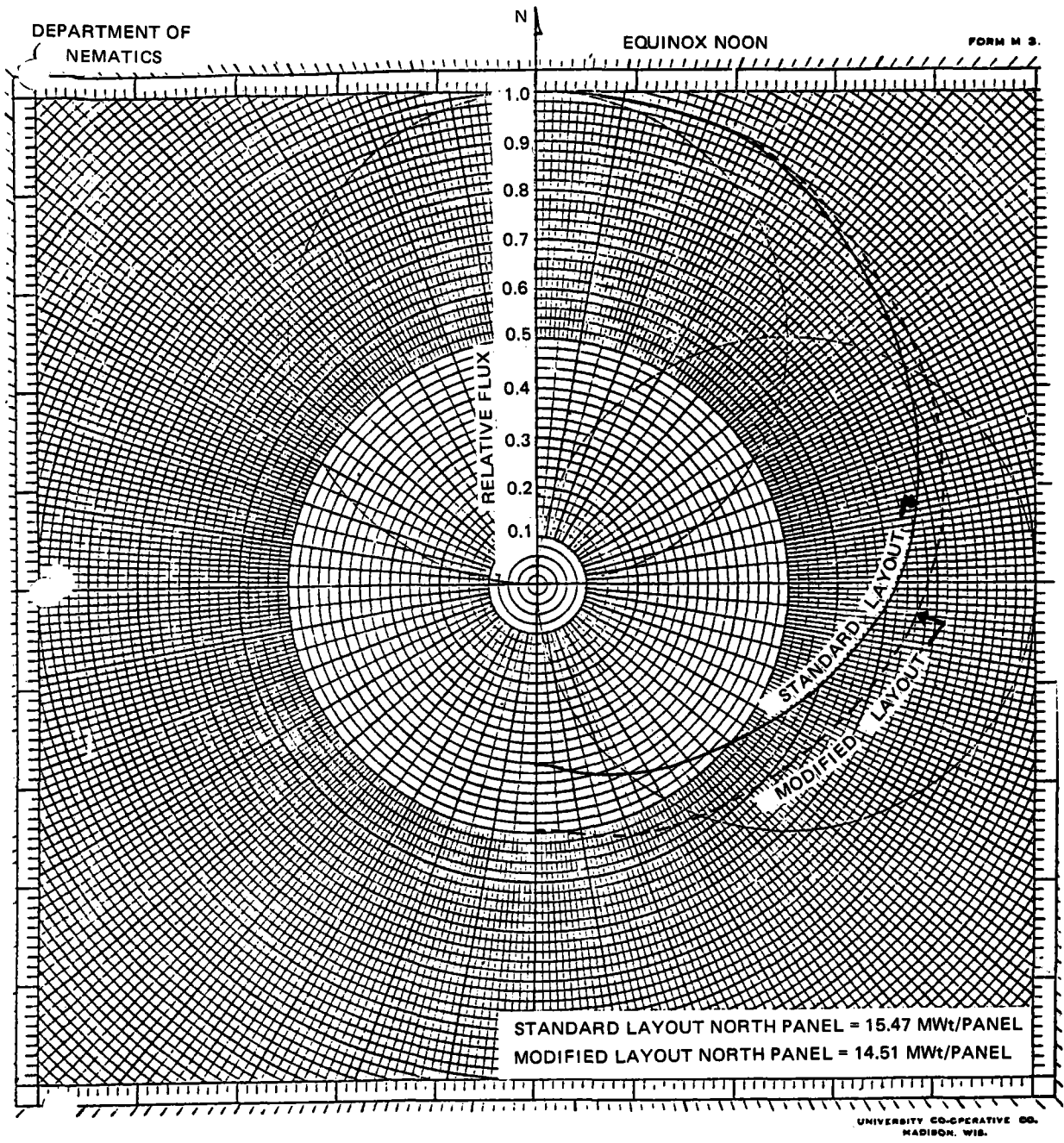


Figure 3-13. Figure of Merit vs Equinox Noon Power



POLAR COORDINATE, GRADUATED IN DEGREES

Figure 3-14. Normalized Incident Flux on Receiver

1.1) that operates at an acceptable reduced peak flux, is the 13.5-m x 10.4-m receiver shown on Curve Z of Figure 3-13.

Receiver Flux Distribution Trade Study

The normal optimization procedure produces a field trimmed such that the field is strongly biased to the north side of the tower. The mechanism controlling the trim is primarily a function of limits set on allowable cosine losses. The standard north field biasing creates a relatively large variation in total panel flux distribution around the receiver when comparing the total flux on north facing panels with that on south facing panels. Trades related to sodium flow control per panel established the desirability of reducing this flux induced flow imbalance in the north/south panel locations. An obvious method of reducing the north/south per panel flux ratio was to move some of the heliostats from the north side of the tower to the south, conversely moving the relative location of the tower/receiver further north in the field. This can be accomplished analytically by modifying the cosine related field trim constraints. Additional runs were made for the selected tower/receiver combination associated with the 0.8 solar multiple baseline system. The results of this modification can be seen in Figure 3-14. This figure shows the normalized incident flux on north panel = 1.00) flux distribution on the receiver at the design point (equinox noon). The solid line is the result of a "standard" field layout, while the dotted line presents the modified cosine trim case. As can be seen, two changes are occurring. First, the incident flux on the north, or maximum flux panel, is reduced from 15.47 MW/panel to 14.51 MWt/panel (a 6.2% reduction) and secondly, the ratio of north/south panel flux is reduced from 2.78 to 2.0 (a 28.1% reduction). A comparison of system figure of merit shows that these beneficial reductions are achieved with less than a 2% increase in system figure of merit at the design total receiver absorbed power. As a result of this trade study, the final field optimizations and the associated performance for both the 0.8 and 1.4 solar multiple 100 MWe reference systems were based on the modified cosine trim constraints.

3.2.3 Heliostat Parametric Analysis

An analysis was made to estimate the optimum size of a heliostat, considering only the minimum capital cost for the heliostat. Semi-empirical cost algorithms are posed based on prototype heliostat capital costs. While these algorithms are oversimplified, it is felt that the results of the analysis are still representative.

The following general conclusions are drawn (based on capital costs):

- 1) The heliostat area and drive unit size for which the design margins in both strength and stiffness are both at the minimum acceptable value should be the lowest cost.
- 2) The prototype heliostat, at 49 m^2 , is about optimum for the above condition.
- 3) Designing to strength considerations (survival wind loads), only, neglecting stiffness (operating wind loads) indicates a 56 m^2 area to be optimum.
- 4) Neglecting survival wind loads and designing to stiffness considerations leads to an optimum size of about 36 m^2 .

A subsequent analysis was done to include the effect of the present value of operating and maintenance (O&M) costs in this optimization. The addition of these costs resulted in a heliostat which was sized by stiffness criteria (operational wind loads) and slightly oversized based on strength considerations being optimum. This minimum cost occurs at a heliostat size of $\sim 63 \text{ m}^2$. However, the optimum is very flat about this point and is only about $\$.60/\text{m}^2$ less than the cost of the 49 m^2 baseline design heliostat including O&M costs.

The results of these analyses are shown in Figure 3-15. The lower set of curves is based on variations in heliostat capital costs only, with the solid line being the cost of a heliostat which meets or exceeds both the strength and stiffness criteria, i.e., to the left of 49 m^2 , the design is strength-critical and to the right of 49 m^2 , the design is stiffness-critical. In the case of the lower (capital cost only) curves, the minimum cost for a heliostat which meets both criteria is achieved with a 49 m^2 heliostat. The upper set of curves shows the results of adding to the capital cost the present value of O&M costs. Again, the solid line is defined as above; however, in this case, the minimum cost on the solid (valid design line) occurs at a heliostat size of approximately 63 m^2 . Because the 49 m^2 size is only slightly higher in cost than the apparent minimum and detailed cost and performance data is available at this size, the 49 m^2 heliostat will be used (including O&M cost) in the initial field optimization analyses. The impacts of reducing heliostat size on the field optimization will be analyzed at a later date using the cost variations (including O&M) presented in this figure.

The following explanation is given to further define the terms "strength critical" and "stiffness critical." A component is considered strength critical when its design is dictated by criteria that it shall not fail based on material yield strength when subjected to the design survival wind loads. A component is considered stiffness critical when its design is dictated by criteria that it shall not deflect beyond limits defined by meeting tracking accuracy requirements when subjected to operational wind loads.

As will be seen in the derivation of the cost algorithms, the drive system and its associated components were considered as either strength-of-stiffness critical, with the other heliostat components being designed by strength, or some other criteria not related to stiffness, as defined above. The following table summarizes the major components of the drive system and how strength and stiffness affect the design.

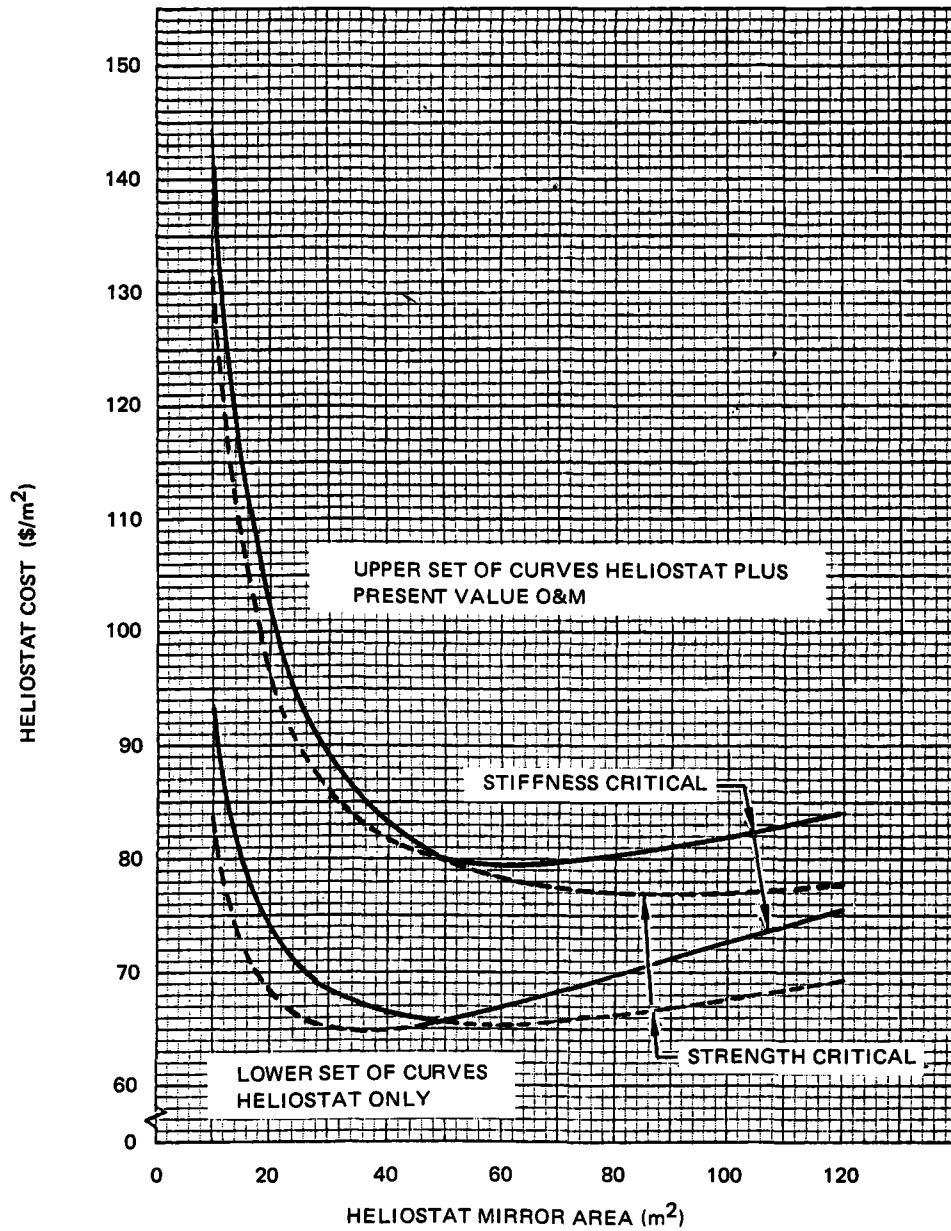


Figure 3-15. Effect of Heliostat Size on Normalized Cost

DRIVE SYSTEM DESIGN SUMMARY

Component	Design Criteria	
	Strength	Stiffness
Jacks & attach points	Size of components	N/A
Harmonic drive unit	Size of gears	Clearances between flex and circular splines.
Azimuth Drive Housing & drag link (material dependent)	Sized based on yield strength	Low yield strength/cost material (ductile iron) selected. This provided large-enough components to meet deflection criteria.
Turret bearing	Primarily strength related to minimizing Brinelling.	

The following describes the derivations of the capital and O&M cost algorithms based on the current 49 m² prototype heliostat:

Each of the algorithms is of the form

$$\text{Cost} = C(a)^n$$

where

C is the cost of the component per prototype heliostat unit (49 m²) in dollars,

a is the area normalized to 49 m², and

ⁿ is an empirically estimated exponent.

Capital Cost Algorithms

The pedestal/foundation loads vary as $(\text{area})^{3/2}$. With the foundation costs dominant, a relationship

$$\text{Cost} = 725 a^{3/2} \text{ is adopted.}$$

Reflector costs vary approximately as the area, or

$$\text{Cost} = 470 a^{1.0}.$$

The support structure loads vary as $(\text{area})^{3/2}$. Stress is a function of MC/I , with the moment varying as $a^{3/2}$. For constant section depth, structure mass will vary as the moment. Optimized sections will vary at a slightly lower power. Hence, adopt

$$\text{Cost} = 363 a^{1.4}.$$

Wiring and control costs are nearly constant with area, with wiring costs varying about as $(\text{area})^{1/2}$ and control constant. Hence, adopt

$$\text{Cost} = 245 a^{+0.2}.$$

Assembly, installation, and checkout costs are substantially independent of area; hence, use

$$\text{Cost} = 279.$$

Drive unit costs depend on whether the drive unit is designed by strength or stiffness. Drive unit loads vary as $(\text{area})^{3/2}$ and strength varies as D^3 , where D is a characteristic dimension, such as pitch diameter. The drive unit mass tends to vary as D^2 . The cost of the drive unit per pound varies as $(\text{weight})^{-.11}$. From the above relations, D varies as $(\text{area})^{1/2}$, mass varies as area, and cost varies as $(\text{area})^{0.89}$. Hence, for strength limited drive units,

Cost = $407 a^{0.89}$ for the azimuth drive, and

Cost = $730 a^{0.89}$ for the elevation drive, or

Cost = $1137 a^{0.89}$ for the total drive unit.

For stiffness limited drives, the moment of inertia for the reflector varies as (area)². The drive unit stiffness also varies as D^3 . Hence, D varies as (area)^{2/3}, mass varies as (area)^{4/3}, cost as (area)^{1.187}, and

$$\text{Cost} = 1137 a^{1.187}$$

for the stiffness limited drive.

The total heliostat cost is then given by

$$C = 725 a^{3/2} + 470 a + 363 a^{1.4} + 245 a \cdot 2 + 279$$

$$+ \begin{cases} 1137 a^{0.89} & \text{(strength limited)} \\ 1137 a^{1.187} & \text{(stiffness limited)} \end{cases}$$

The cost per unit area is

$$\frac{C}{a} = 725 a^{.5} + 470 + 363 a^{.4} + 245 a^{-.8} + 279 a^{-1}$$
$$+ \begin{cases} 1137 a^{-.11} & \text{(strength)} \\ 1137 a^{.187} & \text{(stiffness)} \end{cases}$$

Analyses

The slope of the cost curve with area is found by differentiating by area

$$\frac{d}{da} \left(\frac{C}{a} \right) = 362.5 a^{-.5} + 145.2 a^{-.6} - 196 a^{-1.8} - 279 a^{-2}$$

$$+ \begin{cases} -125 a^{-1.11} \\ 212.6 a^{-.823} \end{cases}$$

For a heliostat area of 49 m^2 , or a reduced area, a , of unity, the equation becomes

$$\frac{d}{da} \left(\frac{C}{a} \right) = 37.2 + \begin{cases} -125 \text{ (strength)} \\ +212.6 \text{ (stiffness)} \end{cases}$$

Inspection of the above equation shows that the selection of stiffness or strength limitations on the drive unit governs the slope of the cost curve.

For a reduced area of unity (area = 49 m^2), $\frac{d}{da} \left(\frac{C}{a} \right) < 0$ for a strength limited drive unit, indicating that the area should be increased. For a stiffness limited drive unit and a reduced area of unity (area = 49 m^2) $\frac{d}{da} \left(\frac{C}{a} \right) > 0$ the area should be reduced. The calculated, optimum reflector area for a strength limited drive unit is 56 m^2 (605 ft^2) and for a stiffness limited drive is 36 m^2 (383 ft^2). The correct conclusion is that the area should be approximately that which makes the drive unit equally critical in strength and stiffness.

For current heliostat loads, the drive unit is about equally critical for strength and stiffness. Hence, the heliostat size is about optimum. Reduced loads which may result from wind loads, considering effects of interference and wind fences, should lead to a smaller heliostat as the optimum size. Under the stiffness limited conditions noted above, the size is about 36 m^2 which, to the level of accuracy of the above algorithms, should be considered to be indistinguishable from the pilot plant collector size of 38 m^2 .

Operations and Maintenance Cost Algorithms

A previous study of O&M costs associated with the prototype heliostat identified O&M costs of \$55/year in the first year and \$30/year in subsequent years (1978 dollars). An analysis of these costs was made which divided the costs into three categories as follows:

- Part A: Those costs which were independent of heliostat size (primarily, reliability-related items associated with unscheduled maintenance).
- Part B: Costs associated with maintenance materials, i.e., cleaning fluids.
- Part C: Costs which were associated with heliostat scheduled maintenance labor.

Part A costs were assumed to vary as

$$\text{Cost} = (\text{Present value of Part A}) \times a^0 \text{ (i.e., constant per heliostat)}$$

Part B costs were assumed to vary as

$$\text{Cost} = (\text{Present value of Part B}) \times a^1 \text{ (i.e., proportional to mirror area)}$$

Part C costs were assumed to vary as

$$\text{Cost} = (\text{Present value of Part C}) \times a^{.5}$$

This assumption came from the fact that the labor for scheduled maintenance was primarily associated with washing the heliostat, and the time to wash each heliostat was a function of heliostat width (i.e., the time

to drive a washing device past the heliostat with the washing being accomplished by a vertical boom which swept across the heliostat). Since the design is almost square, the width becomes a function of the square root of the area.

Therefore, the O&M cost per heliostat is given by the following equation:

$$\text{Cost} = A_{PV}a^0 + B_{PV}a^1 + C_{PV}a^{.5}$$

where a is as defined in the capital cost analysis and A_{PV} and C_{PV} are the present values of O&M Parts A, B, and C as defined above.

The cost per unit normalized area is therefore

$$\frac{\text{Cost}}{a} = A_{PV}a^{-1} + F_{PV} + C_{PV}a^{-.5}$$

A breakdown of these costs on a per year basis is as follows:

	<u>1st Year</u> (1978 \$)	<u>2nd - 30th Year</u> (1978 \$)
A	40.70	17.10
B	7.70	7.20
C	<u>6.60</u>	<u>5.70</u>
Total	55.00	30.00

The present value of these costs was then calculated using the prescribed EPRI/DOE methods using the following assumptions:

Operational Date	1990
O&M	8%
Discount Rate	10%
System Life	30 Years

This leads to the following present values:

$$\text{Present value of Part A: } A_{PV} = \$415$$

$$\text{Present value of Part B: } B_{PV} = \$165$$

$$\text{Present value of Part C: } C_{PV} = \$131$$

Therefore, the cost algorithm for O&M present values is as follows:

$$\frac{\text{Cost}}{a} (\text{O\&M})_{PV} = 415 a^{-1} + 165 + 131 a^{-.5}$$

The present value cost (in 1978 dollars) for the 49 m² heliostat is \$711 or \$14.52/m².

3.3 RECEIVER SUBSYSTEM

Parametric analyses of the receiver subsystem and its components are discussed in the following section. The Receiver Subsystem contains the receiver, the receiver pump, the steam generator units, and the main sodium piping, including the riser and downcomer.

Since several alternatives exist for piping the solar receiver and fossil-fired sodium heater into the sodium process system for the hybrid plant, a trade study was made to compare these alternatives. Options considered were one parallel and two series arrangements: one of the series arrangements consisted of a receiver piped ahead of the heater, and the other with the heater piped ahead of the receiver.

In the parallel arrangement, the temperature rise across the components is maintained constant while the sodium flow is proportioned in the series arrangement, the sodium flow is fixed and the temperature rise across the components is varied with respect to load change. Refer to Section 4.3 for more specific details concerning this system trade study.

Results showed that the parallel configuration is the preferred choice. It is easier to control such a configuration because the sodium inlet and outlet temperatures are fixed and the power level is controlled by varying the sodium flow; carbon steel can be utilized for sodium riser and inlet piping to receiver; thermal cycling is minimized; and it is the most cost-effective arrangement.

Therefore, the parallel configuration was selected for the hybrid plant conceptual design.

3.3.1 Receiver Concepts

The receiver is a critical component in the solar hybrid plant as it is the interface between the collector and the heat transport subsystems. The receiver is exposed to a heat flux in excess of 1000 suns. At any given instant, the heat flux on the receiver varies by at least a factor of 30 at different locations. During the course of a day, a typical point on the receiver will have an incident flux that varies by at least a factor of four. The temperature difference across the tube wall receiving the greatest flux may be up to 100°C (180°F) while on the rear half of the same tube there will be little or no thermal gradient.

The heat flux on the receiver is such that a loss of coolant can cause severe overheating in a matter of seconds. The heat flux pattern on a panel varies in space and time such that the thermal stresses in a rigid panel can lead to deformation and failure. About 13% of the incident radiation will be lost to the surroundings, while about 5% of the arriving energy misses the receiver altogether. If the receiver is made smaller to reduce the heat losses then the interception will increase. Or if the receiver is made large to intercept more radiation, then the thermal losses will increase. The receiver is sized to minimize the losses.

If a gap between the receiver tubes occurs then the incident heat flux can seriously overheat any structures behind the tubes. Any uncooled strip of metal exposed to the heat flux has a chance of being overheated; therefore, the gap between the receiver tubes is restricted to <1.5 mm (60 mils).

The receiver is exposed to all the elements such as rain, snow, hail, wind, lightning, and earthquake and is designed to survive these environments. Even so, access for maintenance is provided. While the receiver spends part of the time exposed to a variable and intense heat flux, the rest of the time it is in darkness and is inactive. If hot sodium is

circulated through the receiver at night, some operational problems are lessened but the thermal losses become high. A thermal shroud can be used on the receiver at night but is a cumbersome and costly component. If the system is drained at night and no thermal shroud is used, the receiver will cool below preheat temperatures. This is a feasible approach and does require the addition of a preheat step in the startup procedure each morning. For the reference design, the receiver is drained at night.

A sodium-cooled receiver has some problems, it also has many favorable features. The sodium has a high heat transfer capability and can accept very high heat fluxes without causing excessive tube metal temperatures. The sodium is well below its normal boiling point (882⁰C or 1620⁰F) so remains as a dense single phase fluid. Since pressure and corrosion problems do not exist, the receiver walls can be relatively thin. This reduces thermal stresses, thermal losses, and material costs.

3.3.1.1 Cavity vs External Receiver

Trade studies of cavity and external receivers were made for the ACR(3-1,6-6,6-15) study at both the system and component levels. The system comparison involved such factors as the receiver view factor, size, shape, and orientation of the collector, spillage, atmospheric attenuation and tower height. The component comparison considered receiver size, weight, complexity, and cost.

The cavity receiver has the advantage of lower overall reflective and thermal losses.

The external receiver has several overall advantages. One is that for a given power the tower is shorter and less expensive, the spillage is less and the receiver is smaller, simpler, lighter, and less expensive.

The receiver consists of many small-diameter, vertical tubes cooled by upward flowing sodium. Manifolding at the top and bottom of the receiver connects the receiver to the cold and hot buffer tanks which are connected to manifolding which connects to the riser and downcomer.

3.3.1.2 1.4 SM Receiver Design Description

Figure 3-16 shows a conceptual sketch of the ACR receiver mounted on the tower. A crane mounted at the top is shown lifting a panel and its support structure into position. Vertical I-beams and associated trusses provide the main receiver structural support.

Figure 3-17 shows some of the structural details of the receiver. The panel and panel structure are supported by the main structure. Sodium piping with bends to allow for thermal expansion connect the panels to the riser and downcomer. The riser is higher than the upper edge of the panels and acts as a standpipe to provide sodium to the panels in case of pump and/or check valve failure. The sodium expansion tank is toroidal in shape and is located near the top of the receiver.

The receiver is of the external type and it is 16.1 m (52.8 ft) in diameter and 16.1 m in height. It consists of 24 separate vertical panels - each panel being constructed of 110 stainless steel tubes. Each tube has a diameter of 1.91 cm (0.75 in.) and a wall thickness of 0.124 cm (0.049 in.). See Figure 3-18.

The panel tubes are placed tangent to one another forming a flat panel 209.3 cm (82.5 in.) wide. The tubes are held mechanically in this position. The tubes are anchored to the support structure at the panel top and are permitted to grow vertically - the maximum growth being in the neighborhood of 13 cm (5 in.). The tubes are supported every 1.2 m (4.0 ft) by a pin and bracket arrangement which firmly mounts the tubes to the support structure while permitting thermal expansion.

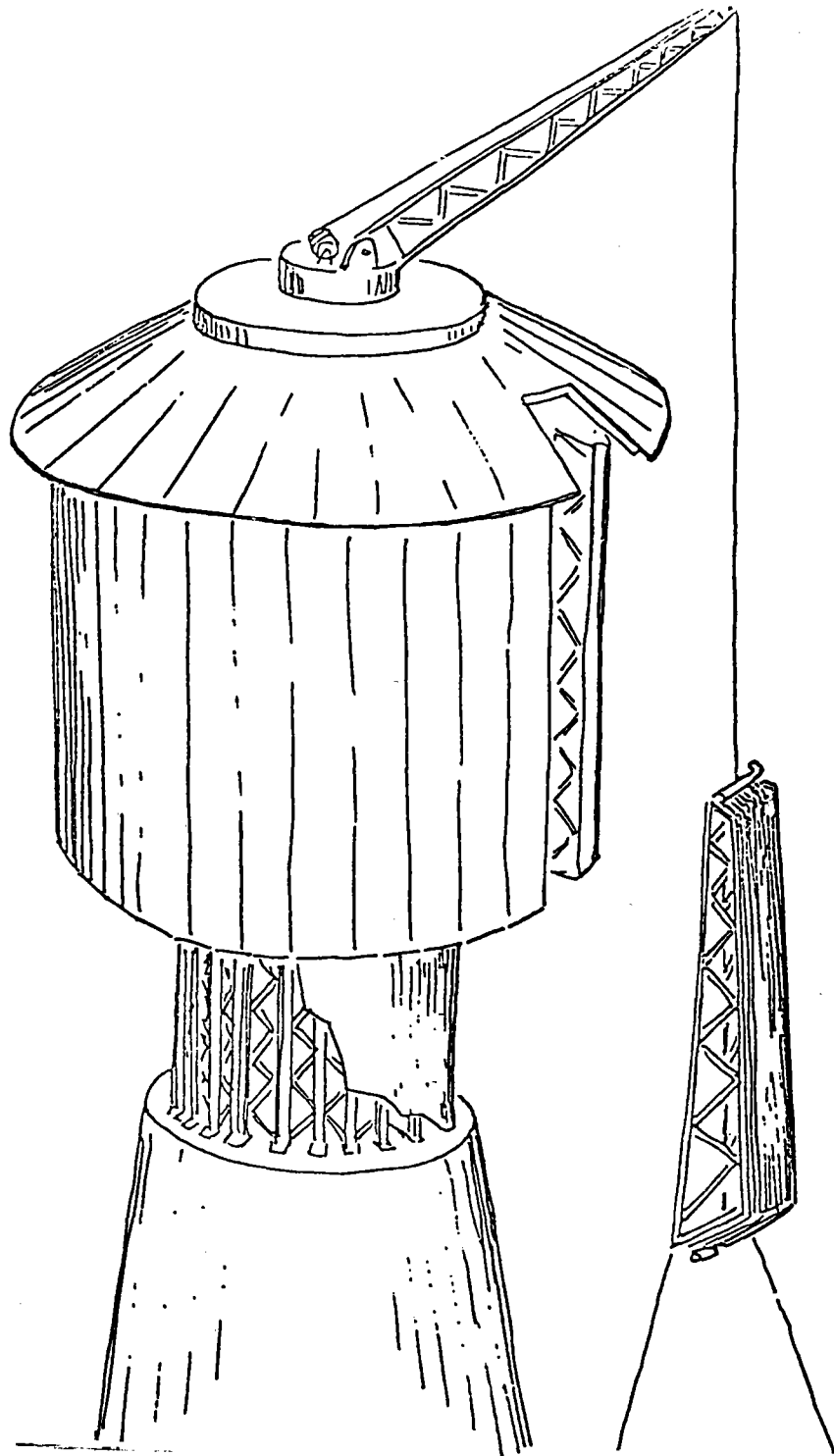


Figure 3-16. External Receiver Concept

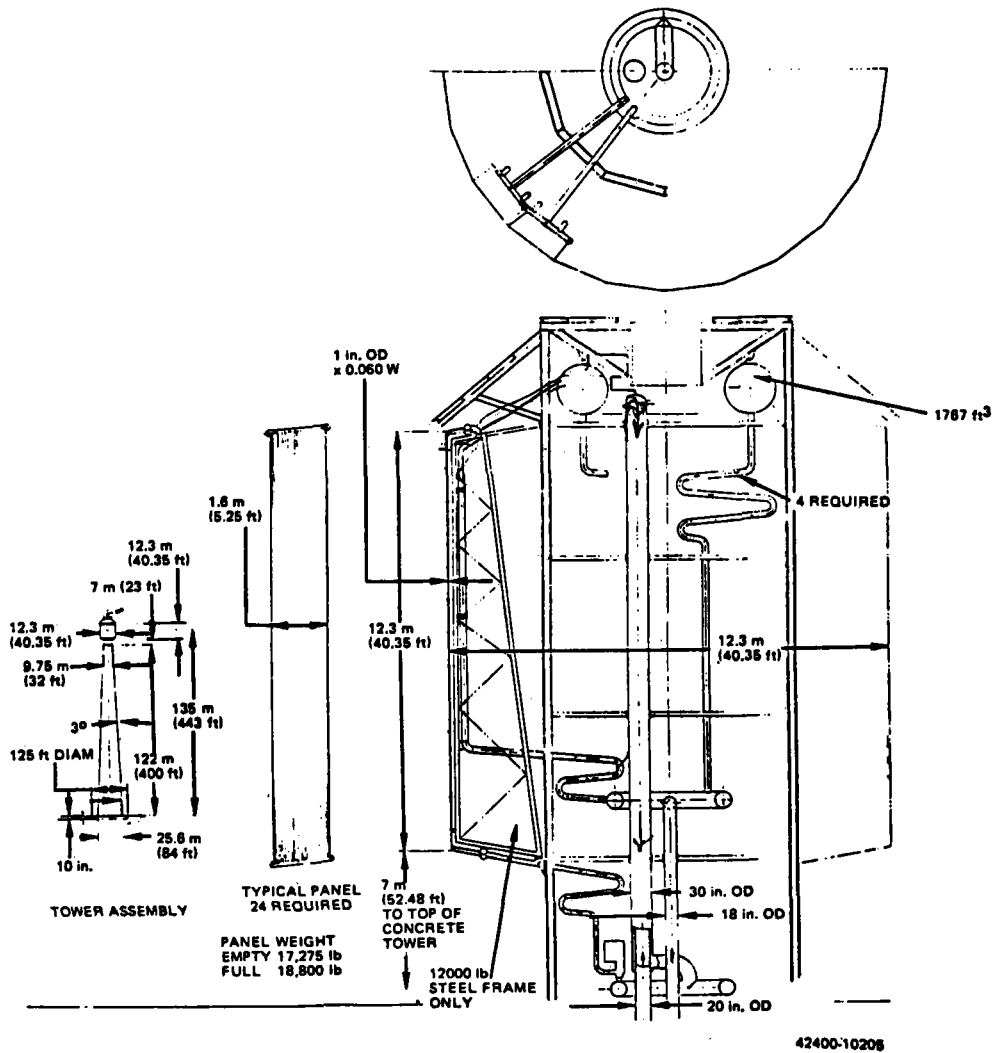
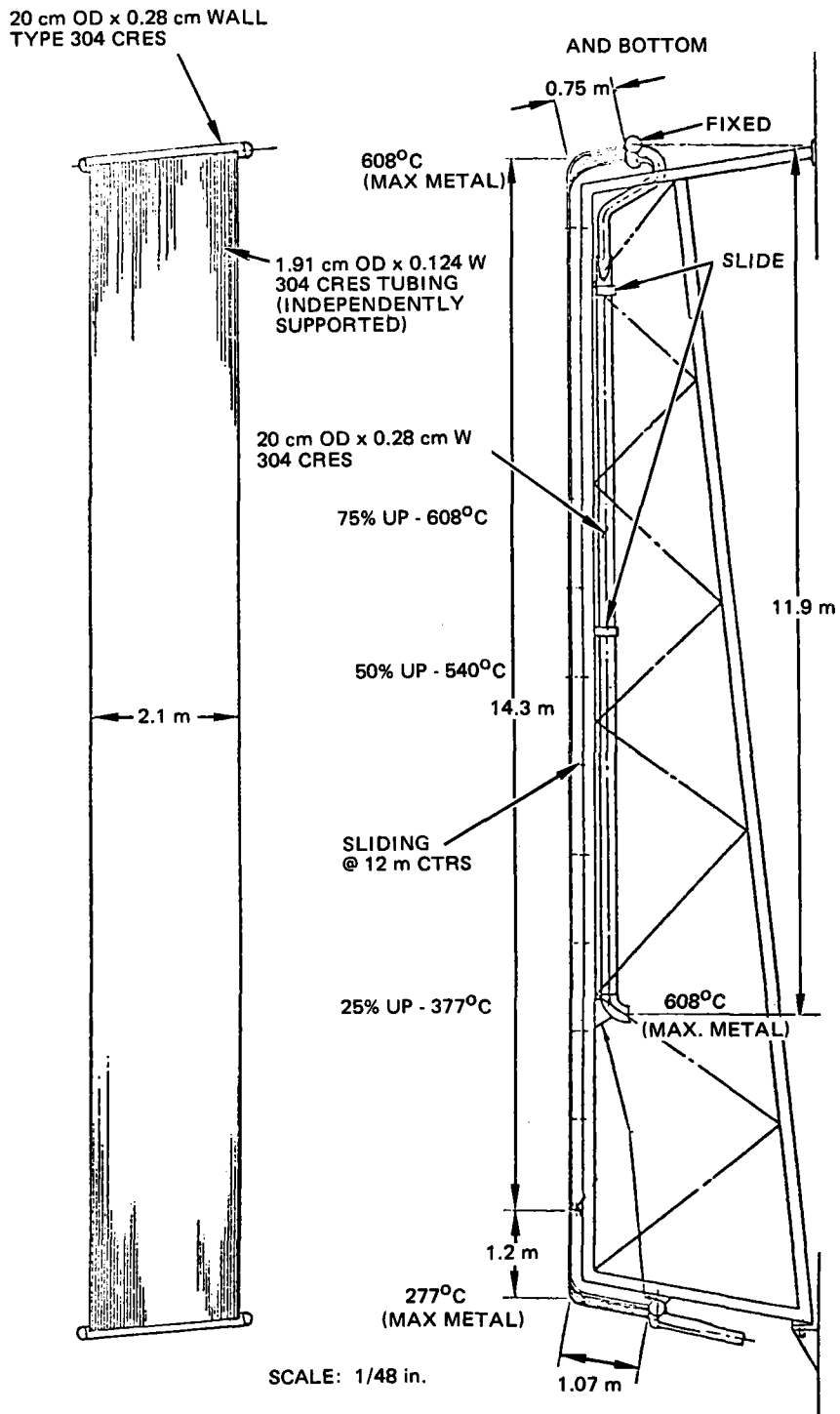


Figure 3-17. Baseline Receiver Design Layout for 0.9 SM Hybrid Plant



REF: 304 CRES @ 538°C
= 0.0000515 cm/°C

Figure 3-18. Panel Concept

The tubes enter manifolds at the top and bottom of the panels. The manifolds are constructed of 20-cm (8-in.) pipe with a 0.277-cm (0.109-in.) wall, and are the width of the panel. The manifolds at the bottom and top are connected to the main sodium riser pipe by means of a 20-cm (8-in.) pipe.

Each panel is supported by a full-length strong-back that is constructed of 15-cm (6-in.) box beams having a steel thickness of 0.953 cm (0.375 in.). Each strong-back is bolted to the vertical I-beam structure that is attached to the top of the tower. Behind each panel is a thin stainless steel thermal shield that serves to intercept any stray light beams that may enter between tubes. There is also thermal insulation between the panels and internal structure to prevent overheating of structures and reduce heat losses.

The riser pipe is connected to an antisiphon pipe which extends from a point below the panel base to well above the panels - a distance of 33 m (72 ft). It consists of an inner 51-cm (20-in.) pipe and an outer concentric 76-cm (30-in.) pipe. Sodium from the riser travels up the inner pipe, then returns down the outer annulus delivering sodium to the toroidal distribution ring at the base of the receiver.

An expansion tank is located near the top of the antisiphon pipe and above the panels and manifolds. It is a hexagonal torus measuring 8 m (26 ft) across the flat diameter and is constructed of six mitered pipes, each having a diameter of 1.8 m (6 ft). The expansion tank accommodates the effect of temperature changes in the sodium and the piping of the receiver loop. A crane hoist will be placed on top of the receiver to lift the panel and strong-back assemblies into position and remove them during maintenance periods. A circular shed roof is installed around the top of the receiver to protect against rain, snow, and hail.

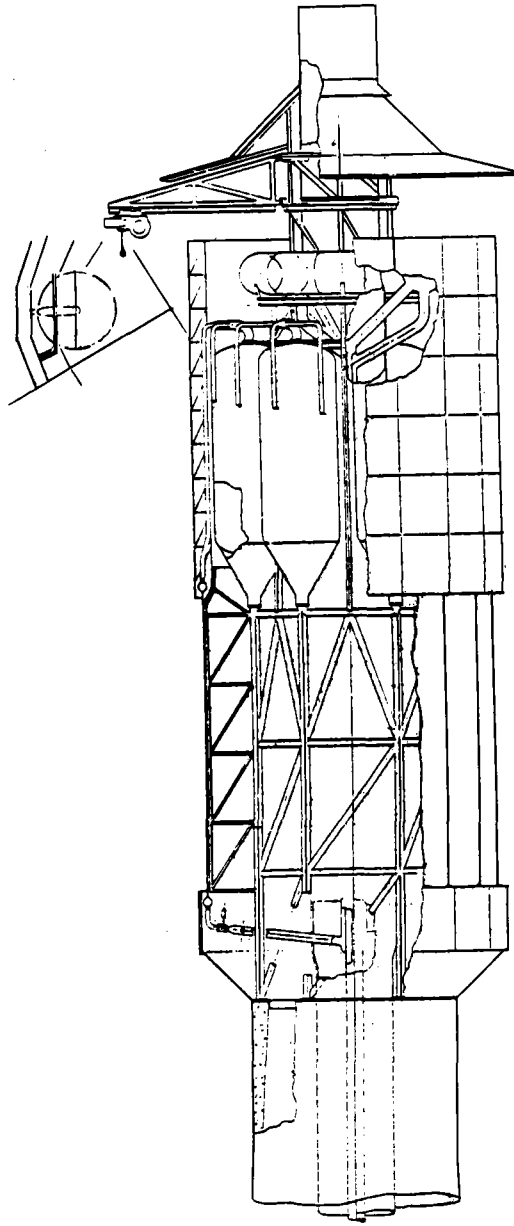


Figure 3-19. 0.8 SM Receiver – Buffer Tanks in Tower

3.3.1.3 Receiver for 0.8 SM Plant

For the 0.8 SM plant, several receiver concepts were evaluated. Figure 3-19 shows a concept with the cold and hot buffer tanks mounted on top of the tower above the external receiver. The cold tank is toroidal in shape, whereas the hot tanks are vertical horizontal components. The fossil-fired sodium heater stack is shown inside the tower and passes up through the receiver. A revised concept of this arrangement is shown in Figure 3-20. In this revised design, the toroidal cold tank is replaced with six cold buffer vertical tanks which are more cost effective than the single tank.

3.3.1.4 Receiver Heat Flux Study

A trade study was made to determine if it is cost effective to increase the receiver height to capture some of the incident heat flux and, at the same time, insulate sections of the receiver to reduce the thermal heat losses. The details of this study are presented in Appendix B. Results indicated that the small savings in cost did not make this concept worthy of any further study for the 100 MWe hybrid plant. However, as the receiver size is increased to the size required for the commercial solar plants, there may be more of a cost incentive to pursue this concept.

3.3.1.5 Receiver Panel Tube Orificing and Control Valve Reduction Study and Selection of Number of Panels

During the Phase I conceptual design study, it was proposed that the panel tube of the central receiver be orificed in order to flatten the temperature profile at the panel outlet. This would reduce panel thermal stresses and allow many more tubes per panel. Also, panel outlet temperature flattening would allow several panels to use the same flow control valve which would increase the system reliability.

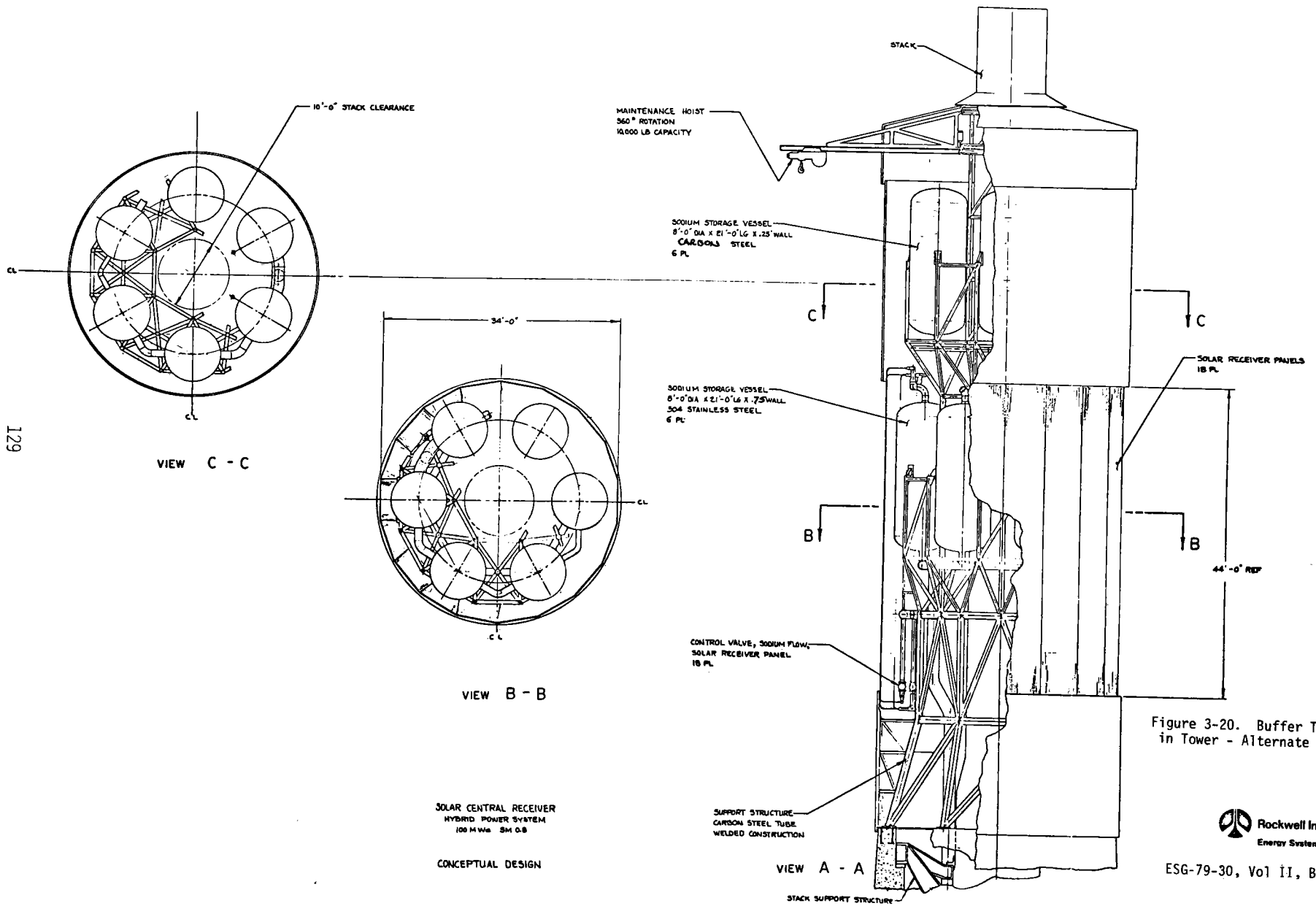
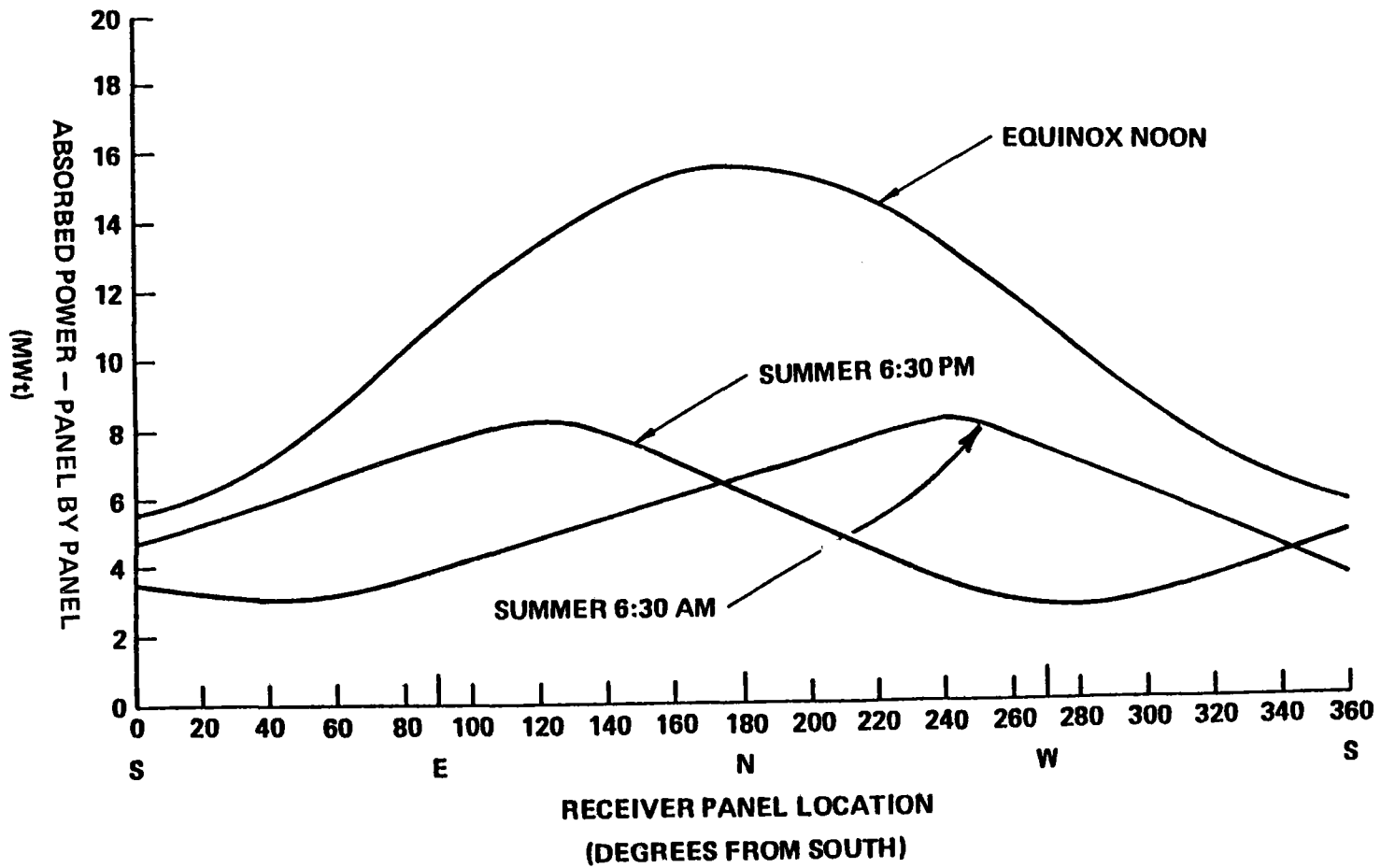


Figure 3-20. Buffer Tanks in Tower - Alternate 1

The technical feasibility of panel tube orificing requires relatively constant horizontal flux gradients across the panel. The outlet temperature of each tube depends upon the ratio of mass flow to heat absorbed by each tube. When a flux gradient exists across a panel and the flow in each tube is equal, the tube outlet temperature will be proportional to the local flux. Consequently, the outlet temperature profile of a panel will be flat if the ratio of mass flow to heat absorbed in each tube is constant. This can be accomplished by orificing individual tubes to achieve a panel flow distribution similar to the panel flux distribution. However, if the flux gradient of a panel which has orificed tubes changes slope, i.e., reverses, the flow distribution will oppose the flux distribution and result in temperature gradients and thermal stresses with higher magnitudes than if the tubes were non-orificed. Consequently, any panel in which a flux gradient reversal is expected to occur must be eliminated as a candidate for tube orificing.

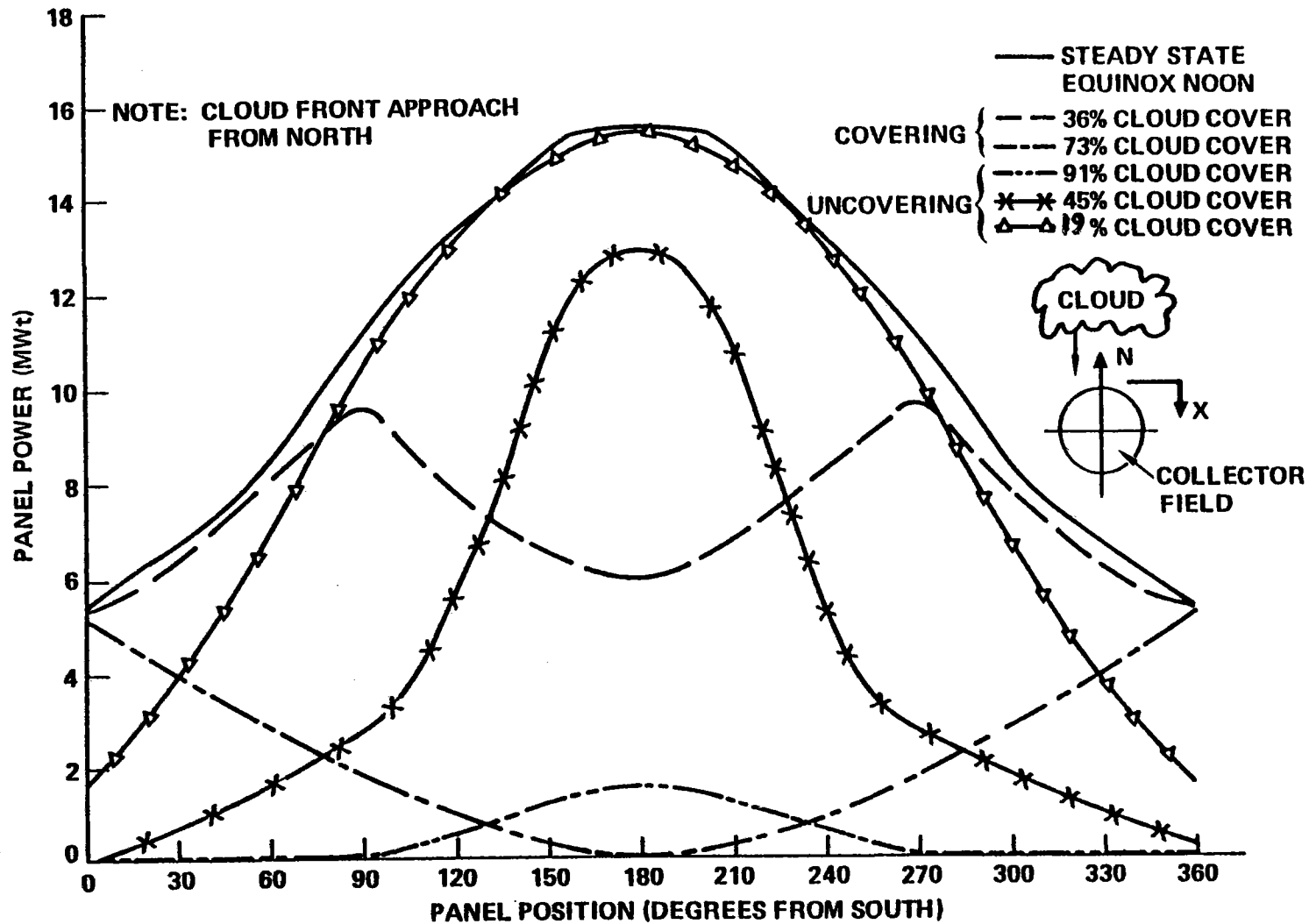
A study of the expected range of flux gradient variations as a function of diurnal variations and collector field assymetry was also made. The results are shown in Figure 3-21. As the sun moves across the sky, the optical interaction of the collector field and receiver results in flux gradient reversals in all panels except a few in the southeast to northeast quadrant and perhaps one or two panels in the northwest quadrant. On this basis, there are a few candidate panels for tube orificing.

Transient flux distributions must also be considered in the selection of candidate panels. If an opaque straight-edge cloud approaches from the north side of the collector field, the resulting flux distributions, as a function of cloud position, are shown in Figure 3-22. For a cloud whose shadow position is 73% of the way from the north field edge to south, the flux gradients of every panel have reversed compared to steady-state operation. Consequently, all panels have to be eliminated as orificing candidates if receiver operation continues beyond the time when the field and cloud shadow interact. Panels identified as candidates during steady-state considerations are still valid, however, if the field has been disengaged prior to the arrival of the cloud shadow.



79-MA31-52-4

Figure 3-21. Diurnal Variation in Circumferential Flux Distribution



79-MA31-52-5

Figure 3-22. Transient Incident Panel Powers

Similar observations can be made with regard to the proposal of using a single control valve for several panels. Flux gradient reversals due to diurnal or transient meteorological phenomena would cause flow maldistribution and result in excessive panel temperature gradients, except in the case where the mirrors are steered off the receiver prior to cloud cover transients.

The selection of the number of panels results from a trade study. A large number of panels results in small temperature gradients across the panel outlets but increased fixed panel fabrication costs and decreased system reliability due to increased valve requirements. Decreasing the number of panels decreases panel unit cost and increases system reliability at the expense of increasing panel outlet temperature gradients.

An engineering judgment of tube/header stress limitations has established 100 to 120⁰F as the allowable nominal temperature gradient across a panel. A study of the nominal temperature gradients across panels for the 0.8 SM, 208 Mwt receiver based on the flux information supplied by MDAC in Figure 3-21 was completed. The results of this study are shown in Table 3-8.

TABLE 3-8
NUMBER OF PANELS VS TEMPERATURE GRADIENT

<u>Number of Panels</u>	<u>Nominal Panel Gradient (⁰F)</u>
30	16 ⁰ C (28 ⁰ F)
24	27 ⁰ C (49 ⁰ F)
18	64 ⁰ C (115 ⁰ F)

Consequently, a 96-tube panel has been selected as the reference design for the hybrid plant receiver. This results in 18 panels.

Summarizing the results of these studies: (1) panel tube orificing and combination of panels to reduce numbers of control valves are not recommended if receiver operation is contemplated during cloud transients; (2) if the receiver can be shut down in a controlled manner, prior to cloud cover passage, such that flux gradient slopes are maintained, then five panels in the southeast quadrant and two panels in the northwest quadrant are good candidates for orificing and combination; and (3) the 18-panel configuration is the recommended starting point for any of these proposed changes.

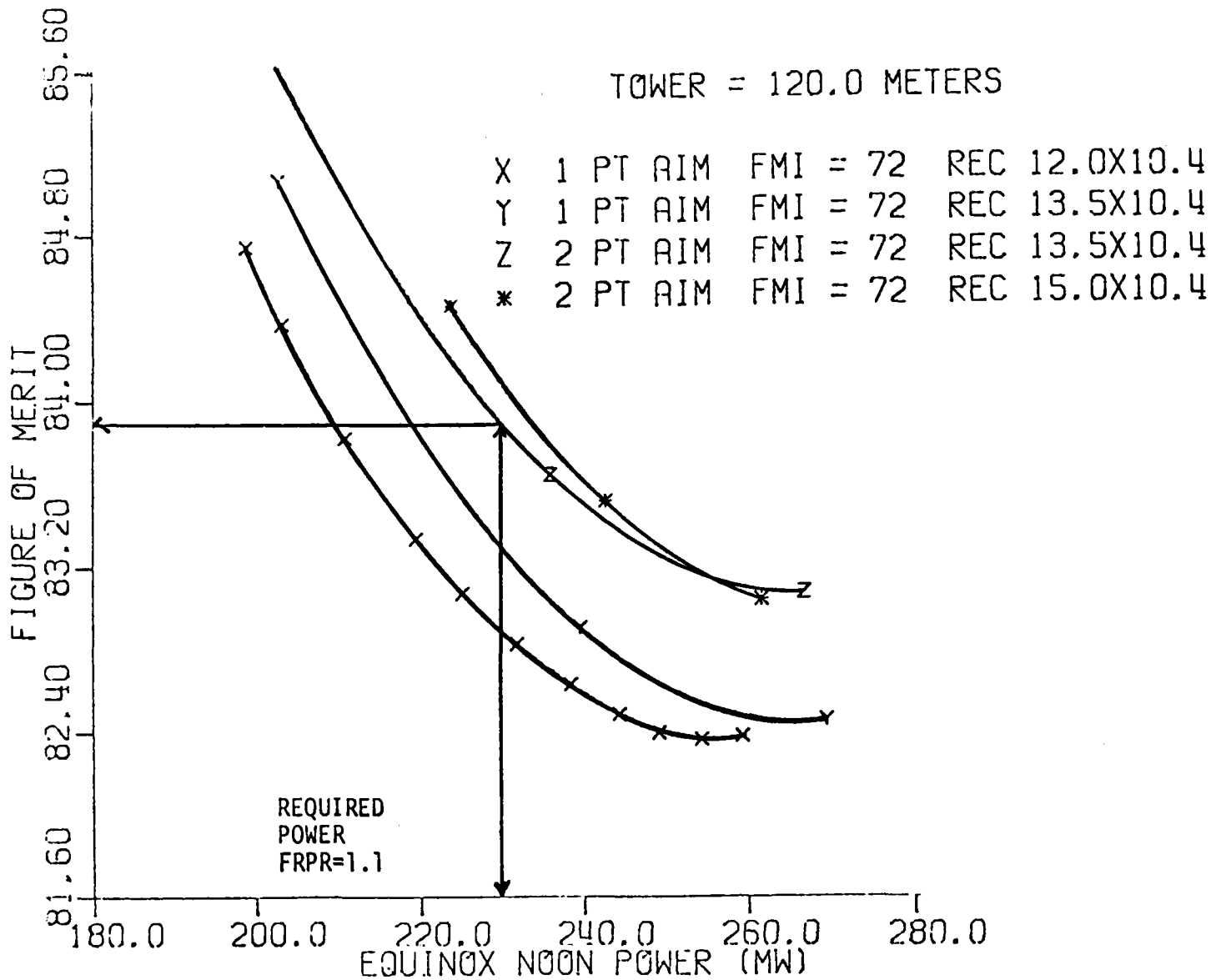


Figure 3-23. Solar Multiple = 0.8 Receiver Size Selection

3.3.2 Receiver Size

Solar Multiple = 0.8 Receiver

The selected receiver size for the 0.8 solar multiple system is 13.5 m in length by 10.4 m in diameter. The selection of this receiver size was a direct result of the aim strategy trade study (see Section 3.2.2) done during the collector field optimization. The lowest figure of merit (\$/Mwt-h annual) system resulted from a solar system with a smaller (10.4 m x 10.4 m) receiver. However, an analysis of the peak flux associated with this size receiver, utilizing single point (receiver equatorial) aim identified a peak flux in excess of the allowable flux from a receiver thermal stress standpoint. This necessitated looking at alternate aim strategies to reduce the peak flux. Because of excess spillage, there was little that could be accomplished in reducing the peak flux on the 10.4 x 10.4 m receiver without a relatively large loss of performance because of the spillage. Therefore, it was necessary to increase the receiver size to minimize the performance loss and still reduce the peak flux to an acceptable level. The system with the lowest figure of merit with an acceptable peak flux utilized a 13.5 m length by 10.4 m diameter receiver operated with two point aim and became the recommended receiver configuration for the solar multiple 0.8 reference system. These data are shown in Figure 3-23.

Solar Multiple = 1.4 Receiver

The results of the collector field optimization showed that the system with the lowest figure of merit at the required peak power of 364 Mwt (solar multiple = 1.4) was the system with a 15.3 m length by 13.0 m diameter. This can be seen in Figure 3-24 showing the family of systems using a 150 m tower.

This initial optimization was shown using one point aim and, as was the case with the solar multiple 0.8 system, resulted in a peak flux which exceeded the allowable value. However, in this case, the receiver was large enough, because of the higher peak power requirements associated with the solar multiple 1.4, to allow two-point aim without creating excess spillage, which would necessitate analyzing a larger receiver. This is due to the relative constant image size reflected on the receiver, which is enough smaller than the receiver to allow

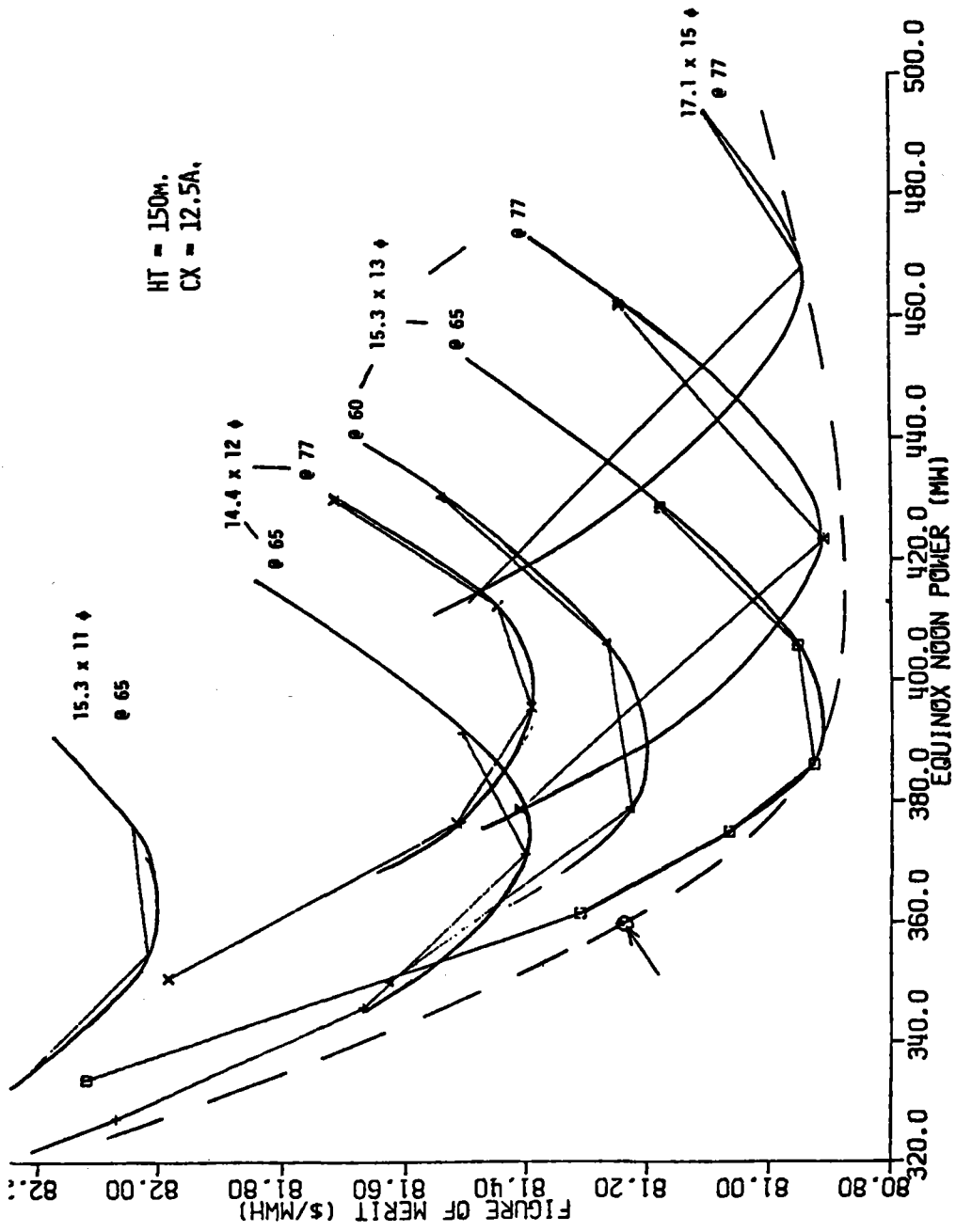


Figure 3-24. Solar Multiple - 1.4 Receiver Size Selection

the necessary spreading of the aim points to achieve acceptable peak flux levels. Therefore, the initial selection of the 15.3 x 13.0 m receiver was upheld. Subsequent analysis and performance estimates for the solar multiple 1.4 system were made assuming the two-point aim resulting in slightly higher figure of merit than initially calculated.

Preferred Commercial System

The selection of 28 m high by 25 m diameter receiver for the preferred commercial system was based, once again, on being the lowest figure of merit system at the chosen power level (1600 MWt). As was the case with the 100 MWe solar multiple 1.4 system, this optimization was done, for the sake of computational simplicity, using single point aim, as expected, resulting in a peak flux which exceeded the receiver design limitation. Again, because of the relatively large receiver size, the selection based on the single point aim data was considered invalid, since the receiver can accommodate multiple (up to three) aim points to reduce the peak flux without adversely affecting spillage losses. The data used in this selection are shown in Figure 3-25 as a family of curves for three different (one smaller and one larger) receiver sizes on a 330 m focal height tower.

3.3.3 Receiver Materials Selection

The material selected for the high-temperature receiver and down-comers is Type 304 stainless steel. Three materials were considered: Type 304, Type 316, and Alloy 800H. Table 3-9 presents the engineering basis for the material selection. While Type 316 and Alloy 800 have higher design allowables, it does not compensate for the higher material and fabrication costs. For the receiver, where fatigue cycling and thermal conductivity are important, Type 304 will have even more of an advantage. In other applications, Type 304 should result in lower cost but Type 316 could be substituted in specific instances where higher

EQUINOX NOON POWER VS. FIGURE OF MERIT
 FOCAL HEIGHT OF TOWER = 330.0 METERS

Y FMI = 75 REC 28.500X25.0
 Z FMI = 75 REC 25.147X23.0
 * FMI = 75 REC 31.853X28.5

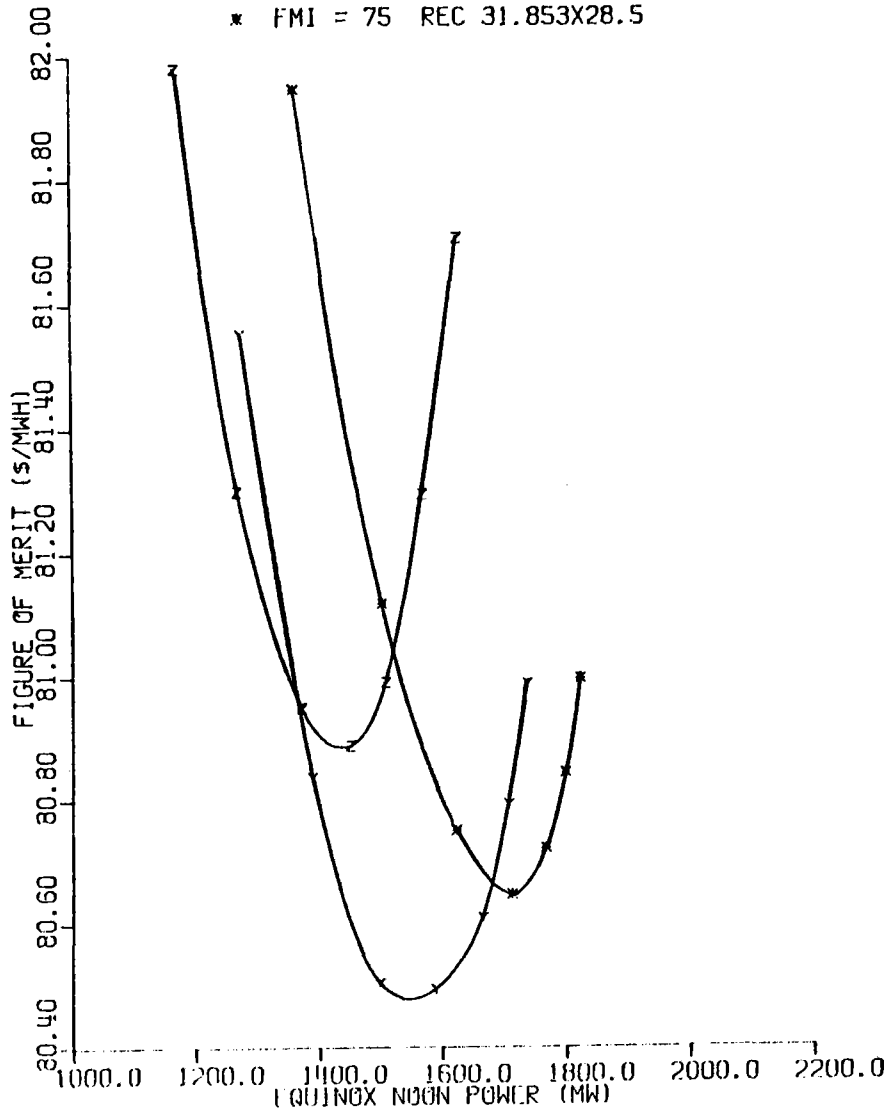


Figure 3-25. Receiver Sizing Preferred Commercial System

TABLE 3-9
ENGINEERING BASIS FOR MATERIAL SELECTION

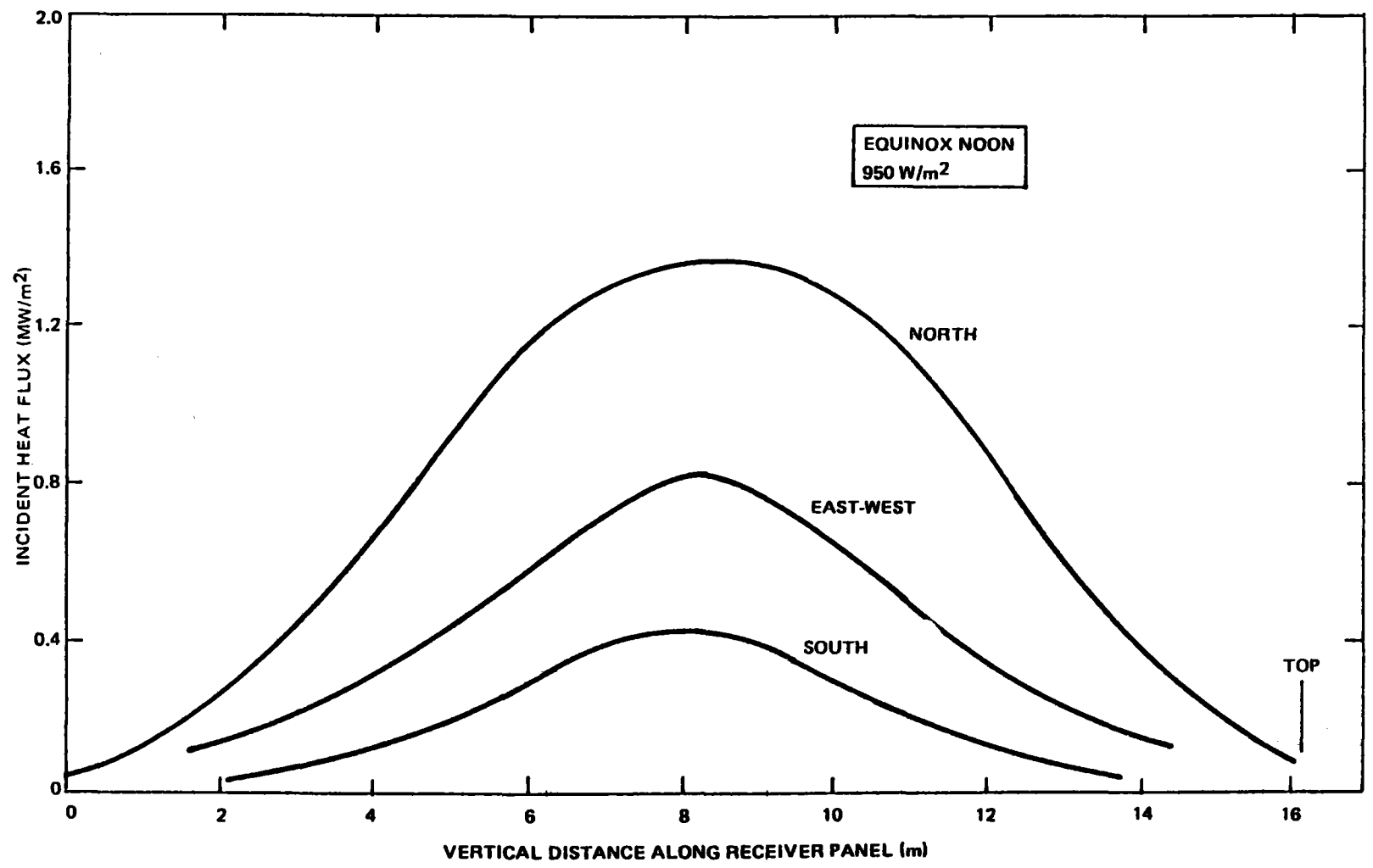
Material Properties @ 1100°F	Sym- bol	Units	Type 304	Type 316	Alloy 800
Design Allowables		ksi	9.8	12.4	13.0
Ratio	A		1.0	1.27	1.33*
Fatigue Strain Range @ 10 ⁴ cycles		10 ⁻³ in./in.	2.2	2.2	2.0
@ 10 cycles		10 ⁻³ in./in.	32.0	32.0	38.0
Ratio			1.0	1.0	1.0
Thermal Expansion (Av. 70°F 1100°F)		10 ⁻⁶ /°F	10.2	10.3	9.6
Ratio			1.0	1.01	0.94*
Thermal Conductivity		Btu/hr-ft-°F	13.6	12.9	12.1
Ratio			1.0*	0.95	0.89
Material Cost	M		1.0*	1.23	2.27†-4.54
Fabrication Cost Ratio (principally weldability)	F		1.0*	1.15	1.25
Total Cost Ratio§	T		1.0*	1.09	1.40

*Best material for given property.

†Material cost of 2.27 is used in the Total Cost Ratio.

§Total Cost Ratio takes into account differences in design allowables.

$$T = 0.333 M/A + 0.666 F$$



42400-10210

Figure 3-26. Receiver Heat Flux Distribution

design allowables or material weight savings are needed. In addition, Type 304 has a proven performance record in high-temperature sodium systems since the 1950's. It possesses adequate strength for the intended application. Its technical base is founded on extensive research, particularly of recent years at the national laboratories such as Oak Ridge and Argonne, as well as widespread practical experience.

Where a very high-strength alloy is required, such as in bolting or in shields against thermal striping, the precipitation-hardenable nickel-base alloy, Inconel 718, will be specified. This alloy is the current choice of material in many high-temperature, high-strength applications.

The low-temperature regions such as the riser will be of carbon steel. Transitions between the low-temperature carbon steel and the high-temperature austenitics will use an alloy, Inco 82, which has essentially the same composition as Inconel 600. This is also a well established, proven transition welding alloy.

The remainder of the high-temperature portion of the system, except for the pumps, will be of Type 304. The pump cases will be of Type 316, and the impellers will be of CF8M, which is the cost equivalent of Type 316. This selection is based on the designs of sodium pumps made of these alloys. Contacting surfaces such as valve seats and pump bearing will be hardfaced with stellite.

3.3.4 Receiver Thermal Performance Analysis

The highest heat flux, as shown by the typical ACR data of Figure 3-26, is on the north facing panel. Tube wall temperatures are calculated using the flux data for the specific collector field. Peak wall temperatures occur at about three-quarters the distance to the top of the panel. From analysis of this type, the thermal stresses within the tube wall are determined. The purpose of these calculations is to determine

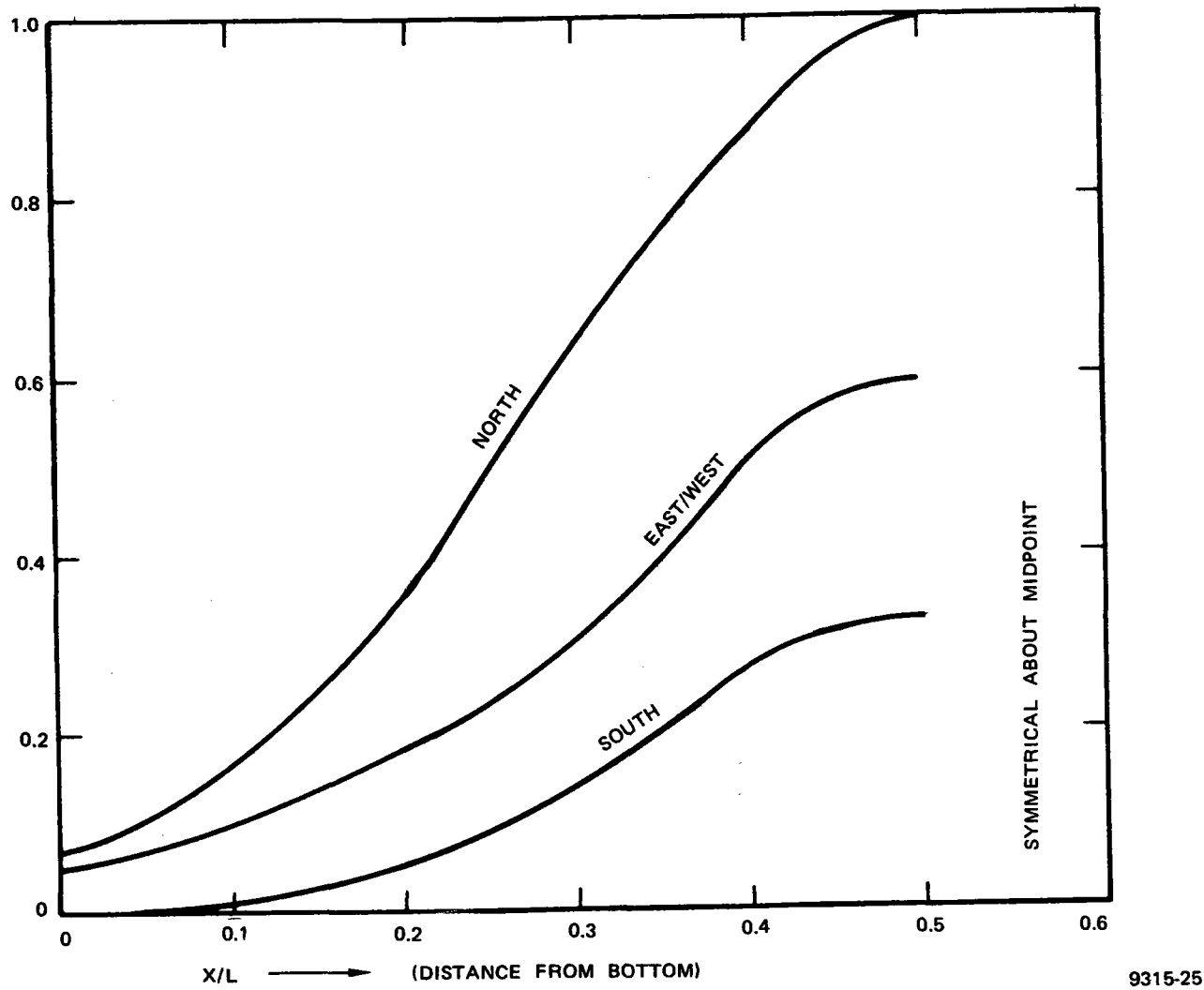


Figure 3-27. Normalized Receiver Heat Flux Profiles: Based on Equinox Noon

panel life and supply design information such that the panel and receiver as a whole may be designed to minimize the effects of thermal expansion, changing and uneven heating and cooling, and to provide the temperature data for the thermal loss calculations.

Calculation of the thermal heat losses from the sodium receiver have been carried out as follows: The reflected insolation loss is calculated from the solar absorptance of Pyromark ($\epsilon = 0.95$). The infrared loss is calculated from an integrated surface temperature for the receiver. Convective losses are estimated using a high Reynolds number average heat transfer coefficient for a roughened cylinder in cross-flow.

A preliminary thermal analysis of the baseline receiver sodium-cooled panels for the ACR was performed. A discussion of this analysis follows and is directly applicable to the hybrid plant.

The incident heat flux was obtained from the University of Houston for the case of equinox noon. These ACR data plotted in normalized form are shown in Figure 3-27 for the north, east-west, and south panels.

The ACR baseline power at the time of the analysis was 429 MWt. The sodium inlet and outlet temperatures were 288°C (550°F) and 594°C (1100°F), respectively. The receiver flow rate at this maximum power condition was 3,975,000 kg/hr (8,744,500 lb/hr).

The receiver had 24 panels, each consisting of 110 tubes, there being 2640 tubes in all. Each tube had an OD of 1.91 cm (0.75 in.) and a wall thickness of 0.124 cm (0.049 in.). These tubes were made of Type 304 stainless steel.

The receiver was divided into four quadrants - north, east, west, and south. At equinox noon, the characteristics of the east and west quadrants were identical. Each of the four quadrants was analyzed on the

basis of its average properties. Table 3-10 shows the flow fraction, flow rate, and heat input for each quadrant.

The heat transfer correlation for sodium flowing in tubes was:

$$Nu = 7.0 + 0.025 (PrRe)^{0.8}$$

TABLE 3-10
RECEIVER QUADRANT FLOW AND HEAT INPUT

Quadrant	Flow Fraction	Flow Rate (kg/hr)	Heat Input (Mwt)
North	0.425	1.69×10^6	182
East	0.235	0.93×10^6	101
West	0.235	0.93×10^6	101
South	0.105	0.42×10^6	45

where (in consistent units)

$Nu = hD/K_w$, Nusselt Number

$Pr = C_p u / K_f$, the Prandtl Number

$Re = DV/u$, the Reynolds Number

h = sodium heat transfer coefficient

D = tube diameter

C_p = specific heat of sodium

u = viscosity of sodium

K_f = thermal conductivity of sodium

ρ = sodium density

V = sodium velocity

K_w = thermal conductivity of stainless steel

Each panel will have the flow metered by the panel control valves so that the outlet temperature is very nearly a constant. Thus, the flow velocity will vary among the panels from 0.933 m/s (3.06 f/s) in the south quadrant to 4.05 m/s (13.3 f/s) in the north quadrant. Because of the temperature and velocity variations, the sodium heat transfer coefficient will range from 30260 W/m²-K (5337 Btu/hr-ft²-°F) at the hot end of the south quadrant to 52170 W/m²-K (9201 Btu/hr-ft²-°F) at the cool end of the north quadrant.

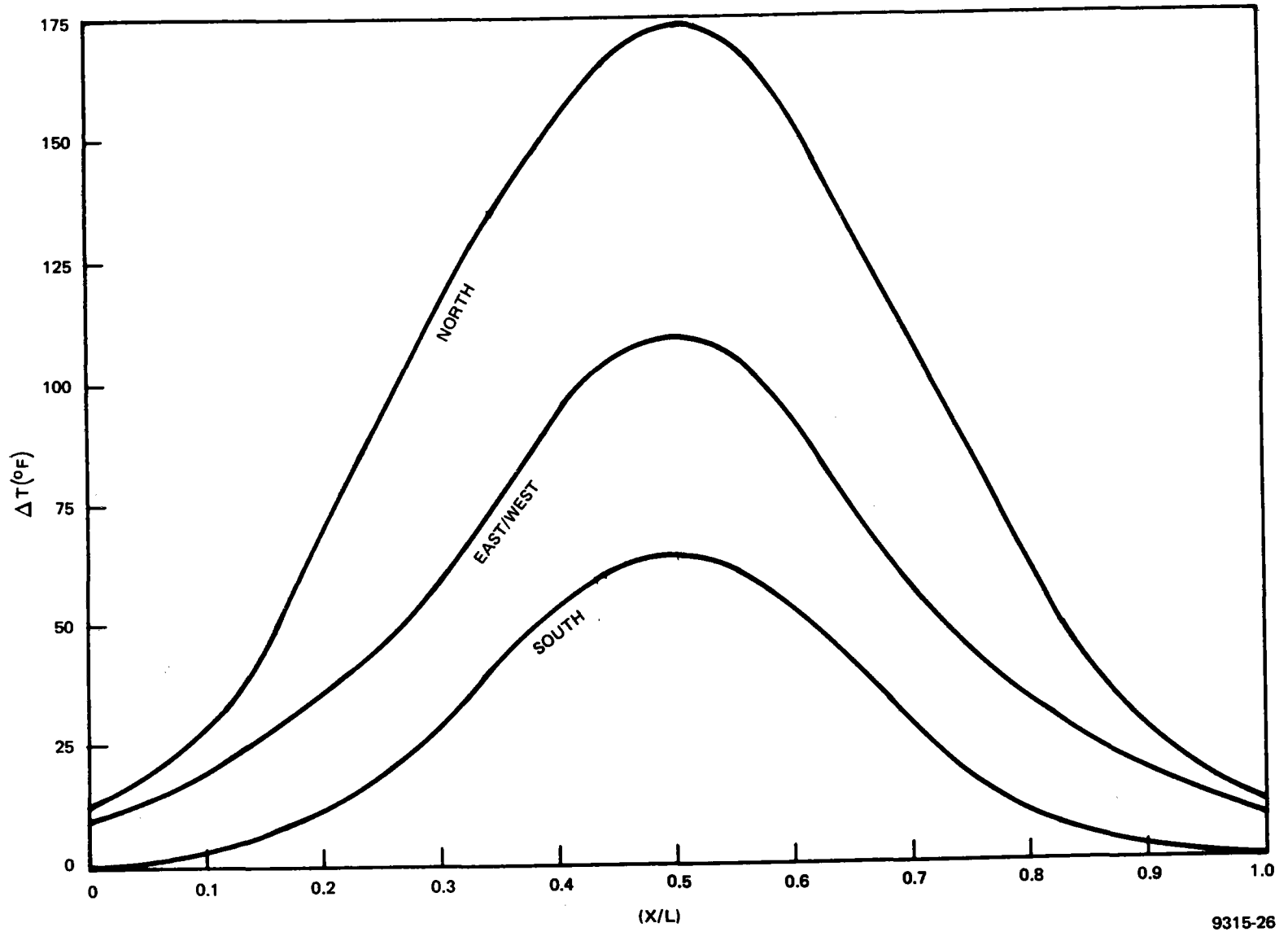
K_w varies from about 18.2 W/m-K (10.5 Btu/hr-ft-°F) to 22.3 W/m-K (12.9 Btu/hr-ft-°F) from the cool inlet of the receiver to the hot exit. The conductance across the wall thickness is K_w/x , where K_w is the thermal conductivity of the wall and x is the wall thickness.

The overall heat transfer coefficient, U , is:

$$U = \frac{1}{\frac{x}{K_w} + \frac{1}{h}}$$

This coefficient is controlled more by the wall conductance than by the sodium conductance. Values of U range from 9871 W/m²-K (1741 Btu/hr-ft²-°F) at the cold end of the south quadrant to 12179 W/m²-K (2148 Btu/hr-ft²-°F).

The ΔT between the outer tube surface and the bulk sodium was calculated assuming that one-half of each tube surface is available for heat transfer and using the values of U at each point on the receiver. The maximum ΔT 's ranged from 35.3°C (63.6°F) at the midpoint of the south quadrant to 96.3°C (173.4°F) in the north quadrant. Figure 3-28 shows the ΔT 's at various points on the baseline receiver. When these ΔT 's are added to the local sodium temperatures then the peak metal temperatures at all points on the receiver are obtained. Figure 3-29 shows these temperatures.



9315-26

Figure 3-28. ΔT Through Tube Wall and Na Film

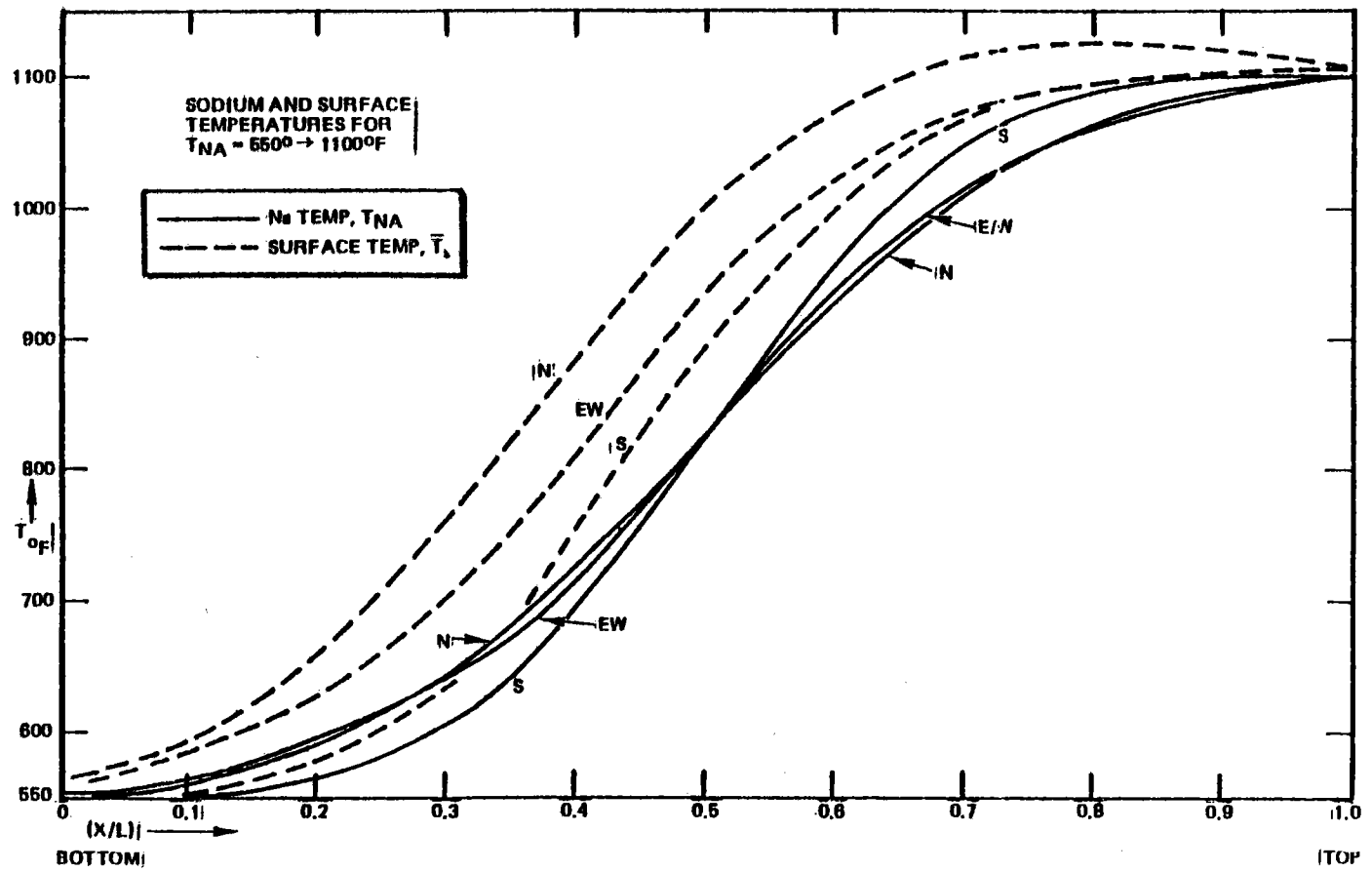


Figure 3-29. Axial Temperature Distribution on Solar Panel Tubes

After this analysis was performed, the maximum receiver power for the ACR was reduced from 429 to 390 MWt. On the other hand, since the temperatures of the north quadrant represent an average case, the peak temperature in that quadrant will be somewhat greater. The current peak ΔT is estimated to be 119°C (214°F), and the peak metal temperature will be 618°C (1144°F) instead of the 608°C (1125°F) shown in Figure 3-29.

A study was made of the thermal losses that occur in the ACR external receiver. Table 3-11 lists the assumptions used in this study. Figure 3-29 shows the normalized equinox noon receiver incident power distribution which was adapted to the ACR baseline 16 m x 16 m (53 ft x 53 ft) receiver. The receiver model was divided into eighty small sections, each of which was losing heat to the surroundings by reflection, radiation, and convection.

TABLE 3-11
ASSUMPTIONS FOR THERMAL LOSS STUDY

Equinox, Noon Incident Power Distribution
288°C Sodium In, 593°C Sodium Out
Four Azimuthal Quadrants
Twenty Vertical Sections
Solar Absorptance in Pyromark = 0.95
Emittance = 0.90 Effective
Roughness of Cylinder = 60×10^{-5}
Achenbach Heat Transfer Correlation Plus Natural Convection
Winds from 0 to 16 m/s (36 mph)

The radiation emittance chosen was 0.90, which is somewhat conservative. For the convection heat transfer, the correlation of Achenbach was used. The Achenbach experiments were performed at a high Reynolds number, but not quite as high as the value of 10^7 that could be reached by an external receiver in a high wind. The effects of natural convection were added to the forced convection value. The results of this study are given in Section 5.3.3. The detailed study is given in Appendix F of Reference 3-1.

References 3.3-1 and 3.3-2 are informal papers presented at the Sandia Laboratories/Department of Energy Workshop on Convective Losses from Solar Receivers, held at Dublin, California, April 17-18, 1979.

In Reference 3.3-3, P. Oosthizen and R. Leung propose $N = 2$ on the basis of experimental data. In Reference 3.3-1, B. Pomeroy and V. Kadambi use $N = 2, 3,$ and 4 just as a mathematical variable.

In the matter of the analysis of the convective heat losses from the solar receiver, the question has been raised from time to time as to how to determine the net effect of both forced convection (due to wind) and natural convection (due to thermal buoyancy).

The method currently being employed generally for this type of analysis is to first calculate the heat transfer coefficients for forced and natural convection as if each were acting alone. Then, an effective heat transfer coefficient is determined according to one of several suggested methods: a simple addition of the two coefficients, choosing the larger of the two coefficients, or combining by a formula that is intermediate to these two methods.

There would seem to be something intuitively satisfying about the root-mean-square ($N = 2$) proposal. It gives the idea of a vectorial resolution of two gas velocities flowing at right angles to one another.

In Figure 3-30, a plot is shown of $h(\text{effective})$ as a function of $h(\text{larger})$, $h(\text{smaller})$, and the assumed value of N . Note that either $h(\text{forced})$ or $h(\text{natural})$ can be $h(\text{larger})$ or $h(\text{smaller})$, merely depending upon their calculated magnitudes. It is obvious that if one of the heat coefficients is much larger than the other, it controls the value of the effective heat transfer coefficient. Only in those cases where the two heat transfer coefficients are of the same order of magnitude is the determination of a combined heat transfer coefficient of interest.

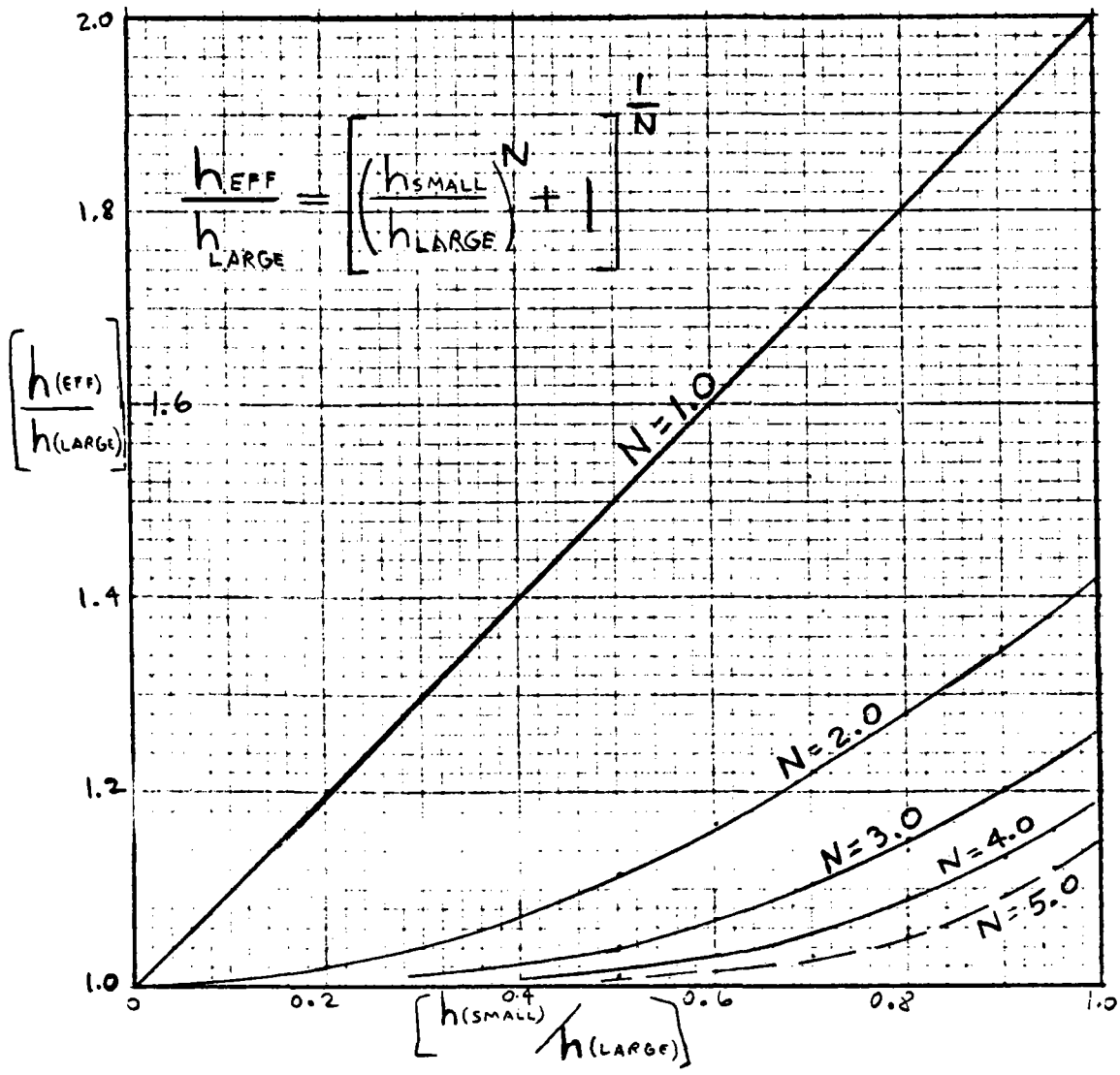


Figure 3-30. Combined Heat Transfer Coefficient

Effective heat transfer coefficient, h_{eff} , based on combining h_{forced} and h_{free} according to the indicated equation.

(Based on considering the larger and smaller values of the two h's.)

Figure 3-31 is a plot taken from Reference 3.3-1. It is proposed to represent some experimental data by the root-mean-square rule ($N = 2$). Curves are presented in Figure 3-31 for $N = 1, 3,$ and 4 to give a better idea of how well the curve of $N = 2$ fits. Notes are added to Figure 3-31 to indicate variables according to the nomenclature used previously.

Calculation sheets are included from which Figure 3-32 has been plotted.

Suppose we assume:

$$h_{\text{eff}} = \left[(h)_{\text{forced}}^2 + (h)_{\text{nat}}^N \right]^{\frac{1}{N}} = \left[(h)_{\text{larger}}^N + (h)_{\text{smaller}}^N \right]^{\frac{1}{N}} \quad 1$$

$$\text{with } 1 \leq N \leq \infty$$

This can be rewritten:

$$\frac{h_{\text{eff}}}{h_{\text{larger}}} = \left[1 + \left(\frac{h_{\text{smaller}}}{h_{\text{larger}}} \right)^N \right]^{\frac{1}{N}} \quad 2$$

$N = 1$ straight addition:

$$h_{\text{eff}} = h_{\text{large}} + h_{\text{small}}; \quad \frac{h_{\text{eff}}}{h_{\text{larg}}} = \left[1 + \frac{h_{\text{small}}}{h_{\text{large}}} \right] \quad 2-1$$

$N = 2$ root mean square:

$$h_{\text{eff}} = \left(h_{\text{large}}^2 + h_{\text{small}}^2 \right)^{\frac{1}{2}}; \quad \frac{h_{\text{eff}}}{h_{\text{larg}}} = \left[1 + \left(\frac{h_{\text{small}}}{h_{\text{larg}}} \right)^2 \right]^{\frac{1}{2}} \quad 2-2$$

$N = 3, 4, \text{ other:}$

$$\frac{h_{\text{eff}}}{h_{\text{larg}}} = \left[1 + \left(\frac{h_{\text{small}}}{h_{\text{larg}}} \right)^N \right]^{\frac{1}{N}} \quad 2-3$$

$N = \infty, \text{ choose larger } h \text{ only:}$

$$h_{\text{eff}} = h_{\text{larg}}; \frac{h_{\text{eff}}}{h_{\text{larg}}} \left[1 + \left(\frac{h_{\text{small}}}{h_{\text{larg}}} \right)^{\infty} \right]^{\frac{1}{\infty}} \rightarrow 1.0 \quad 2-N$$

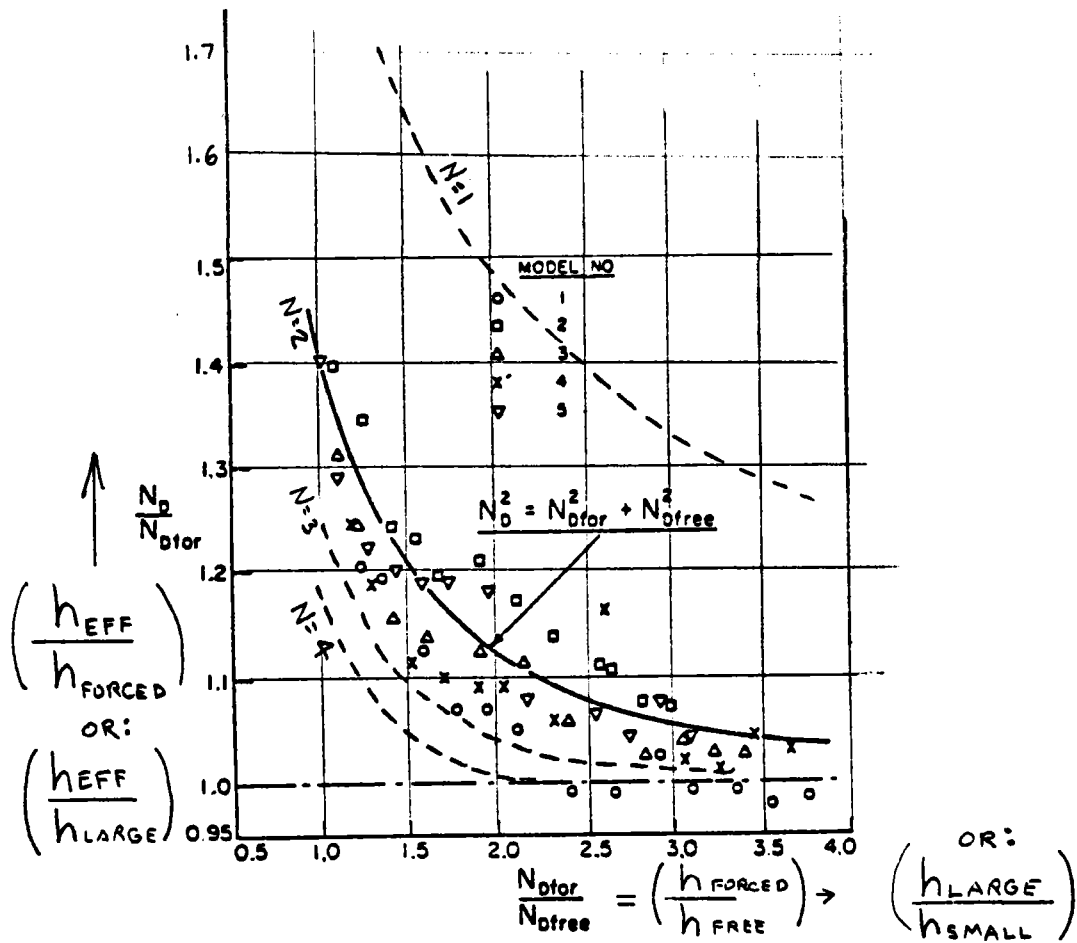
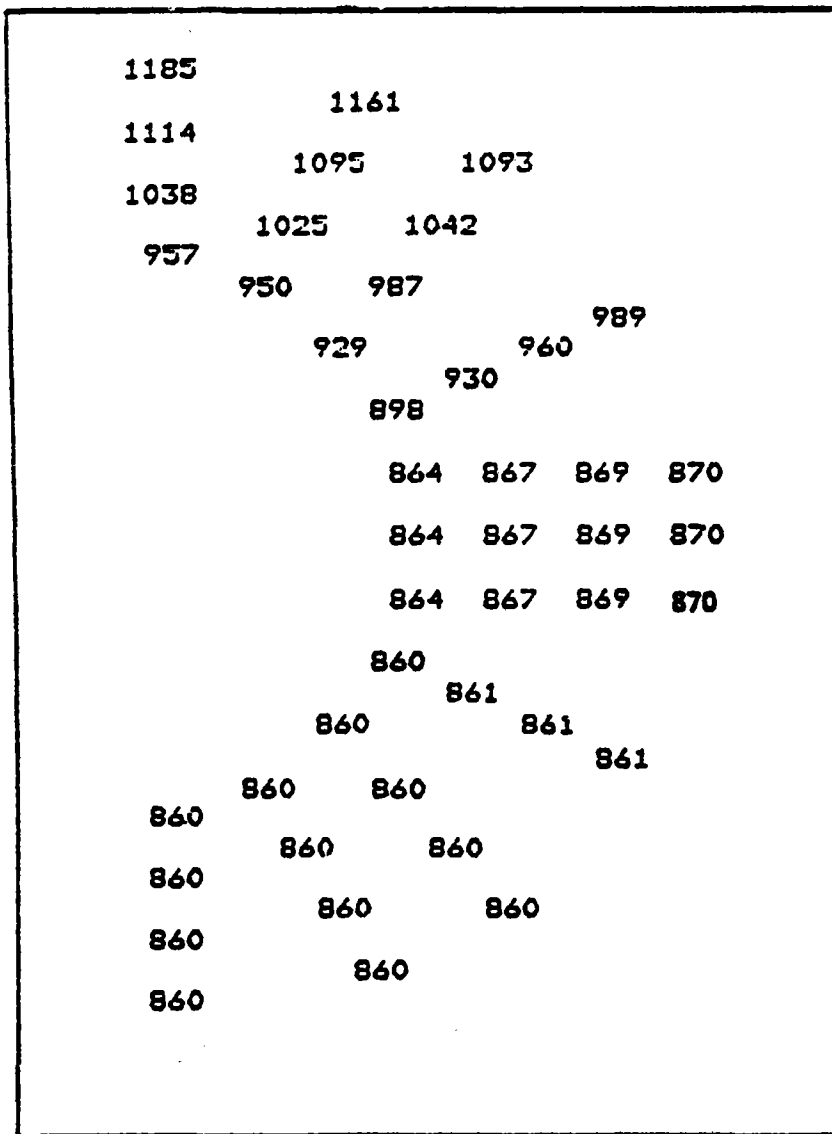


Figure 3-31. Heat Transfer in Combined Free and Forced Flows

Curve taken from Oothuizen and Leung (Ref. 3.3-3).

Curves for $N = 1, 3$ & 4 have been added, along with "clarifying" notes.



NOTE:
Temperature
in °F

Figure 3-32. Advanced Receiver Tube Temperature Profile
 Equinox Noon - North Side
 1.9 cm (3/4-in.) OD - 0.127 cm (0.05-in.) Wall
 Elevation 8.5 m, Heat Flux at Crown 2.15 MW/m²
 One-Point Aim Strategy, 15 m Receiver, CRES 304 Tubes

3.3.5 Absorber Panel Life Analyses

Structural analyses of the receiver subsystem were confined to those sub-components most influenced by solar flux changes during service, i.e., the solar panel tubing, manifolds, and outlet piping. A piping flexibility/stress analysis was performed using an in-house, finite-element computer code, DRIPS* to predict deadweight and thermal expansion stresses in the solar panel tubing and outlet piping. The thermal inputs to this analysis were based on tubing cross-section temperature distributions for the conceptual receiver design at the north side - equinox noon. Thermal gradient stress analyses were performed based on closed-form cylinder equations with the same thermal inputs as used in the piping flexibility/stress analysis. Evaluations of predicted results were performed utilizing ASME B&PV Code criteria and material data generated to support development of Code rules for construction of pressure vessel components in elevated temperature service. It was concluded that the design of the receiver can meet the requirements of Section VIII of the Code and the strain cycle criteria of Code Case N-47(1592) of Section III, Class 1, of the ASME B&PV Code. The following paragraphs provide a more detailed summary of these conceptual design activities and results.

3.3.5.2 Thermal Inputs

Both the piping flexibility/stress analysis and thermal gradient stress analysis required a detailed definition of thermal profiles in the solar panel tubes at all locations along the length of the tubes. The north side tube panel was selected as the reference case since the highest solar flux exists at this location and, therefore, the highest thermal stresses will also occur here. Conceptual thermal analyses were performed which resulted in predicted tube (hot-side) outside temperatures and sodium temperatures at this location as a function of axial location in the receiver. Figure 3-29 presents these results. Detailed thermal flux analyses have been performed which predicted tube cross-section thermal profiles for various flux levels. Figure 3-32 is a typical predicted thermal profile. An equivalent tube (hot-side) outside temperature was developed for these various profiles and equations established which could relate key temperature values and gradients in the tube cross-section to the difference between outside tube temperature and sodium temperature. Thus, utilizing these equations, the key temperature values and gradients for the conceptual design could be

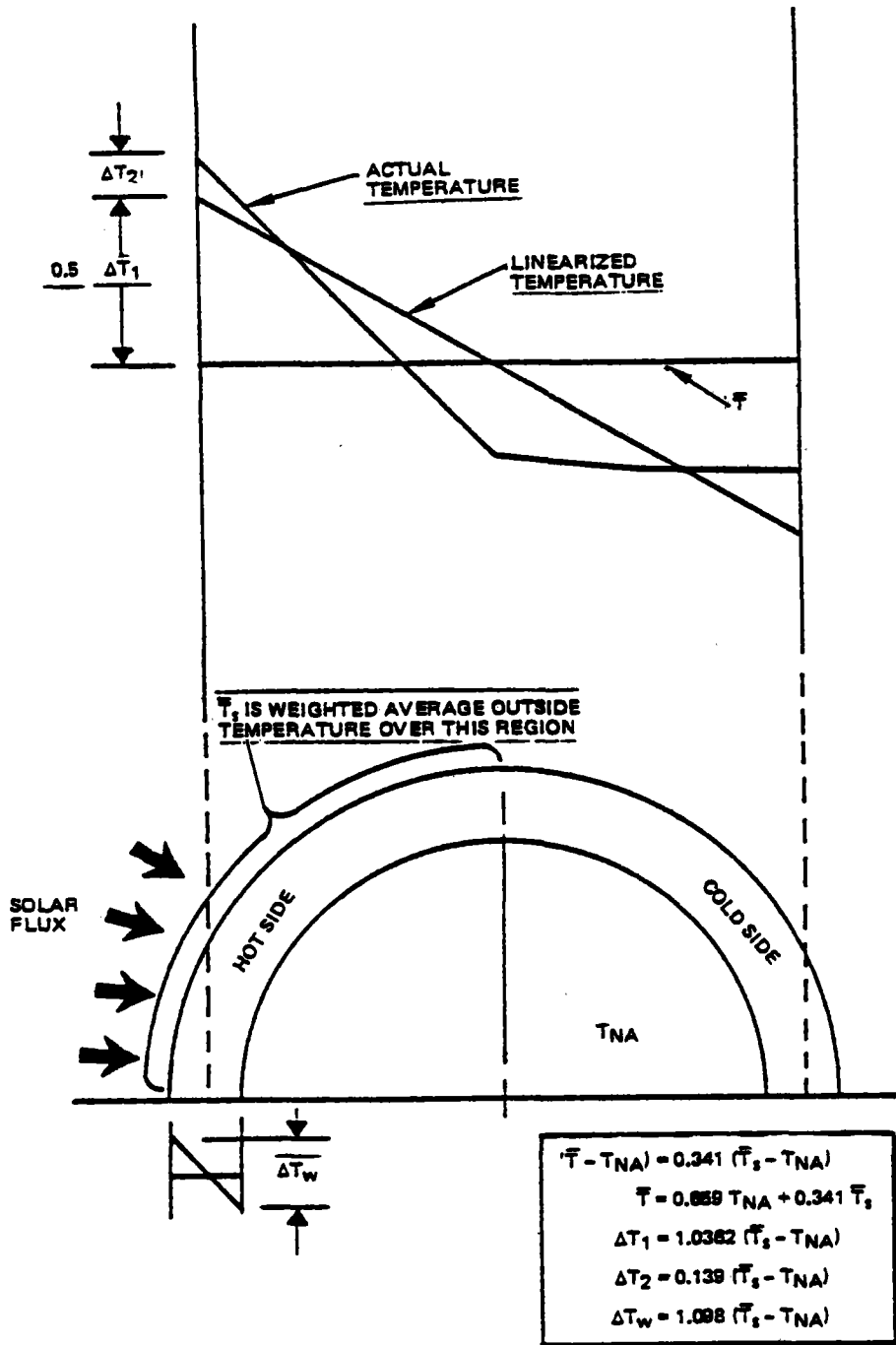


Figure 3-33. Derived Temperature Relationships

determined. Figure 3-33 presents these equations and temperature definitions while Table 3-12 summarizes the results of this effort.

3.3.5.3 Piping Flexibility/Stress Analysis

Figure 3-34 is the model of the solar panel tubes and outlet piping employed in the DRIPS flexibility/stress analysis. Hand calculations were utilized to determine an optimum location of anchor points to minimize the stresses at the outlet piping bends. Basically, the axial thermal expansion of the solar panel tubes away from the lower axial support was matched to the axial thermal expansion of the outlet piping away from its axial support location. By inputting the linearized across-the-tube temperature gradients (ΔT_1) and bulk metal temperatures (T) for the solar panel tubing, the program could compute thermal induced moments at all nodal locations along the computer model. ASME Code B31.1 stress intensification factors were then used to calculate stresses at all piping locations.

Stresses due to weight and pressure loadings were calculated using DRIPS computed moments and conventional ASME Code B31.1 design procedures.

The results of these analytical efforts are summarized in Table 3-13. Figure 3-35 is a computer plot of exaggerated piping displacement due to the thermal loadings. Note that the utilization of solar panel tube supports essentially provides full restraint of the across-the-tube thermal moments as evidenced by minimal bowing of the tubes between support locations. This is important with respect to gapping considerations that exist when an individual tube concept is employed versus alternate integral tube wall concepts.

3.3.5.4 Thermal Gradient Analyses

Stresses due to linearized across-the-tube thermal gradients and overall thermal expansion were considered in the piping flexibility/stress analysis. This leaves only consideration of peak across-the-tube thermal gradients (ΔT_2) and through-the-wall thermal gradients (ΔT_w), to complete the thermal loading evaluation. This was done by assuming the maximum values of these gradients, located at the crown of the hot side of the tube, acted uniformly around the

TABLE 3-12

DERIVED TEMPERATURE VALUES IN SOLAR PANEL

X/L*	T _{Na} (°F)	T _s (°F)	T (°F)	ΔT ₁ (°F)	ΔT ₂ (°F)	ΔT _w (°F)
0	550	562	554.1	12.4	1.7	13.2
0.033	550	571	557.2	21.7	2.9	23.1
0.066	554	580	562.9	27.0	3.6	28.5
0.106	561	595	572.6	35.3	4.7	37.3
0.146	572	617	587.3	46.6	6.3	49.4
0.187	583	647	604.8	66.3	8.9	70.3
0.227	601	683	629.0	85.0	11.4	90.0
0.268	622	725	657.1	106.7	14.3	113.1
0.308	648	770	689.6	126.3	17.0	134.0
0.348	678	819	726.1	146.1	19.6	154.8
0.389	713	870	766.5	162.6	21.8	172.4
0.329	751	920	808.6	175.0	23.5	185.6
0.470	793	970	853.4	183.4	24.6	194.3
0.510	834	1010	894.0	182.4	24.5	193.2
0.550	877	1040	932.6	168.8	22.7	179.0
0.591	918	1065	968.1	152.3	20.4	161.4
0.631	952	1088	998.4	140.9	18.9	149.3
0.672	985	1106	1026.3	125.3	16.8	132.9
0.712	1015	1116	1049.4	104.6	14.0	110.9
0.752	1041	1122	1068.6	83.9	11.3	88.9
0.793	1061	1124	1082.5	65.2	8.8	69.2
0.833	1073	1123	1090.1	51.8	6.9	54.9
0.873	1084	1120	1096.3	37.3	5.0	39.5
0.914	1091	1118	1100.2	28.0	3.8	29.6
0.954	1096	1114	1102.1	18.6	2.5	19.8
0.977	1098	1111	1102.4	13.4	1.8	14.3
1.000	1100	1108	1102.7	8.3	1.1	8.8

*X/L denotes the vertical location along the receiver solar panel as a fraction of the panel height.

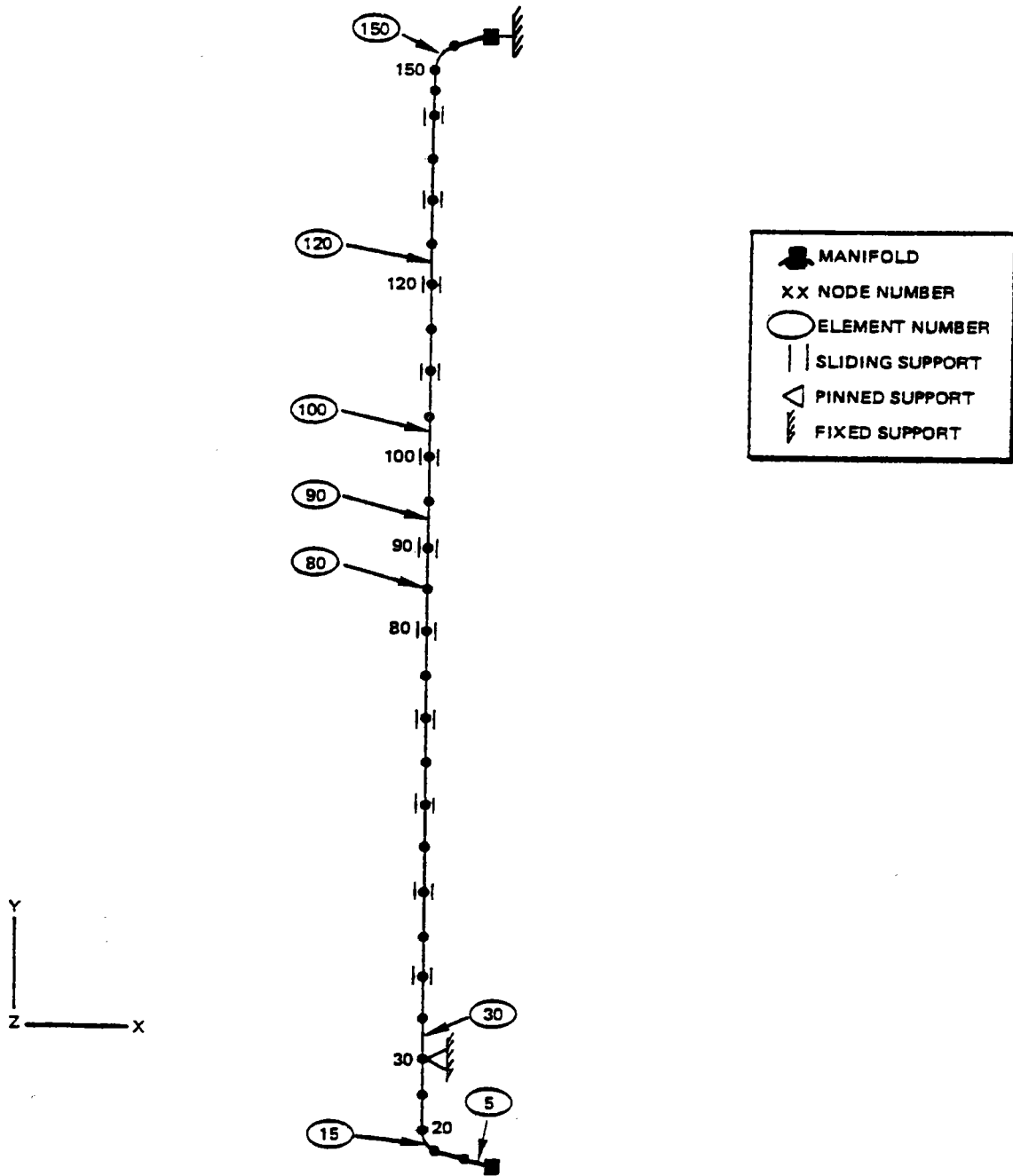


Figure 3-34. DRIPS Computer Model of Solar Receiver

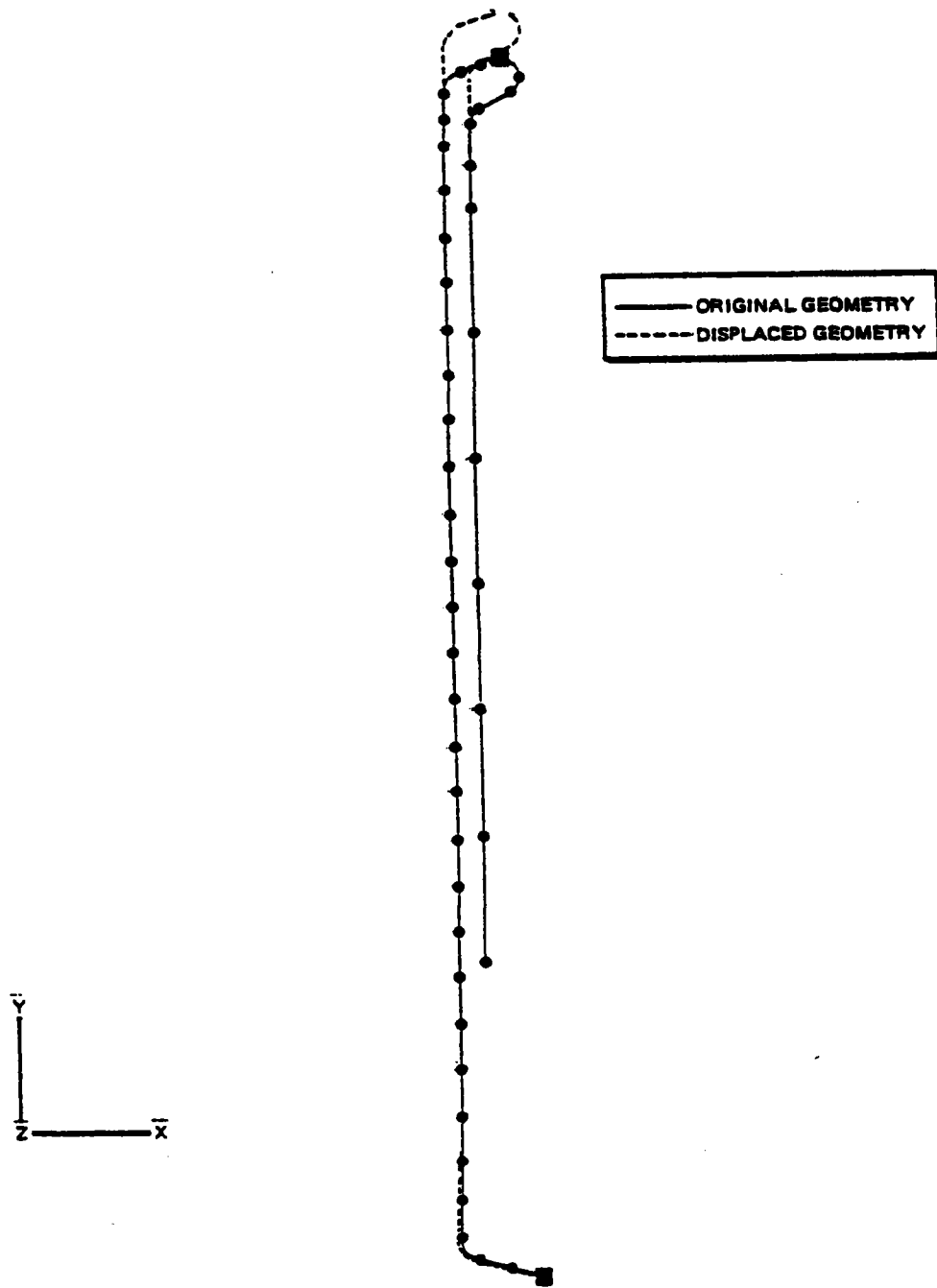


Figure 3-35. DRIPS Predicted Thermal Displacements (Exaggerated)

TABLE 3-13
DRIPS PREDICTED STRESSES (psi)

Element	Node	σ_{z_P} Pressure Membrane	σ_{z_W} Weight Membrane	σ_{z_B} Weight Bending	σ_{z_M} Thermal Membrane	σ_{z_1} Thermal Bending
5	5	125.0	-0.9	-277.2	-118.2	-10720
15	20	122.1	5.1	-112.1	-136.4	6231
30	30	116.7	-218.4	37.2	61.5	-8379
80	80	82.9	-122.9	0.1	61.5	-22353
90	90	76.3	-103.8	-0.7	61.5	-20470
100	100	69.6	-84.7	2.6	61.5	-16947
120	120	56.3	-46.5	36.2	61.5	-7931
150	150	39.2	-2.7	-120.0	59.2	-2662
165	170	138.3	-102.9	-3421.6	-192.9	-15096
180	180	147.4	-81.4	-2442.3	-77.6	-4373
195	195	225.5	-291.4	451.6	-275.3	12
220	225	484.7	-590.6	0.5	-272.7	0

circumference of a cylinder. This assumption allowed utilization of classical cylinder thermal stress equations and resulted in the predicted stresses summarized in Table 3-14.

3.3.5.5 Evaluation of Stress Results

Two approaches were taken to evaluate the predicted stresses: (1) utilization of the damage definitions, criteria, and material allowables contained in ASME Code B31.1, and (2) utilization of the strain cycle criteria of Code Case N-47 (1592) of Section III, Class 1 of the ASME B&PV Code.

TABLE 3-14
COMPUTED THERMAL GRADIENT STRESSES

Element	Node	$\sigma_{z_2}^*$ ΔT_2 Bending	$\sigma_{z_3}^\dagger$ ΔT_w Bending
5	5	0	0
15	20	0	0
30	30	-817	-4661
80	80	-5584	-31777
90	90	-5153	-29274
100	100	-4290	-24417
120	120	-1998	-11317
150	150	-248	-1439
165	170	0	0
180	180	0	0
195	195	0	0
220	225	0	0

$$*\sigma_{z_2} = E\alpha\Delta T_2$$

$$\dagger\sigma_{z_3} = \frac{E\alpha\Delta T_w}{2(1-\nu)}$$

3.3.5.6 ASME Code B31.1 Evaluation

An ASME Code B31.1 design evaluation establishes acceptable stress levels dependent on the nature of loading, the material strength at temperature, and the type of stress field resulting from the loading. Cyclic loadings are addressed by a reduction factor, based on the number of service cycles, which is used to lower the allowable stresses. Many years of service experience in the power industry has demonstrated this design approach can result in reliable piping designs.

Table 3-15 which summarizes the results of the B31.1 evaluation of the ACR receiver indicates the conceptual receiver design will satisfy the criteria at all locations except in the solar panel tubes local to the maximum flux location. Here, the cyclic thermal expansion stresses exceeded the allowables, however, only by 5%. For the hybrid system, the reduction in peak flux from 1.7 MW/m² to 1.5 MW/m² provides a positive margin at each point and thus satisfies the B31.1 criteria.

TABLE 3-15
SUMMARY OF B31.1 STRESS EVALUATION

Element	Node	Pressure Plus Weight Stress Evaluation			Thermal Stress Evaluation		
		Computed Stress (psi)	B31.3 Allowable (psi)	Design* Margin	Computed Stress (psi)	B31.3 Allowable (psi)	Design* Margin
5	5	333	15900	High	10720	21880	1.04
15	20	206	15900	High	6231	21880	2.51
30	30	145	15900	High	8379	21880	1.61
80	80	83	14060	High	22353	21512	-0.05
90	90	77	12420	High	20470	21184	0.03
100	100	72	10280	High	16947	20756	0.22
120	120	83	8740	High	7931	20488	1.58
150	150	129	9380	High	2662	20576	6.73
165	170	2704	9700	2.59	15096	20640	0.37
180	180	1979	9700	3.90	4372	20640	3.66
195	195	564	9700	High	12	20640	High
220	225	485	9700	High	0	20640	High

*Design margin = $\frac{\text{Allowable stress}}{\text{Computed Stress}} - 1.0$

3.3.5.7 Solar Panel Relaxation-Fatigue Damage Evaluation

Over the past 6 to 8 years, considerable attention has been given to the cyclic behavior of metals subjected to temperatures where creep can be significant. This was the result of an observation that the introduction of slow cyclic rates or periods of sustained loading between cycles can reduce fatigue life below that of conventional continuous cycling test data. Although cyclic behavior at elevated temperature is complex and not completely understood, interim failure theories have been developed by the Nuclear Code committees which, with appropriate safety factors, provide an adequate design basis for nuclear power plant components.

In order to be applicable to a wide range of loading situations and geometries, the ASME Section III Code design criteria contains various assumptions which increase the design conservatism as the sophistication of the design analyses decreases. Unfortunately, it was not possible to justify performing rigorous (inelastic) analyses for the receiver conceptual design effort whereby the less conservative design criteria could be employed. However, the material data base and failure theories forming the basis for the nuclear design criteria can be used to establish a "screening criteria" particular to the stress behavior and design confidence needs of the solar receiver.

A key observation supporting this effort was that the regions of maximum thermal gradient stresses (hot side of the tubes) would be subjected to compressive stresses at the hot end of the load cycle. Also the tension stress field existing on the cold side of the tubes decreased in value going up the receiver from the maximum flux location so that at those locations where this region was hot enough to exhibit creep effects, the stresses were not extremely large. Finally, equilibrium (primary) stresses were small at the maximum gradient locations and the piping system was such that elastic follow-up should be minimal. This led to the conclusion the critical regions would be governed largely by relaxation-fatigue with compressive hold periods. For Type 304 stainless steel, hold-time fatigue test data indicates this type of fatigue behavior is the least detrimental of the four basic cyclic stress mechanisms (tension vs. compressive hold periods-relaxation vs. creep-fatigue interaction. In fact, only a minimal reduction in fatigue life is observed in the test data with respect to the continuous cycling fatigue curve.

For these reasons, it was felt a conceptual design level "screening" criteria" could be used which employed the continuous cycling fatigue curves contained in Code Case N-47 (1592). Additionally, in light of the design confidence needs of a solar power plant, it was decided to adjust the curves to provide a safety factor of 1.5 on strain range and 10 on cycles rather than the implicit factors of 2 on strain range and 20 on

cycles contained in the code case. This would bring the safety factors more in line with design practices conventionally employed by high-reliability non-nuclear technologies such as those found in the aerospace industry.

The results of this evaluation are presented in Table 3-16 which indicates the design is adequate. However, at the maximum flux locations, calculated strain ranges approach limiting values. Several design modifications are available to increase design margins in these areas.

3.3.5.8 Conclusions

Based on the conceptual design calculations, the design of a structurally adequate receiver subsystem appears feasible.

TABLE 3-16
RELAXATION-FATIGUE EVALUATION

Element	Node	Computed Strain Range (%)	Allowable Cycles	Design* Margin
30	30	0.036	>10 ⁶	>100
80	80	0.263	10,000	0.00
90	90	0.248	12,800	0.28
100	100	0.211	26,000	1.63
120	120	0.099	>10 ⁶	>100
150	150	0.020	>10 ⁶	>100

$$*Design\ margin = \frac{1.0}{10,000/Allowable\ cycles} - 1.0$$

3.3.5.9 Recommended Future Structural Design Activities

Due to marginal nature of the conceptual design evaluations, the lack of rigorous detailed analyses, and in the interest of developing an optimum design, it is recommended three design options be further evaluated, each of which can significantly increase the receivers structural adequacy:

- 1) Reduction of solar panel tube thickness
- 2) Multipoint aiming techniques (to reduce the desk flux)
- 3) Alternate materials (such as Alloy 800H)

3.3.5.10 Analysis of Tube Ends

Analysis is currently being performed on other programs to optimize the length of the 1.9 cm (3/4 in.) OD - 0.127 (0.05 in.) wall receiver tubes in the regions before and after the flux absorption area. This analysis is required because of the change in design from what was previously analyzed. There exists a definite trade-off between thermal expansion flexibility and deadweight/seismic stiffness that must be considered. Also, it is believed that deadweight hangers may be required in the horizontal runs of the expansion loop. Expansion joints would shorten expansion loops, but would add complexity to the system. The possibility is under consideration.

The receiver tubes are being analyzed to ANSI B31.1, with guidance on fatigue damage (due to through-the-wall thermal gradients) from ASME Section III Class 1, Code Case N-47 (previously known as Code Case 1592).

A thermal histogram is expected to be compiled to provide analyst with a tool to remove some of the conservatism of previous analyses.

Obviously, more sophisticated thermal and structural evaluations need to be performed with particular emphasis placed on development of an appropriate design criteria. However, this is a natural occurrence in any design activity progressing out of the conceptual stage into preliminary design.

Since previous work on the receiver tubes has shown acceptable stresses and design life, it is anticipated that no basic conceptual design problems will be encountered during this detailed analysis effort. As before, a finite element piping model will be developed and loaded with the previous thermal distributions--both along the length of the tubes and across the tube thermal distributions. The number of guides to prevent gross bowing of the receiver tubes will be determined as optimizing the number of these supports has a significant cost savings.

3.3.6 Receiver Structural Support Analysis

The receiver structural supports are being analyzed on other programs to Section III, Subsection NF (Component Supports) of the ASME Code. The stress criteria in this code are similar to the American Institute of Steel Construction (AISC) criterion, except temperature considerations are taken into account.

The receiver structural supports must withstand the thermal effects due to flux, any interaction between the supports and the receiver-tubes, wind and earthquake effects, as well as deadweight loads.

A brief look at the seismic loadings indicated that the receiver structural supporting system has sufficient bracing to prevent failure during the projected earthquake and that cost optimization is possible.

3.3.7 Tower Analysis

The tower must be designed to support the receiver and auxiliary components, provide access for maintenance and inspection of the receiver, instruments and controls, piping and other equipment that may be located on the tower, and adequate provisions must be made to insure crew safety at all times for required operations, inspection, maintenance, and repair.

3.3.7.1 Tower Design Criteria for 0.8 SM Plant

Seismic Loads

Ground Response Spectra from NRC Regulatory Guide 1.60

Damping Values from NRC Regulatory Guide 1.61 = 0.07

Peak ground accelerations (UBC Zone 3, Modified Mercalli Intensity VIII):

Horizontal	0.35 g
Vertical	0.36 g

Wind Loads

Wind velocity, including gusts, = 40 m/s (90 mph) at 10 m (30 ft). Wind loads based on ANSI A58.1-1972.

3.3.7.2 Tower Analysis Method for 0.8 Plant

The receiver tower was modeled as a fixed-base, multi-mass cantilever beam structure. The tower was divided into fifteen segments of equal length, with the mass of each segment located at the segment centroid. The tower masses consisted of the tributary mass from the tower structure itself plus the tributary mass from the FRP liner and riser and downcomer piping. The masses were connected by prismatic beam elements, with section properties based on the gross uncracked concrete section using the average radius and thickness along the length of the element.

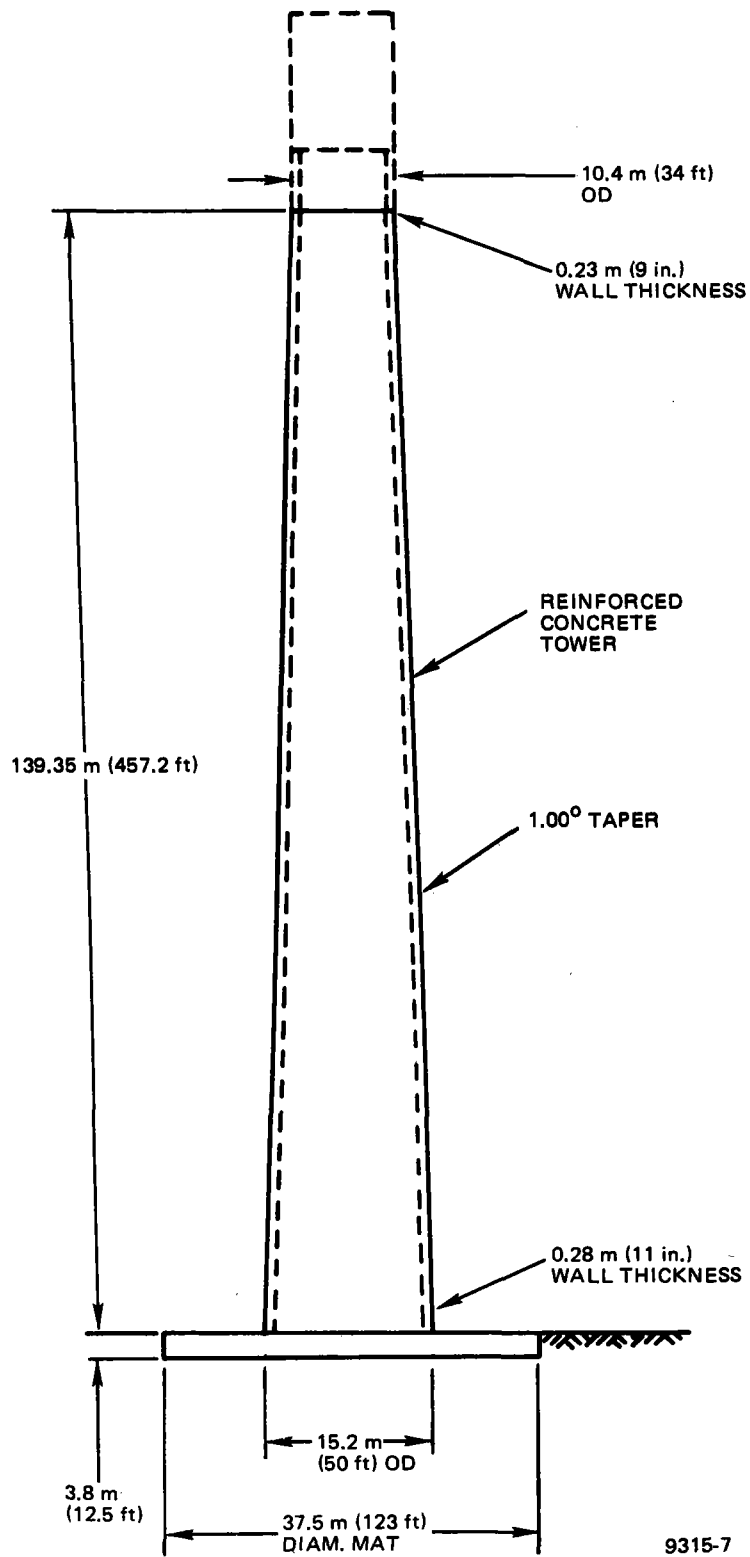


Figure 3-36. Receiver Tower
(100 MWe, 1.4 SM)

The receiver was modeled by beam elements having an assumed stiffness of 0.2 times the stiffness of the topmost tower element. The receiver model and assumed mass distribution may be found in Appendix D of this report.

Tower response to both horizontal (one component) and vertical earthquake loading was computed using the response spectrum method. Drag wind effects were considered using the provisions of ANSI A58.1-1972. The calculated wind velocity to produce vortex shedding is 72 mph. At this wind velocity, it was assumed that there is sufficient turbulence to preclude the formation of vortices and, hence, dynamic wind effects due to vortex shedding were presumed nonexistent.

Minimum shell wall thickness and minimum circumferential reinforcement were determined in accord with Sections 4.1.3 and 4.7.3, respectively, of the "Specification for the Design and Construction of Reinforced Concrete Chimneys (ACI 307-69)." Vertical reinforcement was calculated using the strength design provisions found in Chapters 9 and 10 of the "Building Code Requirements for Reinforced Concrete (ACI 318-71)."

3.3.7.3 Tower Analysis Method for 1.4 SM Plant

The tower analysis method used for the 1.4 solar multiple tower is the same as that described in Section 3.3.7.2. The tower/receiver model and assumed weight distribution may be found in Appendix D of this report.

3.3.7.4 Tower Analysis Results for 1.4 SM Plant

Figure 3-36 shows the concrete tower and mat dimensions for the 100 MWe, 1.4 solar multiple baseline plant.

Table 3-17 shows the tower/receiver displacements and accelerations for the 0.35 g earthquake design condition.

Appendix D contains the computer program input and output data for the 139.35 m (457.2 ft) concrete tower analysis.

The design of the foundation mat was controlled by stability to resist seismic overturning moments. It was required that positive pressure be maintained over at least 80% of the mat contact area. The calculated net bearing pressure for this condition (2.65 ksf) was much less than the allowable net bearing pressure (10 ksf), thus providing a comfortable design margin on bearing pressure.

TABLE 3-17
TOWER DISPLACEMENTS AND ACCELERATIONS
(0.35 g Lateral and Vertical Earthquake)
(100 MWe, 1.4 SM)

Location	Relative Displacements				Absolute Accelerations			
	Horizontal		Vertical		Horizontal		Vertical	
	m	ft	m	ft	m/s ²	ft/s ²	m/s ²	ft/s ²
Base of Tower 0 m (0 ft)	0.000	0.000	0.000	0.000	3.435	11.270	3.435	11.270
Top of Tower 139.35 (457.2 ft)	0.454	1.490	0.009	0.029	5.684	18.649	11.168	36.642
Mid-Point of Receiver 154 m (505.2 ft)	0.535	1.754	0.010	0.034	8.656	28.398	13.977	45.856
Top of Receiver 161.65 m (530.3 ft)	0.578	1.896	0.010	0.034	13.277	43.559	13.977	45.856

3.3.7.5 Tower Analysis Results for 0.8 SM Plant

Figure 3-37 shows the concrete tower column and mat dimensions for the 100-MWe, 0.8 solar multiple baseline plant.

Table 3-18 shows the tower/receiver displacements and accelerations for the 0.35 g earthquake design condition.

Appendix D contains the computer program input and output data for the 113.3 m (365 ft) concrete tower analysis.

3.3.8 Riser/Downcomer Analysis

3.3.8.1 Piping Configuration and Materials Selection

For the ACR study, four downcomer piping configurations were developed and studied to determine the simplest routing for a 51-cm (20-in.) sodium downcomer line from the receiver. This study titled "Pipe Routing Study of Sodium Downcomer" is presented in Reference 3-1, and is directly applicable to the hybrid plant design which also uses a 51 cm (20 in.) sodium downcomer line. The reference design is designated as Type I in that appendix.

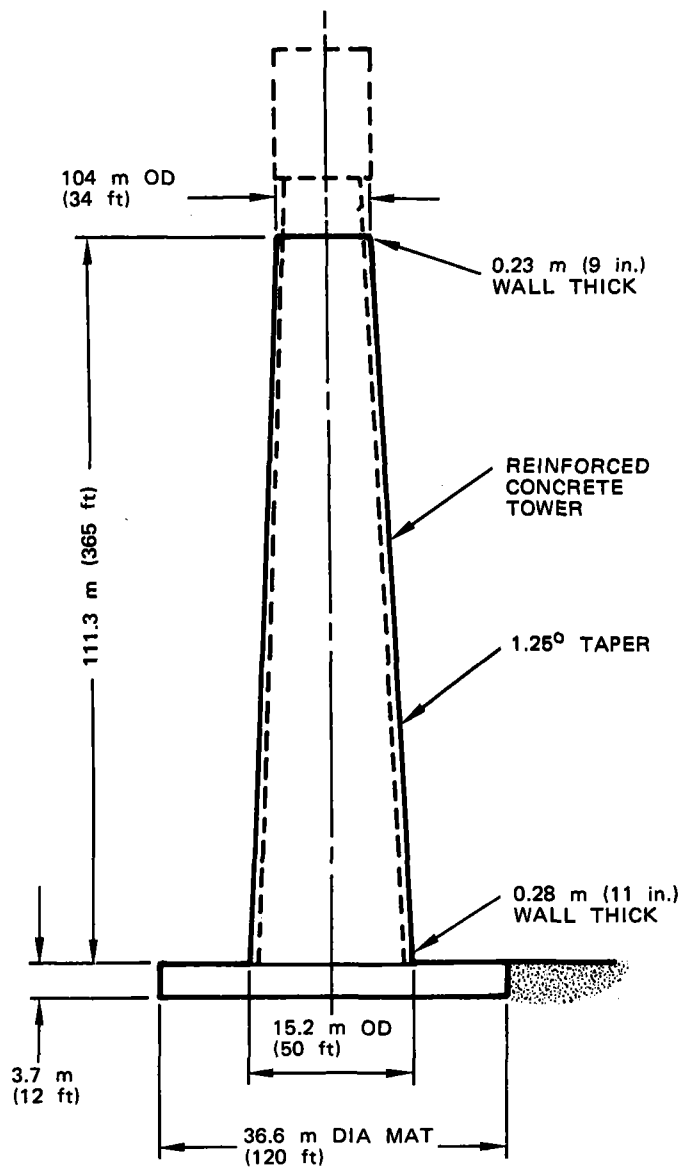
Piping materials selected are carbon steel for the sodium riser piping and stainless steel for the sodium downcomer piping. Refer to Section 3.3.3 for a discussion on the use of austenitic stainless steels for sodium service.

3.3.8.2 Tower Riser and Downcomer Pipe Selection

0.8 SM Plant Concept

In addition to surveying the riser/downcomer trade studies performed during the Advanced Central Receiver Program, a trade study which examined the total cost of the riser and downcomer of an 0.8 solar multiple hybrid system as a function of pipe size was completed. This trade study was part of the single vs multiple free-surface sodium loop trade study documented in Section 3.4.1. Riser and downcomer friction head losses calculated in this study were used to size the receiver pump and the balance of sodium loop piping.

In this study, the total cost consisted of the following components: Pipe capital cost, pump capital cost to overcome pressure drop in each leg, present value of electricity required to overcome the pressure drop discounted to account for dynamic heating recovery and plant capital cost required to support the



9315-27

Figure 3-37. Receiver Tower (100 MWe, 0.8 SM)

TABLE 3-18
TOWER DISPLACEMENTS AND ACCELERATIONS
(0.35 g Lateral and Vertical Earthquake)
(100 MWe, 0.8 SM)

Location	Relative Displacements				Absolute Accelerations			
	Horizontal		Vertical		Horizontal		Vertical	
	m	ft	m	ft	m/s ²	ft/s ²	m/s ²	ft/s ²
Base of Tower 0m (0 ft)	0.000	0.000	0.000	0.000	3.435	11.270	3.435	11.270
Top of Tower 111.3m (365 ft)	0.276	0.905	0.006	0.019	6.336	20.786	10.317	33.847
Midpoint of Receiver 124.0 m (406.5 ft)	0.332	1.089	0.007	0.024	6.874	22.551	12.983	42.596
Receiver Crane 141.7 m (465 ft)	0.419	1.376	0.005	0.026	18.198	59.705	14.794	48.328

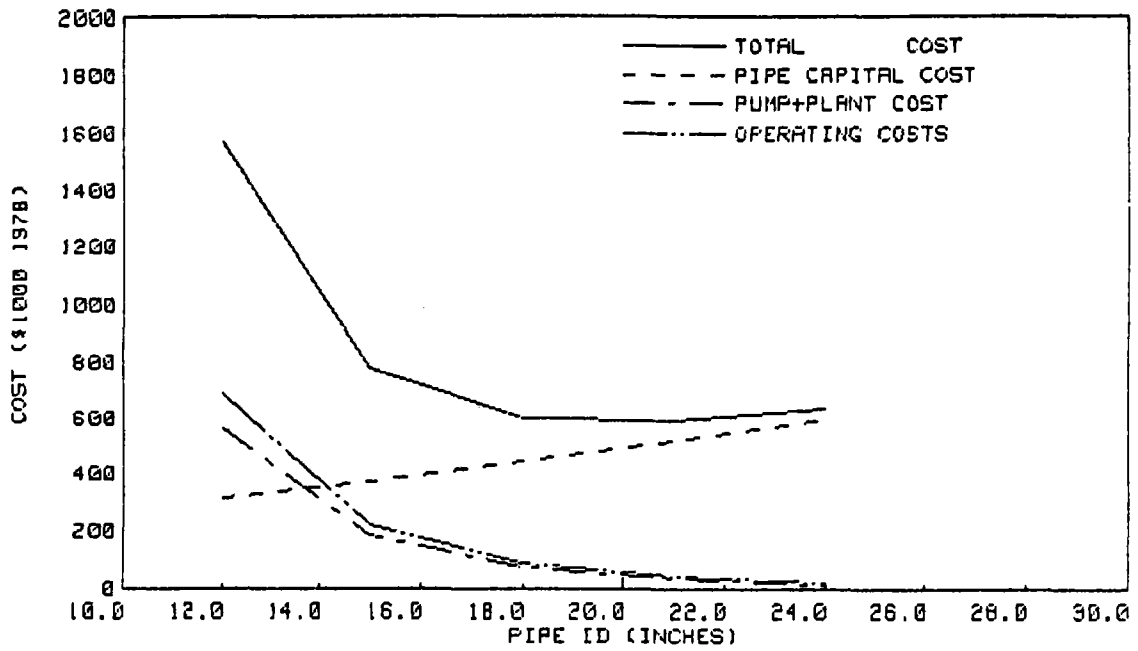


Figure 3-38. Coal Fired Hybrid Riser Costs vs Pipe ID

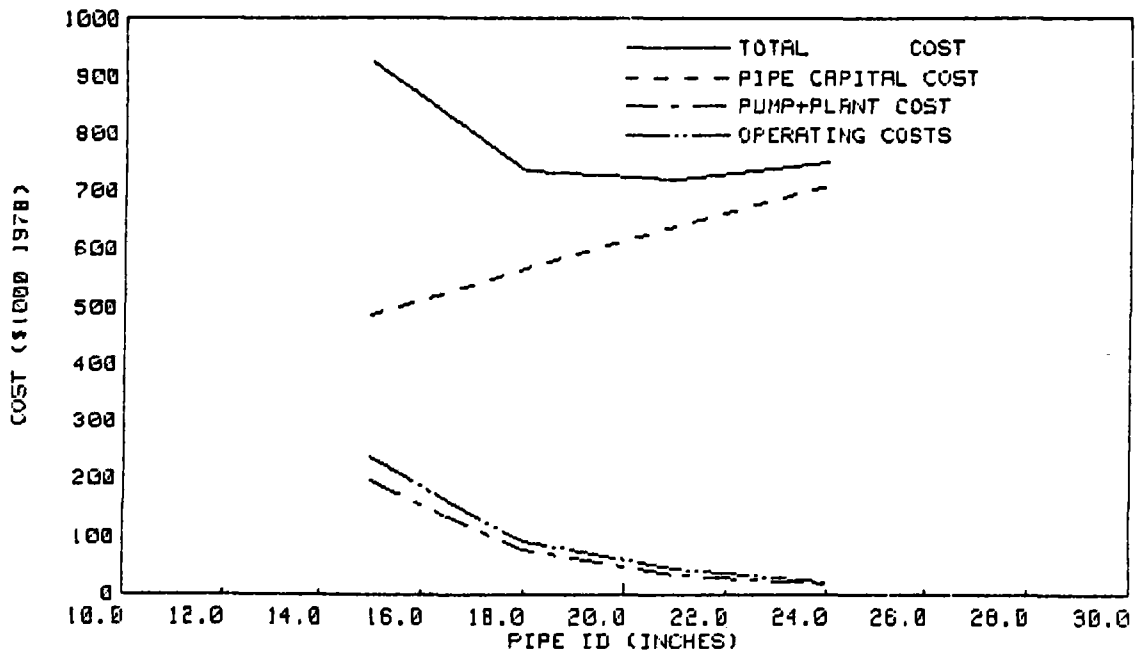


Figure 3-39. Coal Fired Hybrid Downcomer Costs

additional pumping power. Generally, as pipe diameters increased, pipe pressure drop decreased, pipe capital costs increased, pump capital costs decreased, pump electricity costs decreased and plant capital costs decreased.

Riser and downcomer total and component costs are shown in Figures 3-38 and 3-39, respectively. Riser pipe sizes in the range of 31 to 61 cm (12 to 24 in.) ID were considered. Downcomer pipe ID sizes in the range of 38 to 61 cm (15 to 24 in.) were also considered. Downcomer minimum pipe ID was set at 38 cm (15 in.) as a result of excessive pressure drop in smaller pipes.

The total costs minimize at a pipe ID of 51 cm (20 in.) for both riser and downcomer. The nearest commercially available pipe size to a 51 cm (20 in.) ID is a 51 cm (20 in.) OD. ID's on a 51 cm (20 in.) pipe vary from 48 cm (18.8 in.) to 49.5 cm (19.5 in.), depending on pipe schedule. Since there is very little total cost penalty in using these slightly reduced ID's, 51 cm (20 in.) pipe was selected as the baseline riser and downcomer pipe. The actual schedule selected will depend upon the actual vs allowable stress in each leg.

For purposes of other trade studies, Schedule 30 pipe was tentatively selected. This resulted in an effective pressure drop of 0.005 psi/straight foot of riser or downcomer.

1.4 SM Plant Concept

In the case of the 1.4 solar multiple plant configuration, the riser and downcomer piping flow and pressure drop requirements are similar enough to the ACR system that the ACR riser and downcomer design was adopted directly. This resulted in a riser pipe nominal OD of 24 in. The downcomer pipe OD was selected in accordance with the recommendations of the tower head recover trade study completed during the ACR program. The selected downcomer nominal pipe OD is 12 in.

TABLE 3-19
CONVENTIONAL FREE-SURFACE PUMP CHARACTERISTICS

	Reactor						
	HNPF	EBR-II	EFFBR	PFR	FFTF	SNR-Stork	SNR-KSB
	Pump Type						
	Hallam	Fermi	Fermi	Fermi	Fermi	Hallam	Hallam
Capacity (gpm)	7,200	5,500	11,800	18,500	14,500	22,000	22,000
Head (ft)	160	200	310	333	502	276	279
Design Temperature (°F)	1,000	800	1,000	752	1,050	1,076	1,076
Motor Speed (rpm)	900	1,075	900	960	1,110	1,000	1,020
Motor Power (hp)	350	350	1,060	2,000	2,100	2,000	2,000
Gas Sealing Arrangement	Mechanical Shaft Seal	Hermetic Motor Seal	Mechanical Shaft Seal	Mechanical Shaft Seal	Mechanical Shaft Seal	Visco-Seal	Mechanical Shaft Seal
Vessel Seal Type* (leakage)	Labyrinth (3%)	-	-	-	-	Piston Ring (2%)	Piston Ring (<1%)
Speed Control	Eddy Current Coupling	Variable Frequency and Voltage	Liquid Rheostat Wound Rotor	Hydraulic Coupling	Liquid Rheostat Wound Rotor	Thyristor	Thyristor
Total Pump Operating Time (h)	125,000	100,000+	129,000	17,000+	-	>5,000	>1,000

*Hallam types only

3.3.9 Pump, Piping, and Valve Analysis

3.3.9.1 Sodium Pumps

A vast amount of experience has been accumulated over the past 25 years of ESG's involvement in the design and development of sodium system components. Pump development was initiated in 1955 at ESG for the Sodium Reactor Experiment (SRE), and continued development lead to design of the free-surface type Hallam pump, the Fast Flux Test Facility pump, the Clinch River Reactor Plant (CRBRP) pump, and the Inducer pump.

Recent main heat transfer system sodium pumps are primarily free-surface, centrifugal impeller pumps, operating in the 850- to 1150-rpm range. Currently, several double-suction centrifugal impeller types are being designed or fabricated, most notably for the CRBRP and the BN-600 reactors. While free-surface (cover gas) pumps are the most common, several freeze-seal types have been operated, such as the BNR-350 and SRE pumps. Table 3-19 summarizes the key characteristics of several types of large pumps. From the table, we see that substantial operating experience exists for liquid sodium pumps. The main problem associated with pumps has been the seizure of bearings, a phenomenon related to designing for optimum clearances for the upper bearing. If the clearance is too large, there are difficulties with radiation streaming; but, if the clearance is too small, there is danger of seizure of the bearings, especially if the drive shaft becomes slightly distorted because of temperature gradients. This problem is associated with nuclear reactor operations, where the large pumps have been used to date. The clearances may be increased for non-nuclear applications, and alleviate this problem. The shaft length may also be shortened to minimize dis-

Some 33 pumps of the class and capacity (15,000 to 20,000 gpm) required for a 100 MWe Solar plant have successfully operated in sodium reactor loops throughout the world (USA, U.K., France, Germany, Italy, Holland and the USSR). Pumps are being presently designed by Rockwell and others under contract to DOE for use in large scale Breeder Reactor plants with capacities in the range of 85,000 gpm. A prototype pump for France's Super Phoenix with a capacity of 79,000 gpm has been tested in water and the pumps full scale rotating works are presently being tested in sodium.

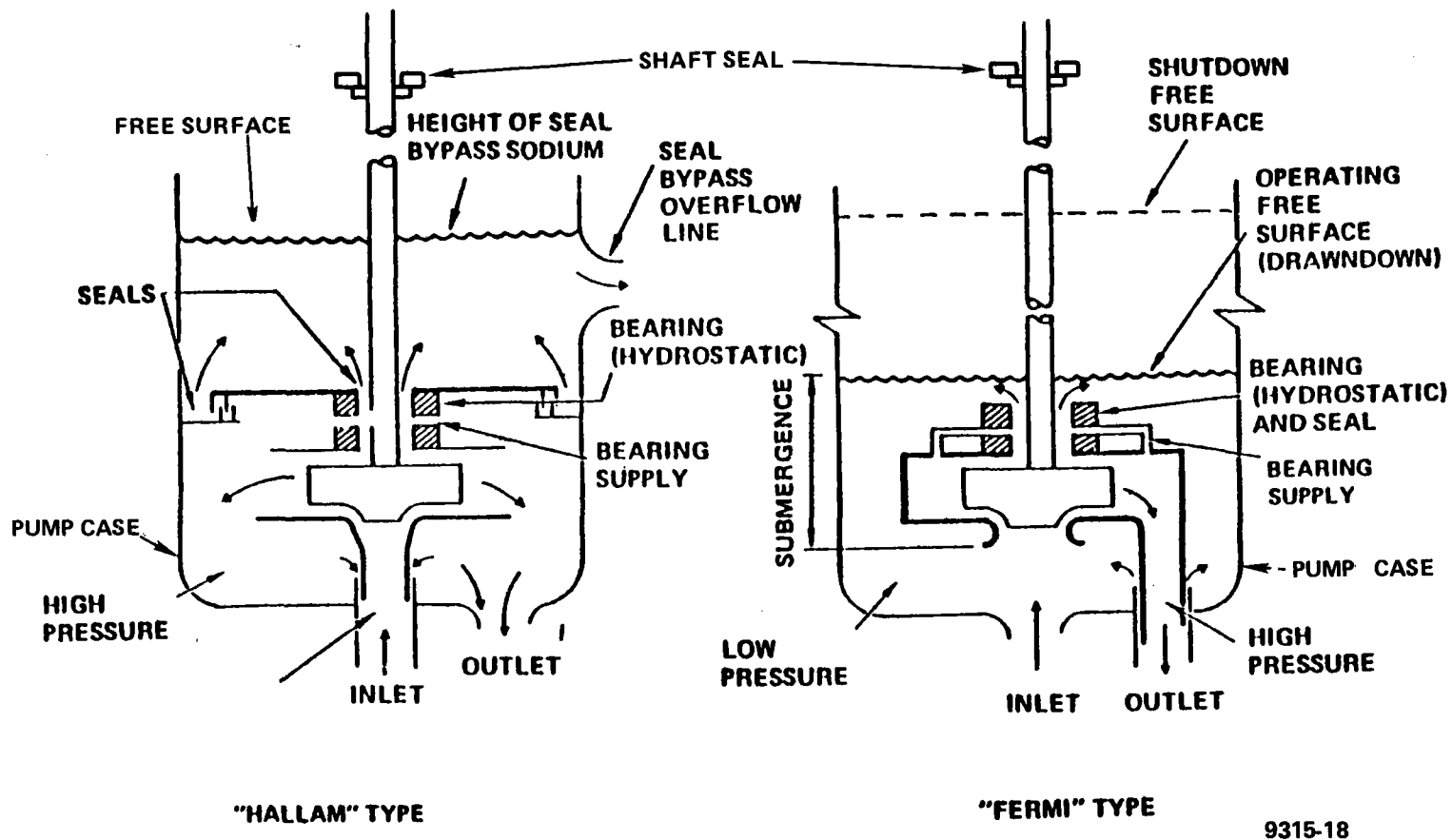


Figure 3-40. Key Differences Between the Fermi and Hallam Free Surface Pumps

A free-surface pump is a vertical mechanical pump placed in a close fitting vessel called the pump case. The liquid level ("free-surface") in the outer case is maintained above the impeller and below the top of the pump case. For this type of pump, a shaft seal is not required to seal in the liquid. Pumps which use an inert cover gas, such as sodium pumps, use a gas seal placed on the shaft to minimize cover gas leakage. Figure 3-40 shows typical free-surface pumps used for sodium applications.

The viable alternative sodium pumps for large-scale sodium systems appear to be ac electromagnetic induction pumps or centrifugal pumps. Electromagnetic induction pumps require no moving parts and no pressure boundary penetration for their operation. These excellent operational characteristics are offset by the difficulty of cooling the windings without freezing the sodium while maintaining the pump in a shutdown condition. In addition, the pumping efficiency of these pumps is less than 50% which leads to an unacceptable economic penalty. A comparison of electromagnetic pumps vs mechanical pumps is given in Reference 3-1.

As previously stated, free-surface pumps for large-scale sodium service have already been developed for the Liquid Metal Fast Breeder Reactor Program. Two basic designs are available: the Hallam-type and the Fermi-type. The key differences are shown in Figure 3-41. For our purpose, the Fermi-type appears to be the better choice since it does not require the seal bypass overflow line; it has a higher efficiency; it is more tolerant of pipe reactions; it has lower pressure boundary stresses; and it is more fully developed than the Hallam type. (The Fast Flux Test Facility and the Clinch River Breeder Reactor Plant utilize a version of this concept.)

3.3.9.2 Piping Analysis

The tower downcomer stainless steel piping expands approximately 50 in. during heatup from ambient to the receiver outlet temperature of 1100⁰F. The

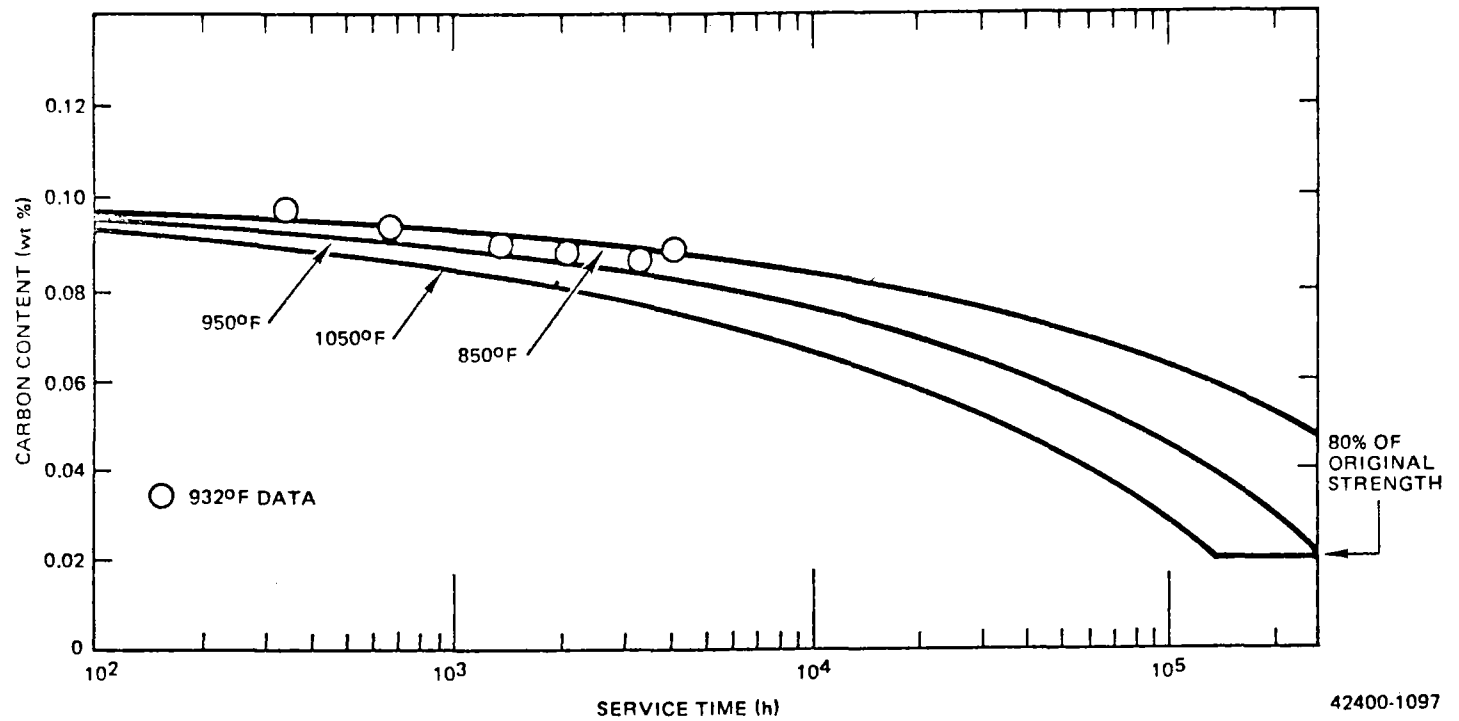


Figure 3-41. Decarburization of 0.095-in. Thick 2-1/4 Cr - 1 Mo Steel by Sodium (One Side)

42400-1097

carbon steel riser piping expands about one-half this amount in heating up to 550⁰F. Several piping configurations were developed and studied during the Phase I ACR conceptual design for accommodating the thermal expansion of the downcomer piping. This ACR pipe routing study of the piping is presented in Reference 3-1. The study indicated that the simplest pipe arrangement is to fix the downcomer at the receiver and pump ends and take the thermal expansion in a single plane with one 5D bend and a horizontal run of pipe. Although this arrangement is geometrically simple, it complicates the pipe hanger requirements because of the large motions. An alternate arrangement utilizes expansion loops and anchor points on the tower. Each loop contains four 5D bends and 20 ft of straight pipe. The pipe hangers would be conventional rigid supports. The reference design for the hybrid plant is designated as Type I.

3.3.9.3 Piping Materials

As previously noted in Section 3.3.3, the austenitic stainless steels have been used as the principal material of construction in nearly all sodium-cooled test loops and nuclear reactors. Their wide acceptance has been associated with their ability to satisfy the material requirements, which include (1) elevated-temperature strength, (2) compatibility with sodium, (3) fabricability, and (4) availability. Their satisfactory performance in test loops and large liquid metal cooled reactors at temperatures to 704⁰C (1300⁰F) has proven their acceptability. Tests have proven that austenitic stainless steels are suitable for long-term use in sodium at temperatures to 704⁰C (1300⁰F) providing the oxygen concentration is maintained below 10 ppm.

The low-alloy steels (2-1/4 Cr - 1 Mo) have been used for sodium containment at temperatures up to 510⁰C (950⁰F). The attractiveness of this material is derived from reasonable strength at temperatures up to 510⁰C (950⁰F), and low cost. The thermal behavior of this material is particularly attractive, because its high thermal conductivity, in combination with its low thermal expansion coefficient, leads to a significant reduction in thermal stress and fatigue. The 2-1/4 Cr - 1 Mo steel is subject to decarburization in sodium (Figure 3-41), which results in a reduction of both long- and short-term mechanical properties. Allowable design stresses for 2-1/4 Cr - 1 Mo must be reduced accordingly. The reduction of structural properties with increasing temperature limits the use of

this material to temperatures below 538⁰C (1000⁰F). The 2-1/4 Cr - 1 Mo is generally harder to weld than the austenitic stainless steels, because it requires preheat and post-weld heat treatment. This occasionally causes problems, if weld repair in service is required.

Transition welds between dissimilar materials, such as austenitic stainless steel to ferritic steel (2-1/4 Cr - 1 Mo), are considered detrimental to plant reliability. High thermal stresses result from differing thermal properties at these welds, and the migration of carbon from ferritic to stainless steel may take place. Another consideration includes the sensitization of the austenitic stainless steel during post-weld heat treat of the ferritic steel.

Transition welds are normally made using nickel-base electrodes or "sleeves" of Inconel between the two materials, provided the welded section is not subject to overly severe thermal transients. The Inconel sleeve has intermediate thermal properties, relative to austenitic and ferritic material, that somewhat mitigates the thermal transients. The Inconel can be welded to the ferritic steel and heat treated before welding to the austenitic steel, thus avoiding the sensitization problem. Thermal stress problems that might be anticipated in such welds can be minimized by adjusting the length of the Inconel sleeve for added flexibility, and by judiciously locating the weld.

3.3.9.4 Valves

A considerable amount of operating experience has been accumulated on valves for high-temperature liquid metal systems. Valves up to 18 in. are in operation at the ETEC, and have proven extremely reliable. The French plan to test a prototype steam generator isolation valve, almost 3 ft in diameter, in water and static sodium. The Germans successfully tested a 24-in. valve for over 4000 hours, with pressure differences up to 60 psi at 1075⁰F and 1500 manipulations. Freeze seals are used as the primary seal, with a secondary backup packed-type seal in the larger valves. Small valves are usually sealed with bellows, with a secondary

backup packed-type seal. The valves are ordered with standard weld preparation ends, for welding into the system. Valves up to 12 in. in diameter are considered state of the art and are available from several valve manufacturers.

3.3.10 Steam Generator Analysis (Heat Exchanger)

3.3.10.1 Current SG Experience

Table 3-20 lists the more recent steam generator operating experience. The following steam generator test loops are currently in operation in foreign countries.

Hengelo, Holland	SNR-300	52.75 MW
Les Renardier, France	Super Phenix	45 MW
BOR 60, Russia	BN-600	30 MW
O'arai, Japan	Monju	40 MW
O'arai, Japan	Monju	10 MW

An extensive Rockwell International-funded program was conducted, covering the design, analysis, and fabrication of a 30-MWt Modular Steam Generator (MSG) Test Unit. Test monitoring and evaluation, plus post-test examination, was also performed on this program. The testing was funded by the Department of Energy (DOE) then Energy Research and Development Administration (ERDA), and was accomplished at the Energy Technology and Engineering Center (ETEC)/Sodium Component Test Installation (SCTI) Facility, where various tests, including over 9000 hr of sodium operation, were run. This company-funded effort, spanning more than 8 years, has formed the basis for the design and fabrication of the Energy Systems Group (ESG) steam generator module for the Clinch River Breeder Reactor Program (CRBRP).

A summary of the test results for the MSG is given in Figure 3-42. It is to be noted that the boss shown in Detail A in this figure is milled out of the solid tubesheet forging, thus, the autogeneous butt weld provides a tube-to-tubesheet weld that can be 100% x-rayed. The performance characteristics of these units correlate well with the engineering predictions. The correlations are shown in Figure 3-43.

TABLE 3-20
SUMMARY OF "COMPACT TUBE" STEAM GENERATOR EXPERIENCE

Facility	Power (MWt)	Configuration	Materials	Type of Operation	Liquid Metal Inlet Temperature (°F)	Exit Steam Conditions (psia/°F)	Operating Time (h)	Problems
<u>Small-Scale Tests</u>								
W-HTMI	1	Single-wall serpentine tube with cover gas	Alloy 800	Once-through	960	2400/950	800	Instability
Grand Quevilley	5	Serpentine tube and shell, helical tube, and Z-tube	2-1/4 Cr - 1 Mo evaporator, Type 321 SS superheater	Once-through	1020	2470/955	8000	Minor flow maldistribution
Interatom KNK Model	5	Serpentine tube and shell	Stabilized 2-1/4 Cr - 1 Mo	Once-through	790	1160/790	5600	None
Monju Z-Tube Model	1	Single-wall helical tube	2-1/4 Cr - 1 Mo	Once-through	1000	2545/955	3600	Two small leaks in HAZ of welds which had not received PWHT
<u>Large-Scale Tests</u>								
Phenix	45	Serpentine tube and shell	2-1/4 Cr - 1 Mo evaporator, Type 321 SS superheater-reheater	Once-through	1020	2545/955	7000	None
Super-Phenix Fives-Call Babcock	45	Helical tube	Incoloy 800 tubes, Type 304 SS shell	Once-through	975	2705/915	1000	None
Super-Phenix Stein Industries	45	Z-tube	2-1/4 Cr - 1 Mo Evaporator, Type 316 SS superheater	Once-through	975	2705/915	~1000	None
SNR Helical Tube	50	Helical tube	Stabilized 2-1/4 Cr - 1 Mo	Once-through	970	2470/932	~1000	None
Monju	50	Helical tube	2-1/4 Cr - 1 Mo	Once-through	940	1940/910	~4000	Flow instability below 30%, liquid level control (sodium side)
AI-MSG	33.8	Hockey stick	2-1/4 Cr - 1 Mo	Once-through	950	2430/930	4000	None
<u>Reactor Plant Operation</u>								
EFAPP	143	Serpentine tube	2-1/4 Cr-1 Mo	Once-through	820	910/780	2000	*
DFR	3	Serpentine shape - separate H ₂ O and Na tubes in Cu laminations	Type 321 SS	Once-through	570	147/518		Chloride stress corrosion
KNK	28	Serpentine single tube in shell	2-1/4 Cr - 1 Mo	Once-through	790	1160/790	5200+	Leak in HAZ of spacer tab on tube
Phenix	15	7-tube serpentine units	2-1/4 Cr - 1 Mo evaporator, Type 321 SS superheater	Once-through	1020	2400/955	6000+	None
BOR-60	30	Serpentine tube	Low-alloy steel	Once-through	900	430	20,000+	None

*Caustic stress corrosion; tube vibration; wear; tube-tubesheet weld leaks; flow instability, corrected by orificing

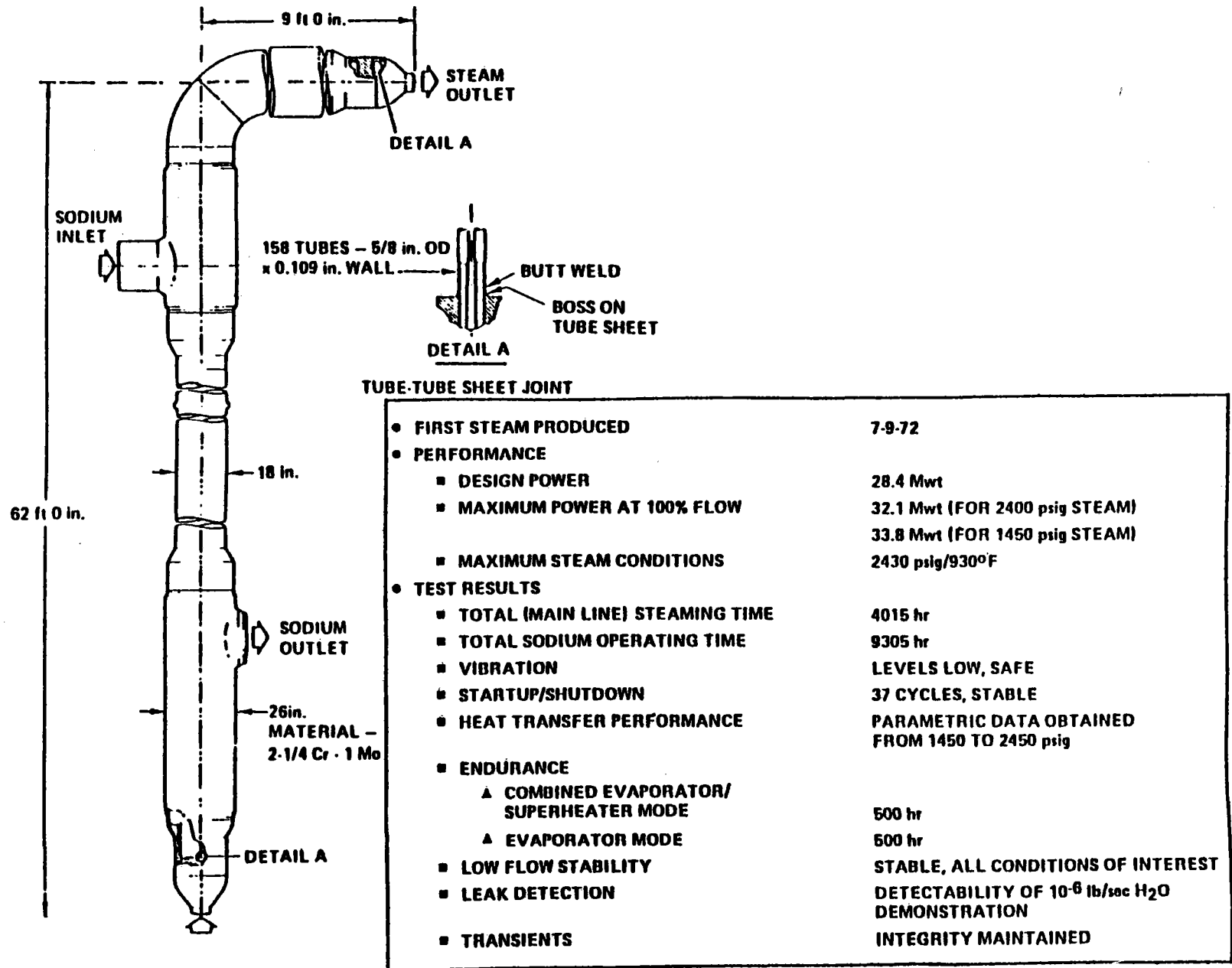
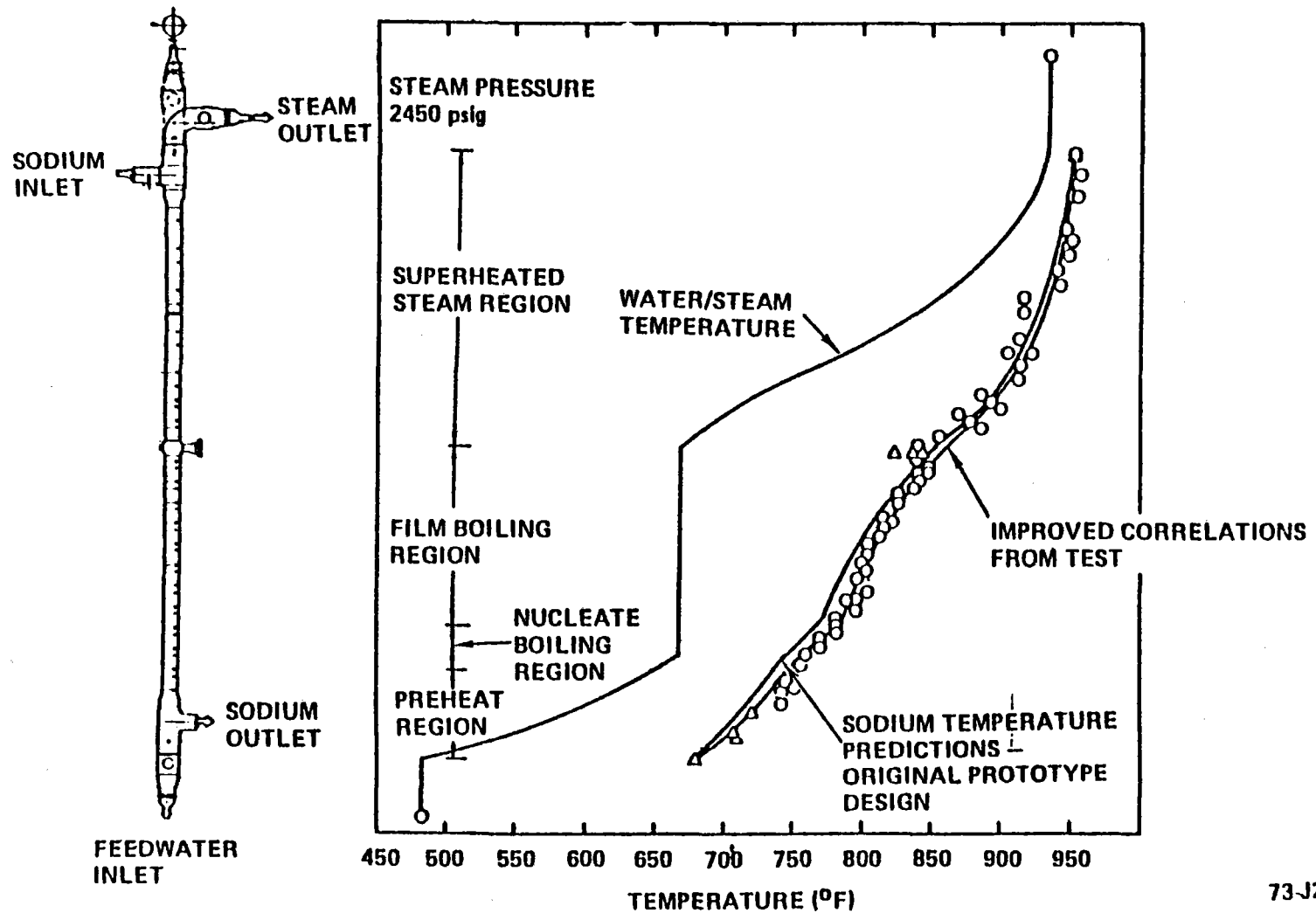


Figure 3-42. Highlights of LMEC/SCTI Test of MSG



73-J26-6-2

Figure 3-43. Heat Transfer Results from LMEC/SCTI Test of MSG
(100% Power in Combined Evaporator-Superheater Mode)

In summary, the steam generators evaluated as part of this hybrid conceptual design effort are based on the ESG modular steam generator (MSG) and the Clinch River steam generator designs. This steam generator design features a hockey stick shape and can be designed for a range of sizes to be used as evaporators, superheaters, and reheaters. At temperatures at or below 510°C (950°F), ferritic tubes of 2-1/4 Cr - 1 Mo would be used. However, at temperatures above 510°C (950°F), the recommended material of construction is Type 304 stainless steel.

The modular approach may be attractive for early plants, but for a large number of standardized plants, the evaporator, superheater, and reheater units designed for the specific purpose greatly simplify the system flow configuration and result in a cost reduction. This simpler arrangement for the power requirements of the revised configuration consists of an evaporator of ~146 Mwt, a superheater of 74 Mwt, and a reheat unit of 40 Mwt. The larger evaporator unit is a 1.2 scale-up of the CRBRP design (~120 Mwt). The superheater is the same size as the current CRBRP design, since with the lower heat transfer characteristics of steam, the unit is estimated to operate at about 74 Mwt as a superheater. As indicated above, Type 304 stainless steel would be selected for both the superheater and the reheater. The reheat unit would be similar to the current ESG-MSG though scaled up slightly. While the ESG-MSG is rated at about 32 Mwt as a combined evaporator and superheat unit, as a superheater only, the power would be reduced to about 25 Mwt, hence necessitating a modest scale-up. The steam generator units are similar to those selected for the ACR study.

3.3.10.2 Recirculation

It is planned to use recirculation only during startup and shutdown. This is to ensure stable flow conditions during low flow operation. At full load, there should be no stability problems as demonstrated by the MSG test. Also, DNB is not considered to be a problem as explained in the following paragraphs.

In some fossil-fired boilers, there have been tube failures due to Departure from Nucleate Boiling (DNB) phenomenon. The solution in this case has been to use a large recirculation ratio and thereby avoid having DNB occur in the evaporator at all. The tube failures are due to two separate phenomena:

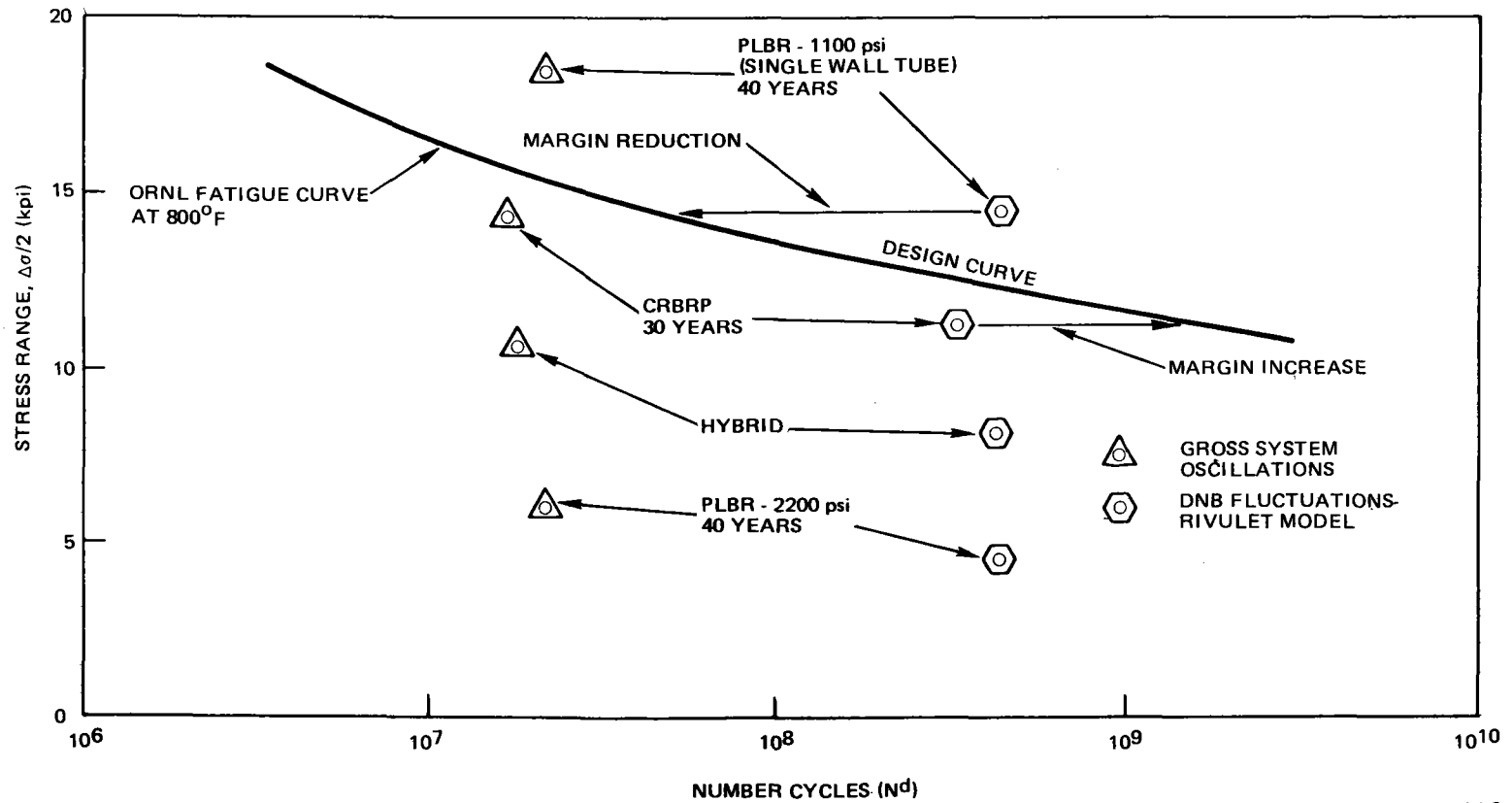


Figure 3-44. Stress Range vs Allowable Stress Cycles

- 1) Overheating due to a high heat flux and the low heat transfer coefficient of film boiling.
- 2) Stress fatigue due to alternate exposure to film boiling and nucleate boiling.

Overheating cannot occur in a sodium-heated steam generator as the steam tubes cannot exceed the temperature of the sodium. This is not the case in a fossil-fired plant where the heat source can considerably exceed the maximum allowable tube temperatures.

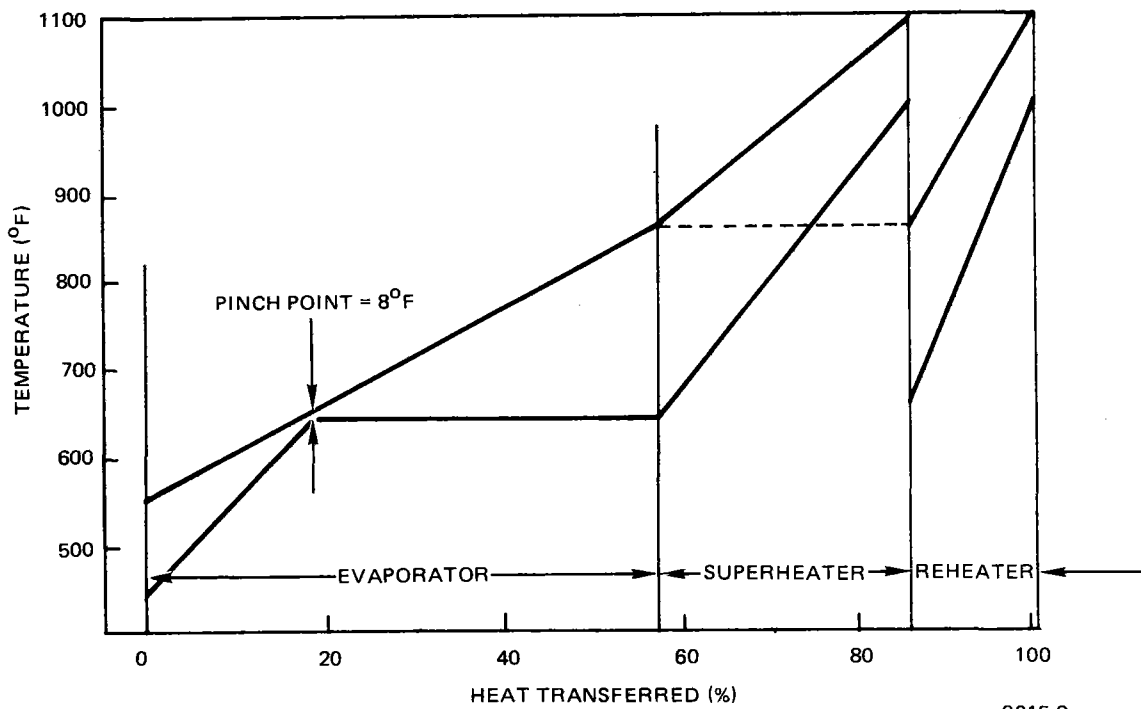
Stress fatigue can occur in the DNB region due to temperature oscillations. During nucleate boiling, large tube wall temperature gradients can occur and are then collapsed during film boiling. This oscillation can be due to power level changes or locally due to the two-phase flow alternately exposing the tube wall to water (nucleate boiling) and steam (film boiling). Figure 3-44 shows approximately where the hybrid system is as far as allowable stress range. For a 30-year tube life, the hybrid system has a comfortable margin. The margin is measured as the ratio of the design point stress cycles to the design curve stress cycles at the design point stress level.

With a sodium-heated heat exchanger and the hybrid steam operating conditions, DNB is acceptable and, therefore, no recirculation is planned at full load.

3.3.10.3 Steam System Materials Selection

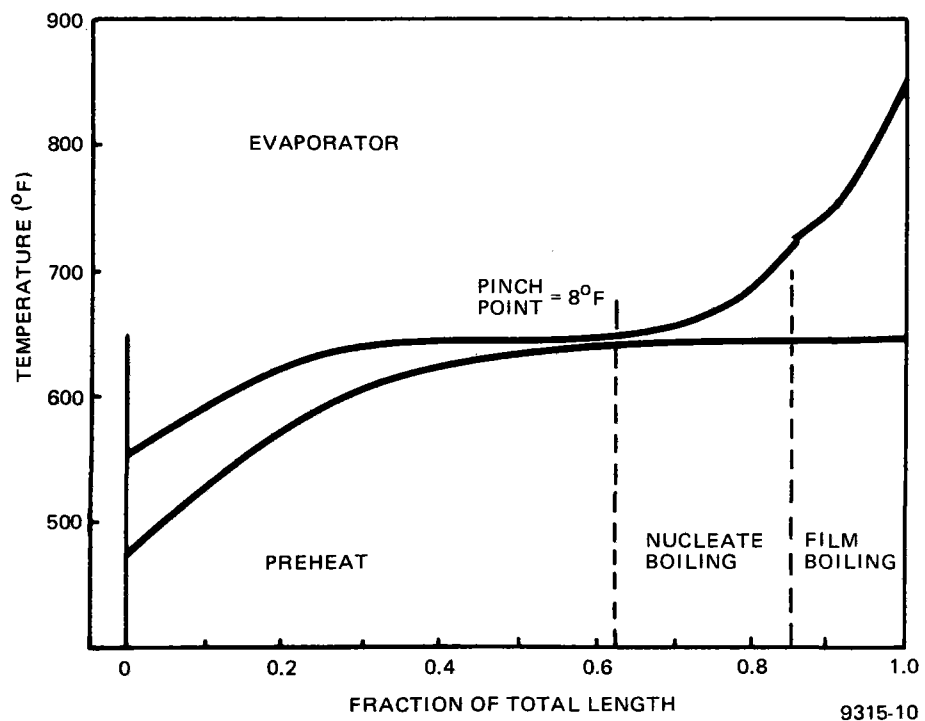
The material to be used in the evaporator will be 2-1/4 Cr - 1 Mo. This alloy is used in over 90% of the liquid metal steam systems in the free world to the present time. It is very forgiving of water chemistry excursions and has been used for many years in fossil-fueled steam generators. It is not subject to chloride stress corrosion cracking. At the temperatures that the evaporator is used, there is no significant problem of decarburization by the sodium.

The higher temperature superheater and reheater are currently planned to be of Type 304 stainless steel. This alloy has been used in superheaters in conventional boilers for over 25 years. B&W alone has fabricated and operated over



9315-9

Figure 3-45. Pinch Point Diagram — % Basis



9315-10

Figure 3-46. Pinch Point Diagram — Length Basis

150 boilers which contain austenitic stainless steel. There have been no reported failures from stress corrosion in any of these boilers in this time period.

Alternate materials to the Type 304 stainless steel are Type 316 stainless steel, Alloy 800, which is essentially a stainless steel containing 30% nickel instead of 8%, and an alloy currently under development by DOE, namely, a stabilized 9 Cr - 1 Mo alloy. As shown in Table 3-9 in Section 3.3.3, Alloy 800 and Type 316 stainless have higher stress design allowables than Type 304, but they are not sufficient to justify their additional material and fabrication costs. However, Alloy 800 enjoys a slightly superior resistance to stress corrosion cracking. It is to be used in the next generation of steam generators built by the French (Phenix). However, it is substantially more expensive than the Type 304 and is not immune to either chloride or caustic stress corrosion cracking. Approximately \$800,000 would have to be saved in water treatment costs in order to justify the use of Alloy 800. Its application at this time is not considered cost-effective for the central receiver solar systems. The 9 Cr - 1 Mo stabilized alloy appears very attractive due to a potentially lower cost, lower expansion coefficient, and higher thermal conductivity than the austenitic materials and what appear to be very promising mechanical properties. The allowables for this alloy may actually be higher than the austenitic materials. However, the alloy is not yet considered to be state-of-the-art or commercially available and is not currently allowed in Section III or VIII of the ASME Code. It may be commercially available when advanced solar plants are designed and built.

3.3.10.4 Effect of Sodium ΔT on Steam Generator Costs

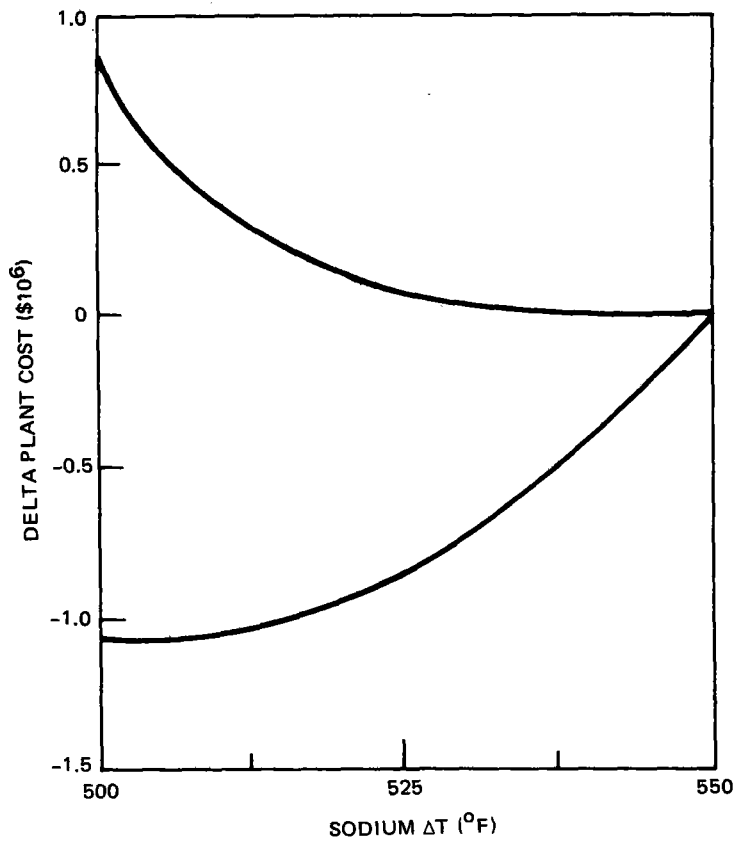
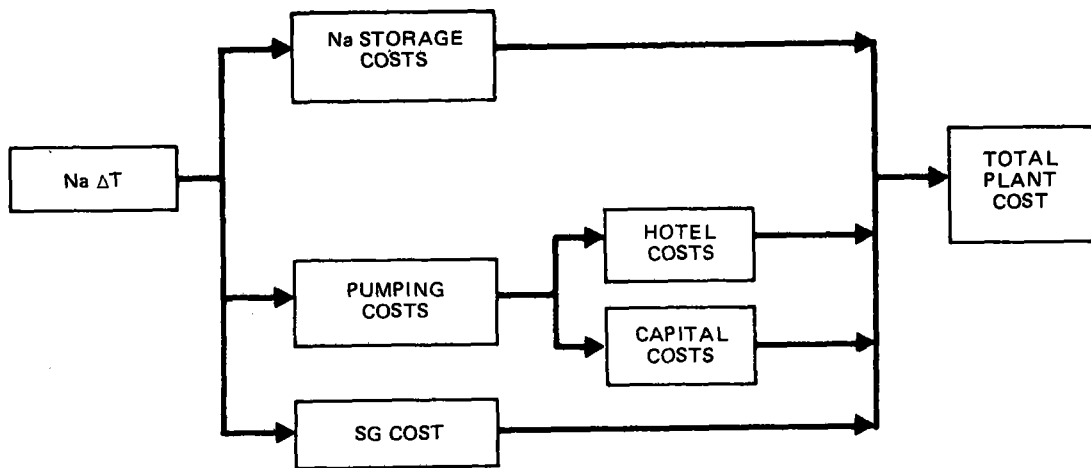
The purpose of the study was to determine if a sodium ΔT of 550^oF still provides the optimal plant costs. Figure 3-45 is a temperature profile for the evaporator unit for the current operating conditions. A sodium ΔT of 550^oF during the ACR program was determined as resulting in an optimum plant cost. Conditions at that time gave a pinch point of 22^oF. More detailed evaluations of the steam cycle have since then resulted in an 8^oF pinch point (Figure 3-46). This small

sodium/water ΔT results in a large evaporator surface area for a given thermal rating. To put it in perspective with another plant cycle, Table 3-21 shows a comparison of solar hybrid with CRBRP.

TABLE 3-21
COMPARISON OF EVAPORATOR SURFACE AREA WITH CRBRP

Parameter	Units	Solar Hybrid	CRBRP
Surface Area	ft ²	15,900	5,697
Pinch Point	°F	8	66
Thermal Rating	MWt	146	115
Surface Area/ Thermal Rating	ft ² /MWt	109	50

The solar hybrid requires over twice the surface area per MWt rating as CRBRP. The effect on overall plant costs was determined for a ΔT of 550°F, 525°F, and 500°F, which corresponds to a sodium cold leg temperature of 550°F, 575°F, and 600°F, respectively. A reduced sodium ΔT requires a higher sodium flow rate for a given thermal rating. Figure 3-47 shows the effect of sodium ΔT on total plant costs. For the case of 0.8 SM with no storage, there is a cost saving of \$1,070,000 using a sodium ΔT of 500°F. For the case of a 1.4 SM and 3-hr sodium storage, the current 550°F is still the optimal plant operation. As the most likely solar hybrid candidate will contain some sodium storage and the potential cost savings not that large, it is not recommended at this time to change the baseline case.



9315-11

Figure 3-47. Effect of Sodium ΔT on Plant Costs

TABLE 3-22
 COMPARISON OF CANDIDATE THERMAL STORAGE CONCEPTS,
 0.8 SOLAR MULTIPLE

Concept	Advantages	Disadvantages
1. Ground level, high pressure, hot and cold tanks	a. Good operational flexibility b. Good steam/sodium system decoupling c. Good reliability d. No steam generator pump	a. High cost b. Large volume, 700 psia tanks required for transient management
2. Ground level, atmospheric pressure, hot and cold tanks	a. Best operational flexibility b. Best steam/sodium system decoupling c. Low pressure tank construction	a. Highest cost b. Lost tower static head c. Least reliability d. Requires steam generator pump
3. Tower level low pressure, hot and cold tank	a. Lowest cost b. Solid sodium piping system c. Best reliability d. Passive receiver protection c. No steam generator pump	a. Tank location b. Adequate steam/sodium system decoupling c. Adequate system flexibility

3.4 STORAGE SUBSYSTEM

3.4.1 Storage Concepts

3.4.1.1 0.8 Solar Multiple

For the 0.8 solar multiple, three storage concepts were examined as candidates for the thermal buffering required by the system. The baseline design system included ground level, pressurized, hot and cold sodium storage tanks. As an alternative to the baseline system, ground level atmospheric pressure tanks in conjunction with an additional sodium pump for steam generator sodium supply was considered. The third alternative is to locate low pressure tanks in the receiver tower separated by an elevation head. The relative advantages and disadvantages of each concept are summarized in Table 3-22. Conceptual schematic representations of the three candidate concepts are shown in Figures 3-48, -49, and -50.

Based on passive thermal protection capabilities and low cost, the tower level, low pressure hot and cold tank thermal buffer system was adopted as the reference storage subsystem for the 0.8 solar multiple system configuration.

3.4.1.2 1.4 Solar Multiple

The all sodium storage system concept developed during the sodium cooled advanced central receiver (ACR) program was adopted as the baseline storage system for the 1.4 solar multiple. This concept is shown schematically in Figure 3-48. The large sodium inventory required for 3 h of storage precludes high pressures or elevated tanks.

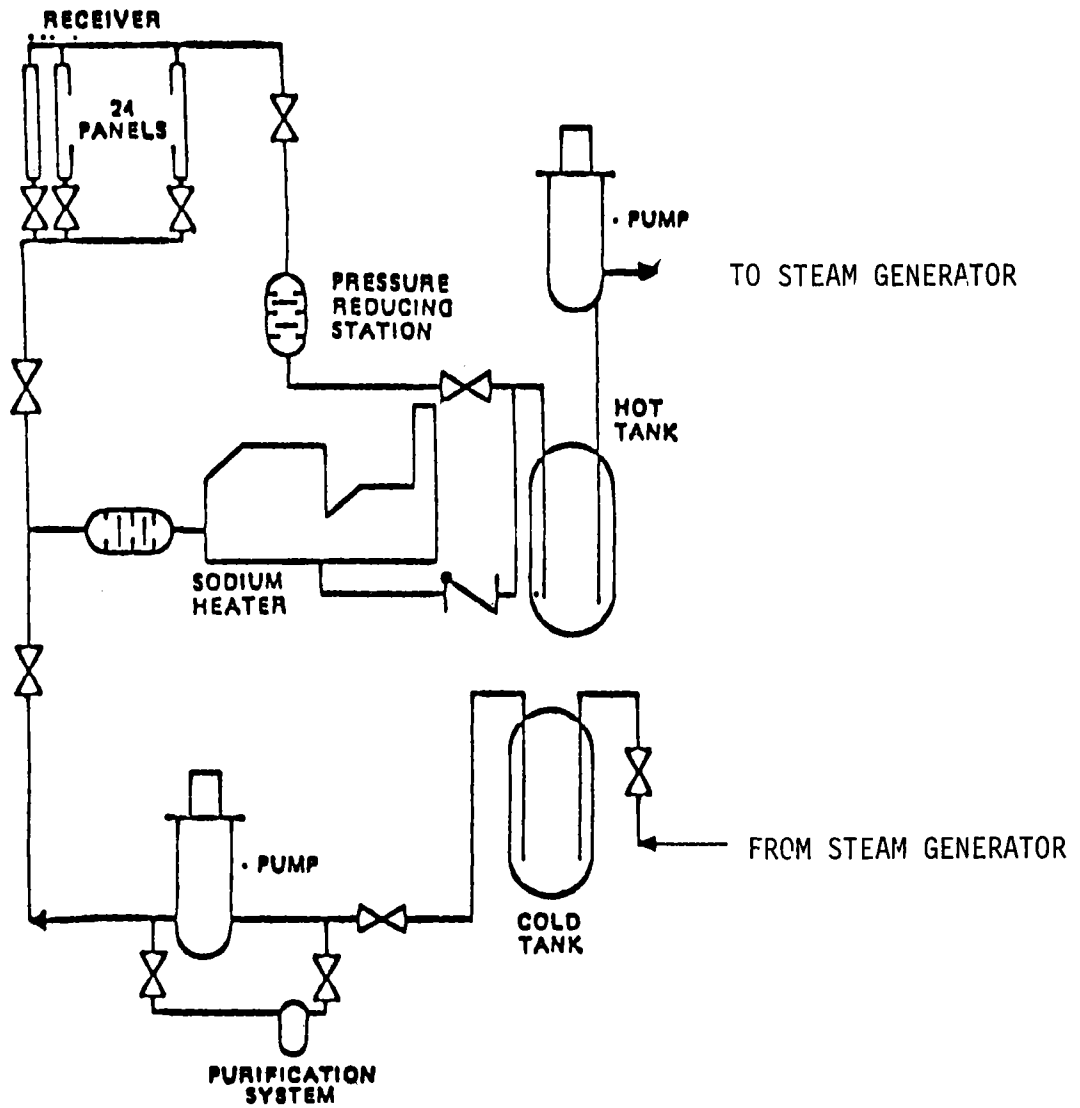
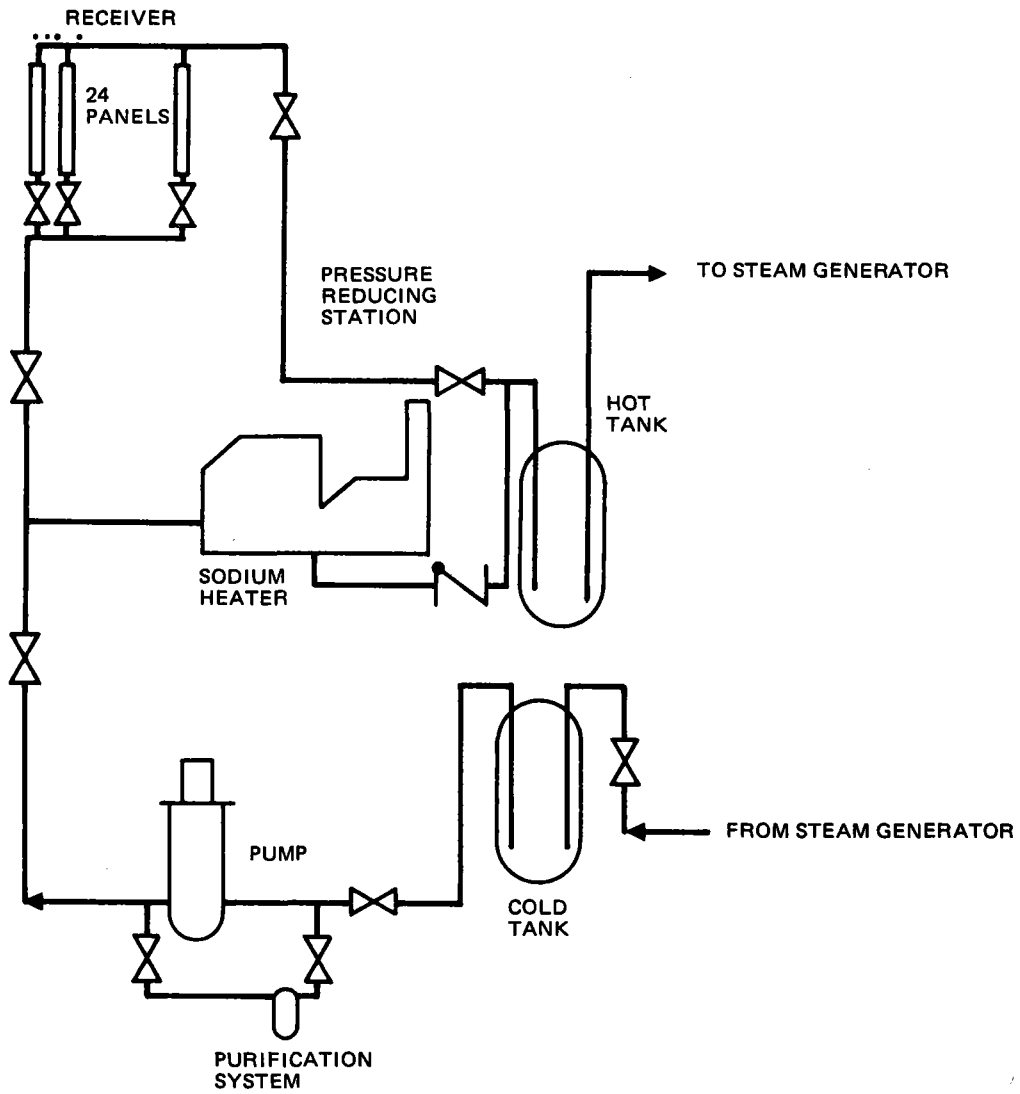


Figure 3-48 Ground Level, Atmospheric Tank Storage Concept



9315-29

Figure 3-49. Ground Level, High Pressure Storage Concept

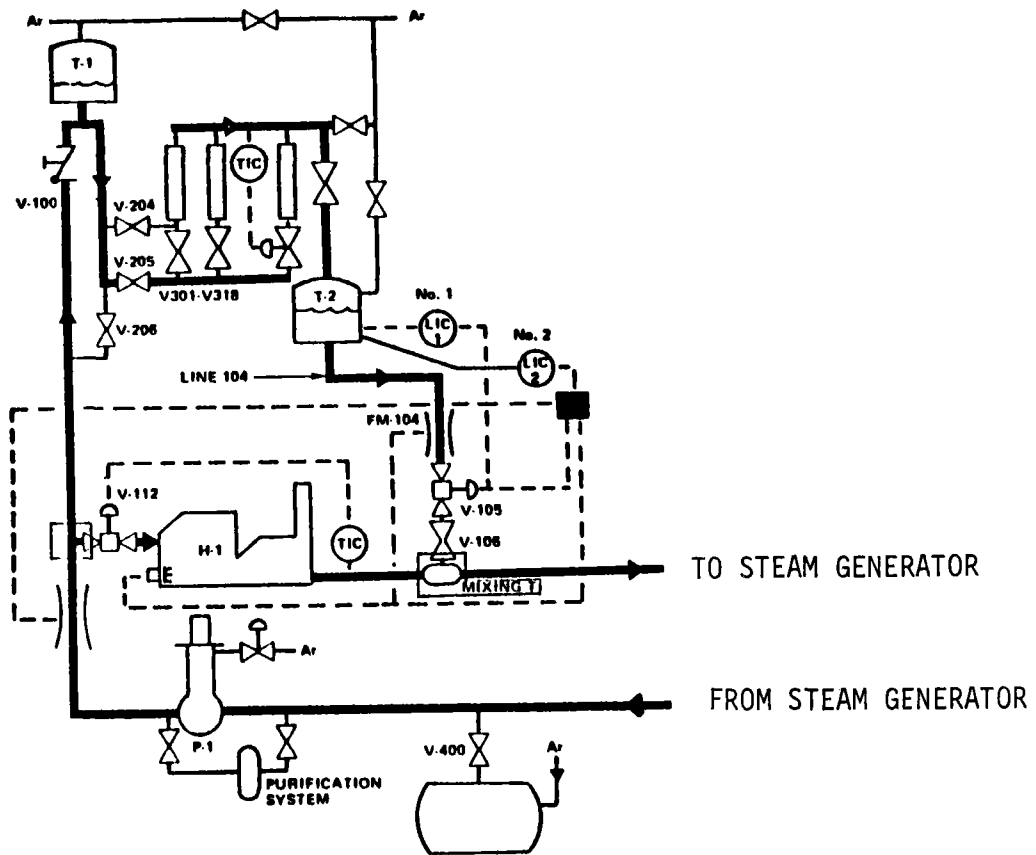


Figure 3-50. Buffer Tanks T₁ and T₂ Located at the Receiver Elevation²

3.4.2 Storage Size

3.4.2.1 0.8 Solar Multiple

For the case of the 0.8 solar multiple plant there is no solar energy thermal storage subsystem provided in the sense of being able to sustain full power operation for any significant time without solar insolation. However, there is buffering provided by means of a system of cold and hot tanks provided in the receiver plumbing system.

These hot and cold buffer tanks (6 each) are approximately 2.4 m (8 ft) diameter by 6.1 m (20 ft) in height and are sized to provide sufficient flow through the receiver in the event of a loss of P-1 pump to prevent excessive receiver outlet temperature. The performance of this buffer system in response to loss of pump and the action of the hot buffer tanks in the case of cloud over transient are discussed in section 3.4.4 below.

3.4.2.2 1.4 Solar Multiple

For the 1.4 solar multiple plant design the thermal storage subsystem consists of a two-tank system (single hot, single cold) sized to provide sufficient thermal energy to operate the plant at net electrical power rating for 3 hours when operating solely from thermal storage. The hot storage tank is approximately 30.5 m (100 ft) diameter by 13.7 m (45 ft) high. This translates to about $1 \times 10^4 \text{ m}^3$ (2.6×10^6 gallons) capacity. The hot tank contains $\sim 17 \times 10^6$ lb of sodium. This quantity allows adequate ullage volume. Both the hot and cold tanks are approximately the same volume despite the minor variation in sodium density between the hot and cold temperatures.

The storage tanks are sized on the basis of the thermal energy requirements, specific heat of sodium, and plant temperature difference between the hot and cold storage tanks. The obvious advantage of a thermal storage system is that the flow to the steam generators is always from thermal storage, and the system isolates the steam generators from the effects of variations in solar insolation and transients caused by pump problems or cloud passage.

3.4.3 Storage Media and Containment Materials Selection

The materials to be used for the high-temperature storage tank will be Type 304 stainless steel. It possesses adequate strength, excellent weldability, reasonably low cost, and a broad base of experience and research. Material selection (Type 304, Type 316, and Alloy 800) is based on data given in Table 3-9 of Section 3.3.3. Components used in the high-temperature sodium system include pumps, which will probably be made of Type 316 stainless steel in the pump case and the cast version of Type 316 stainless steel, Alloy CF8M. The basis for this selection is that the pumps designed and built of these materials are commercially available. Valves will be of Type 304 stainless steel, while valve hardfacing and pump bearing will be Stellite 6B, a proven hardfacing alloy that has been used in many sodium applications.

The lower temperature regions will be of carbon steel. Transitions between the low-temperature carbon steel and the high-temperature austenitics will use an alloy, Inco 82, which has essentially the same composition as Inconel 600. This is also a well established, proven transition welding alloy.

3.4.4 Storage Thermal Performance Analysis

The hot and cold buffer tanks of the plant with the 0.8 solar multiple (Figure 3-50) provide passive protection against a loss of P-1 pump accident. The relative motion of the sun will drift the image off the receiver and reduce the input thermal power with time. Concurrently, with the receiver control valves unchanged, the net head difference between the hot and cold buffer tanks continues the flow through the receiver. The ullage in the cold and hot tanks in conjunction with the initial argon gas pressures in these tanks is designed to provide an approximate match between the flow decrease through the receiver and the absorbed drop-off in the receiver so that the receiver outlet temperature remains approximately constant.

The details of the performance analysis of the hot and cold buffer tank system with respect to loss of P-1 pump is covered in Appendix A to this report.

The maximum ramp rate of the sodium heater cannot meet the sharp-edged cloud passage transient requirements. Sodium flow from the hot buffer tanks (T-2) through the steam generator system and into the cold buffer tanks (T-1) supplements the sodium heater delivery to maintain constant thermal power to the steam generator during this transient.

For the case of the 1.4 solar multiple plant, (Figure 3-48) the operation of the plant is always from the hot storage tank whether the thermal energy is being provided by the fossil-fired sodium heater, from the solar plant receiver, or from a combination of both. That is, the solar receiver and the fossil heater are in parallel. This arrangement provides isolation of the steam generators from the effects of transients and is an inherent advantage of a thermal storage system with respect to plant operation.

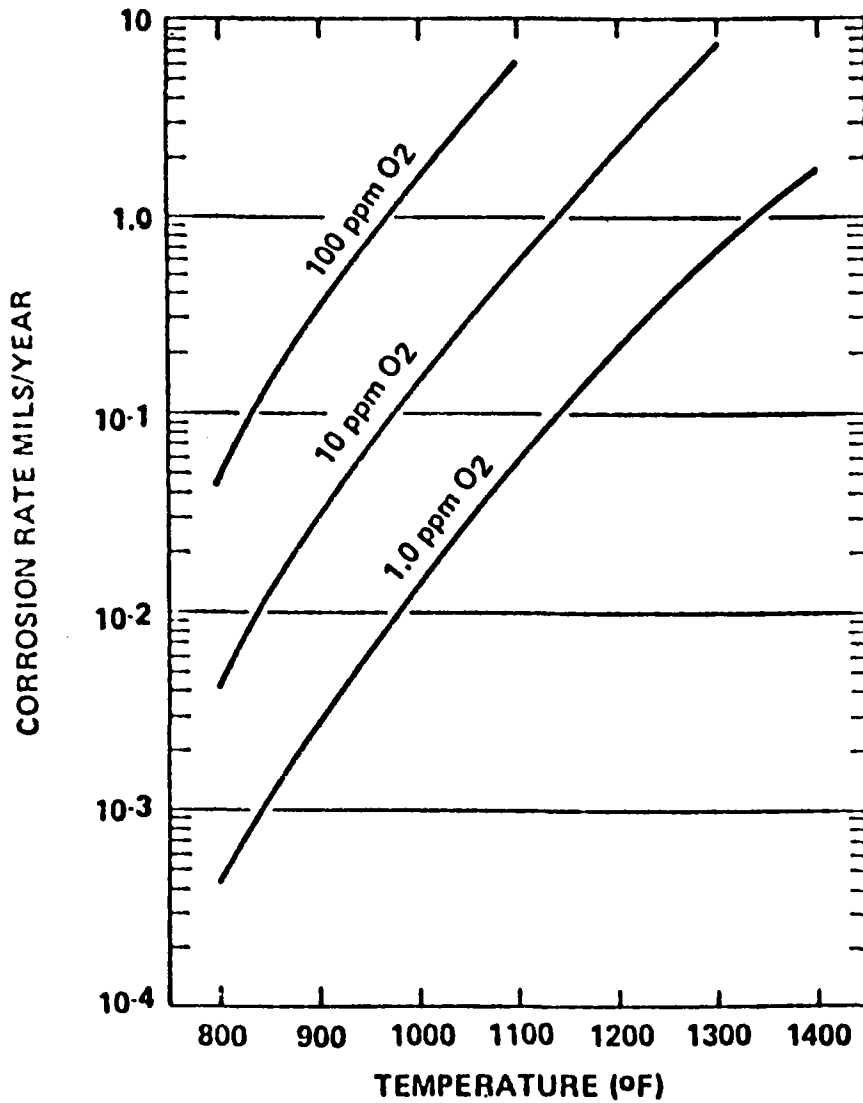
3.4.5 Containment Vessel Structural Analysis

The sodium containment vessels are to be designed to the API Standard 620 supplemented with selected paragraphs from the ASME Code, Section III.

The major loading of these vessels and support structures is expected to be due to seismic activity. The support method must allow for thermal growth of the vessels, yet must provide a suitable load path for deadweight and seismic loads. No major conceptual problems are expected due to the conventional braced frame design of the current concept.

3.4.6 Ullage Maintenance Analysis

It is planned to recycle the argon ullage gas during drain and fill operations. Thus, extremely small amounts of gas would be used. Consequently, there would be very little make-up and therefore a high quality gas could be employed cost effectively.



NOTES

- 1) FOR SODIUM VELOCITY >10 ft/s, LOWER CORROSION AT LOWER FLOW
- 2) OXYGEN ANALYZED BY VANADIUM WIRE; USUALLY 1/10 OF RESULTS BY OTHER METHODS
- 3) MULTIPLY BY 2 FOR HIGH dT/dx (i.e. CORE)

REFERENCE: NUCLEAR SYSTEMS MATERIALS HANDBOOK

Figure 3-51. Corrosion of Type 316 Stainless Steel by Flowing Sodium

3.4.7 Fluid Maintenance Analysis

The principal contaminant of concern in sodium systems is oxygen. The concern stems from: (a) The possibility of plugging small lines <2.54 cm (1.0 in.) in diameter which have sections operating below the oxygen solubility temperature limit of the sodium and operates for long times (>1.0 h) in this condition, and (b) increasing the receiver tube corrosion rate by operating above 2 or 3 ppm oxygen (at 3 ppm, the initial corrosion rate is ~ 0.013 mm per yr (0.5 mils/yr). The average value would be less than half this amount over the 30-year life of the panel. See Figure 3-51.

For the 0.8 SM system, the surface area is $\sim 60,000$ ft². The initial surface contamination would amount to ~ 12 lb of O₂ (using the generally accepted value of 2×10^{-4} lb of O₂/ft²) of surface for clean argon purged system.

The sodium used to fill the system will be filtered at a temperature of 300°F and will add about 2 lb of oxygen to the inventory for a total of 14 lb. This is about 14 ppm. The initial cleanup would take about 150 hr (3 days) using conservative cleanup techniques and a 30 gpm cold trap.

For the 1.4 solar multiple case, the surface is about twice the 0.8 plant. The total oxygen would be ~ 24 lb of O₂ from surface contamination and 32 lb from the initial fill. This would amount to a concentration of approximately 3.5 ppm. The initial cleanup would require about 25 days using a 60 gal/min cold trap. Actually, plant operations would start immediately in either case and cleanup would proceed during normal operation.

The equipment to be used for these operations is described in Paragraph 3.4.5 "Fluid Maintenance Design."

3.4.8 Pumps, Piping, and Valve Analysis

The discussion presented in Section 3.3.9 on sodium pumps, piping, and valve analysis is applicable to this section for the storage subsystem.

3.5 NON-SOLAR SUBSYSTEM

3.5.1 Non-solar Concepts (0.8 and 1.4 Solar Multiple)

The only non-solar concept given detailed consideration in the program is that of a fossil-fired sodium heater. Other concepts are available for supplying auxiliary heat to the Electric Power Generation Subsystem. These include a molten salt primary loop and heater, a water-steam primary loop and boiler, or a conventional fossil boiler in parallel with the steam generators. The first two alternatives have been and are being considered by other investigators,* and for this reason, are considered only as benchmarks in this program. The last alternative would require a detailed assessment of parallel source two-phase flow interfaces. For this reason, the selected sodium primary loop and heater system was chosen over this alternative to avoid a dilution of the detail. In theory, a single-phase sodium heater should be simpler to design, construct, operate, and maintain and, therefore, more reliable and cost effective than a boiler.

Within the selected nonsolar concept, several system and component level trade studies were completed. The component level trade studies and analyses including nonsolar size, thermal performance, life analysis, pumps, piping, and valves, and waste handling system selection are summarized in this section. System level nonsolar subsystem trade studies are described in Section 4 and include fuel selection, parallel versus series configuration, and heater response requirements.

3.5.2 Non-solar Subsystem Size (0.8 and 1.4 Solar Multiple)

The size requirement for the nonsolar subsystem is set by the requirement of full-capacity credit for the plant. The nonsolar subsystem must be capable of supplying 100% of the steam generator power requirements, 260 MWt, whenever the receiver is not able to do so. In the case of the 0.8 solar multiple, this means that a minimum nonsolar subsystem power requirement of 20% of steam generator power or 52 MWt

*Martin Marietta and McDonnell Douglas

is also required. The 1.4 solar multiple sodium heater and non-solar subsystem would only be used when the receiver and storage subsystem outputs are zero. Consequently, the non-solar subsystem will be of a significant fraction of the time. In this case, the simultaneous requirements for full-capacity credit and filling storage from solar alone have overly constrained the plant and added to the amortized cost of the non-solar subsystem.

It is suggested that an investigation of the consequences of relaxing the full-capacity credit requirement be made. The possible benefits of such a relaxation include decreased capital cost and the ability of the plant to operate in a utility load following mode without suffering from excess non-solar subsystem capacity capital costs.

3.5.3 Non-solar Materials Selection

The materials identified in Table 3-23 have been selected for the furnace and convection surfaces of the sodium heater. Considerations involved in choosing these materials include gas-side fuel-ash corrosion and sodium-side decarburization.

TABLE 3-23
HEAT TRANSFER SURFACES

	Material	Tube OD (in.)	Surface Area (ft ²)
Low-Temperature Convection Surface	Carbon Steel	2.50	60800
High-Temperature Convection Surface	Type 304 Stainless Steel	2.50	26700
Radiant Surface	2-1/4 Cr - 1 Mo	1.25	9120 (effective at full load) 7460 (effective at 20 percent load)

The rate of coal-ash corrosion at a given metal temperature increases as flue gas temperature increases. Based on research and field data, a correlation

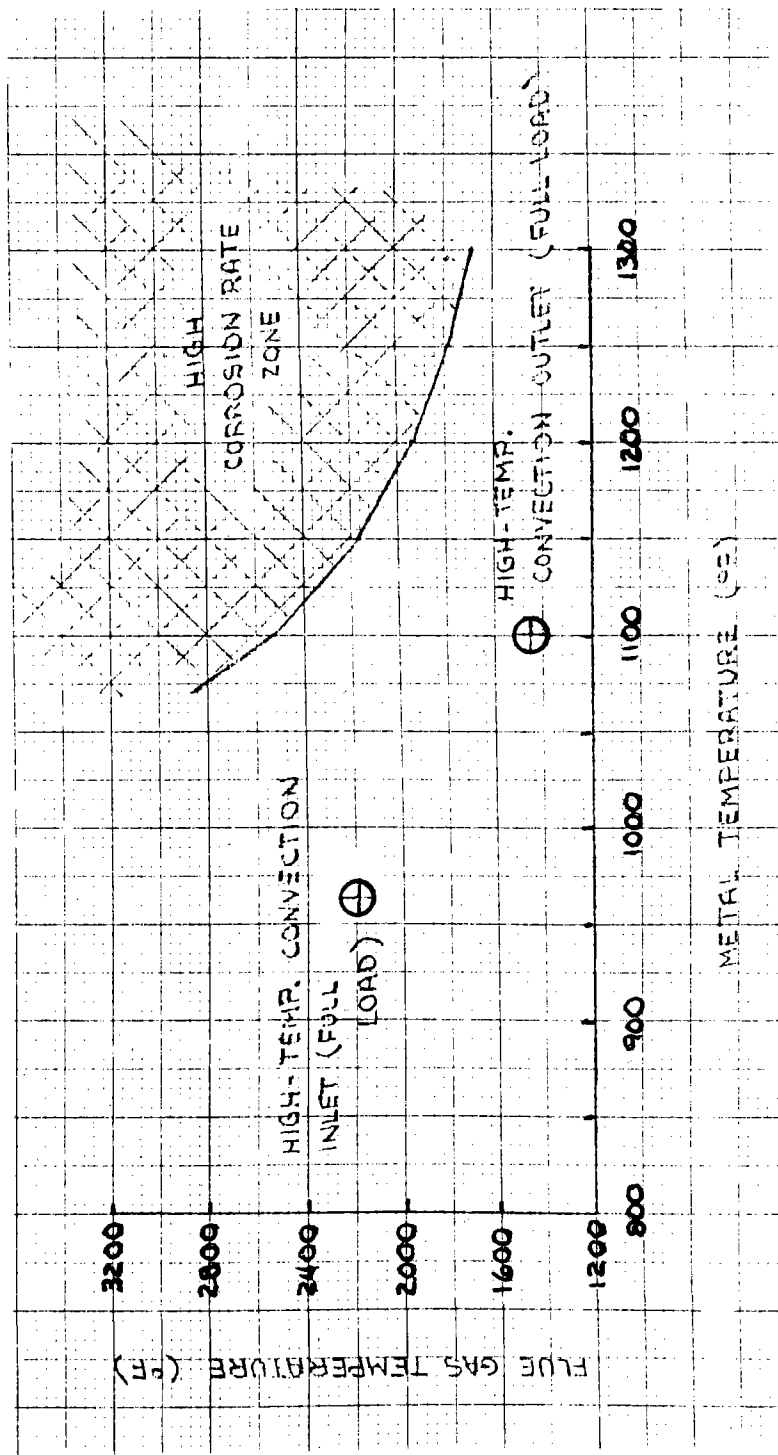


Figure 3-52. Coal-Ash Corrosion

of corrosion rate as a function of gas and metal temperature has been developed. Experience indicates that little or no corrosion is to be expected when temperatures do not exceed the limits defined in Figure 3-52. The design parameters characteristic of the sodium heater fall well outside the "corrosion zone." Flue gas velocities in the convection regions have been limited to approximately 55 ft/s to preclude metal loss by coal-ash erosion.

For the sodium heater, the only question regarding decarburization relates to the 2-1/4 Cr - 1 Mo alloy composing the furnace tubes. The characteristics of this material in sodium are shown in Figure 3-53. The maximum metal temperature varies from $\sim 963^{\circ}\text{F}$ to 1028°F over the operating load range. As shown in Figure 3-53, decarburization rates at these temperatures are within suitable design limits.

3.5.4 Non-solar Fuels Selection (0.8 and 1.4 Solar Multiple)

The non-solar subsystem fuel selection trade study was considered a system level study and such is documented in the systems analysis section. It is located in Section 4.3.6.

3.5.5 Non-solar Thermal Performance Analysis (0.8 and 1.4 Solar Multiple)

A detailed description of the thermal performance of the heaters for the 0.8 and 1.4 solar multiple systems is located in the design data sheets (Appendices E and F).

A bin system and a direct firing system were considered for application with the sodium heater. Components common to both systems include feeders, pulverizers, primary-air fans, and coal and air conveying lines. With the bin system, raw coal is dried, pulverized, transported to cyclone separators where moist air is exhausted, and discharged to storage bins. The coal is subsequently aerated and pumped to utilization bins near the furnace. With the direct-firing system, the raw coal is dried, pulverized, and delivered to the burners in a single continuous operation.

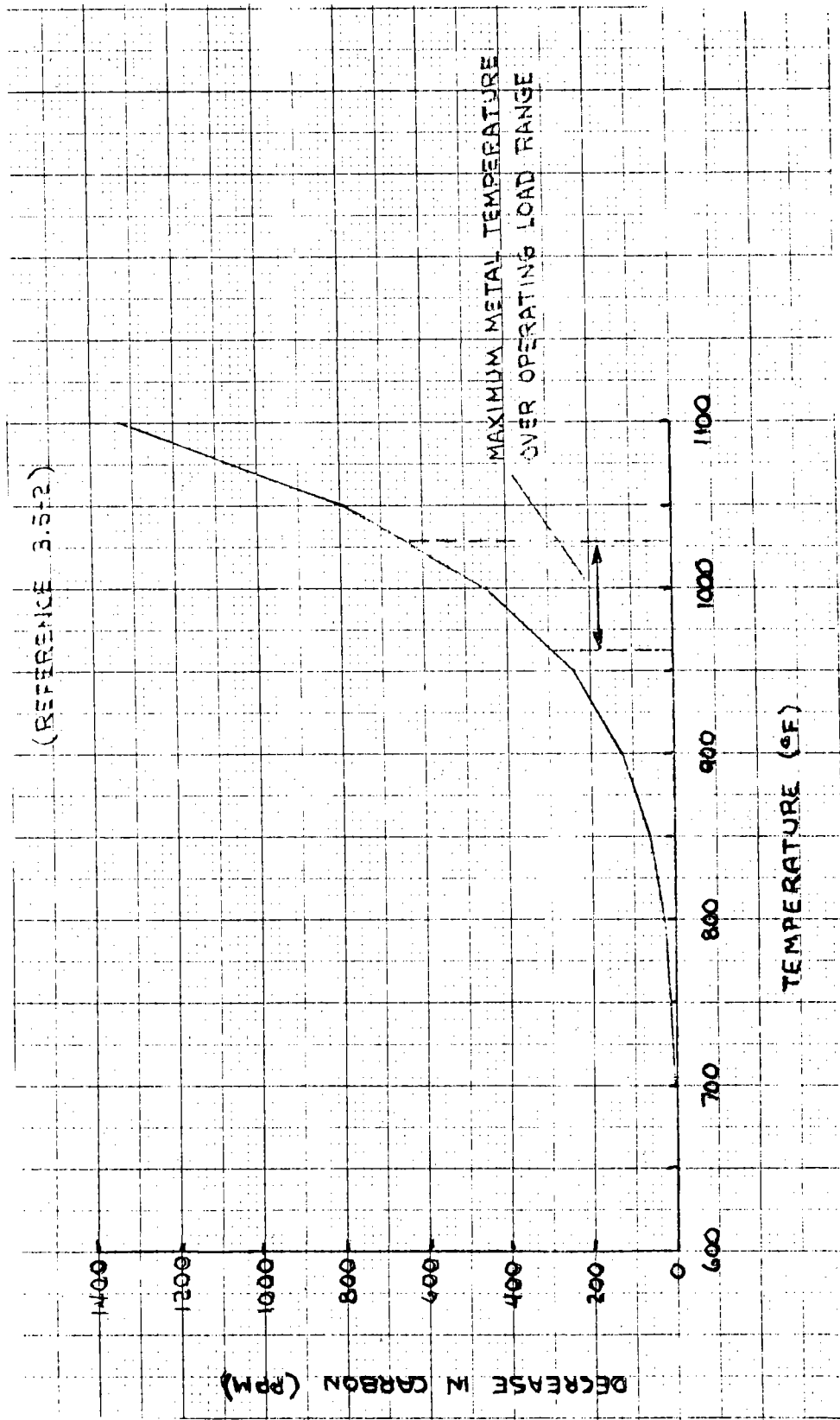


Figure 3-53. Decarburization of 2-1/4 Cr - 1 Mo Alloy Furnace Tube in Sodium

Direct-firing eliminates the need for separately-fired dryers and storage facilities and simplifies the transport system. However, the operating range of an individual pulverizer is limited to about 2.5:1 because air velocities must be maintained above minimum values to keep the coal in suspension and to assure burner flame stability.

Load variations greater than 2.5:1 are usually accomplished by starting up (or shutting down) pulverizer-burner sets (see Section 5.6.3). Therefore, increases in load demand slightly greater time with the direct-firing system than with the bin system, where an inventory of processed coal is readily available. Despite this minor disadvantage, the direct-firing system has been selected for this application because of its greater simplicity, significant reductions in capital and operating expense, and reduced space requirements. The arrangement of components in the direct-firing system is shown in Figure 3-54. Additional performance information is given in Sections 5.5 and 5.6.

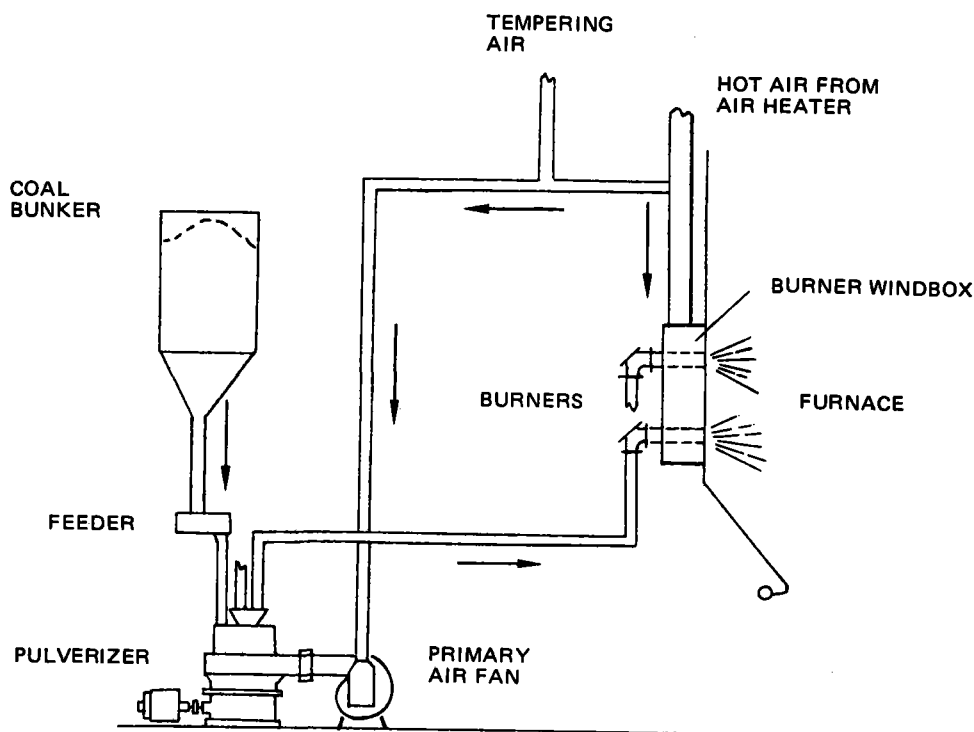


Figure 3-54. Direct Firing System for Pulverized Coal

3.5.6 Absorber (Furnace Life Analysis)

The sodium heater was designed in accordance with the standards for fossil-fired boilers developed from the considerable experience acquired by Babcock & Wilcox (B&W) in this field and the operating and maintenance experience with sodium heaters of Energy Systems Group (ESG). While no specific life analysis has been performed, the review of the design, conducted by B&W, ESG, Stearns-Roger, and Salt River Project, on April 19 and 20, 1979, has led to a general engineering judgment that the design is similar enough to successful boiler and heater designs that there is no obvious reason that the heater life would be less than the required 30 years.

3.5.7 Pumps, Piping, and Valve Analysis

3.5.7.1 0.8 Solar Multiple

In this configuration, the sodium piping is arranged such that it represents a quasi closed-loop system. The only truly free surfaces are located in the receiver, high above the non-solar subsystem. Consequently, the 0.8 solar multiple heater does not require an upstream drag valve for pressure reduction. A simple control valve suffices to properly allocate flow to the heater. This type of valve is discussed in Section 3.3.9.

3.5.7.2 1.4 Solar Multiple

This system requires a drag valve upstream of the heater to reduce the heater inlet sodium pressure such that the pressure at the mixing tee joining the receiver and non-solar subsystems insures a proper flow distribution to these subsystems. In both the 0.8 and 1.4 solar multiple configurations, the receiver pump supplies the motive force for the required flow.

3.5.8 Waste Handling Selection (0.8 and 1.4 Solar Multiple)

3.5.8.1 Ash Handling

Two ash conveying schemes were studied. The first scheme, shown in Figure 3-55, utilizes a negative pressure pneumatic conveying system powered by a mechanical vacuum producer. The second scheme shown in Figure 3-56, utilizes a combined negative and positive pneumatic conveying system with a vacuum/pressure transfer tank. The type of conveying system selected depends on the size of the unit, plant elevation, and conveying distances. For the baseline 100-MW solar hybrid plant, a negative pressure pneumatic conveyor system was selected, with the ash storage bin located within the central core area. If the ash storage bin were located outside of the collector field, requiring a conveying run of approximately 7067 m (3,500 ft), the combination vacuum/pressure conveyor system would be required. A comparison between the two methods of ash removal is shown in Table 3-23. The negative pressure pneumatic conveying system was selected for the 0.8 and 1.4 solar multiple system based on cost effectivity.

3.5.8.2 Chimney Sizing

It is desirable in chimney design to have a chimney which is self-drafting (requiring no additional fan power) and operating at a slightly negative pressure relative to the atmospheric pressure. As shown in Figure 3-57, the stack diameter required for natural draft at the sodium heater rating (265 MWt) is approximately 3.5 m (11.5 ft) ID, with a corresponding exit gas velocity of approximately 16.7 m/s (55 fps). However, in the solar hybrid plant design, the stack diameter is constrained due to available space limitations at the receiver structure. For the baseline 100-MW plant design, a stack ID of 2.4 m (8.0 ft) passing through the receiver structure was selected by ESG. The smaller stack diameter results in a pressurized stack (approximately 81 mm (3.2 in.) water column) with an exit gas velocity of approximately 34.5 m/s (113 fps) at rated load and requiring about 150 MW additional fan power over the natural draft case.

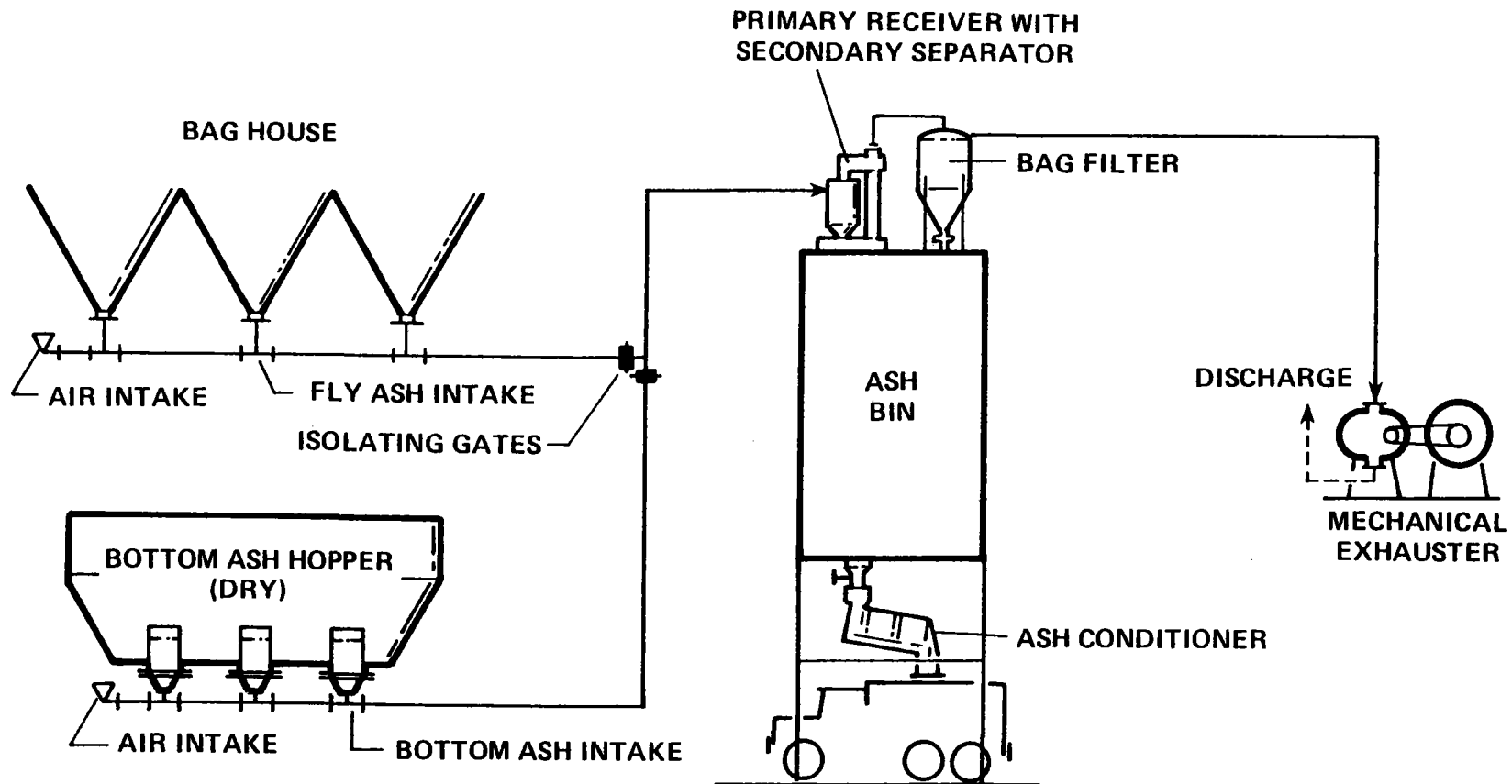


Figure 3-55. Negative Pressure Pneumatic Conveyor

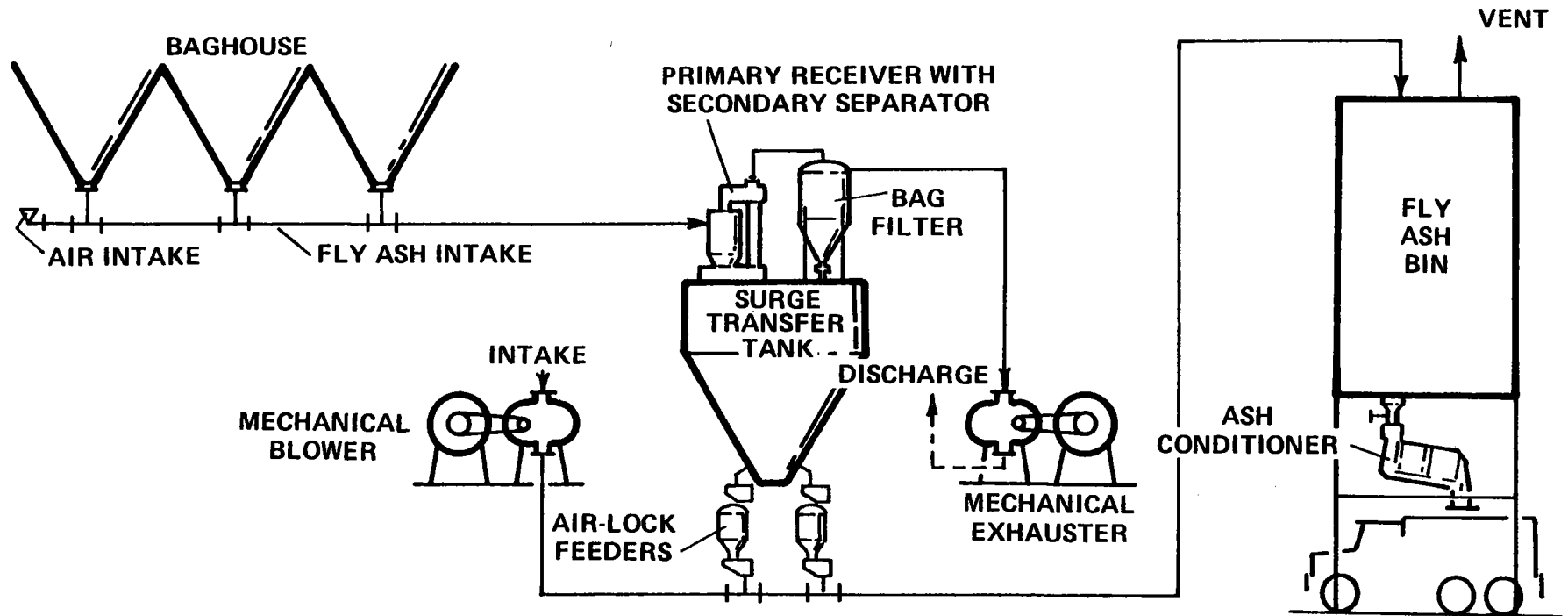
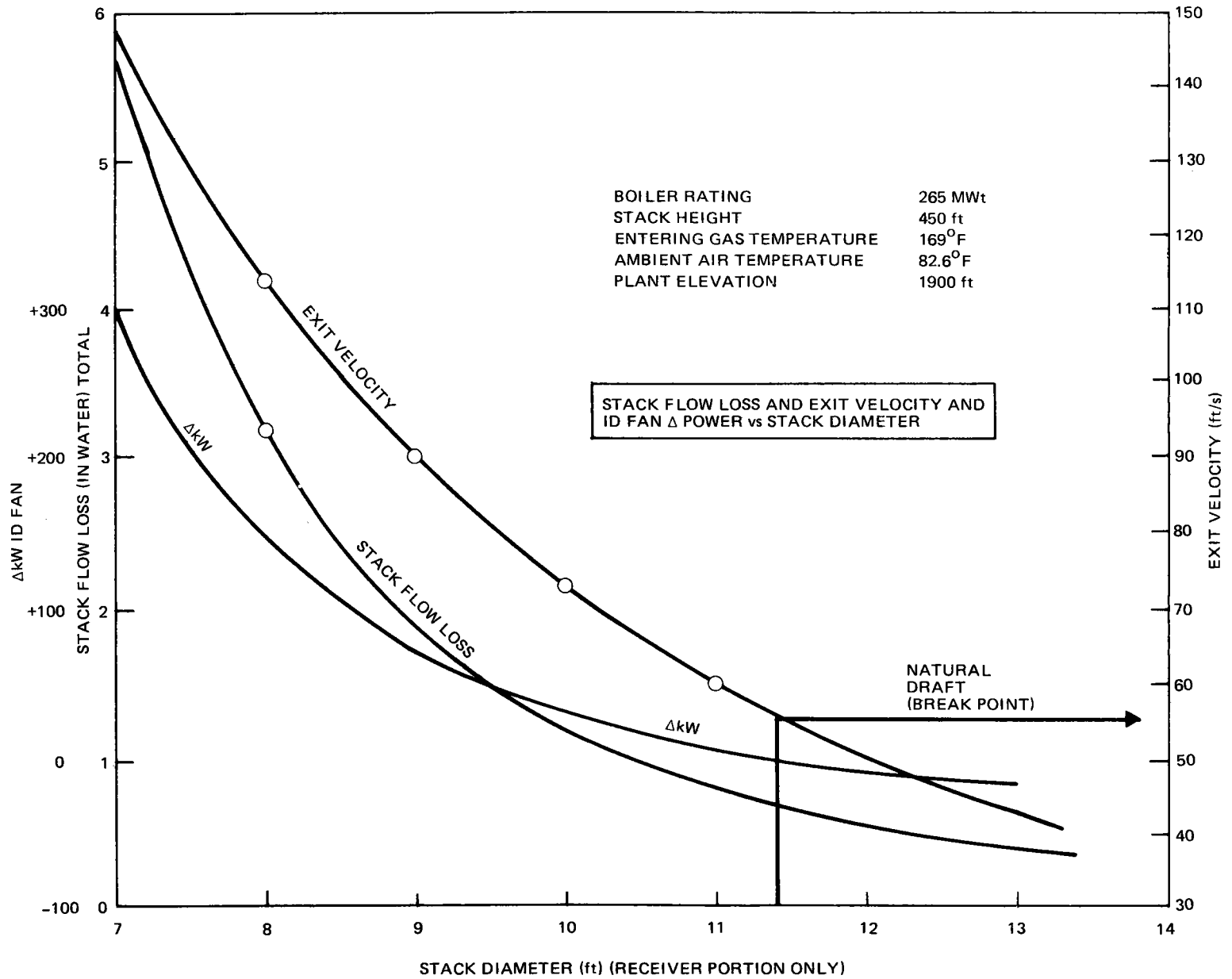


Figure 3-56. Negative and Positive Pressure Pneumatic Conveyor

TABLE 3-24
ASH SYSTEM COMPARISON

Type of Ash Conveying	(Selected) Vacuum System	Vacuum/ Pressure System
Ash Storage Bin Location	Close-In (Within Center Area)	Remote (Outside Collector Field)
Ash Piping Length	500 ft	3500 ft
Mechanical Blower	None Required	1 @ 400 hp
Mechanical Exhauster	1 @ 100 hp	1 @ 100 hp
Capital Cost (1979) (Installed)	\$1,100,000	\$1,585,000
Operating Cost	Lower	Higher
O&M Cost	Lower	Higher



9315-12

Figure 3-57. Solar Central Receiver Hybrid Power System

3.6 ELECTRICAL POWER GENERATION SUBSYSTEM (EPGS)

3.6.1 EPGS Concepts

The EPGS concept considered in the parametric analysis task was limited to the steam Rankine cycle utilizing a reheat steam turbine for the following, important reasons:

- 1) Proven, reliable technology
- 2) Utility acceptance
- 3) Complements sodium-cooled receiver technology (permits high-temperature, reheat steam cycles)
- 4) Meets or exceeds program requirements

One of the attractive features of sodium as a heat transport fluid in a central receiver concept is that it can permit the use of efficient, high-temperature, high-pressure steam turbines; turbines that represent current state-of-the-art technology. It also allows the use of reheat. Because of these features, the technical approach on the EPGS was to select the most efficient and cost-effective turbine generator system and then to design the sodium heat transport systems to meet the EPGS requirements.

3.6.2 EPGS Size

The baseline solar hybrid EPGS size selected was 100 MWe net as specified.

3.6.3 Cycle Selection

Parametric analyses of the electrical power generation subsystem (EPGS) are discussed in the following section. The EPGS is a power conversion cycle consisting of a steam turbine-generator, heat rejection equipment, feedwater heating equipment, feedwater pumps, steam and condensate piping and electrical system. This configuration is shown in Figure 3-58.

A wide range of steam inlet pressures and temperatures, including single and double reheat, were examined to determine the cost benefits due to efficiency improvements to be gained with the use of higher turbine pressures and temperatures and alternate turbine cycle configurations.

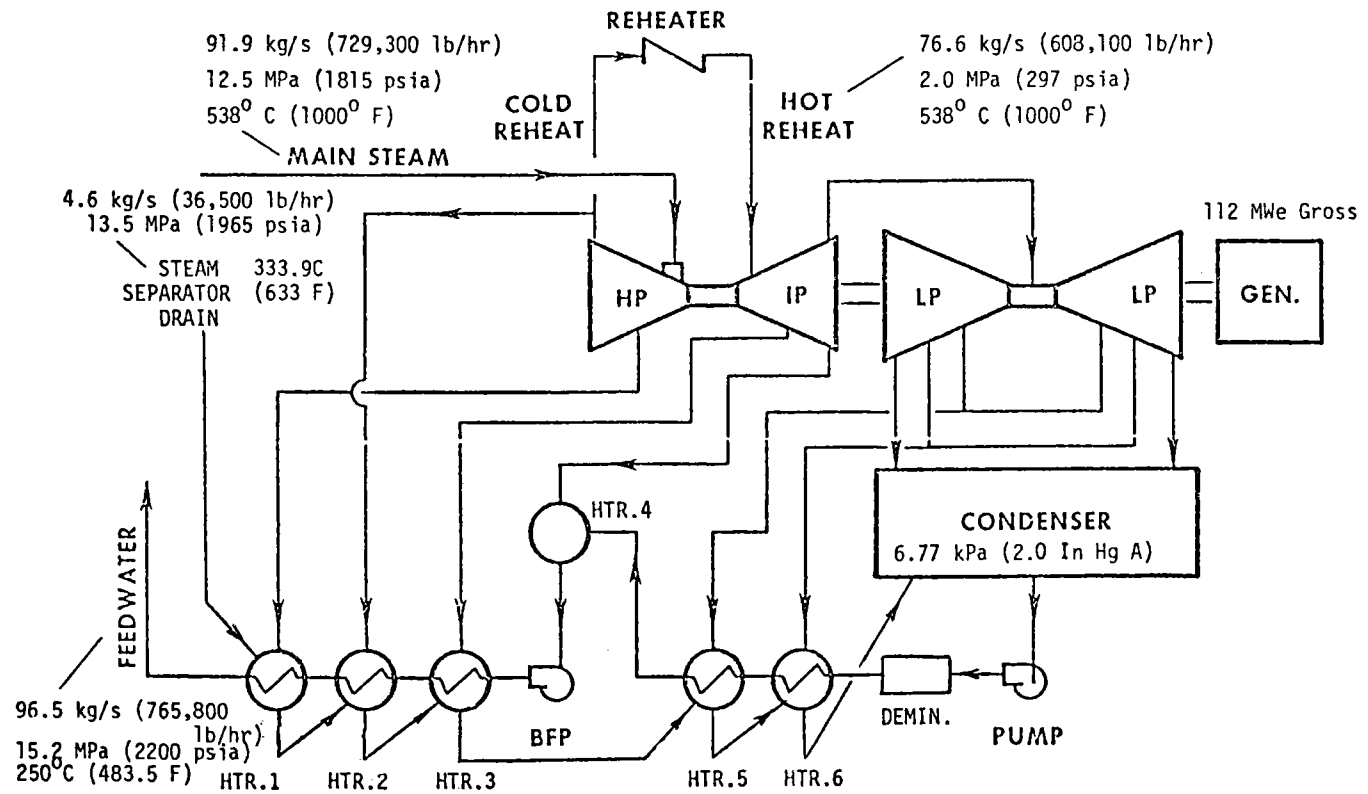
Results showed a 12.5 mPa (1815 psia), 538°C (1000°F) and six heater (HARF) cycle is the preferred choice for the 100-MWe baseline plant. The results are shown in Table 3-25. Returning the 5% steam separator drain through the No. 1 heater shows results in a small increase (10 Btu/RW h) in the heat rate (Table 3-26).

3.6.4 Typical Steam Cycle Startup and Shutdown Operation

Following is a brief startup and shutdown outline procedure for a typical Sulzer steam cycle similar to the one proposed for the large commercial-scale 430-MWe solar hybrid plant. The flow diagram is shown in Figure 3-59. The case shown is a superheated steam cycle utilizing two evaporators in parallel, a steam drum, and a superheater providing steam at 2400 psig and 1000°F. The two evaporators generate wet steam which is superheated after passing through a moisture separator. An outline of the plant startup sequence is given in 5.3.1.2.

3.6.4.1 Startup Procedure

- 1) Start the auxiliary boilers. Seal the turbine glands; start the circulating water pumps and condenser vacuum pumps to establish condenser vacuum. Provide auxiliary steam to assist deaeration in the condenser hotwell.



Estimated Gross Turbine Heat Rate = 8300 kJ/kW hr
(7868 BTU/kW hr)

Figure 3-58. Turbine Cycle Configuration

TABLE 3-25
EPGS PERFORMANCE CHARACTERISTICS (NO BLOWDOWN)

C 2/725

GENERATOR OUTPUT = 112000. KW MECH. AND ELEC. LOSS = 1803. KW

CYCLE PERFORMANCE

HEAT RATE = $(735870. (1480.1 - 468.7) + 606491. (1526.2 - 1305.0)) / 112000.$
Gross = 7843.4 BTU/KWH
 BOILER DUTY = 278457600. BTU/HF BOILER BLOWDOWN = 0.0 PERCENT
 CONDENSER DUTY = 496458272. BTU/HF CONDENSER PRESSURE = 2.0 IN HGA

	FLOW LB/HR	PRESS. PSIA	TEMP. DEG F	ENTHALPY BTU/LB	QUALITY	
TURBINE THROTTLE	735870.	1815.00	1000.00	1480.10		
HP TO LP LEAKAGE	28773.	1340.34	934.35	1456.20		
COLD REHEAT	606491.	330.60	536.01	1305.04		
HOT REHEAT	606491.	297.54	1000.00	1526.25		
LP TURBINE INLET	635264.	297.54	994.00	1523.07		
LP TURBINE EXHAUST	504463.	0.98	101.14	1044.27	0.94	
MAKEUP TO CONDENSER	0.					
HOTWELL	568320.	0.98	101.14	69.14		
HIGH PRESSURE TURBINE EFFICIENCY =	83.75 PERCENT					
LOW PRESSURE TURBINE EFFICIENCY =	91.91 PERCENT					
TURBINE FIRST EXTRACTION PRESSURE RATIO =	3.00					
BOILER FEEDPUMP EFFICIENCY =	75.00 PERCENT					
BOILER FEEDPUMP POWER REQUIREMENT =	1999. KW / 2680. HP					
HEATER NO.	HP 1	HP EXH 2	IP 3	IP EXH 4	LP 5	LP 6
TTD	-3.	0.	-5.	0.	5.	5.
DC	10.	10.	10.	0.	10.	10.
STAGE PRESS	605.00	330.60	148.30	61.03	22.90	6.23
LINE PRESS LOSS	35.30	19.84	8.90	3.66	1.37	0.37
EXT FLOW	53773.	46833.	35223.	31721.	32444.	31413.
EXT ENTHALPY	1355.67	1305.04	1435.29	1337.43	1246.35	1149.60
HTR SHL PRESS	569.70	310.76	139.40	57.37	21.53	5.86
HTR SHL TEMP	480.48	420.59	352.70	299.79	231.91	169.02
HTR SHL ENTHALPY	465.05	397.55	324.61	259.22	200.26	136.99
FW IN FLOW	735870.	735870.	735870.	568320.	568320.	568320.
FW IN PRESS	2225.35	2245.35	2265.35	67.37	123.24	143.24
FW IN TEMP	420.59	357.70	294.82	226.91	164.02	101.14
FW IN ENTHALPY	399.46	333.11	268.56	195.31	132.27	69.51
FW OUT FLOW	735870.	735870.	735870.	735870.	568320.	568320.
FW OUT PRESS	2205.35	2225.35	2245.35	57.37	103.24	123.24
FW OUT TEMP	483.48	420.59	357.70	299.79	226.91	164.02
FW OUT ENTHALPY	468.65	399.46	333.11	259.22	195.31	132.27
DR IN FLOW	0.	53773.	100006.	135829.	0.	32444.
DR IN TEMP	0.0	430.59	367.70	304.82	0.0	174.02
DR IN ENTHALPY	0.0	408.76	340.68	274.81	0.0	142.04
DR OUT FLOW	53773.	100006.	135829.	0.	32444.	63957.
DR OUT TEMP	430.59	367.70	304.82	0.0	174.02	111.14
DR OUT ENTHALPY	408.76	340.68	274.81	0.0	142.04	79.13

TABLE 3-26
EPGS PERFORMANCE CHARACTERISTICS
(5% BLOWDOWN)

GENERATOR OUTPUT = 112000. KW			MECH. AND ELEC. LOSS = 1803. KW			
CYCLE PERFORMANCE						
HEAT RATE = 7853.6 BTU/KWH						
BOILER DUTY = 879607552. BTU/HR			BOILER BLOWDOWN = 0.0 PERCENT			
CONDENSER DUTY = 497872384. BTU/HR			CONDENSER PRESSURE = 2.0 IN HGA			
	FLOW LB/HR	PRESS. PSIA	TEMP. DEG F	ENTHALPY BTU/LB	QUALITY	
TURBINE THROTTLE	729249.	1815.00	1000.00	1480.10		
HP TO LP LEAKAGE	28514.	1340.34	934.35	1456.20		
COLD REHEAT	608112.	330.60	586.00	1305.03		
HOT REHEAT	608112.	297.54	1000.00	1526.25		
LP TURBINE INLET	636625.	297.54	994.06	1523.11		
LP TURBINE EXHAUST	505915.	0.98	101.14	1044.28	0.94	
MAKEUP TO CONDENSER	0.					
HOTWELL	569955.	0.98	101.14	69.14		
RETURN FROM BOILER	36462.	2015.00	636.86	673.89	1	
HIGH PRESSURE TURBINE EFFICIENCY = 83.75 PERCENT						
LOW PRESSURE TURBINE EFFICIENCY = 91.91 PERCENT						
TURBINE FIRST EXTRACTION PRESSURE RATIO = 3.00						
OILER FEEDPUMP EFFICIENCY = 75.00 PERCENT						
OILER FEEDPUMP POWER REQUIREMENT = 2080. KW / 2789. HP						
HEATER NO.	HP 1	HP EXH 2	IP 3	IP EXH 4	LP 5	LP 6
TTD	-3.	0.	-5.	0.	5.	5.
DC	10.	10.	10.	0.	10.	10.
STAGE PRESS	605.00	330.60	148.30	61.03	22.90	6.23
LINE PRESS LOSS	36.30	19.84	8.90	3.66	1.37	0.37
EXT FLW	45744.	46880.	35266.	31405.	32537.	31503.
EXT ENTHALPY	1355.66	1305.03	1435.32	1337.45	1246.37	1149.61
HTR SHL PRESS	568.70	310.76	139.40	57.37	21.53	5.86
HTR SHL TEMP	480.48	420.59	352.70	289.79	231.91	169.02
HTR SHL ENTHALPY	465.05	397.55	324.61	259.22	200.26	136.99
FW IN FLOW	765711.	765711.	765711.	569955.	569955.	569955.
FW IN PRESS	2225.35	2245.35	2265.35	67.37	123.24	143.24
FW IN TEMP	420.59	357.70	294.82	226.91	164.02	101.14
FW IN ENTHALPY	399.46	333.11	268.56	195.31	132.27	69.51
FW OUT FLOW	765711.	765711.	765711.	765711.	569955.	569955.
FW OUT PRESS	2205.35	2225.35	2245.35	57.37	103.24	123.24
FW OUT TEMP	483.48	420.59	357.70	289.79	226.91	164.02
FW OUT ENTHALPY	468.65	399.46	333.11	259.22	195.31	132.27
DR IN FLOW	36462.	92206.	129086.	164352.	0.	32537.
DR IN TEMP	636.86	430.59	367.70	304.82	0.0	174.02
DR IN ENTHALPY	673.89	408.76	340.68	274.81	0.0	142.04
DR OUT FLOW	82206.	129086.	164352.	0.	32537.	64040.
DR OUT TEMP	430.59	367.70	304.82	0.0	174.02	111.14
DR OUT ENTHALPY	408.76	340.68	274.81	0.0	142.04	79.13

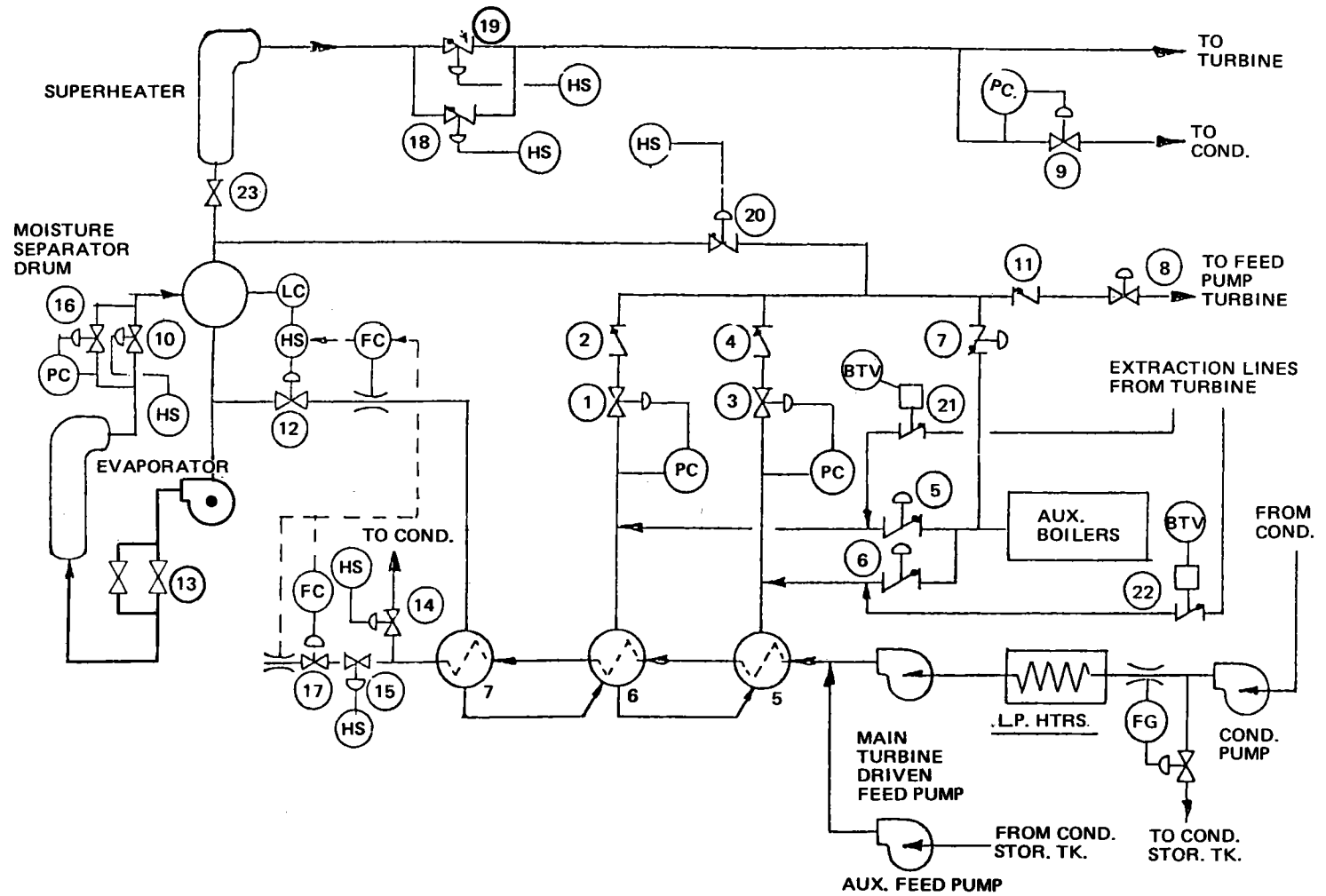


Figure 3-59. Sulzer Cycle Startup/Shutdown System

- 2) Open startup recirculation Valve 14 near the feedwater inlet to the steam generator. Flush the condensate and feedwater system by pumping deaerated condensate through the piping and recirculating to the condenser.
- 3) When the feedwater reaches the quality required for power generation, open evaporator inlet Valve 15, admitting feedwater to the steam generator modules. Close the startup recirculation valve. Open evaporator outlet Valve 10. Fill feedwater side of the steam generator.
- 4) Close the evaporator outlet valve. Open the evaporator outlet isolation Valve Bypass 16 to the moisture separator. The evaporator is maintained at about 500 psig by pressure control on the valve. Open blowdown Valve 12 to recirculate to the condenser; use the feedwater control to automatically establish a flow of about 10% rated flow. The flow from the moisture separator discharges to the blowdown cooler and cascades to the condenser.

A slight amount of steam flashes in the moisture separator drum. Open the superheater inlet isolation Valve 23 and outlet isolation Valve Bypass 18, exposing the superheater to low-temperature dry saturated steam.

- 5) Open Valves 5 and 6, admitting steam from auxiliary boilers to one shell of Heaters 5 and 6 to heat feedwater to 400⁰F minimum.
- 6) When the cleaning and warmup operation is completed, fill the shell side of the steam generator with sodium. Start the sodium pump and operate the systems at full flow on the feedwater cycle. Start the auxiliary feed pump to pump 10% rated flow through each steam generator module and evaporator outlet Valve Bypass 16 into the moisture separator. Adjust the pressure controller on the evaporator outlet bypass valve to maintain 2500 psig back-pressure to suppress boiling in the evaporators.

The hot feedwater from the evaporator discharges into the moisture separator. A level is maintained in the moisture separator by control of the blowdown flow to the condenser. The condensate pump continues to operate to divert excess condensate in the hotwell to the condensate storage tank.

As the sodium temperature increases, the feedwater temperature increases. The pressure in the moisture separator increases to correspond with the feedwater saturation temperature.

- 7) When the sodium temperature reaches about 575⁰F, bring the sodium heater on line and reduce the sodium flow to 40%.
- 8) Hot feedwater discharges from the evaporator into the moisture separator with part of it flashing into steam.

Open Valve 20 to bleed off steam for auxiliary use. Also open the superheater Bypass Valve 18 to warm up the main steam header.

As the flash steam flow increases, it replaces auxiliary boiler steam as the heating medium in feedwater Heaters 5 and 6. When sufficient steam is generated, start one of the turbine-driven feed pumps and remove the auxiliary feed pump from service. Excess steam is dumped to the condenser via the turbine bypass system.

- 9) When the main steam line is warmed, open the superheater isolation Valve 19 and close the bypass Valve 18. Continue to dump excess steam to the condenser.
- 10) When the steam temperature reaches 700⁰F, admit steam to roll the turbine.
- 11) When the evaporator reaches saturation at 2500 psig, open the evaporator outlet isolation Valve 10 and close the evaporator outlet bypass Valve 16.
- 12) When the steam from the superheater reaches operating pressure and temperature, increase load and put the turbine on automatic control.

3.6.4.2 Normal Shutdown Procedure

- 1) Shutdown is initiated by a turbine trip which, in turn, trips the steam generator feed pumps. However, the condensate pumps remain operational.

- 2) Main steam pressure rises and actuates the turbine bypass system to dump steam to the condenser. One condensate pump operates to pump excess condensate from the hotwell to the condensate storage tank. As the feedwater pressure decays, the check valve on the recirculation line from the moisture separator opens to allow natural recirculation. On loss of extraction pressure, automatic Valves 5 and 6 open to supply steam from the moisture separator to one train of Heaters 5 and 6 to maintain the temperature at 400°F.
- 3) At this time, the moisture separator level is dropping, but within 30 s the auxiliary feed pump is started and supplying makeup feedwater to the steam generator.
- 4) As the steam from the steam generator approaches saturation at 2500 psia, close the superheater outlet isolation Valve 19 and open the outlet bypass Valve 18 to keep the superheater warm. Steam from the moisture separator is bled off to the auxiliary steam system. Excess steam is dumped to condenser via the turbine bypass system. Blow down water to the condenser to maintain steam generator water chemistry within limits.
- 5) Close the evaporator outlet Valve 10 and open the evaporator outlet bypass Valve 16 to maintain 2500 psia on the feedwater to suppress boiling in the evaporator. Admit steam from the auxiliary boilers to provide pegging steam to Heaters 5 and 6. Shut off Valve 12 in header supplying steam from the moisture separators to these heaters.
- 6) If a long shutdown is contemplated, cool the sodium and empty it from the steam generator. Fill the space with inert gas. Close the superheater bypass valve and fill the tube side with feedwater and chemicals as required for layup.

3.7 MASTER CONTROL

The master control system developed for the Advanced Central Receiver Power Plant study was selected as a baseline for the Solar Hybrid Central Receiver system. Because of the close similarity in operating philosophy and regime, the design concept from the previously mentioned study was used unchanged and the analysis of this system was limited to assessing the impact of integrating the nonsolar system (sodium heater) control function into the already defined system. Section 3.7.1 presents a synopsis of the concept and Section 3.7.2 discusses the integration of the heater controls.

3.7.1 Master Control Concepts

The design of the Master Control Subsystem for the Solar Hybrid Central Receiver system must address the same objectives of the Advanced Central Receiver Solar Power Plant of high reliability, cost effectiveness and simplicity. To achieve these objectives, the design must incorporate proven hardware components; low cost hardware, software and interfaces; and a simple operational approach.

Looking ahead in the mid-1980 time-frame when an advanced system would be consummated into a working plant, several opportunities will be available to the power plant control system designers that have a distinct advantage over present power plant control hardware techniques. These advantages include: (1) lower cost electronic products of all kinds, (2) high speed, very reliable information transmission techniques, (3) low power consuming electronic devices, and (4) high density electronic packaging. These opportunities are becoming prominent in all industries today and will see significant improvements and development in the years ahead.

Digital microprocessors today are proliferating in the control market. The computational power of these devices is approaching the minicomputer class at fractions of the cost and considerably smaller in size. Evidence on the present and projected improvements that dramatize the future for these devices is shown in Figures 3-60 through 3-62. A single microprocessor chip in 1980 will contain over two times as many logic gates with an increase of only 37% in size (see Figure 3-60). Secondary information storage costs are expected to decline

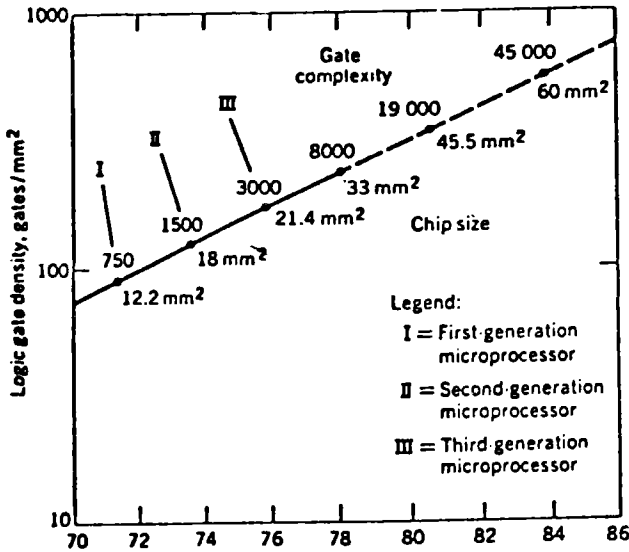


Figure 3-60. Annual Improvement in Logic Gate Density

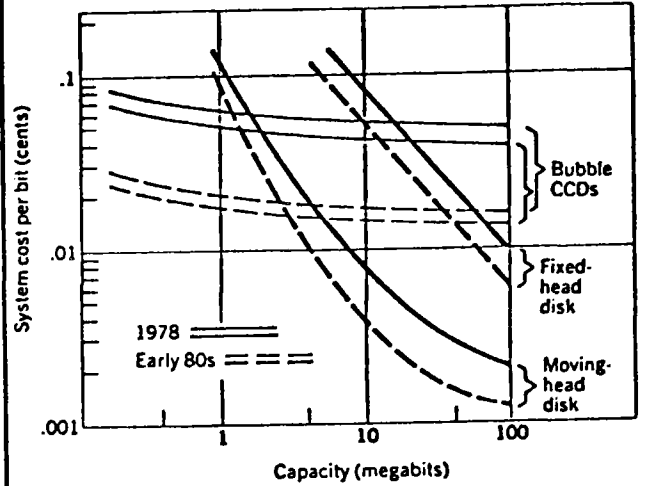


Figure 3-61. Cost per Megabit of Data Storage - 1978 and 1980

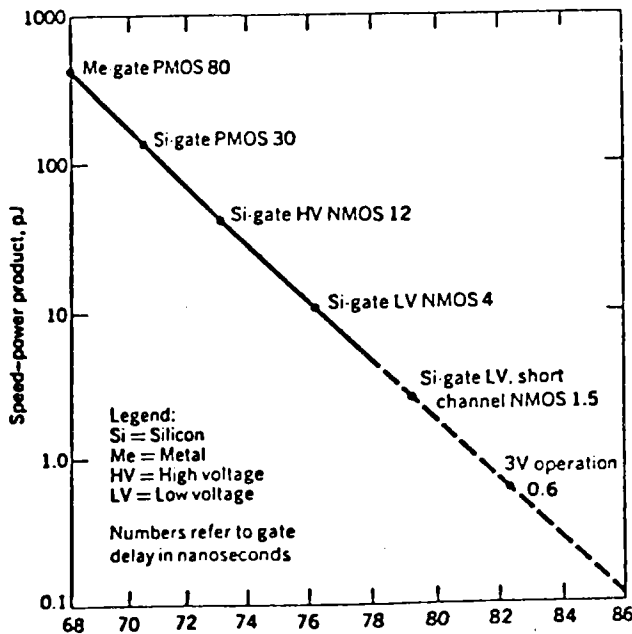


Figure 3-62. Annual Improvement for Power Consumption

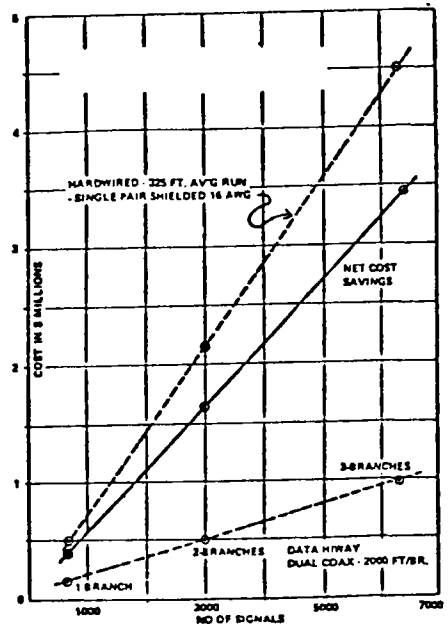


Figure 3-63. Data Acquisition Costs - Conventional Hardwired vs Data Hiway

significantly (Figure 3-61) and the speed and power consumption for these solid state devices is expected to improve dramatically (Figure 3-62).

The serial digital data transmission bus has been growing in popularity in the process industry because of: (1) the reduced wiring costs (see Figure 3-63), (2) high immunity to external noise sources, and (3) the increased use of digital computers for process monitor and control applications. Fiber optic techniques are gradually replacing the coaxial and twisted pair serial data transmission busses. This technique retains the attributes of the conventional serial digital information transmission bus, but has the capacity to handle transmission speeds approaching the speed of light. With the extremely wide frequency bandwidth of fiber optics (over 200 megaHertz) many individual signal paths can be accommodated on a single strand.

All of these devices and techniques mentioned heretofore utilize solid state integrated circuit technologies almost exclusively. This technology continues to show MTBF for components greater than fifty thousand hours (approximately 5.5 years). Furthermore, the lower power requirements to operate these devices, coupled with the materials and packaging techniques used, have extended the environmental limits of temperature, humidity and shock within which these components will operate. Consequently, sequence programmers, microprocessors, and digital converters do not have to be placed in stringently controlled environments. These devices will operate in many field environments.

All of these advantages are being implemented into the mast control design for the Solar Hybrid Central Receiver system design. This design incorporates the following general features:

- Distributed digital control of the power plant processes
- Remotely located controllers
- Serial redundant digital control and data communications between the control center and the subsystems
- Single operator for plant and subsystem control and monitoring

- Control processor terminals used for plant and subsystem control and monitoring.
- Microprocessor based controller hardware throughout
- Maximum use of CRT display devices for monitoring plant status
- Three modes of operation: (1) automatic, (2) semi-automatic, and (3) manual.

3.7.2 Master Control System Analysis

Early in the study a decision was made to utilize the master control system design formulated during the Advanced Central Receiver (ACR) Solar Power Plant Study for the Solar Hybrid Central Receiver system. This eliminated the necessity to perform any lengthy or major perturbation type analysis on this subsystem. However, there is a major single difference between this system and the ARC system arising from the utilization of a fossil fired sodium heater in parallel with the solar heated receiver.

Because of this, it was necessary to assess the impact of integrating the heater control function into the existing design. An analysis of the defined hardware led to the conclusion that there was ample capability to integrate the coordinated control functions of the fossil fired heater into any of the four processors defined in the ACR MCS. Because of the close operational and functional coupling of the heater with the receiver and thermal storage/buffer systems, the logical choice was the receiver and thermal storage/buffer control processor. The coordinated control of the heater can be accomplished via software by providing receiver/heater ramp control, thermal storage make-up (if required) and steady state flow/temperature control from combined receiver/heater, heater only, or receiver only output. The justification for the above conclusions is based on the assumption that the fossil fired heater utilizes hardware control and monitors elements conventional to other subsystems of the distributed plant control architecture. Other operating assumptions and assumed features include: heater control/monitor elements are located near the heater and will communicate with the MCS via the data hiway utilized by other subsystem control elements and that CRT monitor and keyboard manual command entry will be provided as for other subsystems.

The significant impact of integrating the heater controls was therefore found to be in the area of additional software, with only second order effects to the hardware associated with providing data links with the data hiway.

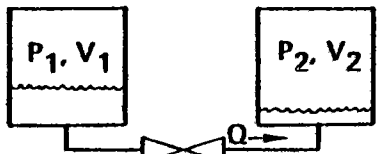
3.8 DYNAMIC ANALYSES

A brief series of dynamic analyses was performed on the 0.8 and 1.4 solar multiple, 100 MWe configurations in order to set the buffer storage requirements and validate the solar/non-solar interfaces. The study drew heavily on the results of the Advanced Central Receiver (ACR) program receiver subsystem simulation study. Consequently, it was not necessary to model the receiver per se as long as receiver coolant supply was adequate during the transients of interest.

3.8.1 0.8 Solar Multiple

In This case, the two transients of interest were the loss of sun incident and loss of pump, P-1, transient. (See Figure 3-50.) In the first case, the object was to ascertain the inventory of sodium required in the hot buffer tanks to insure an orderly transition from all-solar operation to all-heater operation. The goal in the second case was twofold: to validate the concept of a pressurized passive receiver protection subsystem and to determine the required initial pressure to insure adequate flow through the receiver as the sun defocuses by retrograde motion.

The results of the first study are summarized in Section 5, Figure 5-59. Based on estimates of heater characteristic time constants, it is possible to estimate the heater response in an idealized manner as shown in the figure. The response of the receiver is based on the results of the detailed receiver simulation. However, the receiver in the 0.8 SM, 100 MWe plant configuration is considerably smaller than the 1.5 SM receiver modeled in the ACR study. Consequently, an idealized response has been estimated for the receiver. It is also shown in Figure 5-59. Based on these idealized response curves, the hot tank sodium inventory required to ameliorate the loss of sun incident was determined to be equivalent to 1.4 minute of full flow for the steam generator. The hot tank active sodium volume was sized accordingly.



$$P_1 V_1^K = C_1 \rightarrow P_1 = C_1 V_1^{-K} \quad (1)$$

$$P_2 V_2 = C_2 \rightarrow P_2 = C_2 V_2^{-K} \quad (2)$$

$$\text{DRIVING HEAD } H = P_1 - P_2 + \frac{\text{SET TO } 0}{\text{STATIC HEAD}} \quad (3)$$

SUBSTITUTE 1 AND 2 INTO 3 AND DIFFERENTIATE NOTING THAT $dV = dV_1 = -dV_2$

$$dH = -K \left[C_1 V_1^{-(K+1)} + C_2 V_2^{-(K+1)} \right] dV \quad (4)$$

$$\text{FRICTION HEAD} = C_3 Q^2 \quad (5)$$

DIFFERENTIATE FRICTION HEAD AND SET EQUAL TO 4

$$dH = -K \left[C_1 V_1^{-(K+1)} + C_2 V_2^{-(K+1)} \right] dV = 2C_3 Q dQ \quad (6)$$

$$\frac{dQ}{dT} = \frac{-K}{2C_3} \left[C_1 V_1^{-(K+1)} + C_2 V_2^{-(K+1)} \right]$$

NOTING THAT $Q dt = dV$

Figure 3-64. Loss of Pump Transient

The second study concerning the loss of pump, P-1, transient was the more serious of the two. In this case, it is assumed that the pump, heliostats, and controllers all lose control power simultaneously. If no supplemental cooling is available subsequent to the loss of pump, P-1, the sodium in the receiver can absorb enough heat to boil sodium in the hottest panels.

Consequently, one of the goals of this study was to ascertain the head flow characteristics to provide adequate cooling during the transient.

A schematic representation of the situation, along with the development of the governing equations, is shown in Figure 3-64. Using the receiver absorbed power decay curve and analytically solving the governing equations for the appropriate constants by the method of successive substitution yields the final result shown in Figure 3-65. These results show that for a reasonable initial cold ullage pressure (35 psig), good flow/power matching can be achieved. The initial ullage volume associated with this pressure was incorporated into the final design of the buffer tanks.

A more detailed presentation of this study can be found in Appendix E.

3.8.2 1.4 Solar Multiple (SM)

The 1.4 SM, 100 MWe hybrid plant configuration is identical to the 1.5 SM ACR configuration with the exception of a slightly smaller receiver and the addition of the sodium heater in parallel with the receiver. Consequently, if it can be shown a priori that the receiver and heater operate in a quasi independent fashion, in the event of a transfer from all-solar to all-heater operation, then the heater/receiver interface can be conceptually verified without a detailed simulation.

The outlet junction of the heater and receiver design was modified such that each empties into the hot tank at atmospheric pressure. For such a configuration, the only remaining determinant of flow independence is the ability of the receiver pump to handle the transfer. If the pump head remains high enough, then the operation is independent.

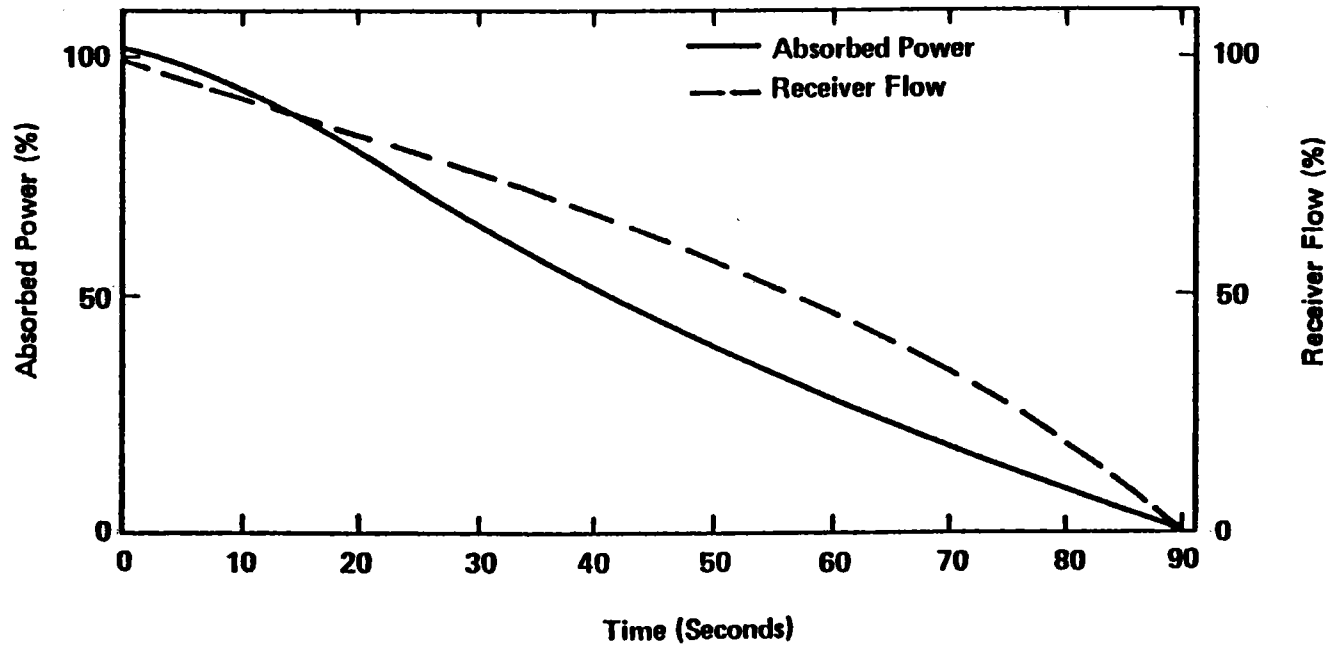


Figure 3-65. Buffered System Response to Loss of Pump Transient

Figure 3-66 shows the projected head pump curve for the 1.4 Solar Multiple System receiver pump operating at 700 rpm. At Point 1, the total receiver/heater flow split is 80/20. If at this time the receiver shuts off due to cloud cover, the flow drops back to Point 1. This represents a change in head of 2%. If the heater control valve remains unchanged, then the heater flow and ΔT will change <1.5%. This change in flow and heater outlet temperature is easily tempered by the mass-capacity of the hot tank, such that the variation of hot tank outlet temperature would be negligible.

The conclusion drawn from these observations is that, due to the required high head of the tower, the receiver pump maintains more than adequate operating margin to maintain independent hydraulics in the receiver and heater.

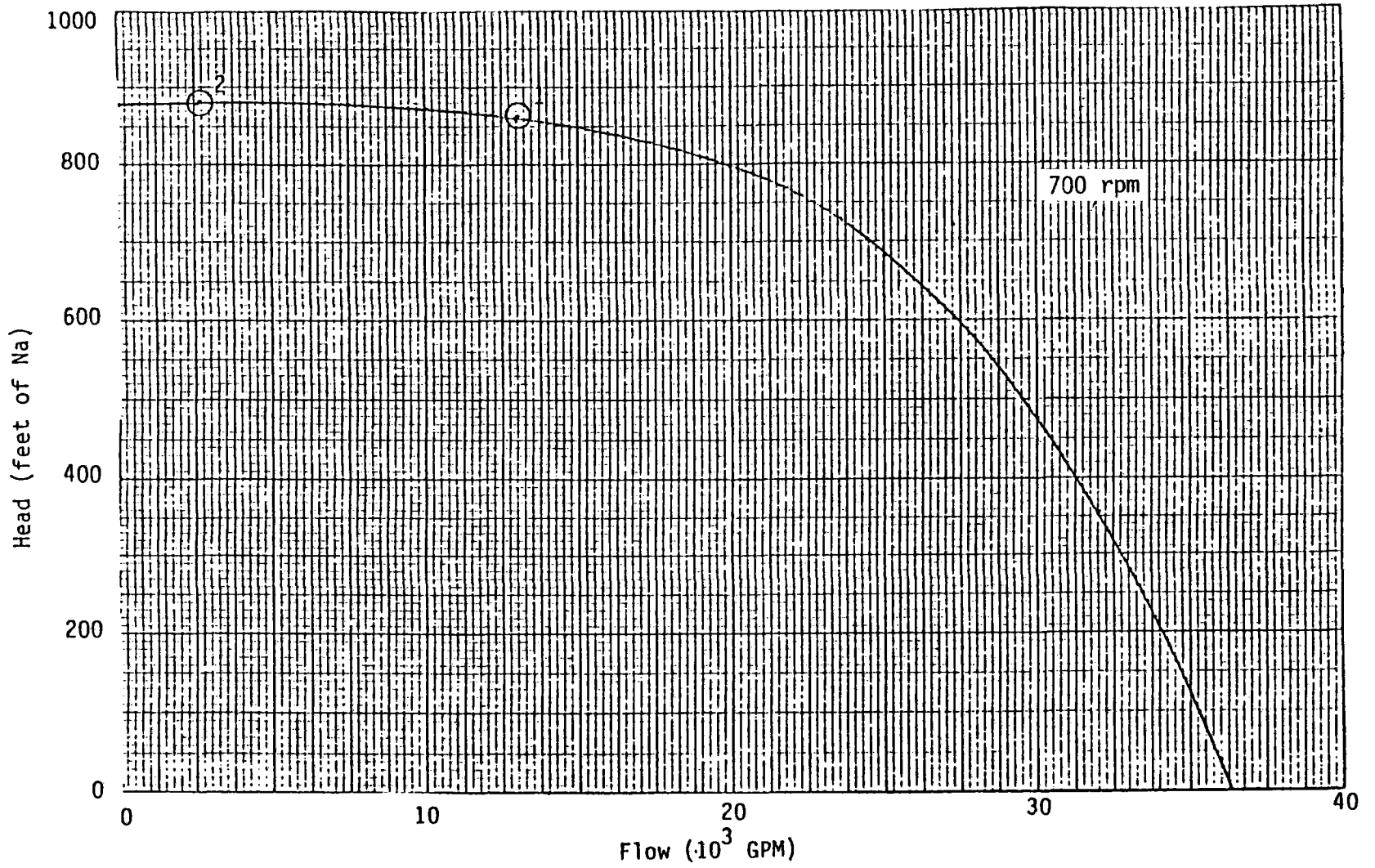


Figure 3-66. 1.4 SM Receiver Pump Head vs Flow Curve

4.0 SELECTION OF PREFERRED SYSTEM

4.1 SELECTION PROCESS (0.8 and 1.4 SM)

The selection process of the system, subsystems, and components of the 0.8 and 1.4 solar multiple sodium-cooled hybrid central receiver configurations all employed the same fundamental methodologies. For any given system or component level selection technically feasible alternatives were compared on an economic basis using the economic parameters delineated in the program requirements definition document.^(4.1) The economic model used to determine the present value, annualized cost, or levelized busbar energy cost of each alternative is outlined in Reference 4.2.

On the component level, an accounting of the indirect costs of each alternative due to impacts of the component on system efficiency, capital, operations, maintenance, and fuel costs was considered, as well as direct cost accounting. In many cases, significant savings in program time were realized by interpolating or extrapolating the results of component cost algorithms developed during the Advanced Central Receiver (ACR) program. In other cases, the ACR cost algorithms were modified to take into account component changes recommended as improvements over the base design. Finally, component selections involving commonly used components such as valves, piping, and auxiliary equipment were made on the basis of previous engineering experience. The details of the component selections are documented in Section 3.

System level analyses, trade studies, and selection studies all used the methodology of Reference 4.2. A computer program was written which incorporated this methodology and allowed rapid variation of input variables and plant operating parameters. For each system alternative, capital cost, fuel cost, solar multiple, fuel type, location meteorological data, and fuel escalation data were generated. Using this input, the program calculated and plotted the levelized busbar energy costs as a function of attained plant capacity. The program is designed for use

with an HP-9845 desk-top computer but is written in BASIC and is easily translated for use on other machines. The program and its methodology is documented in Appendix A. Individual system trade studies and analyses are documented in Section 4.3.

4.2 SELECTION CRITERIA

4.2.1 0.8 Solar Multiple

The 0.8 Solar Multiple System configuration trade studies were constrained only in terms of the required plant output, 100 MWe. Consequently, the primary criterion for selection was cost effectivity, i.e., the system with lowest levelized busbar energy cost was selected. In the case of the fuel selection trade study, additional criteria included: fuel abundance, availability, convertibility, handling, environmental impact, waste handling, waste optics impact, and usage restrictions.

Selection conflicts that required technical trade-offs were resolved by estimating or calculating operating, maintenance, or fuel cost impacts and factoring them into the calculation of system levelized busbar energy costs. In cases where significant cost advantages between alternatives were not found, alternatives were selected on the basis of technical merits, such as, reliability, operability, utility preference, or previous experience.

4.2.2 1.4 Solar Multiple

Within the constraint of the 3-h storage requirement of this configuration, the primary selection criterion was again cost effectivity. Alternatives not showing significant cost differences were compared on the technical criteria listed in Section 4.2.1.

4.3 SYSTEM ANALYSES

4.3.1 Plant Size and Configuration

4.3.1.1 0.8 Solar Multiple

The overall plant size requirements are defined in the Requirements Definition Document.^(4.1) The plant output is 100 MWe, net, regardless of solar insolation levels.

Using the required overall plant size and the resulting steam generator power requirements, derived in the parametric trade study documented in Section 3.6.3, the design sodium loop power requirement for a solar multiple of 1.0 and a field receiver power ratio of 1.0 was established as 260 MWt. The actual sodium loop power handling capability analyses were carried out in a series of trade studies discussed in Sections 4.3.2, 4.3.3, and 4.3.4. In the case of the 0.8 SM, the design sodium loop capacity was set at the design power of the steam generator, 260 MWt based on the solar multiple trade study described in Section 4.3.2.1.

4.3.1.2 1.4 Solar Multiple

In the case of the 1.4 solar multiple configuration, the steam generator requirements remain unchanged from those of the 0.8 solar multiple configuration. However, the system was further constrained to include 3 h of full power storage, capable of being filled on the best solar day, with a solar multiple of ~1.5. The trade study which finally set the solar multiple of this configuration at 1.4 is described in Section 4.3.2.2.

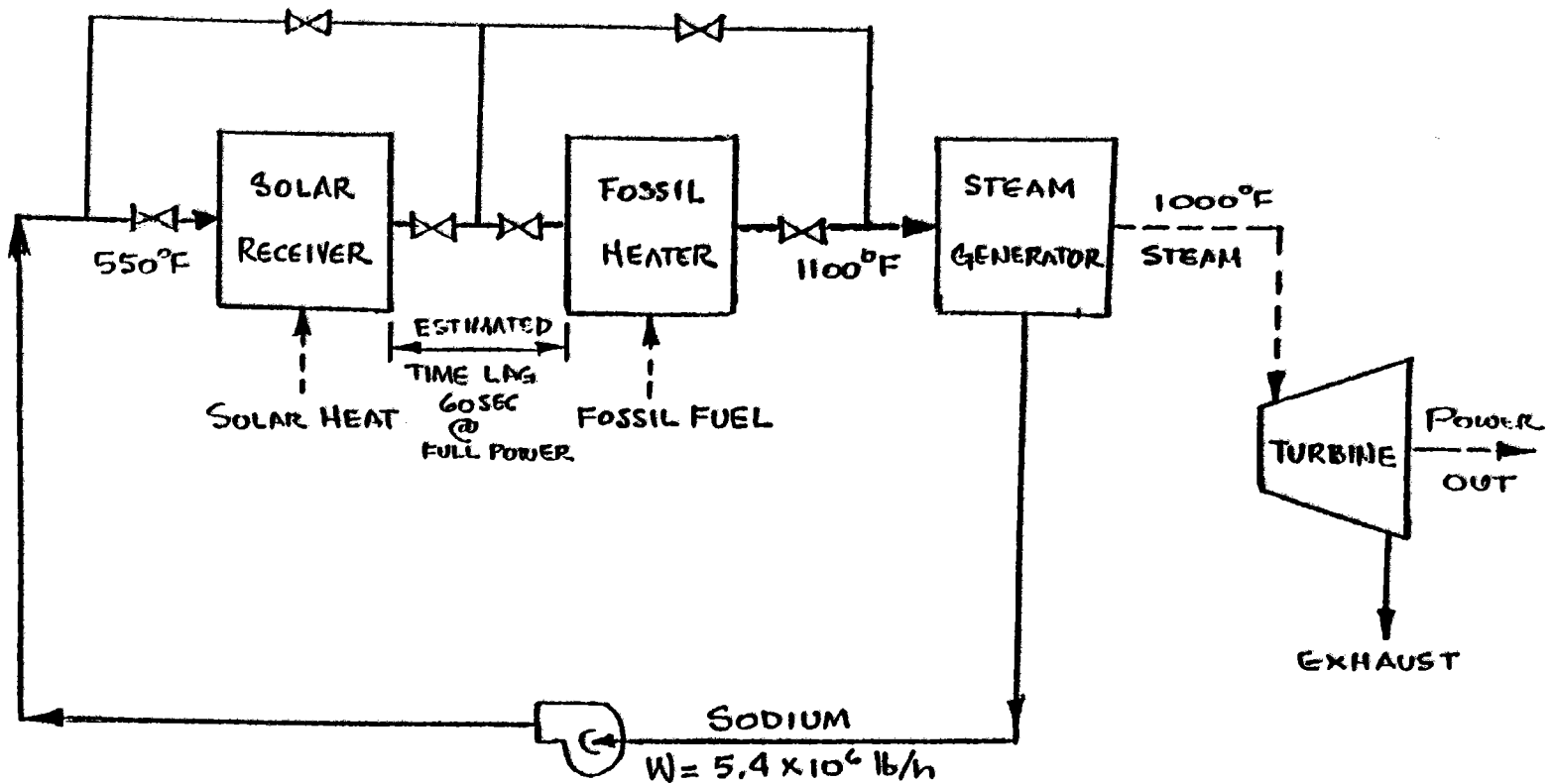


Figure 4-1. Simplified Diagram Solar Hybrid Plant Series Configuration
Solar Receiver Followed by Fossil Heater

4.3.1.3 Solar -- Non-solar Configuration (0.8 and 1.4 Solar Multiple)

Several alternatives exist for piping the solar receiver and fossil-fired sodium heater into the sodium process system for the solar central receiver hybrid power system conceptual design study. These two components can be connected either in parallel or series. Two options also exist for the series connection. The solar receiver can be connected in series either upstream or downstream of the heater. A study was made to compare the relative merits of these alternatives in order to make a selection to be used as the baseline design.

The two options that exist for designing the plant with a series configuration for the heater and receiver are shown in Figures 4-1 and 4-2. In Figure 4-1, the receiver is piped upstream of the heater, whereas in Figure 4-2, the receiver is connected downstream. In either case, for full-load operation, the sodium flow rate through the two components is maintained constant at 5.4×10^6 lb/h and the temperature rise across each component is varied in direct proportion to its load.

Figure 4-3 shows a simplified diagram of the hybrid plant with the solar receiver and fossil-fired heater connected for parallel operation. In this configuration, either component may be operated by itself up to its rated load, or else the total plant load may be split between the two heat sources. The heater has a rated load of 100%; however, the receiver rated load is 80% due to the requirement of 20% minimum safe firing rate of the heater.

An assessment of the economic factors which influence the choice between the series and parallel configurations was made. The economics favor the parallel arrangement for the following reasons:

- 1) Stainless steel piping would be required for the piping connecting the receiver to the heater when connected in series. Replacing the carbon steel piping and valve,

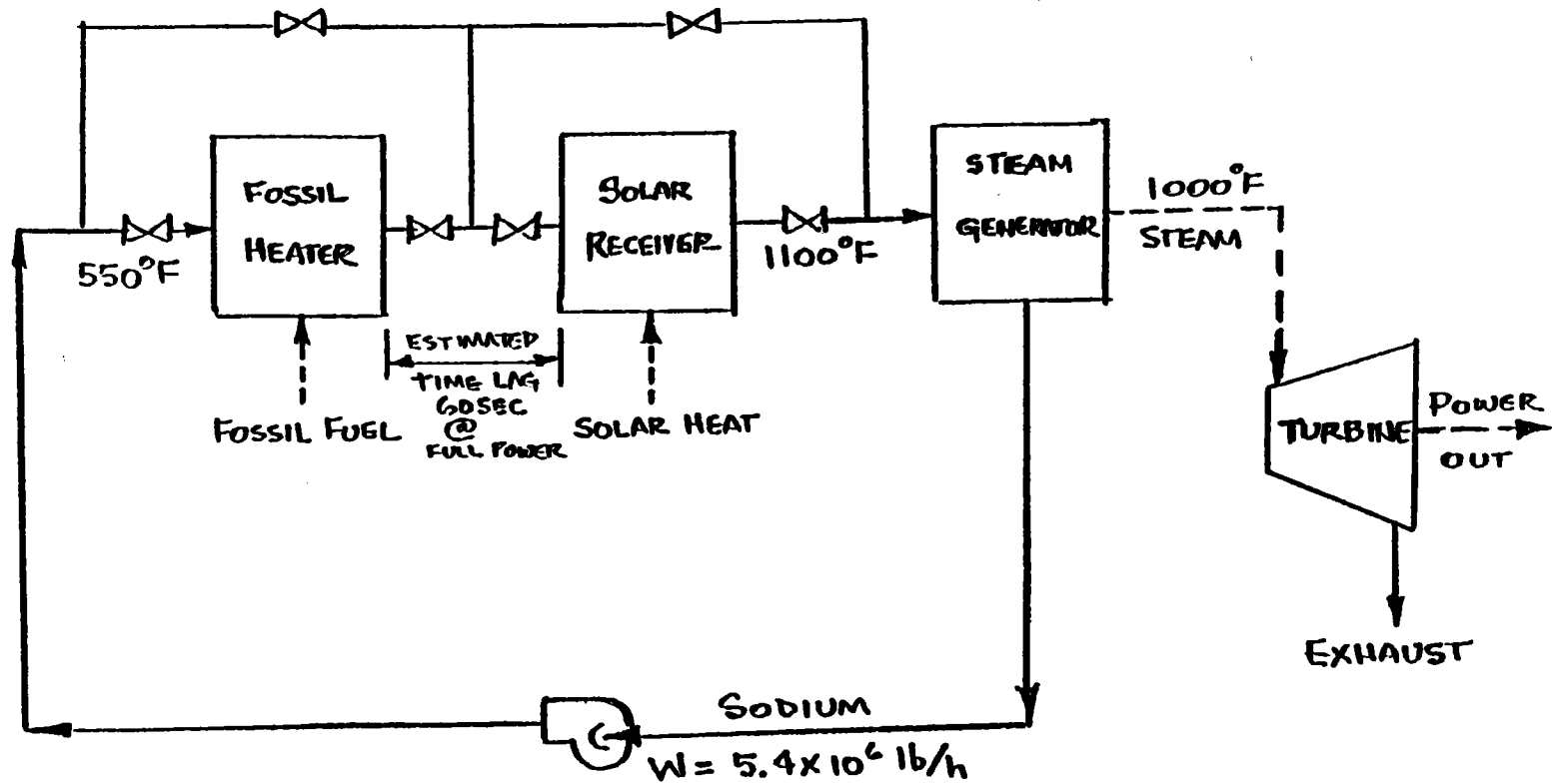


Figure 4-2. Simplified Diagram – Solar Hybrid Plant Series Configuration
Fossil Heater Followed by Solar Receiver

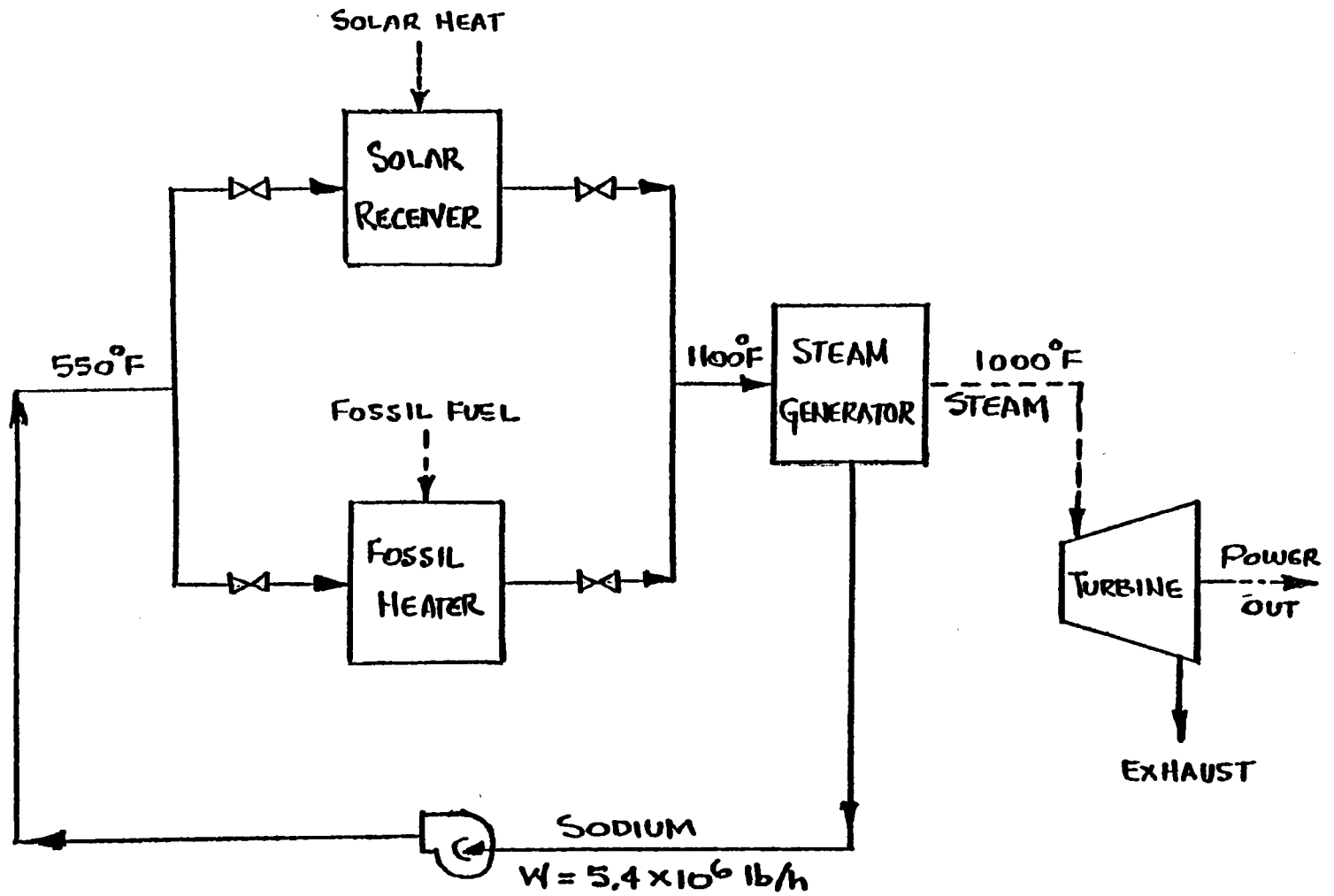


Figure 4-3. Simplified Diagram – Solar Hybrid Plant Parallel Configuration

which can be used for parallel operation, with stainless steel piping and valves is estimated to cost an additional \$160,000 in 1978 dollars.

- 2) Stainless steel piping and valves are also required for the bypass piping for the series arrangement. It is estimated that this extra piping and valving will cost an additional \$700,000 in 1978 dollars.
- 3) Average heat losses for the series configuration are greater than for the parallel configuration when the receiver is installed downstream of the heater. The higher average receiver-operating temperature results in the larger heat losses which are made up by increasing the power output of the heater.

It is estimated that heat losses equal to about 2 MW of thermal energy must be provided by the heater. Assuming a coal-fired heater, additional annual fuel costs of \$47,000 per year are estimated based on a fuel escalation rate of 10%. This is equivalent to a present worth of \$450,000 in 1978 dollars.

- 4) Rapid load changes between the receiver and heater when connected in series will require excessive thermal storage. This is because the receiver can change load at $\sim 1\%/s$, whereas the heater is limited to a temperature change of $10^{\circ}F/min$, which is equivalent to a load change of $1.8\%/min$. Storage of about $1/4$ h will be required in this case to provide the necessary thermal power to maintain constant output during the transfer of the load from the receiver to the heater.

It is estimated that $1/4$ h of thermal storage is equivalent to $\sim \$1.6M$ in 1978 dollars.

- 5) Larger number of thermal cycles will require more expensive design analyses and design requirements to mitigate thermal stresses for the series connected components.

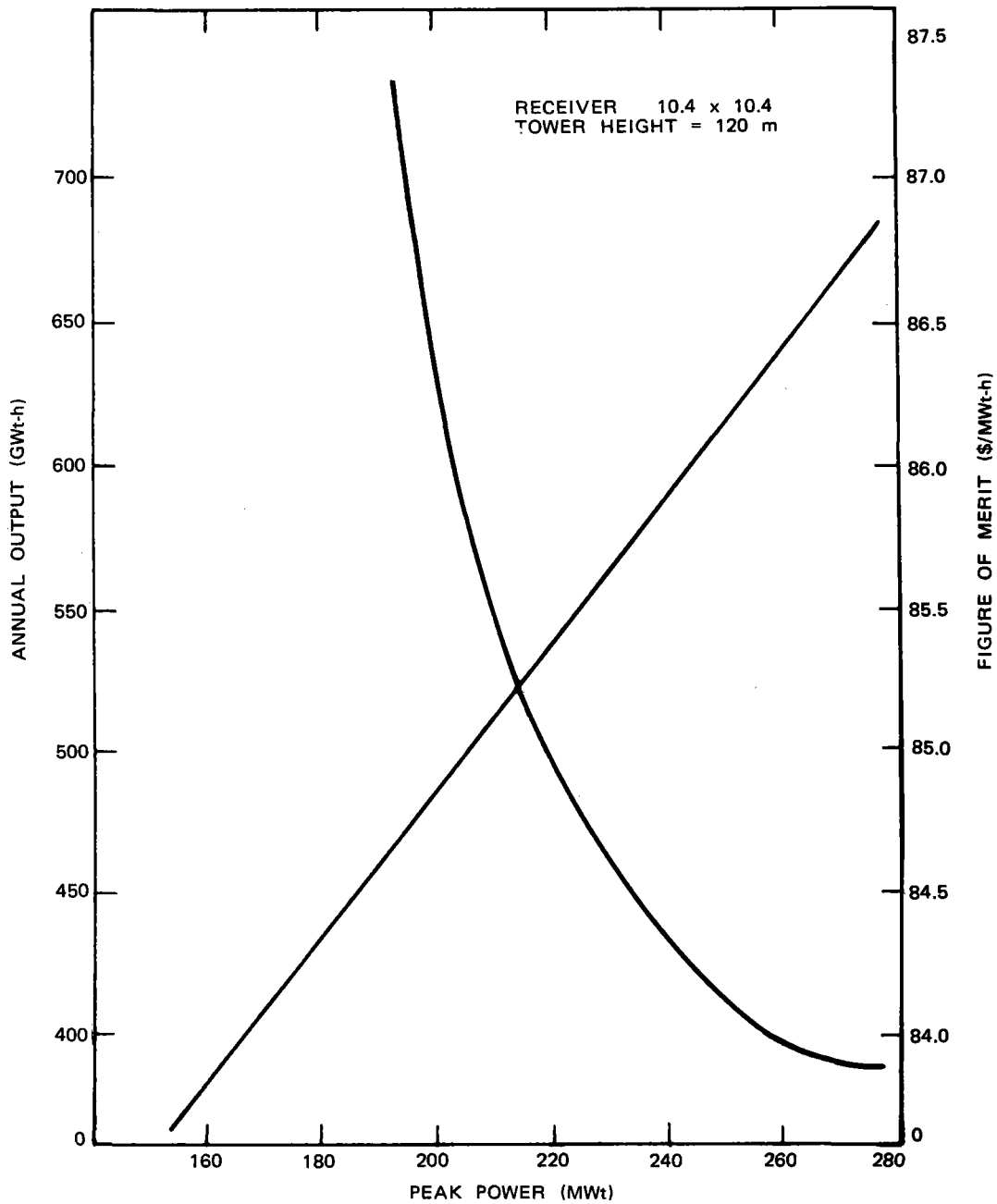
It is estimated that the engineering design and analysis costs for the series connected components could result in increased costs of up to 30%. The life and reliability of these components will be severely impaired by the continuous thermal cycling with load changes. This is a one-time nonrecurring cost for the hybrid plant.

Table 4-1 presents a summary of the estimated additional capital price required for the series configuration and indicates that an additional price of \$2.9 million would be required for the series configuration when compared to the parallel configuration. In addition, \$900,000 of nonrecurring capital price would be required for the design and analyses associated with the thermal cycling problem.

TABLE 4-1
ESTIMATED ADDITIONAL CAPITAL COST
REQUIRED FOR SERIES CONFIGURATION

Item	Capital Price \$1000 (1978)
1. Replace carbon steel piping and valves with stainless steel	160
2. Install stainless steel piping and valves for bypass	700
3. Make up for heat losses using coal-fired sodium heater	450
4. Provide 1/4 hr of thermal storage for rapid load changes	1,600
Subtotal	2,910
5. Additional design and analyses for thermal cycling*	900
TOTAL	3,810

*Nonrecurring price



9315-28

Figure 4-4. Figure of Merit and Annual Output vs Peak Power

Based on the foregoing, it was concluded that the parallel configuration for the solar receiver and the fossil-fired sodium heater is the preferred arrangement for the baseline hybrid plant. This configuration offers the following major technical advantages over the series arrangements:

- 1) Thermal cycling of components is minimized, because load changes are affected by variation in flow rate and not temperature rise, since outlet temperature from heater and receiver is maintained constant at all loads
- 2) Sodium system is easier to control by varying flow rate
- 3) Carbon steel can be utilized for sodium riser and inlet piping to receiver
- 4) Thermal storage may not be a requirement for this mode of operation.

A detailed documentation of the system level trade study briefly described here is located in Appendix B.

4.3.2 Solar Multiple/Field Receiver Power Ratio

The effect of Field Receiver Power Ratio (FRPR) on solar system optimization was investigated for the solar multiple 0.8 baseline system. Solar system optimization and performance data for a 120 m tower with a 10.4 m x 10.4 m receiver were used in the analyses. It is not felt that the subsequent selection of a slightly longer receiver (see Section 3.2.2) would change the results or conclusions of this analysis.

Figure 4-4 presents a detailed look at the 120 m tower, 10.4 m x 10.4 m receiver optimization data. In addition to figure of merit, the annual output is also shown as a function of peak power for this system. The product of these two curves at any given peak power yields the solar system cost. This cost includes all of the solar-related costs including tower, receiver, sodium plumbing, and pump associated with the tower, as well as heliostats, land (including central exclusion area), and field control.

A study was conducted to determine the effect on a modified figure of merit (cost of energy to the receiver at a fixed power level) of operating systems designed at field/receiver power ratio of greater than one. The optimization data were based on operating at a field/receiver power ratio of 1.0. Figure 4-5 shows the nondimensional diurnal variation in clear day output from a system of this type based on a compatible isolation model for each solar month. A nondimensional area inside each monthly curve was determined. Each monthly value was reduced based on the monthly clear day percentages shown in Table 4-2.

These reduced monthly values were averaged to obtain a yearly average. This yearly average was multiplied by 365 days to obtain a nondimensional relative field output for a field sized at a field/receiver power ratio of 1.0. This output was based on a sun acquisition elevation angle of 10° . This process was then repeated for three field/receiver power ratios of >1.0 shown by the horizontal lines on Figure 4-5. The relative output of the fields operating with these field/receiver power ratio cutoffs were calculated as a percent of the unconstrained output of these fields. Data are summarized in Table 4-3 where field receiver power ratio (FRPR) is defined as the ratio of unconstrained peak power to constrained peak power, with the constrained peak power equal to 208 Mwt (solar multiple of 0.8 for the baseline 100 MWe system).

TABLE 4-2
UNIVERSITY OF HOUSTON ISOLATION MODEL MONTHLY CLEAR DAY PERCENTAGES

Month	Percent Clear Days	Month	Percent Clear Days
January	75	July	90
February	75	August	92
March	80	September	92
April	85	October	92
May	90	November	85
June	90	December	85

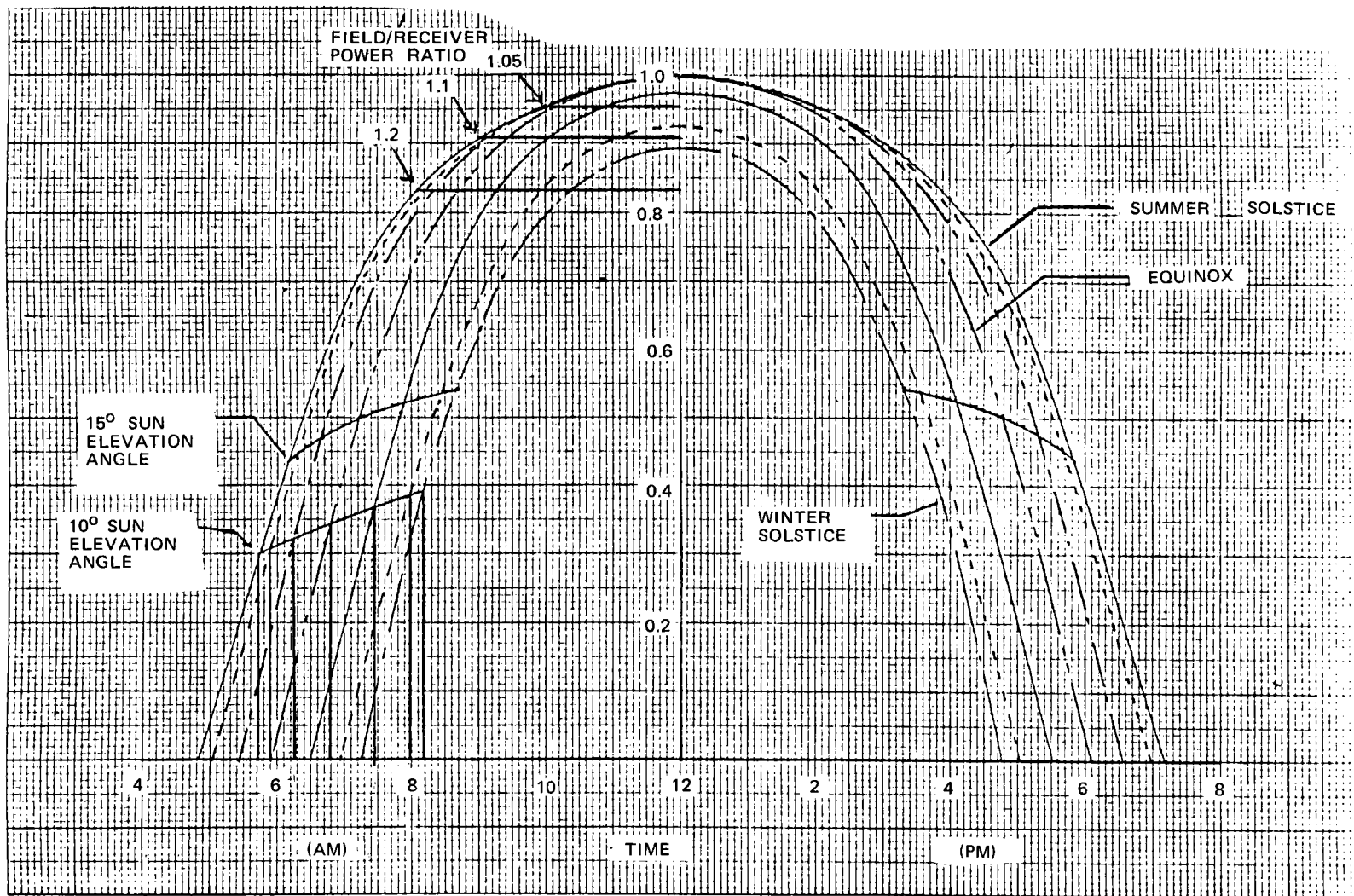


Figure 4-5. Commercial System Collection Characteristics
(U of H Insolation Model)
Absorbed Power
(Nondimensional)

TABLE 4-3
RELATIVE OUTPUT OF FIELDS OPERATING WITH VARIOUS FRPR CUTOFFS

FRPR	Unconstrained Peak Power (Mwt)	Output (Annual)	
		% Unconstrained	Mwt-h
1.0	208	100	508,000
1.05	218.4	98.3	526,000
1.10	228.8	96.5	541,100
1.20	249.6	91.7	565,100

The system cost was determined at each FRPR by calculating the product of figure of merit and unconstrained annual output at each FRPR. This cost was reduced by difference in tower and receiver cost when compared to the cost at 208 Mwt for each FRPR. This difference in cost is associated with the increase in sodium pump and plumbing costs in going to higher peak power levels, which is not required since the systems are constrained to 208 Mwt. These delta costs were determined from Figure 4-6. A summary of the derived system costs for the system constrained to operate at 208 Mwt peak but sized at the higher FRPR are shown in Table 4-4. Also shown is the figure of merit of these systems obtained by dividing the system cost by the constrained output given in Table 4-3.

TABLE 4-4
DERIVED SYSTEM COSTS FOR SYSTEM CONSTRAINED TO OPERATE AT 208 Mwt PEAK BUT SIZED AT HIGHER FRPR

FRPR	System Cost (10 ⁶ \$)	Modified FOM (\$/Mwt-h)
1.0	43.46	85.56
1.05	45.36	86.24
1.10	47.27	87.36
1.20	51.41	90.98

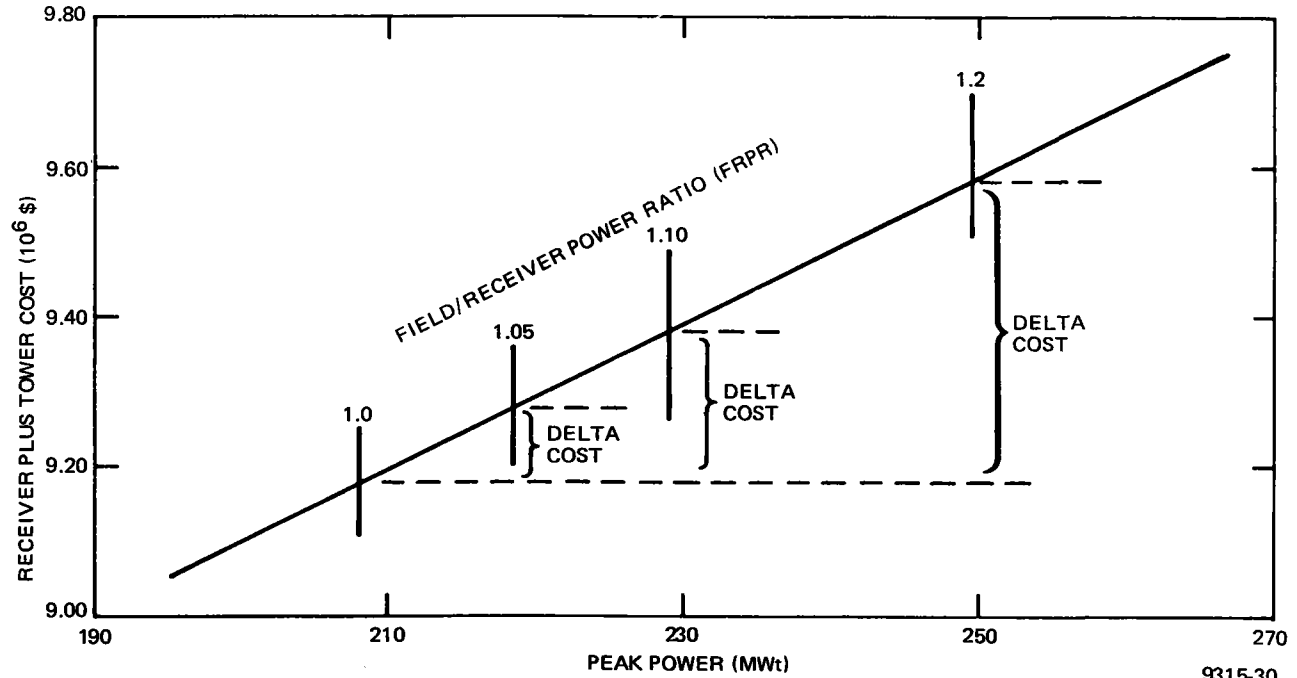
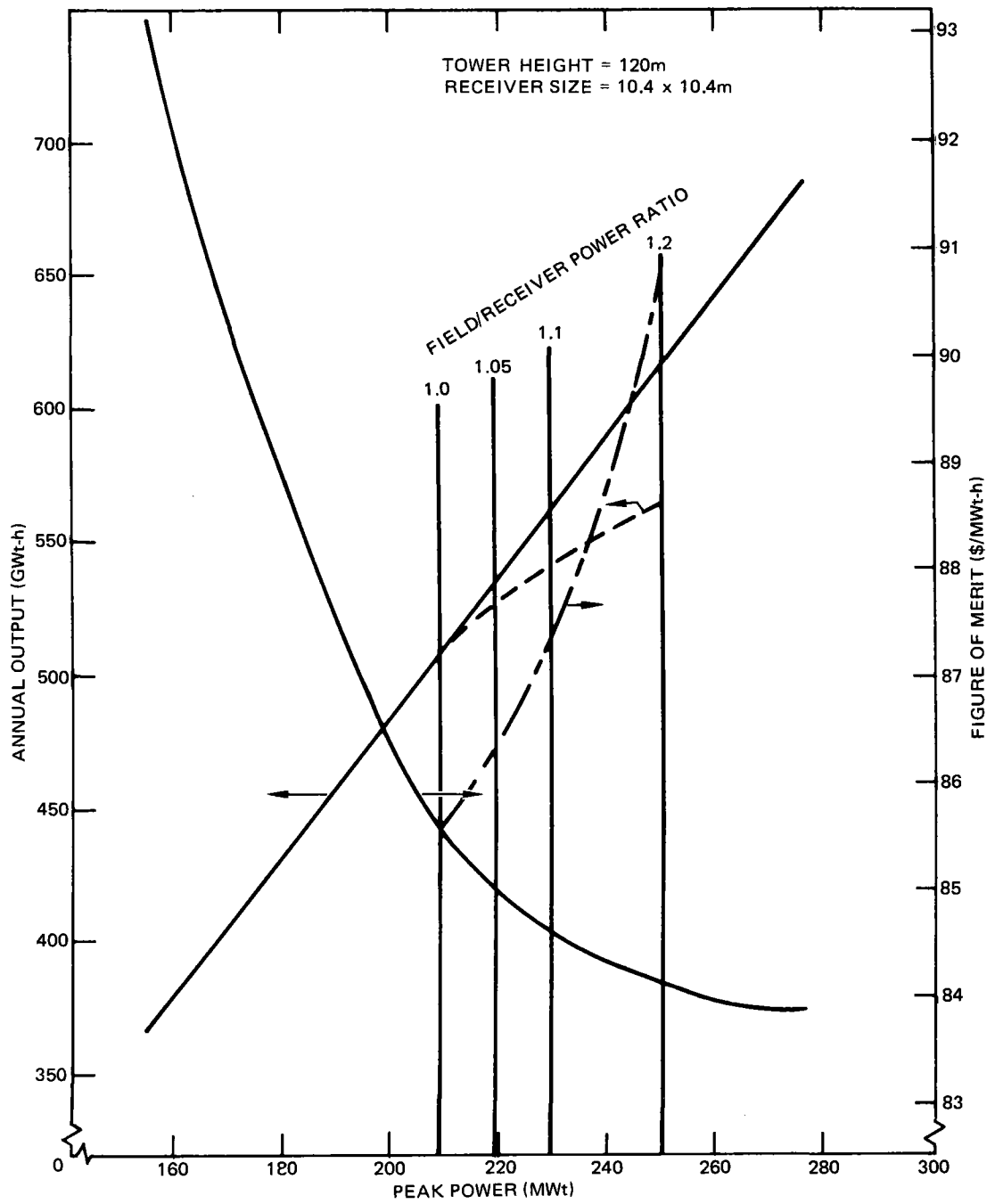


Figure 4-6. Tower Cost vs Peak Power



9315-31

Figure 4-7. Effect of Field/Receiver Power Ratio on FOM

These data (FOM and constrained output) are shown in Figure 4-7 superimposed with the data given in Figure 4-4. The dotted line shows the reduced (constrained output), while the dashed line shows the modified figure of merit at each FRPR. The vertical FRPR lines are shown at the appropriate unconstrained peak power levels. As can be seen, the output increases above that for the FRPR of 1.0 (208 Mwt) with the difference between the unconstrained and dotted constrained lines being the amount of intentionally spilled energy in a year. From a figure of merit or solar effectiveness standpoint, it can be seen that operating at a FRPR of 1.0 provides the most effective solar system (in terms of minimum modified FOM). Studies were then made to determine the effect of operating at higher FRPR on annualized busbar energy costs.

The field receiver power ratio (FRPR) as defined here is the ratio of the power that could be accepted by an idealized receiver compared to the power the actual receiver of the same geometry can accommodate at the design point. In effect, this determines how many additional heliostats can be profitably added to the collector field and which are used only during off-peak insolation periods.

The curves of the differential busbar energy cost vs the FRPR for the 0.8 solar multiple 100-MWe plant are shown on Figure 4-8. The top curve is based on standard economic assumptions for the project. The bottom curve is based on the assumption that the additional heliostats can be purchased at the bulk rate but that their procurement would be at the end of the construction period and would be treated as a post-construction option. Utilizing the bottom curve, the optimum occurs at an FRPR of 1.1 which is the value selected for the hybrid design.

4.3.2.1 0.8 Solar Multiple

The parallel receiver/heater configuration was selected as baseline for the hybrid system. In this configuration, the heater is required to be at temperature during sunlight hours in order to be capable of rapidly supplementing meteorological-induced shortfalls in receiver power. This requirement means that either the receiver power must be large enough such that the heater can be kept warm by solar-heated sodium or that fuel be burned to keep the heater at

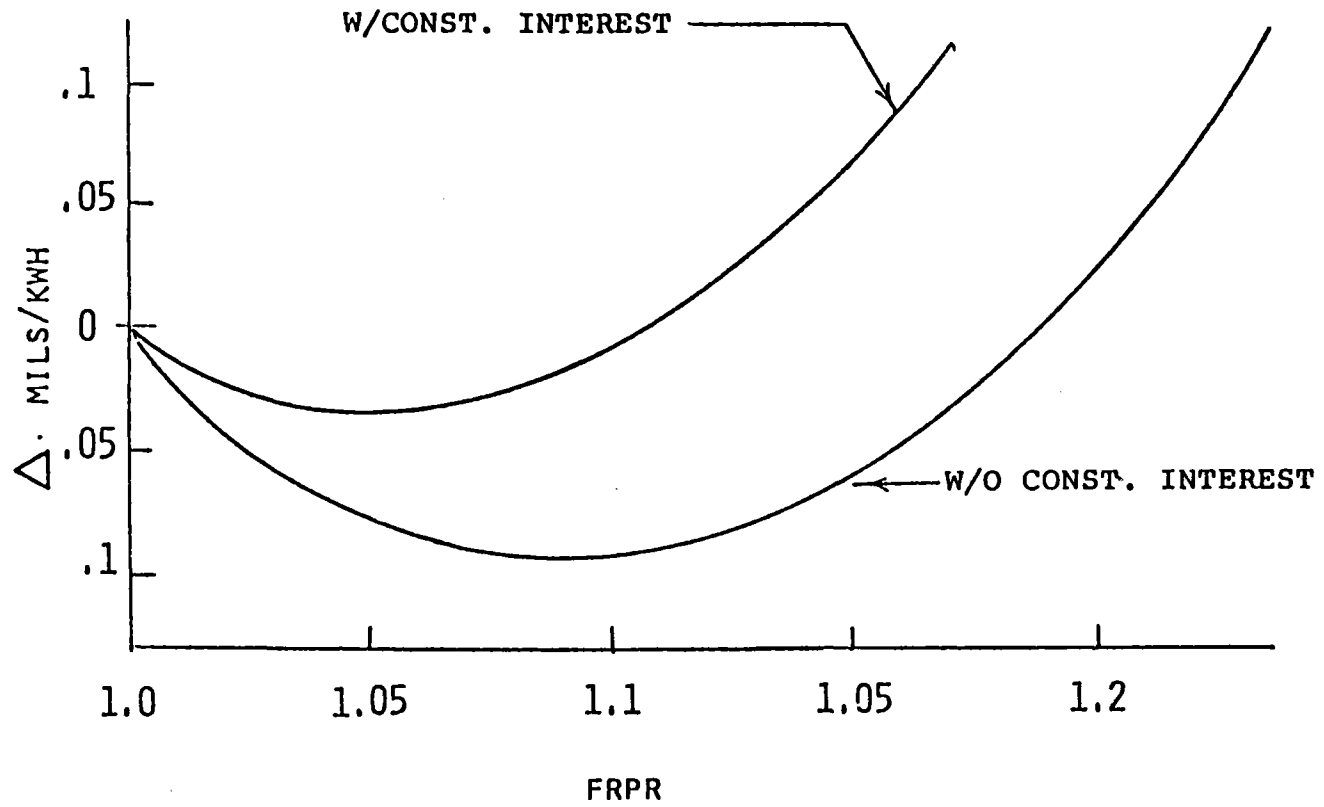


Figure 4-8. Busbar Energy Cost vs Field/Receiver Power Ratio

temperature. Only the latter case was considered in this study. Depending on the fuel selected, the minimum heater power required to maintain combustion stability and sodium temperatures concurrently ranges from 10 to 20% of full power. Full heater power is set by the steam generator power level of 260 Mwt.

Variations in the solar receiver thermal energy output, because of the diurnal variation in absorbed thermal power, are supplemented by the fossil-fired sodium heater to provide a constant net electrical plant output of 100 MW. As the receiver output drops, the heater output increases. Load changes are made by varying the sodium flow through the components. Changes in the seasons, time of day, and weather patterns all affect the solar heat input which requires adjustments in the fossil-fired sodium heater thermal input to maintain a fixed plant output. At some specified minimum solar load, the receiver will be shut down and all the power generated by the sodium heater.

If oil or either of the candidate gases (natural gas or syngas) are used as fossil fuels in the hybrid plant, the minimum heater power is 10% of full power. The minimum power of a coal-fired sodium furnace is 20%. This means that as a point of departure, the nominal power required of the receiver at peak design conditions would be 90% for an oil or gas system, and 80% for a coal system.

There is no technical restriction on the amount of total energy the receiver can contribute to the system. Consequently, the receiver can contribute more or less than the foregoing percentages of total required instantaneous steam generator power. As a minimum, however, a fossil fuel displacement of at least 50% of the steam generator rating. As a maximum, the design receiver power has been limited to 266% of the required steam generator power. This would effectively supply the steam generator 100% power all day and night if storage facilities were available. Thus, it can be seen that for receiver powers equal to or less than the point of departure, no storage is required. For higher powers, storage is required. A convenient single factor which describes the receiver power capability relative to the turbine requirements at name plate rating and simultaneously indicates the relative storage is the solar multiple. Selecting a solar multiple defines the peak design solar/fossil power split of the plant and indicates the magnitude of storage.

The economic assumptions used in this trade study are summarized in Table 4-5.

TABLE 4-5
ECONOMIC ASSUMPTIONS*

Discount Rate = 10%
Economic Life = 30 years
Fixed Charge Rate = 18%
Annual Capital Escalation Rate - 10%
Startup Year = 1990
Annual Fuel Escalation Rates = 6, 8, 10, and 15%
Oil Cost = \$2.00/MMBtu (1978 \$)
Coal Cost = \$1.00 MMBtu (1978 \$)
Natural Gas Cost = \$2.10/MMBtu (1978 \$) (See Reference 4.5)
Syngas Cost = \$3.75/MMBtu (1978 \$) (See Reference 4.5)

*All assumptions as per Reference 4.1 except as noted.

The economic comparisons of solar multiples between 0.5 and 2.66 for various fuel escalation rates in the range of 6 to 15% were made in terms of busbar energy costs vs capacity factor using the J.P.L. Methodology.^(4.2) The methodology was programmed into the computer code described in Section 4.1 and Appendix A.

Using the computer program, the busbar energy costs of coal- and oil-fired hybrid plants as functions of capacity factor, and fuel escalation rates were generated for solar multiples in the range of 0.5 to 2.15. The results are shown for coal with solar multiples 0.5, 0.8, and 1.5 in Figure 4-9 for a fuel escalation rate of 10%. Also shown are the capital costs of each plant in millions (1978) dollars). All plant capital costs were generated by estimates of heater costs provided by Babcock and Wilcox and balance of plant component costs determined by scaling the costs from previous solar studies.

For coal with low fuel escalation rates, Figure 4-9 shows that the lowest solar multiple is marginally cost-effective due to the relatively low cost of fuel. It can be shown that the difference in incremental fuel costs would cause

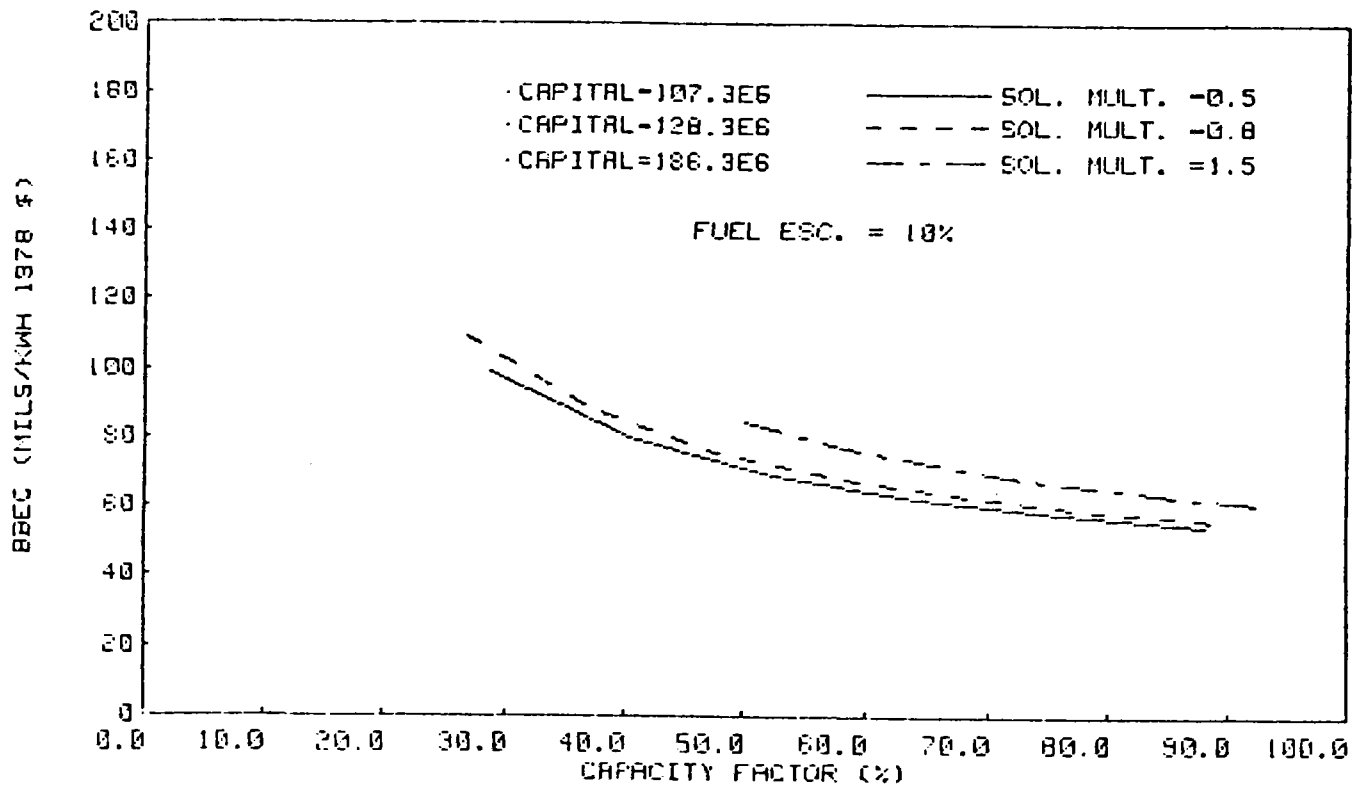


Figure 4-9. Coal Solar Multiple Trade Study

a plant with a solar multiple of 0.8 to be used at a higher capacity than a plant with a solar multiple of 0.5. Consequently, the total busbar energy costs of the 0.8 solar multiple plant would be less than those of the 0.5 solar multiple plant. At a 10% fuel escalation rate, the 1.5 solar multiple is still not competitive.

On the basis of the foregoing trade study, the optimum solar multiple appears to be 0.8 for coal.

A similar trade study for oil showed that the optimum solar multiple at a fuel escalation rate of 10% was greater than 1.5 due to the high cost of fuel. In this case, the margin of superiority of the 1.5 solar multiple was not large. However, the incremental fuel cost drives the solar multiple up.

A detailed description of this study is located in Appendix A.

4.3.2.2 1.4 Solar Multiple

Using the results of the 0.8 solar multiple trade study in conjunction with the requirement of 3 h of storage based on the best possible day dictates that the lowest solar multiple which will fill storage on summer solstice be selected for the storage system configuration. Since the storage thermal losses for the sodium storage system are essentially negligible, the storage energy requirement is 780 Mwt-h thermal. Integration of the energy at the base of the tower less steam generator requirements for several solar multiples showed that a 1.4 solar multiple supplied the required energy with a margin of approximately 18 Mwt-h. Consequently, a solar multiple of 1.4 was selected for the 3-h storage system configuration.

4.3.3 Storage Capacity

4.3.3.1 0.8 Solar Multiple

The economic analysis for the unconstrained system, as described in Section 4.3.2.1, indicated that from an economic standpoint a no storage configuration was the most cost-effective for a 0.8 solar multiple system. However, from a

technical standpoint, this configuration is unattractive. During the design receiver cloud cover transient, the receiver will ramp down from 80% to 0% of steam generator power in 90 sec. The selected coal-fired heater is capable of ramping up in 5 min. from 70 to 100% power. The difference between these ramp rates, when integrated over the transient, represents an energy shortfall. This shortfall is made up by the thermal buffer system. The sizing of the thermal buffer system is described in Section 3.4.2.

4.3.3.2 1.4 Solar Multiple

The 3-h storage size constraint of the 1.4 solar multiple system is set by input from the Customer. It is sized so that a direct comparison may be made between the hybrid system and previously studied central receiver systems with 3 h of storage.

4.3.4 Solar Fraction

4.3.4.1 0.8 Solar Multiple

For the 0.8 solar multiple configuration, the solar fraction of energy and power is determined by an annual integration of solar energy at the base of the tower. The baseline configuration, 0.8 solar multiple, 1.1 field/receiver power ratio system is expected to deliver 540,289 MWh annually. The solar fraction of energy delivered is given by Equation 4.1.

$$\text{Solar energy fraction} = \frac{23.72\%}{\text{attained capacity fraction}} \quad (4.1)$$

For the target capacity factor (70%), this results in a solar energy fraction of 33.9%. The solar power fraction is set by the solar multiple at 80% at design conditions.

4.3.4.2 1.4 Solar Multiple

The expected annual energy from the 1.4 solar multiple configuration is 898,328 MWh. The solar energy fraction for this configuration is given by Equation 4.2.

$$\text{Solar energy fraction} = \frac{39.44\%}{\text{attained capacity fraction}} \quad (4.2)$$

This results in a solar energy fraction of 56.3% at the target capacity factor of 70%.

The solar power fraction of the 1.4 solar multiple is 140% at design conditions.

4.3.5 Non-Solar System Size (0.8 and 1.4 Solar Multiple)

For both storage and nonstorage configurations, the size of the non-solar system is determined by the steam generator power requirements and the requirement for 100% capacity credit. This results in a requirement for a 260-MWt sodium heater. The heater is sized at 265 MWt to provide a small design margin in plant gross power for unforeseen parasitic loads.

4.3.6 Fuel Selection (0.8 and 1.4 Solar Multiple)

The alternate candidate fuels considered for the non-solar subsystem included: coal, oil, natural gas, and syngas. If oil or either of the candidate gases are used as non-solar energy sources in the hybrid system, the minimum power of the sodium heater, based on the minimum safe firing rate, is 10% of required power. If coal is used, the minimum heater safe firing rate is 20%.

The noneconomic advantages and disadvantages of each fuel alternative are shown in Table 4-6. The most abundant of the alternatives is coal. This fact is reflected in its low fuel cost. Coal is also the most available fuel. While it is recognized that its availability is subject to labor negotiations, last winter's coal strike did not seem to seriously impact the operation of western

TABLE 4-6
FUEL SELECTION NON-ECONOMIC CONSIDERATIONS

	Coal	Oil	Natural Gas	Syngas
Abundance	+	-	-	+
Availability	+	-	-	-
Convertibility	+	-	-	-
Freedom from Usage Restrictions	+	-	-	+
Ease of Handling	-	+	+	0
Lack of Flue Gas Cleanup	-	-	+	0
Mirror Fly Ash Precipitation	-	0	+	0
Plant Location Flexibility	-	+	+	0

- + Advantage
- Disadvantage
- 0 No significant effect

coal-fired plants in the major solar market areas. Oil availability is subject to the production changes of foreign suppliers. Natural gas is expected to be unavailable to new power plants as a result of fuel management requirements. "Syngas" appears at present to be unavailable at economically attractive prices.

Ultimately, coal and syngas are the only fuel alternatives expected to remain or become available with reasonable certainty. A number of utilities expect that oil would not be used in new power plants. The use of natural gas in new power plants is currently prohibited in many western states.

Oil and natural gas are the easiest fuels to handle of the two alternatives. Coal is the most difficult. The handling problems of syngas depend upon where gas is manufactured. If it is manufactured onsite from coal, then the handling difficulties would be the same as those for coal. If, however, syngas is purchased from an outside supplier, the handling difficulties would be similar to those of natural gas.

Both coal and oil are expected to require flue gas scrubbers and electrostatic precipitators or equivalent SO₂ removal and particulate control equipment.

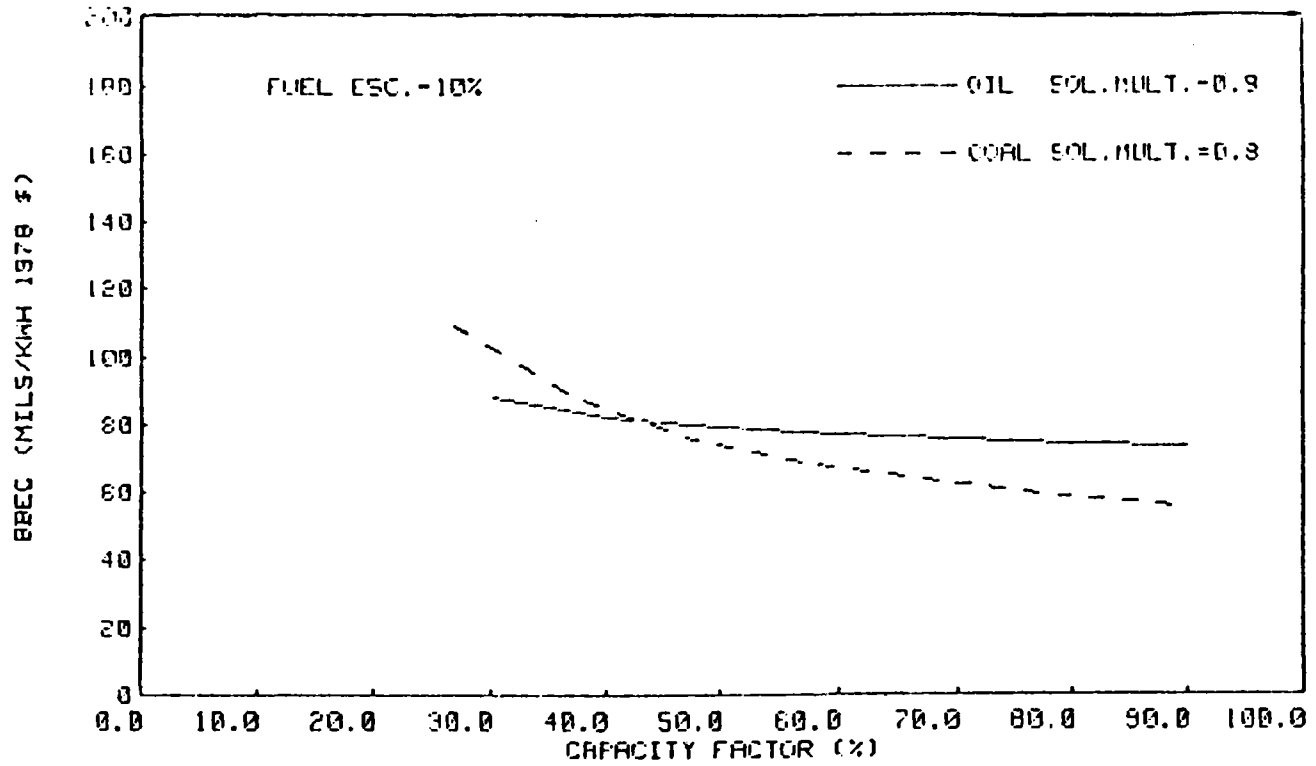


Figure 4-10. Oil and Coal Hybrid Busbar Energy Costs

This problem is critical in that it impacts heliostat fly ash deposition rates. Stearns-Roger has indicated that with properly operating particulate removal equipment, the deposition rate should be manageable. It is not known whether fly ash deposition will be a serious problem with oil firing at this time. Firing natural gas eliminates the scrubber and precipitator requirements as well as the fly ash problem. The precipitator and scrubber requirements as well as fly ash deposition resulting from syngas firing depend upon syngas plant design and location.

Another non-economic fuel selection criteria is plant site flexibility. Coal is the least flexible alternative as reflected in increasing transportation costs as a function of distance from mine mouth. Oil and natural gas have the most flexibility with regard to site location. The site location flexibility of syngas will depend upon the syngas plant location.

It is probable that gas may be unavailable at any price as a result of fuel management decisions. Syngas is, at this time, high enough in cost to be ruled out from an economic consideration. Since oil is more abundant than natural gas, the final economic choice is between oil and coal.

Finally, one of the most important noneconomic considerations is the capability of fuel conversion. A coal heater, because it is the largest for a given rating, is the only heater that, once selected, can be converted to all the other fuel alternatives economically.

Using the economic assumptions summarized in Table 4-5 and the computer model described in Section 4.1 and Appendix A, an economic trade study between coal and oil was performed. The busbar energy cost of electricity as a function of attained capacity fraction, fuel type, and fuel escalation rates were plotted. The results for a fuel escalation rate of 10% are shown in Figure 4-10.

As shown in the figure, coal is a more cost effective fuel above a capacity factor of 42%. As a result of the lower fuel costs of coal, the incremental fuel cost of electricity from a coal plant will also be less than that of an oil plant. Consequently, a dispatcher would be reasonably expected to select a coal

hybrid over an oil hybrid if two otherwise equivalent plants existed. This would result in the coal hybrid attaining a relatively higher capacity factor. It was concluded, therefore, that from an economic and non-economic standpoint, coal should be the baseline fuel for the hybrid system.

4.3.7 Preferred Commercial Plant Selection Study

After completing the detailed design of the 0.8 and 1.4 solar multiple, 100-MWe plants, a trade study was initiated to select the preferred commercial plant configuration. The goal of this study was to select the plant with a rating and storage capacity capable of good market penetration and utility acceptance. The selection criteria and requirements used are defined in Section 4.3.7.1. The selection methodology employed is outlined in Section 4.3.7.2. The results of the study are described in Section 4.3.7.3, and some of the potential options available in building and operating the preferred commercial plant are located in Section 4.3.7.4.

4.3.7.1 Requirements and Selection Criteria

The requirements and selection criteria used in the search for the preferred commercial plant (PCP) are outlined in Table 4-7. In addition to minimizing bus-bar energy costs, the most important requirement of power plants installed between now and the end of the century may well be the minimization of utility dependence on single fuel sources. The rapid escalation of oil during just the duration of this program alone graphically illustrates this problem. At the start of the hybrid program, oil could be bought for roughly \$2.00/MMBtu. A recent conversation with the Los Angeles Department of Water and Power revealed that they are currently paying as much as \$3.80/MMBtu for low-sulfur No. 6 fuel oil. Consequently, it was felt that the preferred commercial plant selection criteria should include some significant consideration of this problem.

In addition to minimizing the problems associated with fuels, it was felt that increasing plant operating flexibility would increase the value of the plant and its marketability. The restriction of plant component sizes to currently available LMFBR components was also included as a criteria in order to assure

TABLE 4-7
REQUIREMENTS AND SELECTION CRITERIA

<u>Minimize</u>
Bus bar energy cost
Fuel type dependence
<u>Maximize</u>
Plant operating mode flexibility
Market penetration
Utilization of existing LMFBR sodium components
Solar energy utilization (50% + energy from sun)

early market penetration and minimum development requirements. Finally, the requirement of at least 50% solar energy contribution was included even though this might require violation of the minimization of busbar energy costs. The justification for this is twofold: it adds considerable plant flexibility and provides hybrid commercial plant for comparison purposes. It may also be that future escalation rates for fossil fuels will greatly exceed current projections and that the extra solar capability would act as a hedge against this possibility. For the hybrid plant, storage is not cost-effective directly, however, in the larger sizes, the differences between plants with and without storage are small and the plants become competitive because the plants with storage are more flexible.

The economic climate and conditions as well as current (as of this trade study) costs of coal and oil are shown in Table 4-8. They are essentially the same as those used in the requirements definition document, with the exception of the oil and coal prices, which have been updated.

4.3.7.2 Selection Methodology

Based primarily on the detailed cost estimates generated during the Advanced Central Receiver Program (ACR) and the updated costs generated during the hybrid program for the 0.8 and 1.4 solar multiple plants, the component and subsystem cost algorithms necessary to cost any given plant configuration were updated.

TABLE 4-8
OPTIMUM PLANT SELECTION STUDY
ECONOMIC CLIMATE AND CONDITIONS

Economic Life	30 years
Fixed Charge Rate	18%
Annual Capital Escalation Rate	10%
Start of Commercial Operation	1990
Oil Cost (1979 Dollars)	\$3.80/MMBtu
Coal Cost (1979 Dollars)	\$1.40/MMBtu
Fuel Escalation Rates:	
Oil	10%/year
Coal	8%/year
Interest During Construction	20% of Capital
Annual O&M Escalation Rate	8%
Discount Rate	10%
O&M	1% of Capital + 30% of Fuel
General Inflation	8%

Using these updated cost algorithms, in conjunction with the previously described JPL bus bar energy cost model, a parametric study examined the viable combinations of the parameters shown in Table 4-9. The top level parameter was receiver power. This parameter was limited to 1600 MWt, that being the receiver power associated with the tallest available tower technology. A definition of a new parameter, α , as the ratio between gross EPGS power and peak receiver power, allows the elimination of either of these variables and considerably simplifies the study. Specifying α and the receiver power completely defines the plant configuration on a basic level and allows a cost and bus bar energy cost estimate to be completed. This is because of the relation between α , the solar multiple, the EPGS gross power, and the gross cycle efficiency, η .

$$\text{Receiver Peak Power (MWt)} = \text{EPGS gross power (MWe)} \\ \times \frac{\text{Solar Multiple}}{\eta}$$

TABLE 4-9
OPTIMUM PLANT SELECTION STUDY PARAMETER RANGES

Receiver Power (MWt)	364 - 1600
Net Plant Size (MWe)	65 - 615
Gross Cycle Efficiency (%)	43.1
Net Cycle Efficiency (%)	38.5
Storage Capacity (hr)	0 - 10

Figure 4-11 is a graphical representation of the relation. Also shown is the relationship between solar multiple and hours of storage for any α , for summer, winter, or equinox operation. Since, at current fuel prices (coal), it was previously found that storage was not cost effective, it was assumed that any storage system would be filled on the best solar day so as to minimize the solar capital investment. The equation which best fits the relation between hours of storage and α is:

$$\text{Hours of Storage} = \frac{\alpha - \eta^2}{0.0053}$$

An entire matrix of busbar energy cost as a function of capacity factor curves was obtained by this method. The two variables of interest were receiver power and α . The results of the study are presented in the next section.

4.3.7.3 Results

Typical computer-generated raw data from this trade study are shown in Figures 4-12 and 4-13. These families of curves show busbar energy costs as functions of attained capacity factor and respective peak receiver powers of 364 and 1,000 MWt. Values of receiver peak power of 500, 750, and 1,600 MWt were also investigated but are omitted in the interests of brevity. Since it would be difficult to ascertain the differences in busbar costs from these figures alone, the results were cross-plotted for a constant-attained capacity factor of 80%. The final trade study family of curves is shown in Figure 4-14. The busbar energy costs for constant storage capacities was plotted against EPGS net power, which was assumed to be 89% of the gross power. Superimposed on these

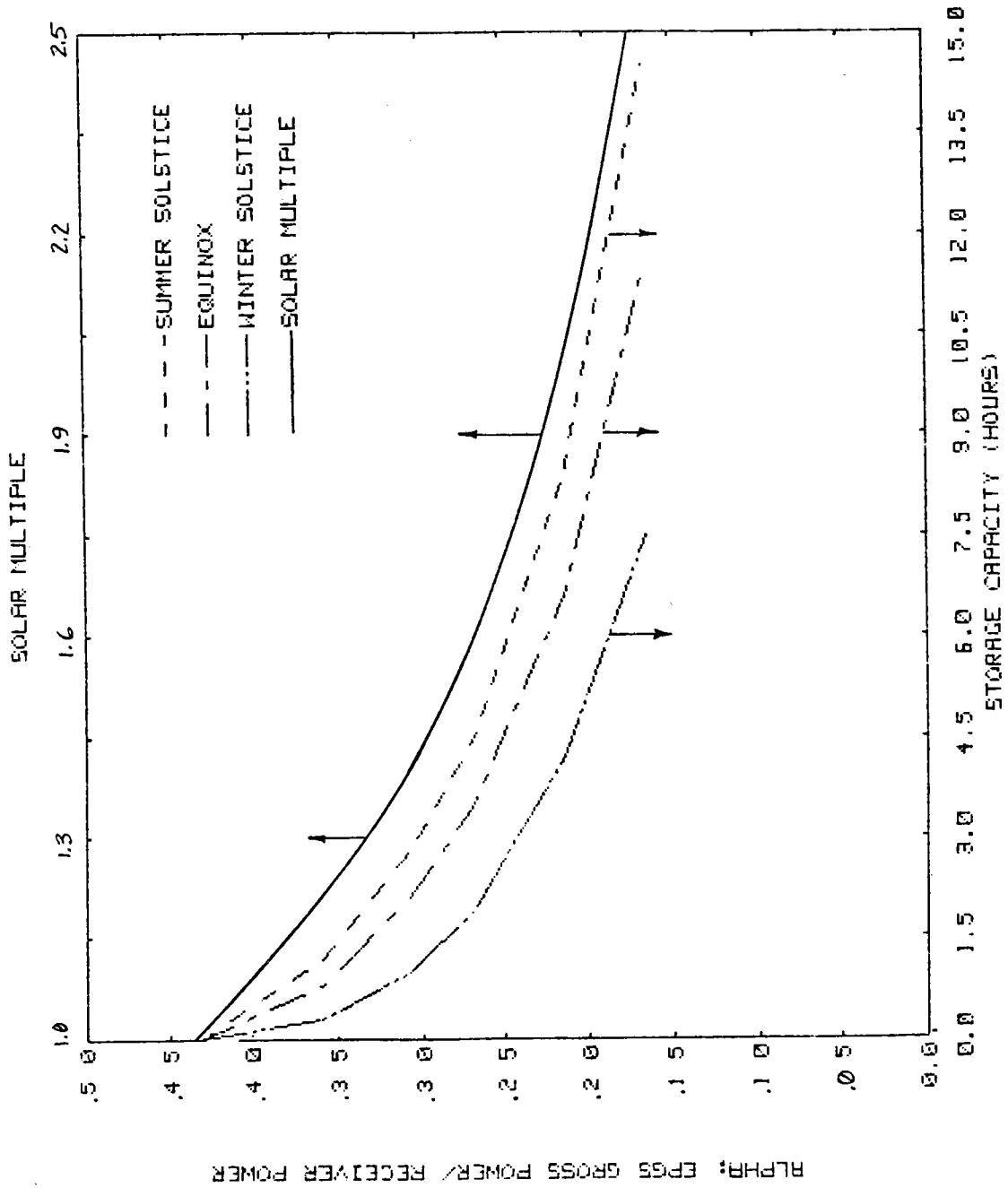


Figure 4-11. EPGG Size vs Storage Capacity

BEEC (MILLS/KWH) (1979\$)

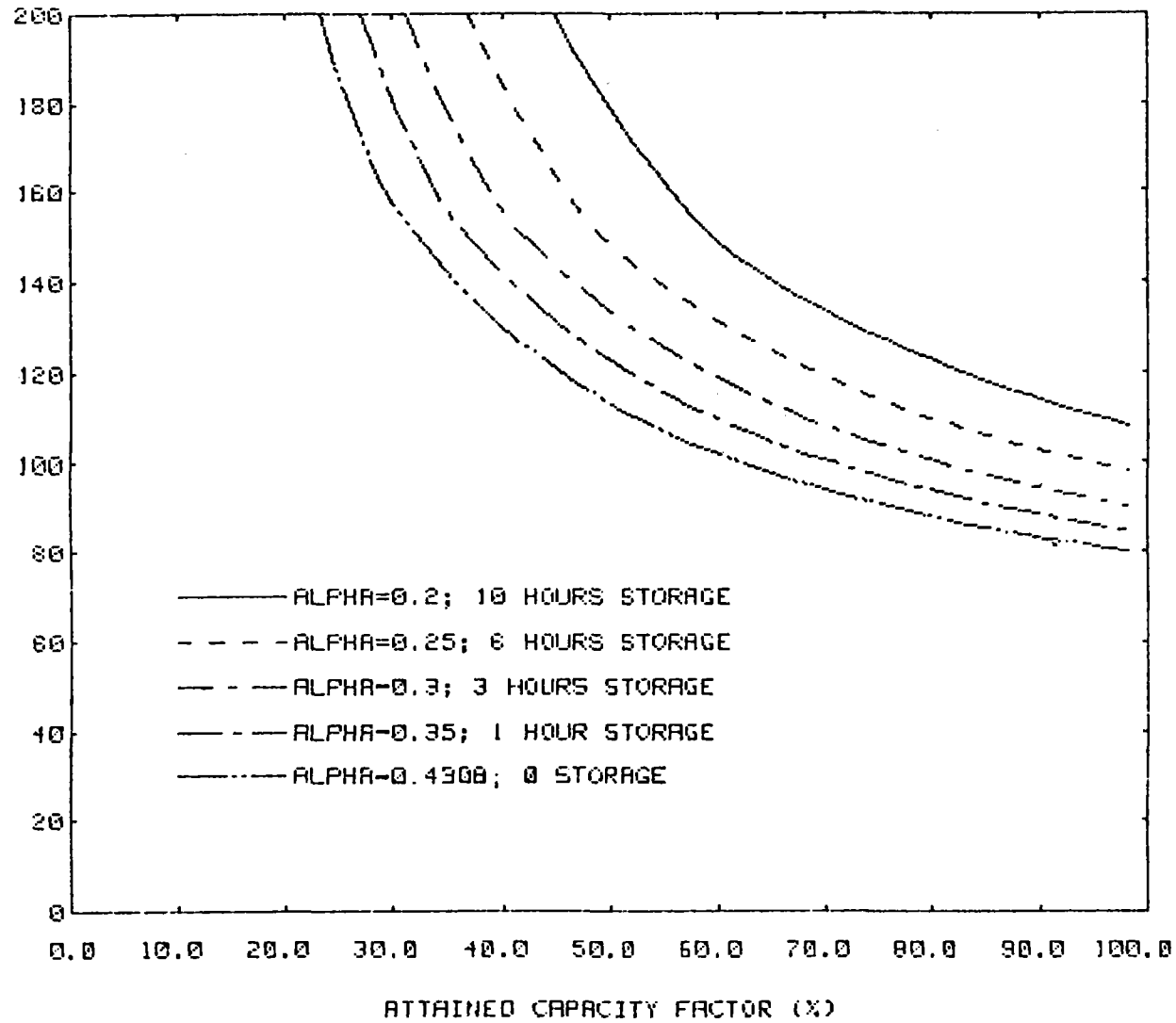


Figure 4-12. Nth Coal Hybrid Busbar Costs; 364 Mwt Receiver

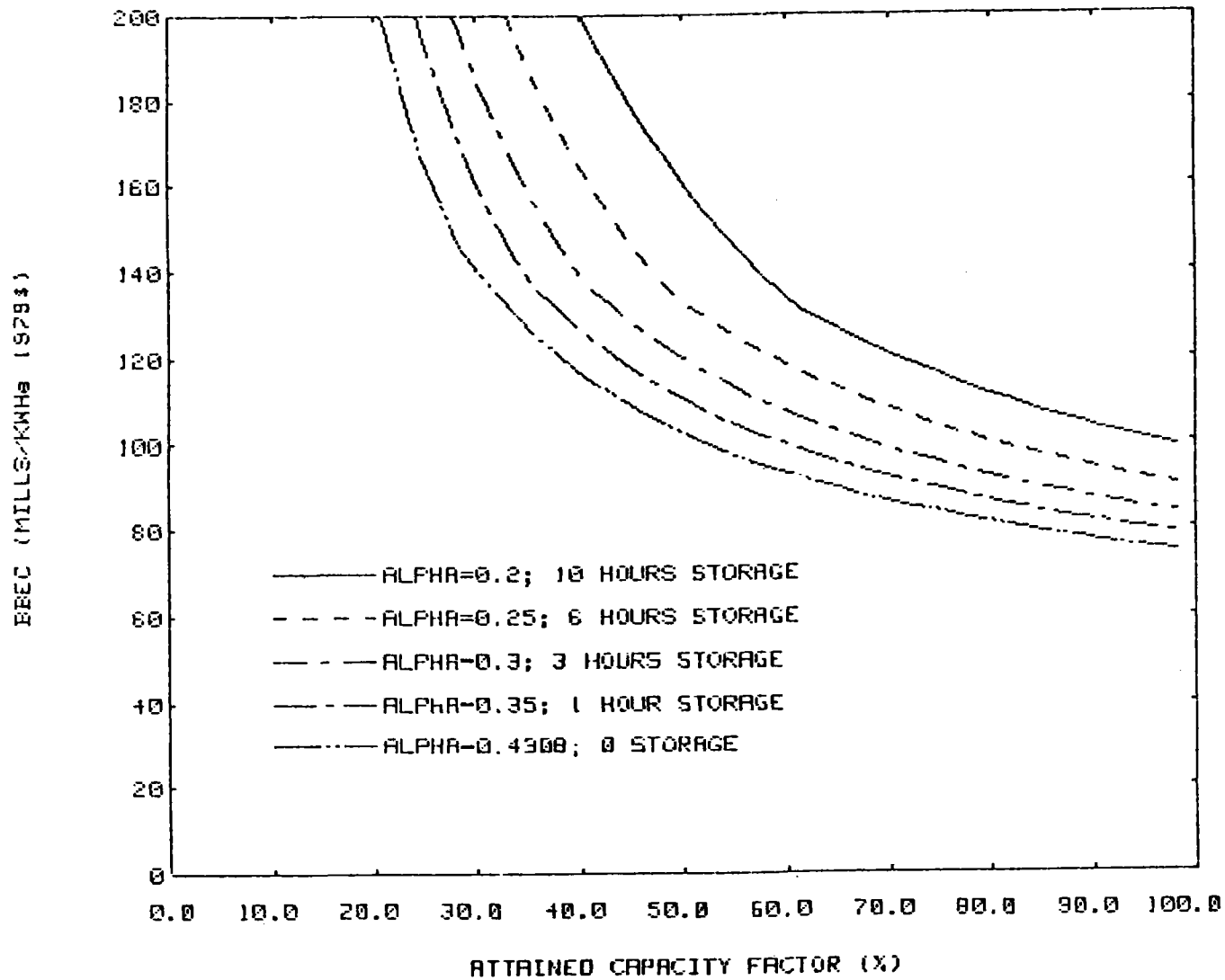


Figure 4-13. Nth Coal Hybrid Busbar Costs; 1000 Mw Receiver

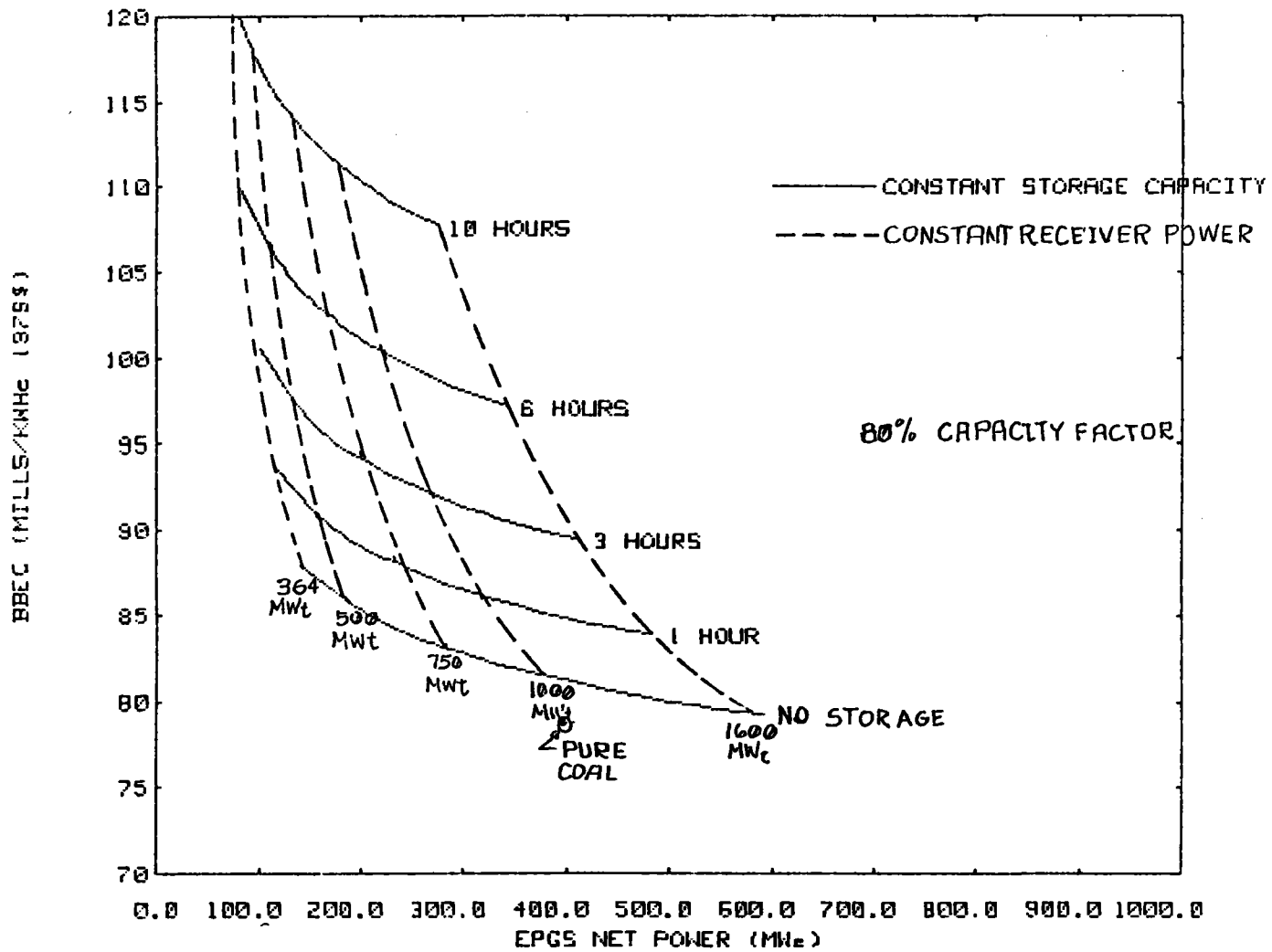


Figure 4-14. Busbar Cost vs Receiver and Plant Size and Storage

plots was a family of curves representing constant receiver peak power. This figure can be used as a "road map" to determine the estimated busbar cost of any viable combination of net plant power, receiver size, and storage. Also plotted as a point of reference is a 400-MWe pure coal-fired power plant.

At \$1.40/MM Btu coal cost, the results show that the nearest cost-competitive coal hybrid plant configuration to a pure coal plant includes no storage. This conclusion is in accord with the results of previously described studies of the 100-MWe plant configuration. However, several other conclusions can also be drawn from this study.

As was observed in the ACR program, increasing the peak receiver power and plant size is cost effective, due to economies of scale, even if storage is not cost-effective in a hybrid plant, due to low fuel costs. The cost penalty in maintaining a 50% solar energy contribution at the maximum available receiver/tower size is roughly 10 mil/kWh.

It was judged that this penalty was not excessive and that satisfactory market penetration could still be achieved with a plant which had storage and, therefore, met all the other selection criteria. Consequently, the 430-MWe, 3+ hours of storage configuration, described in detail in Section 6.1.1, was selected as the initial preferred commercial configuration. This plant size is also consistent with the current utility trend toward 500-MWe-baseloaded plant sizes, away from 1,000 MWe.

The addition of extra non-solar filled storage (~2 h) gives the plant considerable operating flexibility as well as accommodating heater operation 24 h/day. The ability to store low-power heater output, and thereby avoid starting and shutting down the heater daily, is expected to be cost effective due to increases in heater reliability. Although no detailed trade-study results are available to support this design feature, a brief consideration of the costs of substitute power, should the heater be disabled for even a few days due to an operator error in starting or securing operations, would easily justify the capital cost of the extra storage.

4.3.7.4 Preferred Commercial Plant Options

The initially-selected preferred commercial plant (PCP) configuration is most effective in a baseload application, due to the use of inexpensive coal. A brief investigation showed that a modified design of this configuration also has potential application in an intermediate load capacity.

The PCP initial configuration includes a coal-fired sodium heater. This heater is also specifically designed such that it is also capable of firing oil if the burners and fuel supply system are changed out. By initially constructing the PCP plant with oil-fired fuel delivery and omitting the flue gas cleanup system, the PCP can be utilized as a cost-effective intermediate load plant operating at a capacity factor of 40% on low-sulfur oil. Figure 4-15 shows that such a plant with between 1 and 3 hours of storage is cost competitive with a pure coal plant operating at the same capacity factor. This plant would essentially operate as a stand-alone solar plant with oil firing <800 h/yr. While there is no technical reason to restrict oil consumption to this value, the economics deteriorate rapidly above this point.

However, if the original plant layout leaves room for the coal-handling equipment and a flue gas cleanup system, the intermediate-load PCP could be converted to baseload as the economics of the using utility dictated.

Still another option for the PCP exists. If the steam generator and EPGS are oversized, the plant can be operated in a peak-load-following (programmed) mode. The size of the storage capacity over and above that required to store excess solar energy would depend upon the utilities' load-duration curve and peak-power requirements. An integration of the load-duration curve for the Salt River Project indicated that the 2-h storage provided for low-power heater output absorption in the PCP is more than adequate to support such a plant-operating scenario.

It should be evident that the flexibility of the PCP has not been completely exploited and that many other operating modes or application are as yet unidentified.

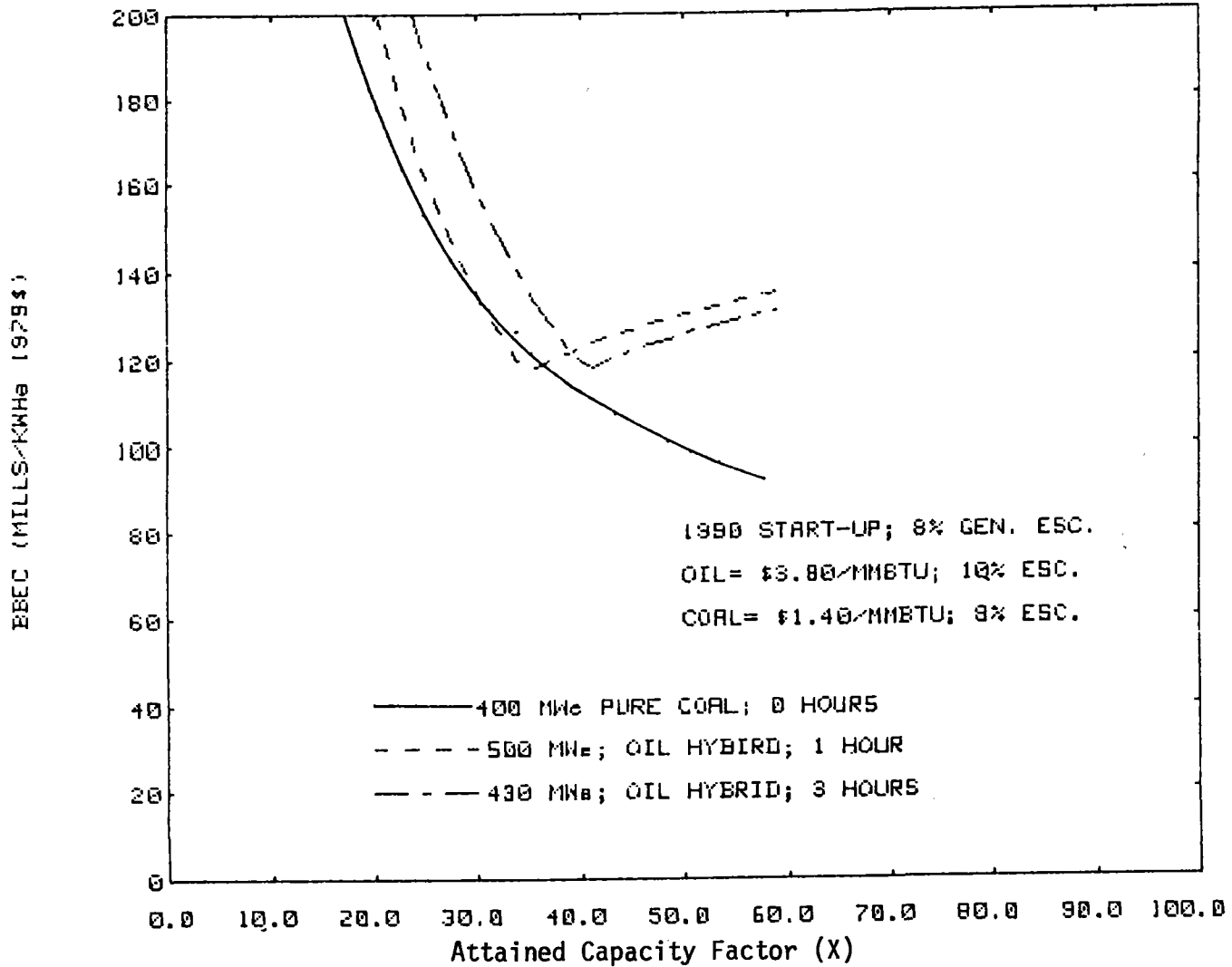


Figure 4-15. Intermediate Load Candidate Comparisons

ABBREVIATIONS AND ACRONYMS

ACR	Advanced Central Receiver
ASME	American Society of Mechanical Engineers
B&PV	Boiler & Pressure Vessel Codes
BN	600 - Russian 600-MW - Sodium Cooled Breeder Reactor
B&W	Babcock & Wilcox
DND	Departure From Nucleate Boiling
EPGS	Electric Power Generation Subsystem
EPRI	Electric Power Research Institute
ERDA	Energy Research and Development Administration
ESG	Energy Systems Group (An organizational element of Rockwell International)
ETEC	Energy Technology Engineering Center (Formerly LMEC - operated for DOE by Rockwell International)
FFTF	Fast Flux Test Facility
FGD	Flue Gas Desulfurization
FMI	Figure of Merit Input
FOM	Figure of Merit
FRP	Fiberglass Reinforced Plastic
FRPR	Field Receiver Power Ratio
GW	Gigawatt
HAC	Heliostat Array Controller
HARP	Heater Above Reheat Point
HNPF	Hallam Nuclear Power Facility
HYB	Hybrid Program
ID	Inner Diameter
LMEC	Liquid Metal Engineering Center (now ETEC)
LMFBR	Liquid Metal Fast Breeder Reactor
Loc. Dep.	Location Dependent
LWR	Light Water Reactor
MCS	Master Control Subsystem
MDC (MDAC)	McDonnell-Douglas Aerospace Corporation
Mo	Molybdenum
MSG	Modular Steam Generator

ABBREVIATIONS AND ACRONYMS

MTBF	Mean Time Between Failures
NRC	Nuclear Regulatory Commission
OD	Outer Diameter
PCP	Preferred Commercial Plant
PDR	Preliminary Design Report
PFR	Prototype Fast Reactor
PID	Proportional Integral Derivative
Resid.	Residual
ROM	Read Only Memory
SCTI	Sodium Component Test Installation
SM	Solar Multiple
SNAP	Space Nuclear Auxiliary Power
SNR-KBS	Dutch Breeder Reactor
SNR-Stork	Dutch Breeder Reactor
SOYD	Sum of the Years Digits
SRI	Stanford Research Institute, International
SRE	Sodium Reactor Experiment
STE	Solar Total Energy
WSCC	Western Systems Coordinating Council